

**Characterization of putative DD-Carboxypeptidase-interacting partners in**

***Mycobacterium smegmatis***

---

**Ditshego Benjamin Ralefeta (462764)**



Dissertation submitted to the Faculty of Health Science, University of the Witwatersrand,

Johannesburg, in fulfilment of the requirements for the degree of Master of Science in

Medicine.

June 2016

## **Declaration**

I, Ditshego Benjamin Ralefeta declare that this Dissertation is my own work. It is being submitted for the Degree of Master in Medicine in the University of the Witwatersrand, Johannesburg. It has not been submitted before for any degree or examination at this or any other University.

---

Ditshego Benjamin Ralefeta

31<sup>st</sup> Day of March 2016

## **Dedication**

I dedicate this work to my mother Maria “Omme” Mosebogadi Ralefeta and my sister Betty “Omgri” Ralefeta for their continued support and presence in my life. I also want to thank my mother for making all the effort, as a single parent, to ensure that I live a normal and happy life. I also want to thank her for the life lessons she taught me and how she raised me. I will forever be grateful for having a parent like you.

To my sister, I am really thankful for making me a priority in your life. That I will never forget and I just want you to know that I appreciate everything you have done for me.

I also want to thank my entire family and every single individual for their positive impact in my life. Without your presence, this would not have been possible.

## **Presentations arising from this MSc**

Conference 6<sup>th</sup> Cross-Faculty Graduate Symposium  
Presentation Poster Presentation  
Year 2014

Conference Molecular Biosciences Research Thrust Research Day  
Presentation Poster Presentation  
Year 2014  
Achievement **Won third prize for best poster presentation**

Conference Pathology Research and Development Congress  
Presentation Poster Presentation  
Year 2015

Conference Molecular Biosciences Research Thrust Research  
Presentation Poster Presentation  
Year 2015

Conference 7<sup>th</sup> Cross-Faculty Graduate Symposium  
Presentation Oral Presentation  
Year 2016  
Achievement **Won third prize for best oral presentation**

## Abstract

*Mycobacterium tuberculosis*, the causative agent of tuberculosis (TB), is responsible for the largest number of deaths due to a single bacterial pathogen. The persistence of TB in society is exacerbated by multiple factors, including the emergence of drug resistant forms of *M. tuberculosis* such as multi-, extensively- and totally-drug strains, which have fuelled a race for the discovery of new drugs with novel modes of action. However, the metabolic flexibility inherent in the tubercle bacillus has made the identification of vulnerable drug targets difficult. The peptidoglycan (PG) layer in the mycobacterial cell wall plays an essential role in bacterial growth, survival and antibiotic resistance but has not been exploited for TB drug development. In this study, we characterized the physiological function of mycobacterial DD-Carboxypeptidases (DD-CPases), a subgroup of Low Molecular Weight penicillin binding proteins (LMW PBPs), implicated in modulating the amount of PG cross-linking, thereby regulating the growth and remodelling of the PG polymer. Given that DD-CPases have not been characterized in actinobacteria, this study comprised the identification of *M. smegmatis* DD-CPases interacting partners, using the mycobacterial Protein Fragment complementation assay (mPFC), and interrogation of the functionality of the *M. tuberculosis* DD-CPase homologues through heterologous complementation in *M. smegmatis*. The Two DD-CPases, encoded by the MSMEG\_2433 and MSMEG\_6113 loci in *M. smegmatis*, were chosen for the identification of putative interacting partners. Screening of a genomic library using the mPFC assay identified 30 and 10 possible interacting partners for MSMEG\_2433 and MSMEG\_6113 respectively. Notably, some of these interacting partners included key regulators of cell elongation (PonA1) or division (PbpA and PbpB) and point to an important function for DD-CPases during mycobacterial growth. To further assess if genetic multiplicity for DD-CPases in *M.*

*tuberculosis* is reflective of an underlying functional redundancy between these enzymes, the *M. tuberculosis* DD-CPase homologues (Rv2911, Rv3627c and Rv3330) were assessed for functionality through ectopic expression in *M. smegmatis*. The resulting heterologous *M. smegmatis* strains displayed altered colony morphology, with smooth colonies that displayed a mucoid surface and cording defects. Ectopic expression of the *M. tuberculosis* DD-CPases in *M. smegmatis* also resulted in aberrant biofilm formation and affected bacterial sliding on semi-solid agar, indicative of an alteration in the three-dimensional packing of cells in a community or changes in membrane properties. Over-expression of Rv2911 and Rv3627c resulted in reduced bacterial cell length accompanied by division defects. Transmission electron microscopy revealed that the *M. tuberculosis* DD-CPase homologues are involved in maintaining normal bacterial cell wall architecture. Over-expression of these homologues in native wild type *M. tuberculosis* H<sub>37</sub>RvS revealed a role for Rv3627c in regulating bacterial colony morphology. Cellular localization studies with rseGFP C-terminally tagged derivatives of these proteins revealed that they localize at the poles, mid-cell or and quarter-cell positions, further suggestive of a role in temporal and spatial co-ordination of cell growth and division. Collectively, the data point to important, possibly redundant roles for the multiple DD-CPases-encoding genes in *M. tuberculosis* and highlights these proteins as possible new drug targets for TB.

## **Acknowledgements**

I would like to thank my financial sponsors, the National Research Foundation (NRF) and the Belgium Technical Cooperation (BTC)

I would also like to thank the University of Cape Town Centre for Imaging and Analysis unit, for offering me the opportunity to use their equipment.

I would also like to thank the CBTR team, both the management and students.

I would also like to thank my two supervisors, Dr. Edith Machowski and Prof. Bavesh Kana.

I am very thankful for your guidance and support. And I am grateful for your patience, especially during the compilation of my dissertation. I am really grateful for that.

## Table of contents

|   |      |
|---|------|
| Declaration.....  | i    |
| Dedication.....   | ii   |
| Presentation arising from this MSc.....   | iii  |
| Abstract.....   | iv   |
| Acknowledgements.....   | vi   |
| List of figures.....  | xi   |
| List of tables.....   | xiii |
| Nomenclature.....   | xiv  |
| <br>  |      |
| 1. Introduction.....  | 1    |
| 1.1. Background.....  | 1    |
| 1.2. Tuberculosis chemotherapy.....   | 2    |
| 1.2.1. Current drug regimen.....  | 2    |
| 1.2.2. Drug-drug interactions.....  | 4    |
| 1.3. The mycobacterial cell envelope.....   | 6    |
| 1.4. Peptidoglycan biosynthesis.....  | 9    |
| 1.4.1. Cytoplasmic step of PG biosynthesis.....                                   | 9    |
| 1.5. Periplasmic step of PG biosynthesis.....                                     | 11   |
| 1.5.1. Hydrolases.....  | 11   |
| 1.5.1.1. Lytic transglycosylases.....   | 11   |
| 1.5.1.2. Resuscitation promoting factors.....                                     | 12   |
| 1.5.1.3. Amidases.....  | 14   |
| 1.5.1.4. <i>N</i> -Acetyl- $\beta$ - <i>D</i> -glucosaminidases.....              | 14   |
| 1.5.2. PG Synthases.....  | 14   |
| 1.5.2.1. L,D transpeptidases.....   | 14   |
| 1.5.2.2. Penicillin binding proteins (PBPs).....                                  | 15   |
| 1.5.2.3. DD-Carboxypeptidases.....  | 17   |
| 1.6. Mycobacterial DD-CPases.....   | 18   |
| 1.7. Hypothesis.....  | 20   |
| 1.8. Aims and objectives of the study.....  | 20   |
| 1.8.1. Study aims.....  | 20   |
| 1.8.2. Study objectives.....  | 20   |
| <br>  |      |
| 2. Methodology.....   | 21   |
| 2.1. Plasmids used and constructs generated in this study.....                    | 21   |
| 2.2. Bacterial growth conditions.....   | 24   |
| 2.2.1. Growth conditions for <i>E. coli</i> DH5 $\alpha$ and derivatives.....     | 24   |
| 2.2.2. Growth conditions for <i>M. smegmatis</i> and <i>M. tuberculosis</i> ..... | 24   |
| 2.3. Mycobacterial DNA extractions.....   | 25   |
| 2.3.1. Large scale DNA extraction for PCR.....                                    | 25   |
| 2.3.2. Small scale DNA extraction for genotypic confirmation.....                 | 26   |
| 2.4. <i>E. coli</i> plasmid DNA extraction.....                                   | 26   |
| 2.4.1. Bulk DNA extraction.....   | 26   |
| 2.4.2. Small scale plasmid DNA extraction.....                                    | 26   |
| 2.5. DNA clean-up and removal of contaminating proteins.....                      | 27   |
| 2.5.1. Sodium acetate precipitation.....  | 27   |



|  |    |
|--|----|
| 2.6. Restriction profiling.....  | 28 |
| 2.7. Agarose gel electrophoresis.....  | 28 |
| 2.8. DNA cloning.....  | 28 |
| 2.8.1. Vector backbone confirmation.....   | 28 |
| 2.8.2. PCR reactions.....  | 29 |
| 2.8.3. PCR and plasmid DNA digestion.....  | 29 |
| 2.8.4. Agarase DNA recovery and clean-up for cloning.....  | 30 |
| 2.8.5. Dephosphorylation of plasmid DNA.....   | 30 |
| 2.8.6. DNA ligations.....  | 31 |
| 2.9. Preparation and transformation of chemically competent <i>E. coli</i> DH5 $\alpha$ .....  | 31 |
| 2.9.1. Preparation of chemically competent <i>E. coli</i> DH5 $\alpha$ .....   | 31 |
| 2.9.2. Transformation of chemically competent <i>E. coli</i> DH5 $\alpha$ .....  | 32 |
| 2.10. Screening and confirmation of positive clones.....   | 32 |
| 2.10.1. Screening for putative clones.....   | 32 |
| 2.10.2. Sequencing.....  | 33 |
| 2.11. Transformation of <i>M. smegmatis</i> .....  | 33 |
| 2.11.1. Preparation of electro-competent mc <sup>2</sup> 155.....  | 33 |
| 2.11.2. Transformation of electro-competent mc <sup>2</sup> 155.....   | 33 |
| 2.12. Transformation of H <sub>37</sub> RvS.....   | 34 |
| 2.12.1. Preparation of electro-competent H <sub>37</sub> RvS.....  | 34 |
| 2.12.2. Transformation of electro-competent H <sub>37</sub> RvS.....   | 34 |
| 2.13. Genotypic confirmation of recombinant strains.....   | 34 |
| 2.14. Genomic DNA library construction.....  | 35 |
| 2.14.1. Genomic DNA extraction and restriction digest.....   | 35 |
| 2.14.2. Preparation of electro-competent <i>E. coli</i> DH5 $\alpha$ .....   | 36 |
| 2.14.3. Transformation of Electro-competent <i>E. coli</i> DH5 $\alpha$ .....  | 36 |
| 2.15. Identification of the respective MSMEG_2433 and<br>MSMEG_6113 putative interacting partners.....                                       | 37 |
| 2.15.1. Assaying for putative interacting partners for MSMEG_2433<br>and MSMEG_6113.....   | 37 |
| 2.15.2. Sequencing and identification of the respective interacting<br>partners.....   | 38 |
| 2.16. Phenotypic characterization of recombinant strains.....  | 40 |
| 2.16.1. Assessment of mycobacterial colony and morphology.....   | 40 |
| 2.16.2. Assessment of mycobacterial biofilm formation.....   | 40 |
| 2.16.3. Assessment of bacterial sliding motility.....  | 41 |
| 2.16.4. Assessment of mycobacterial growth.....  | 41 |
| 2.16.5. Scanning electron microscopy preparation and imaging.....  | 42 |
| 2.16.6. Transmission electron microscopy preparation and imaging.....  | 42 |
| 2.17. Fluorescence microscopy.....   | 43 |
| 2.18. Statistical analysis.....  | 43 |
| 3. Results.....  | 44 |
| 3.1. Protein interactions studies.....   | 44 |
| 3.1.1. Confirming the efficacy of the mPFC assay by assessing protein-interaction<br>of the two peptidoglycan hydrolases, RipA and RpfB..... | 44 |
| 3.1.2. Construction and generation of wild type mc <sup>2</sup> 155 genomic<br>DNA library.....  | 50 |

|  |     |
|--|-----|
| 3.1.3. Cloning and PCR confirmation of MSMEG_2344 and MSMEG_6113 into the bait vector, pUAB400.....  | 52  |
| 3.1.4. Screening for interaction partners using the mPFC assay and trim resistance.....  | 56  |
| 3.1.5. Identification of the respective MSMEG_2433 and MSMEG_6113 putative interacting partners.....   | 57  |
| 3.2. Ectopic expression of <i>M. tuberculosis</i> DD-CPases in <i>M. smegmatis</i> .....   | 68  |
| 3.2.1. Generation and genotyping of heterologous <i>M. smegmatis</i> strains ectopically expressing <i>M. tuberculosis</i> DD-CPases.....  | 68  |
| 3.2.2. Ectopic expression of <i>M. tuberculosis</i> DD-CPases in <i>M. smegmatis</i> significantly affects bacterial colony morphology.....  | 70  |
| 3.2.3. Ectopic expression of <i>M. tuberculosis</i> DD-CPases affects bacterial sliding on semi-solid agar.....  | 71  |
| 3.2.4. Ectopic expression of <i>M. tuberculosis</i> DD-CPases in <i>M. smegmatis</i> results in delayed and aberrant biofilm formation.....  | 74  |
| 3.2.5. Ectopic expression of <i>M. tuberculosis</i> DD-CPases in <i>M. smegmatis</i> results in retarded growth in axenic culture.....   | 75  |
| 3.2.6. Ectopic expression of Rv2911 and Rv3627c significantly alters mycobacterial cell length and mechanisms of division.....   | 77  |
| 3.2.7. Ectopic expression of Rv3330 in <i>M. smegmatis</i> significantly affects cellular morphology.....  | 80  |
| 3.2.8. Ectopic expression of <i>M. tuberculosis</i> DD-CPases disrupts normal cell wall architecture in <i>M. smegmatis</i> .....  | 83  |
| 3.3. Ectopic expression of <i>M. tuberculosis</i> DD-CPase homologues in wild type H <sub>37</sub> RvS strain.....   | 86  |
| 3.3.1. Construction and genotypic analysis of H <sub>37</sub> RvS strains that ectopically express individual DD-CPases-encoding genes.....  | 87  |
| 3.3.2. Ectopic expression of Rv3627c in H <sub>37</sub> RvS significantly affects bacterial cording.....   | 89  |
| 3.3.3. Ectopic expression of Rv3627c in H <sub>37</sub> RvS significantly delays biofilm formation and maturation.....   | 90  |
| 3.3.4. The H <sub>37</sub> RvS recombinant strains ectopically expressing the <i>M. tuberculosis</i> DD-CPases displayed no growth retardation in liquid 7H9 media.....                  | 93  |
| 3.3.5. Recombinant H <sub>37</sub> RvS strains ectopically expressing <i>M. tuberculosis</i> DD-CPases displayed an increase in bacterial cell length as revealed by SEM.....            | 95  |
| 3.3.6. Ectopic expression of <i>M. tuberculosis</i> DD-CPases in H <sub>37</sub> RvS does not affect normal bacterial cell wall architecture as revealed by TEM.....                     | 99  |
| 3.4. <i>M. tuberculosis</i> rseGFP tagged DD-CPases derivatives displayed polar, Mid-cell and quarter cell position localization when ectopically expressed in <i>M. smegmatis</i> ..... | 101 |
| 4. Discussion.....   | 106 |
| 4.1. Interaction between MSMEG_2433 and MSMEG_6113 with PBPs.....  | 108 |
| 4.1.1. MSMEG_6113 and Beta lactamase penicillin-binding protein.....   | 108 |
| 4.1.2. MSMEG_2433 and Penicillin binding protein transpeptidase domain protein (PbpA).....   | 108 |

|  |     |
|--|-----|
| 4.1.3. MSMEG_2433 and the bifunctional penicillin-binding protein A1/1B (PonA1).....   | 109 |
| 4.1.4. MSMEG_2433 and the penicillin-insensitive transglycosylase/penicillin-sensitive transpeptidase (PonA2).....                               | 109 |
| 4.1.5. MSMEG_6113 and Penicillin binding proteins B(PBPB).....   | 110 |
| 4.2. Interaction between MSMEG_2433 and MSMEG_6113 with other periplasmic/ membrane bound proteins.....  | 110 |
| 4.2.1. MSMEG_2433 and the ATP-dependent zinc metalloprotease FtsH.....   | 110 |
| 4.2.3. MSMEG_2433 and UDP-diphospho-muramoylpentapeptide beta- <i>N</i> -acetylglucosaminyltransferase (MurG).....                               | 112 |
| 4.2.4. MSMEG_2433 and UDP- <i>N</i> -acetylenolpyruvoylglucosamine reductase (MurB).....   | 112 |
| 4.2.5. MSMEG_6113 and the cell division control protein Cdc48.....   | 112 |
| 4.3. Proposed model for biological role of MSMEG_2433 and MSMEG_6113.....  | 113 |
| 4.4. Ectopic expression of <i>M. tuberculosis</i> DD-CPase homologues.....   | 113 |
| 4.4.1. <i>M. tuberculosis</i> DD-CPases and maintenance of normal colony morphology.....   | 113 |
| 4.4.2. <i>M. tuberculosis</i> DD-CPases and their role in bacterial motility.....  | 114 |
| 4.4.3. <i>M. tuberculosis</i> Rv3627c and biofilm formation.....   | 115 |
| 4.4.4. <i>M. tuberculosis</i> DD-CPases and their role in bacterial growth.....  | 115 |
| 4.4.5. <i>M. tuberculosis</i> Rv2911 and Rv3627c and their role in maintaining normal bacterial cell length and mechanisms of cell division..... | 116 |
| 4.4.6. <i>M. tuberculosis</i> Rv3330 bacterial cell morphology.....  | 118 |
| 4.4.7. DD-CPases and the bacterial cell envelope.....  | 119 |
| 4.5. Polar, mid-cell and quarter cell position localization of rseGFP tagged <i>M. tuberculosis</i> DD-CPase homologues.....                     | 119 |
| 4.6. A proposed model for the function of <i>M. tuberculosis</i> DD-CPases.....  | 120 |
| 5.1. Conclusion and future prospects.....  | 121 |
| 5.1.1. Conclusion.....   | 121 |
| 5.1.2. Future prospects.....   | 121 |
| 6. Appendices.....   | 123 |
| 6.1. Appendix A: DNA molecular weight markers used in this study.....  | 123 |
| 6.2 Appendix B: PCR primers.....   | 124 |
| 6.2.1. Bacterial two hybrid primers.....   | 124 |
| 6.2.2. Untagged <i>M. tuberculosis</i> DD-CPases primer sets for cloning into pSE100 and genotypic confirmation of generated strains.....        | 124 |
| 6.2.3. rseGFP and <i>M. tuberculosis</i> DD-CPase primer sets for 3-way cloning into pSE100 and genotypic confirmation of generated strains..... | 125 |
| 6.3. Appendix C: Restriction digests.....  | 126 |
| 6.3.1. Restriction profile of the mPFC backbone vectors.....   | 126 |
| 6.3.1.1. Restriction profile of pUAB300.....   | 126 |
| 6.3.1.2. Restriction profile of pUAB400.....   | 127 |
| 6.4. Appendix D: Restriction profile of pSE100 vector backbone   |     |

|   |     |
|---|-----|
| and derivatives.....  | 128 |
| 6.4.1. Restriction profile of pSE100 vector backbone.....   | 128 |
| 6.4.2. Restriction profile of untagged Rv2911 cloned into pSE100.....   | 129 |
| 6.4.3. Restriction profile on untagged Rv3330 cloned into pSE100.....   | 130 |
| 6.4.4. Restriction profile on untagged Rv3627c cloned into pSE100.....  | 131 |
| 6.5. Appendix E: Restriction profile of rseGFP tagged <i>M. tuberculosis</i> DD-CPase derivatives cloned into pSE100..... | 132 |
| 6.5.1. Restriction profile of C-terminally rseGFP tagged Rv2911 cloned into pSE100.....                                   | 132 |
| 6.5.2. Restriction profile of C-terminally rseGFP tagged Rv3330 cloned into pSE100.....                                   | 133 |
| 6.5.3. Restriction profile of C-terminally rseGFP tagged Rv3627c cloned into pSE100.....                                  | 134 |
| 6.6. Appendix F: Culture media.....   | 135 |
| 6.6.1. <i>E. coli</i> culture media.....  | 135 |
| 6.6.2. <i>M. smegmatis</i> culture media.....   | 135 |
| 6.6.2. <i>M. tuberculosis</i> culture media.....  | 135 |
| 6.7. Appendix G: Specialized media.....   | 135 |
| 6.7.1. Minimal Sauton's.....  | 135 |
| 6.7.2. Sliding motility semi-solid media.....   | 135 |
| 6.8. Appendix H: DNA extraction solutions.....  | 135 |
| 6.8.1. Plasmid DNA extraction solutions for <i>E. coli</i> .....  | 135 |
| 6.8.2. Genomic DNA extraction solutions for mycobacteria.....   | 136 |
| Bibliography.....   | 137 |

## List of figures List of figure

|   |    |
|---|----|
| <b>Figure 1.1.1.</b> A global representation of TB incidence in 2014 as reported by the World Health Organization.....  | 2  |
| <b>Figure 1.1.2.</b> A diagrammatic representation of the mycobacterial cell wall.....  | 6  |
| <b>Figure 1.1.3.</b> Diagrammatic representation of the cytoplasmic step of PG biosynthesis.....  | 10 |
| <b>Figure 1.1.4.</b> The site of action of PG remodelling enzymes in mycobacteria.....  | 12 |
| <b>Figure 2.1.1.</b> The concept of the mPFC assay.....   | 38 |
| <b>Figure 2.1.2.</b> The strategy employed using the mPFC assay to identify putative interacting partners for MSMEG_2433 and MSMEG_6113.....  | 39 |
| <b>Figure 3.1.2.</b> Restriction profiling of MSMEG_3145 cloned into pUAB300.....   | 46 |
| <b>Figure 3.1.3.</b> Restriction profiling MSMEG_5439 cloned into pUAB400.....  | 47 |
| <b>Figure 3.1.4.</b> PCR confirmation of strains carrying control vectors.....  | 48 |
| <b>Figure 3.1.5.</b> Genomic DNA library of mc <sup>2</sup> 155 designed with <i>TaqI</i> .....   | 51 |
| <b>Figure 3.1.6.</b> Restriction profiling of MSMEG_2433 cloned into pUAB400.....   | 53 |
| <b>Figure 3.1.7.</b> Restriction profiling of MSMEG_6113 cloned into pUAB400.....   | 54 |
| <b>Figure 3.1.8.</b> Genotypic confirmation of the bait strains.....  | 55 |
| <b>Figure 3.1.9.</b> The results obtained using the mPFC assay for screening of putative MSMEG_2433 and MSMEG_6113 interacting partners.....  | 56 |
| <b>Figure 3.2.1.</b> PCR confirmation of presence of <i>M. tuberculosis</i> DD-CPases in <i>M. smegmatis</i> .....  | 69 |
| <b>Figure 3.2.2.</b> Colony morphology of the recombinant <i>M. smegmatis</i> strains ectopically expressing <i>M. tuberculosis</i> DD-CPases.....  | 71 |
| <b>Figure 3.2.3.</b> Sliding motility of the heterologous <i>M. smegmatis</i> strains on semi-solid media.....  | 73 |
| <b>Figure 3.2.4.</b> Biofilm formation of the heterologous <i>M. smegmatis</i> strains ectopically expressing <i>M. tuberculosis</i> DD-CPases.....   | 75 |
| <b>Figure 3.2.5.</b> Growth curve analysis of the heterologous <i>M. smegmatis</i> strains.....   | 76 |
| <b>Figure 3.2.6.</b> Cell length alteration and division defects displayed by the heterologous <i>M. smegmatis</i> strains as a result of ectopic expression of <i>M. tuberculosis</i> DD-CPases.....             | 78 |
| <b>Figure 3.2.7.</b> Cell length distribution of the heterologous <i>M. smegmatis</i> strains.....  | 79 |
| <b>Figure 3.2.8.</b> Abnormal cell wall morphology displayed by the mc <sup>2</sup> (pSE3330) strain.....   | 81 |
| <b>Figure 3.2.9.</b> Quantification of abnormal cellular morphology resulting from ectopic of Rv3330 in <i>M. smegmatis</i> .....   | 83 |
| <b>Figure 3.2.10.</b> Transmission electron micrographs of the heterologous <i>M. smegmatis</i> strains ectopically expressing <i>M. tuberculosis</i> DD-CPases at log, lag and exponential phases of growth..... | 85 |
| <b>Figure 3.2.11.</b> Quantification of cells displaying aberrant cell wall architecture resulting from increased expression of <i>M. tuberculosis</i> DD-CPases in <i>M. smegmatis</i> as revealed by TEM.....   | 86 |
| <b>Figure 3.3.1.</b> PCR confirmation of recombinant H <sub>37</sub> RvS strains carrying the <i>M. tuberculosis</i> DD-CPases ectopically expressed in H <sub>37</sub> RvS.....                                  | 88 |
| <b>Figure 3.3.2.</b> Colony morphology of the recombinant H <sub>37</sub> RvS strains ectopically expressing <i>M. tuberculosis</i> DD-CPases.....  | 90 |
| <b>Figure 3.3.3.</b> Biofilm formation of the recombinant H <sub>37</sub> RvS strains ectopically expressing <i>M. tuberculosis</i> DD-CPase homologues.....  | 93 |
| <b>Figure 3.3.4.</b> Growth of the recombinant H <sub>37</sub> RvS strains in Middlebrook 7H9 media.....  | 94 |

|   |     |
|---|-----|
| <b>Figure 3.3.5.</b> Cell surface of the recombinant H <sub>37</sub> RvS strains at lag, log and stationary phases of growth as revealed by SEM.....                            | 97  |
| <b>Figure 3.3.6.</b> Cell length distribution of the recombinant H <sub>37</sub> RvS strains.....   | 98  |
| <b>Figure 3.3.7.</b> Transmission electron micrographs of the recombinant H <sub>37</sub> RvS strains obtained for stationary phase cultures.....                               | 100 |
| <b>Figure 3.4.1.</b> PCR confirmation of rseGFP C-terminally tagged <i>M. tuberculosis</i> DD-CPase derivatives.....  | 102 |
| <b>Figure 3.4.2.</b> Cellular localization of C-terminally tagged rseGFP <i>M. tuberculosis</i> DD-CPase derivatives in <i>M. smegmatis</i> .....                               | 104 |
| <b>Figure 3.4.3.</b> Quantification of cellular localization of rseGFP tagged <i>M. tuberculosis</i> DD-CPase fusion proteins ectopically expressed in mc <sup>2</sup> 155..... | 106 |
| <b>Figure 4.1.1.</b> A proposed model for the function of MSMEG_2433 and MSMEG_6113.....  | 113 |
| <b>Figure 4.1.2.</b> A model depicting the role <i>M. tuberculosis</i> DD-CPase homologues.....   | 120 |
| <b>Figure A.1.1.1.</b> Molecular weight DNA markers.....  | 123 |
| <b>Figure A.1.1.2.</b> Restriction profiling of the mPFC prey vector, pUAB300.....  | 126 |
| <b>Figure A.1.1.3.</b> Restriction profiling of the mPFC bait vector, pUAB400.....  | 127 |
| <b>Figure A.1.1.4.</b> Restriction profiling of pSE100.....   | 128 |
| <b>Figure A.1.1.5.</b> Restriction profiling of untagged Rv2911 cloned into pSE100 producing the pSE2911 construct.....   | 129 |
| <b>Figure A.1.1.6.</b> Restriction profiling of untagged Rv3330 cloned into pSE100 to generate the pSE3330 construct.....   | 130 |
| <b>Figure A.1.1.7.</b> Restriction profiling of untagged Rv3627c cloned into pSE100 to generate the pSE3627c construct.....   | 131 |
| <b>Figure A.1.1.8.</b> Restriction profiling of rseGFP C-terminally tagged Rv2911 cloned into pSE100 to generate the pSE2911-rseGFP construct.....                              | 132 |
| <b>Figure A.1.1.9.</b> Restriction profiling of rseGFP C-terminally tagged Rv3330 cloned into pSE100 to generate the pSE3330-rseGFP construct.....                              | 133 |
| <b>Figure A.1.1.10.</b> Restriction profiling of rseGFP C-terminally tagged Rv3627c cloned into pSE100 to generate the pSE3627c-rseGFP construct.....                           | 134 |

## List of Tables

|  |     |
|--|-----|
| <b>Table 2.1.1.</b> Plasmid generated and/or used in this study.....   | 22  |
| <b>Table 2.1.2.</b> Strains used and/or generated in this study.....   | 23  |
| <b>Table 3.1.1.</b> The total number of colonies for each test conducted for screening of putative MSMEG_2433 and MSMEG_6113 interacting partners including the appropriate controls using the mPFC assay..... | 57  |
| <b>Table 3.1.2.</b> Putative MSMEG_2433 interacting partners obtained using the mPFC assay.....  | 60  |
| <b>Table 3.1.3.</b> Putative MSMEG_6113 interacting partners obtained using the mPFC assay.....  | 65  |
| <b>Table 4.1.1.</b> Cell length displayed by the heterologous <i>M. smegmatis</i> and recombinant <i>M. tuberculosis</i> H <sub>37</sub> RvS strains at different growth phases.....                           | 117 |
| <b>Table A.1.1.1.</b> Bacterial two hybrid primers.....  | 124 |
| <b>Table A.1.1.2.</b> Untagged <i>M. tuberculosis</i> DD-CPase primer sets for cloning into pSE100 and genotypic confirmation of generated strains.....  | 124 |
| <b>Table A.1.1.3.</b> rseGFP and <i>M. tuberculosis</i> DD-CPase primer sets for 3-way cloning into pSE100 and genotypic confirmation of generated strains.....  | 125 |

## Nomenclature

|                         |                                      |
|-------------------------|--------------------------------------|
| <b>AG</b>               | Arabinogalactan                      |
| <b>bps</b>              | base pairs                           |
| <b>CTAB</b>             | Cetyltrimethylammonium bromide       |
| <b>DD-CPase</b>         | DD-Carboxypeptidase                  |
| <b>dNTPs</b>            | Deoxynucleotide triphosphates        |
| <b>Hyg</b>              | Hygromycin                           |
| <b>Kan</b>              | Kanamycin                            |
| <b>kbps</b>             | Kilo base pairs                      |
| <b>LA</b>               | Luria Bertani                        |
| <b>LB</b>               | Luria broth                          |
| <b>LMW</b>              | Low molecular weight                 |
| <b>MA</b>               | Mycolic Acids                        |
| <b>mPFC</b>             | mycobacterial Protein Fragment Assay |
| <b>PBPs</b>             | Penicillin binding proteins          |
| <b>PG</b>               | Peptidoglycan                        |
| <b>sdH<sub>2</sub>O</b> | Sterile distilled water              |
| <b>SDS</b>              | Sodium deodecyl sulphate             |
| <b>SEM</b>              | Scanning electron microscopy         |
| <b>TB</b>               | Tuberculosis                         |
| <b>TEM</b>              | Transmission electron microscopy     |
| <b>Trim</b>             | Trimethoprim                         |

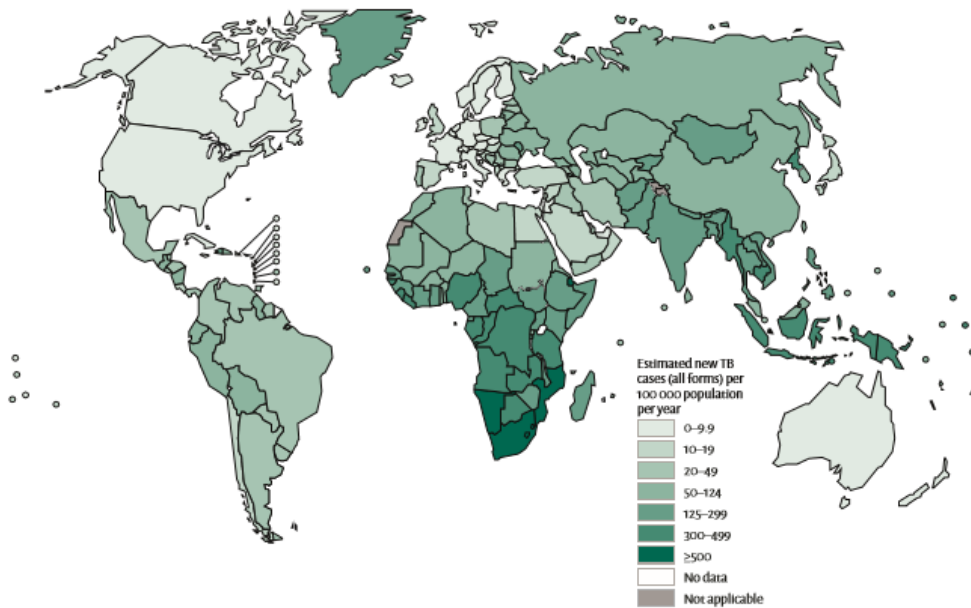


## **1.1. Introduction**

### **1.1.1. Background**

*M. tuberculosis*, a slow growing bacterium and the causative agent of tuberculosis (TB), is a significant cause of morbidity and mortality globally. TB causes approximately 1.3 million deaths annually, with 8-10 million new infections (Corbett et al., 2003). The World Health Organization (WHO) estimated that in 2014, TB claimed 1.5 million lives, wherein 1.1 and 0.4 million were reported to occur in HIV-negative and HIV-positive individuals, respectively (WHO, 2015). A similar trend was documented in 2013, with an increasing number of deaths reported for women and children. Furthermore, the WHO reported for the first time that TB associated deaths in 2014 surpassed that of HIV associated deaths (WHO, 2014). TB infection and associated active disease is prevalent in developing countries and further exacerbated by increased HIV infection rates. The high burden endemic countries with reportedly high numbers of TB infection in 2014 according to the WHO are as follows; India, Indonesia, China, Nigeria, Pakistan and South Africa, figure 1.1.1. In these countries, various socio-economic factors such as urbanization, over-crowding, poor nutrition and stigma facilitate sustained transmission of TB and failure to address these will ensure that human society continues to face a massive on-going and future burden of TB disease.

Estimated TB Incidence rates, 2014



**Figure 1.1.1.** A global representation of TB incidence in 2014 as reported by the World Health Organization. The high burden regions include Asia and Sub-Saharan Africa. (WHO, 2015)

## 1.2. Tuberculosis chemotherapy

### 1.2.1. Current drug regimen

Combinatorial chemotherapy involving numerous first line drugs is used for treatment of drug susceptible TB. These antibiotics comprise rifampicin, isoniazid, pyrazinamide and ethambutol for first two months of treatment, followed by chronic treatment for four months with rifampicin and isoniazid. This approach, to a greater extent, has been used to effectively manage TB in many countries (Duncan, 2013; Zumla et al., 2013). The above mentioned treatment regimen forms the basis of the WHO recommended directly observed therapy short course strategy, adopted in the early 1990's, where a patient is required to take medication in the presence of a health care provider, ensuring compliance (Raviglione and Pio, 2002; Dye et al., 1998). These efforts, together with administration of the Bacille

Calmette-Guérin vaccine (BCG) for prevention of disseminated TB in early childhood, (Colditz et al., 1994; Anderson et al., 2005) have significantly reduced rampant spread of TB globally. However, despite this, TB continues to claim millions of lives, a situation that requires urgent and effective interventions.

Much of the success of *M. tuberculosis* as a human pathogen is related to the amazing responsiveness of the tubercle bacillus to stress conditions, which is illustrated by: (I) the ability of the bacterium to escape host defence mechanisms such as the production of reactive oxygen/nitrogen species and the maturation of the phagosomes (Tufariello et al., 2003) (II) the inherent ability to spontaneously evolve drug resistance through chromosomal mutation of essential drug targets (Nachamkin et al., 1997; Telenti, et al., 1993; Heep et al., 2001) (III) the propensity to adopt alternative growth states (active growth vs. non-replicating persistence vs. the lack of culturability), an effect which is dependent on the host immune status (Zhang et al., 2004; Parrish et al., 1998; Ahmad et al., 2010) (IV) the occupation of different niches during infection, with different physiological conditions which affect the biochemical properties and efficacy of antibiotics (Iseman and Madsen, 1991; Elliott, et al., 1995) (V) the presence of a complex hydrophobic cell envelope, which does not allow for easy diffusion of small molecules such as antibiotics and (VI) the presence of numerous drug efflux systems that pump out antibiotics, thereby reducing their intracellular concentration (Domenech et al., 2005; Rossi et al., 2006; Louw et al., 2009).

These and other factors have essentially fuelled the current TB pandemic as they create a clinical spectrum of disease that is difficult to manage through national control programs in endemic countries. Drug resistant TB [multi-(MDR), extensively (XDR) and totally (TDR)-drug resistant] are a particular challenge and require extended periods of treatment with a combination of both first and second line drugs (Centers for Disease Control and Prevention,

2006; Suárez et al., 2002; Gandhi et al., 2006). The second line drugs in this case include, aminoglycosides (kanamycin, capreomycin and amikacin), fluoroquinolones (moxifloxacin, gatifloxacin) (Ma et al. 2010; Stass et al. 1998) and bedaquiline (Diacon et al. 2013; Mahajan, 2013), which are extremely toxic and cause severe side effects. However, another major obstacle to the design of effective anti-TB drugs is drug-drug interaction, especially in immune compromised HIV-infected individuals taking both anti-TB drugs together with antiretroviral treatment (ARV).

### **1.2.2. Drug-drug interactions.**

Currently, the emergence of drug resistant forms of *M. tuberculosis* have necessitated the design of effective new anti-TB-drugs, but success will only be achieved through integration of both old and new drug regimens together with antiretroviral therapy or any other form therapy, in a combination that will allow for each drug to effectively act on its target (Koul et al., 2011). Additionally, negative interactions between TB drugs and other drugs intended to treat a different condition (diabetes, cholesterol, hypertension etc.), are not the only forms of interaction that can occur as anti-TB drugs can cross react with each other (Bhutani et al., 2005). This limits the combinations of drugs that can be prescribed for a patient with co-morbid TB diseases.

Rifampicin, an essential anti-TB drug, that together with isoniazid, allows for effective early bactericidal activity and increased cure rates (Fox et al., 1999) reduces the serum concentration of protease inhibitors in HIV-infected individuals on ART (Ribera et al., 2001; Haas et al., 2009). Rifampicin also induces expression of the hepatic cytochrome P450 enzyme systems and *P*-glycoproteins, which increase the metabolism of efavirenzi and nevarapine (Ribera et al., 2001) and a number of other antiretroviral agents (Haas et al., 2009; Requena et al., 2005), thereby reducing serum concentrations and ultimate

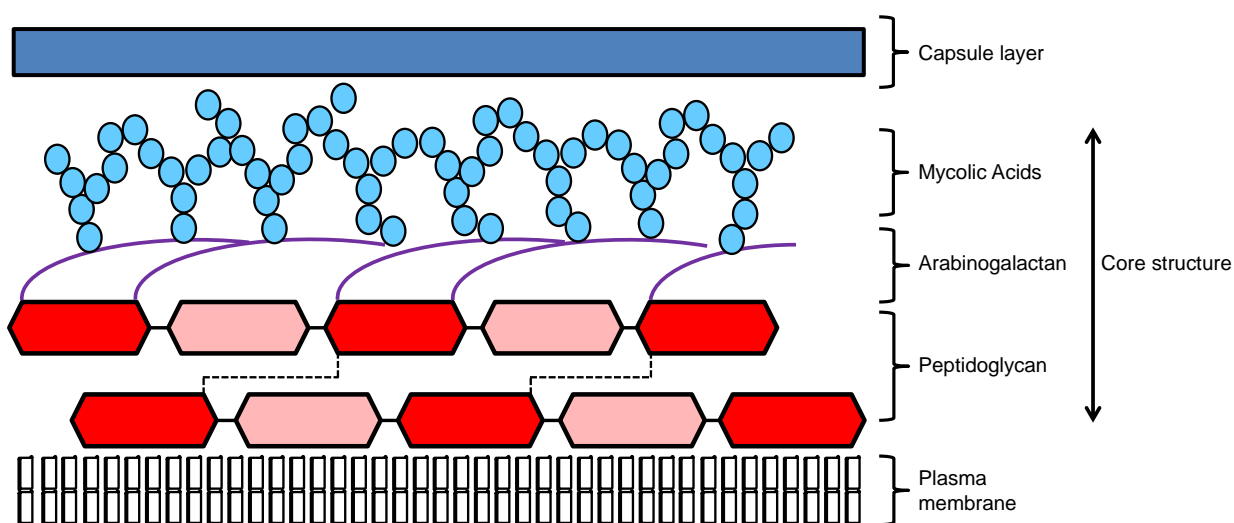
effectiveness of ART. Alternatively, rifabutin provides a tractable replacement for rifampicin, which also induces the cytochrome P-450 enzyme system and *P*-glycoproteins but at lower levels compared to rifampicin (Gonzalez-Montaner et al., 1994; Carto 3<sup>rd</sup> et al., 1998). However, a safe dosage of rifabutin, when co-administered with antiretroviral therapy was not determined (Khachiet al., 2009) until recently (Lan et al., 2014), thus providing a new therapeutic option for TB-HIV infected individuals.

An additional impediment with treatment of HIV-TB co-infection is the general toxicity of both regimens, especially in the case of drug resistance. Therefore, in the case of TB-HIV co-infection, patients will present multiple or overlapping side effects and this will potentially result in the disruption/discontinuation of optimized therapy to minimize the toxicity of the drugs to the patient (Dean et al., 2002). As such, new drugs with novel modes of action that would be active on both drug susceptible and drug resistant forms of TB, that exhibit no cross interactions with ART, now present as an urgent necessity.

The capacity of an organism to establish disease in a host, to persist and disseminate as in the case of TB infection, requires two fundamental processes; growth and division, both of which have to occur under substantive immune assault and drug treatment. The study of mycobacterial cell division and elongation is still in its infancy and further in-roads are required to develop a holistic understanding of these essential processes. A key feature of successful bacterial cell division is the ability to rapidly remodel the multiple layers of the cell envelope to allow for insertion of new cell wall units and degradation of the septum to facilitate daughter cell separation. This MSc focuses on the remodelling of the peptidoglycan (PG) layer in the mycobacterial cell wall, with the aim of uncovering new drug targets that are essential for remodelling this polymer during growth.

### 1.3. The mycobacterial cell envelope

The mycobacterial cell envelope, like in any bacterial species, is central to growth and survival as it provides a barrier to external stress (Mikušova et al., 2000). It consists of three distinct layers including the plasma membrane, the envelope core, and membrane bound lipids or extractable proteins that form part of the capsule-like layer (Alteens et al., 2008; Daffe and Etienne, 1999), figure 1.1.2.



**Figure 1.1.2.** A diagrammatic representation of the mycobacterial cell wall. The image shows the three distinct layers of the mycobacterial: cell wall consisting of the capsule layer, the core structure and the plasma membrane. The core structure encompasses the mycolic acids, arabinogalactan and the peptidoglycan layer.

The unique composition of these layers, detailed further below, has resulted in variable gram staining of mycobacteria, making it difficult to place these organisms under conventional classifications such as gram positive or gram negative (Smithwick, 1976; Miller, 1972)

The outer layer of the mycobacterial cell wall consists of various lipids, proteins and glycoprotein, (Daffe and Etienne, 1999), figure 1.1.2. The sugar components are

predominantly arabinomannan,  $\alpha$ -glucan and mannan (Sani et al., 2010; Deffe and Etienne, 2010). The surface exposed lipids include; lipopolysaccharides (Drapper et al., 1973), a variety of structurally related phenolic glycolipids (Boddingius et al., 1989) and Phthiocerol dimycocerosates (Hunter et al., 1983). The Phthiocerol dimycocerosates and lipopolysaccharides are major virulence factors, modifying the host immune response at the initial host-pathogen encounter (Astarie-Dequeker et al., 2009; Tobian et al., 2003; Moreno et al., 1988). The protein component of the outer layer consists largely of various ESX secretion protein complexes (Sani et al., 2010), malate synthase, the MtrA proteins (Marques et al., 1998) and  $\beta$ -lactam degrading proteins such as the  $\beta$ -lactamase BlaS (Poset et al., 2006).

The core structure consists of 3 distinct layers; mycolic acids (MAs), arabinogalactan (AG) and the PG layer. The MAs are the defining feature of the mycobacterial cell envelope (Daffe and Drapper, 1997) and represent a unique feature to actinomycetes. MAs are  $\beta$ -hydroxyl fatty acids consisting of a long alkyl chain. (Asselineau et al., 1950). Mycobacterial species synthesize three different types of MAs; the  $\alpha$ -, methoxy-, and keto-mycolic forms, and the  $\alpha$ - form is the most abundant of the three (Qureshi et al., 1978; Watanabe et al., 2001). These groups of fatty acids are ester linked to the galactofuran unit of AG (Liu et al. 1996). They are hypothesized to contribute considerably to the hydrophobicity of the cell envelope, thereby determining the fluidity and permeability of the cell (Liu et al., 1996). The reduced general permeability of mycobacteria is the result of tightly packed MAs, which form a pseudo outer membrane that can be seen on electron micrographs (Sani et al., 2010) and contributes to increased drug tolerance, which eventually results in resistance, despite the presence of porins that facilitate diffusion of substances across the cell wall into the cytosol (Kartmann et al., 1999).

MAs are crucial in maintaining other cellular processes such as bacterial cording, biofilm formation and the associated drug tolerance of biofilm-derived bacteria (Ojah et al., 2008). In *M. tuberculosis*, MAs are modified by cyclopropanation and this type of modification is proposed to increase tolerance to oxidative damage (Yuan et al., 1995). The oxygenated forms of MAs are essential for virulence of *M. tuberculosis* in the murine model of TB infection (Dubnau et al., 200). The first line drug, isoniazid, targets biosynthesis of MAs (Takayama et al., 1972; Takayama et al., 1975, Winder et al., 1970), signifying the importance of this unique mycobacterial structure in growth, survival and disease progression in *M. tuberculosis*.

The second layer of the core structure, AG, consists of two distinct units, arabinan and galactose (Daffe et al., 1990). The galactose component forms a polymer of 30 galactose residues and the arabinan component forms branches by attaching at position 5 of the galactose residues (Daffe et al., 1990; McNeil et al., 1990). This structure is sandwiched between the MA and PG layer, and acts as a point of attachment for these two polymers. The PG is linked to AG by a linker unit ( $-\alpha\text{-l-Rhap-(133)-d-GlcNAc-P-}$ ) (McNeil et al., 1990; Mikušova et al., 2000; Bhamidi et al., 2011). The three distinct MAs are esterified to the AG polymer (Liu et al. 1996). Ethambutol, another first line drug for TB treatment, targets polymerization of the arabinan units (through inhibition of the arabinosyl transferases) and mutations in the *embB* operon results in resistance to ethambutol (Belanger et al., 1996; Alcaide et al., 1997; Telenti et al., 1997).

The third layer in the core structure of the mycobacterial cell envelope is the PG layer. This layer is unique to bacterial cells (Severin and Tomasz, 1996). In bacterial species, this structure fulfills a number of processes such as: (I) the maintenance of normal and uniform bacterial cell shape (Scheurwater and Burrows, 2011) (II) the prevention of cell lysis under



stress conditions such as increased internal cytoplasmic turgor/osmotic pressure (Royet et al., 2007; Prigozhin et al. 2013) (III) it presents as a key component in the synthesis of the septum for bacterial growth and division (Begg and Donachie, 1985; Typas et al., 2012) (IV) involvement in inter- and intra-species cell signalling and signal transduction (Dworkin, 2014; Wang et al., 2003) (V) it also plays role in immune modulation (Boneca et al., 2007; Davis et al., 2011).

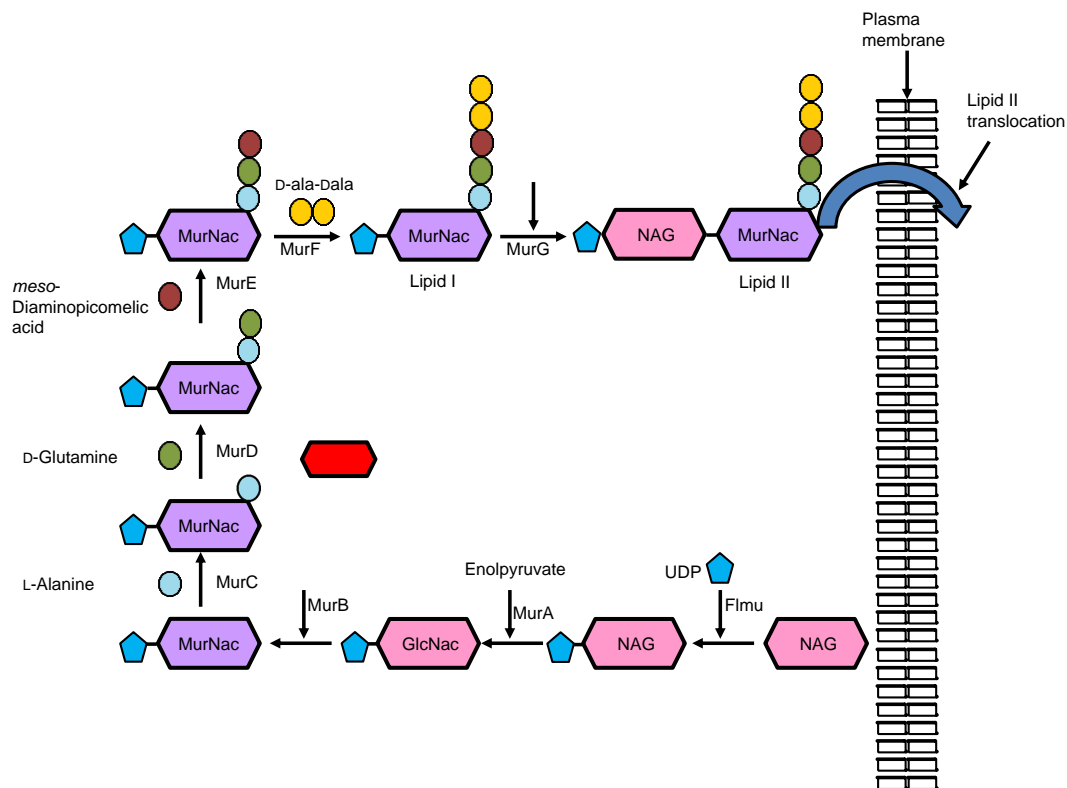
As mentioned above, biosynthesis of MAs and the AG components of the mycobacterial cell wall are targeted with frontline anti-TB drugs, isoniazid and ethambutol. This suggests that the PG layer, by virtue of its role in bacterial growth and physiology, is a promising candidate for the design of effective and target based anti-TB drugs. The next section will focus on the biosynthesis and remodelling of this polymer in bacteria.

## **1.4. Peptidoglycan biosynthesis**

### **1.4.1. Cytoplasmic steps in PG biosynthesis**

The biosynthesis of the PG layer is mediated by a variety of cytoplasmic and periplasmic enzymes. The cytoplasmic enzymes synthesize PG units, which are translocated across the membrane for incorporation into the existing PG polymer to facilitate cell growth and division, figure 1.1.3. The first committed to PG synthesis involves the conversion of NAG (*N*-acetylglucosamine) sugar residues into UDP-NAG (uridinediphosphate *N*-acetylglucosamine) and this is hypothesized to be catalyzed by FlmU in mycobacteria (Hett and Rubin, 2008). This is followed by the addition of the enolpyruvate at the third position of NAG from phosphoenolpyruvate to produce enolpyruvyl UDP-GlcNAc (Undecaprenyl *N*-acetylglucosamine), a reaction catalyzed by MurA (Du et al., 2000). The enolpyruvyl UDP-GlcNAc is reduced by MurB into UDP-MurNAc (uridinediphosphate *N*-

acetylmuramic acid) (Lovering et al., 2012; Hett and Rubin, 2008). Following this, amino acids that make up the stem peptide side chain are sequentially added onto UDP-MurNac. These amino acids are added in the following order: L-alanine, D-glutamine, *meso*-Diaminopimelic acid (*meso*-DAP) and the two terminal D-alanine residues by MurC, MurD, MurE and MurF, respectively to form Lipid I, which is converted into Lipid II upon addition of the UDP-NAG residues by MurG (Mahapatra et al., 2005; Hett and Rubin, 2008; Fan et al., 1994; Bouhss et al., 2008), figure 1.1.3. Lipid II is translocated across the membrane for further remodelling in the periplasm by PG remodelling enzymes.



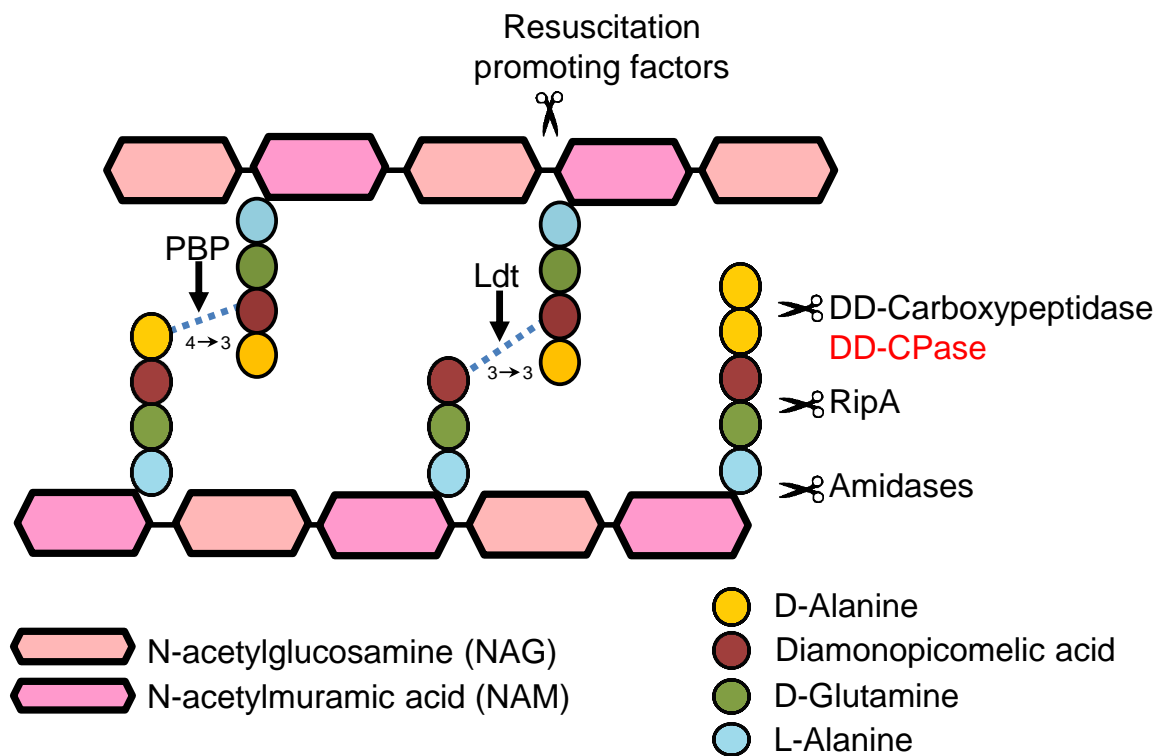
**Figure 1.1.3.** Diagrammatic representation of the cytoplasmic step of PG biosynthesis. The figure shows the conversion of NAG (*N*-acetyl glucosamine) residues to UDP-MurNac (uridinediphosphate *N*-acetylmuramic acid), followed by addition of the amino acids that form the stem peptide side chain which makes up the Lipid I. After this, UDP-NAG (uridinediphosphate *N*-acetyl glucosamine) is added to Lipid I by MurG to form Lipid II which is translocated across the plasma membrane for remodelling by PG remodelling enzymes in the periplasm. (Lovering et al., 2012).

## **1.5. Periplasmic step of PG biosynthesis**

### **1.5.1. Hydrolases**

#### **1.5.1.1. Lytic transglycosylases**

Lytic Transglycosylases hydrolyze the internal  $\beta$ ,1-4 glycosidic bonds between the NAM and NAG sugar residues (figure 1.1.4) with the same specificity as lysozymes, releasing 1,6-anhydromuramoyl product consisting of NAG sugar residues linked to the amino acid side chain (Scheurwater et al., 2008; Zahrl et al., 2005). The difference between lytic transglycosylases and lysozyme is that lytic transglycosylases exhibit exo-lytic activity, only cleaving the terminal NAG sugar residues (Höltje et al., 1975). Lytic transglycosylase facilitate the formation of large gaps within the PG layer that act as sites for the assembly of protein complexes (e.g. Bacterial secretion systems) and related structures such as flagella (Koraimann, 2003; Scheurwater et al., 2008). The formation of these gaps is also essential for expansion of the existing PG polymer, as these allows for addition of new PG subunits (Höltje, 1998). These enzymes also play an essential role, together with amidases, at the septum to allow for efficient and regulated cell division (Heidrich et al., 2002). In addition, they are involved in PG recycling, wherein the NAM containing PG units released after hydrolysis are in turn taken up by the cell for recycling (Park and Uehara, 2008; Lee et al., 2009). Lytic transglycosylases are involved in  $\beta$ -lactam antibiotic resistance as the 1,6-anhydro-muropeptide product that they produce is responsible for the induction of  $\beta$ lactamase (Tayler et al., 2010; Hanson and Sanders, 1999; Korsak et al., 2005; Jacoby, 2009). Lytic transglycosylases are also responsible for PG derived cytotoxicity in host cells and interact with secretion systems involved in the export of virulence factors (Cloud and Dillard, 2002; Höppner et al., 2005)



**Figure 1.1.4.** The site of action of PG remodelling enzymes in mycobacteria. The image shows that PG is remodelled by hydrolase and synthases. The activity of the PG remodelling enzymes is tightly regulated to ensure normal growth and survival of mycobacterial cells. (Machowski et al., 2015).

### 1.5.1.2. Resuscitation promoting factors

Resuscitation promoting factors (Rpf) are a group of secreted proteins with hydrolytic activity that targets the  $\beta$ ,1-4 glycosidic bonds within the PG backbone (Vollmer et al., 2008; Machowski et al., 2014), figure 1.1.4. These proteins contain a lysozyme like domain (Cohen-Gonsaud et al., 2004), suggesting that they function as Lytic transglycosylases. Consistent with this, a recent study demonstrated that Rpf-mediated cleavage of purified PG yielded 1,6-anhydro-muropeptides (Nikitushkin et al., 2015). *M. smegmatis* encodes four Rpf homologues (designated as MSMEG\_5700, MSMEG\_5439, MSMEG\_4643, MSMEG\_4640) and *M. tuberculosis* has five Rpf homologues (designated [*rpfA*] Rv0867c,

[*rpfB*] Rv1009, [*rpfC*] Rv1884c, [*rpfD*] Rv2389c, [*rpfE*] Rv2450c) (Machowski et al., 2014). Despite the high level of genetic multiplicity, a series of studies have implicated the catalytic activity of RpfB in a variety of processes. These include: (I) facilitating normal cell division through spontaneous association of RpfB (MSMEG\_5439) with RipA (an endopeptidase) at the division site (Hett et al., 2007) (II) reactivation of bacterial growth during infection, through the resuscitation of dormant bacteria (Kana et al., 2008; Kana and Mizrahi, 2008; Nikitushkin et al., 2015) and (III) a role in *M. tuberculosis* virulence during acute infection in the murine model of TB infection (Kana et al., 2008; Biketov et al., 2007).

An interesting aspect of the physiological role of RpfB, is their predicted association with reactivation of dormant bacteria that remain viable but non-culturable, a phenomena that was first demonstrated in *Micrococcus luteus* (Mukamolova et al., 1998). It is estimated that one-third of the world's population harbours latent TB infection (LTBI), a form of infection that was hypothesized to be associated with dormant *M. tuberculosis* and reactivation of disease in these individuals was ascribed to reactivation of growth in dormant organisms (Kana and Mizrahi, 2010). Whilst it is tempting to speculate that RpfB play a role in this process during TB disease in humans, no definitive evidence has been presented that associated LTBI with dormant mycobacteria. Moreover, the mechanisms used by RpfB to reactivate dormant bacteria is unknown but it is hypothesized that the PG-derived muropetides released by RpfB, act as signalling molecules, initiating a signal transduction cascade through association with the protein kinase B (PknB) (Kana and Mizrahi, 2010; Shah et al., 2008). A detailed understanding of the mechanisms of reactivation in dormant bacteria is paramount, considering the large proportion of the global population that carries LTBI, a collective that poses a serious public health risk.

### **1.5.1.3. Amidases**

Amidases are zinc containing metalloenzymes that cleave the bond between L-Alanine and MurNac, releasing the stem peptide from the PG backbone, figure 1.1.4. These enzymes are specifically involved in cleavage of the septum and separation of daughter cells during the final stages of cell division (Bernhardt and de Boer, 2003; Höltje and Heidrich, 2001; Heidrich et al., 2001; Heidrich et al., 2002). Amidases are not solely present in bacteria, but have also been found in eukaryotic and viral species and are further classified into two subgroups; amidase\_2 (PF01510) or amidase\_3 (PF01520) containing proteins (Vollmer et al., 2008).

### **1.5.1.4. N-Acetyl-β-D-glucosaminidases**

N-Acetyl-β-D-glucosaminidases are hydrolases which cleave the bonds between the NAG and NAM sugar residues. This group of proteins have received little attention in their role in bacterial physiology and PG remodelling.

## **1.5.2. PG synthases**

### **1.5.2.1. L,D Transpeptidases**

L,D transpeptidases (Ldt) catalyse peptidoglycan cross-linking between adjacent PG subunits. They are specifically involved in the formation of the 3 → 3 cross-links (figure 1.1.4) by hydrolysing the D-Ala-*meso*-DAP bond of the donor pentapeptide stem and transfers the peptide bond to the adjacent side chain *meso*-DAP of the tripeptide acceptor stem (Erdemli et al., 2012). In mycobacteria this specific type of cross-linking within the PG layer was first observed in *M. smegmatis* (Wietzerbin et al., 1974). Subsequent analysis revealed that approximately 80% of the peptide crosslinks are 3 → 3 cross-links, with remainder consisting of 4 → 3 crosslinks, which are synthesized by another distinct group of PBPs (discussed in section 1.5.2.2) (Lavollay et al., 2008; kumar et al., 2012). In *E. coli*, the 3 → 3 PG cross-links comprise between 3 and 10% of all cross-linked (Pisabarro et al., 1985) and in this

context, the high percentage of 3→3 cross-links in *M. tuberculosis* highlights an important role of this specific type of bond during TB pathogenesis. *M. tuberculosis* encode for five Ldt (designated Ldt<sub>Mt1</sub>-Ldt<sub>Mt5</sub>), all of which are susceptible to carbapenem treatment *in vitro* (Kumar et al., 2012; Dubée et al., 2012). Carbapenems are a group of β-lactam antibiotics wherein the carbon at position 4 of the thiazolidinic moiety is replaced by sulfone (Bonfiglio et al., 2002; Nicoletti et al., 2002). Deletion of Ldt<sub>Mt2</sub> results in morphological defects accompanied by reduced virulence and increased susceptibility to amoxicillin during disease progression (Gupta et al., 2010). Ldt<sub>Mt1</sub> and Ldt<sub>Mt2</sub> both play a role in virulence, growth and maintenance of bacterial cell surface morphology, cell size and shape (Schoonmaker et al., 2014). The high abundance of 3→3 peptide cross-links in mycobacteria and the sensitivity of the enzymes that synthesize them to carbapenem, provides a novel area for the development of new drugs that target PG cross-linking.

#### **1.5.2.2. Penicillin binding proteins (PBPs)**

PBPs are a group of structurally related proteins that have the ability to recognize and bind β-lactam molecules, such as penicillin (Ghosh et al., 2008; Mottl and Keck, 1991). They are classified into two distinct groups; Low Molecular Weight PBPs (LMW PBPs) or High Molecular Weight PBPs (HMW PBPs) depending on their electrophoretic mobility as examined by SDS PAGE (Ghuysen, 1991; Spratt, 1977; Spratt 1983).

The HMW PBPs share a common structural organisation with three distinct domains, the cytoplasmic tail, a membrane anchoring transmembrane domain and the two catalytic transglycosylase and transpeptidase domains (Lovering, et al., 2007; Macheboeuf et al., 2006; Goffin and Ghuysen, 2002). These proteins are generally targeted to the cell wall facing the outer surface of the cytoplasmic membrane where PG remodelling occurs (Lovering et al., 2007; Macheboeuf et al., 2006; Goffin and Ghuysen, 2002). The HMW

PBPs are further classified into two subgroups: Class A PBPs with both transglycosylase (catalysing cross-linking of the glycan sugar component of PG subunits) and transpeptidase activity (catalysing cross-linking between stem peptides of adjacent PG strands) (Ghosh et al., 2008; Romeis and Höltje, 1994; Lovering et al., 2007) and Class B PBPs with a single transpeptidase domain (Höltje, 1998; Machowski et al., 2014). The N-terminal domain is used in the classification of these two groups of proteins as either Class A or B HMW PBPs. The transglycosylase and transpeptidase domain of Class A HMW PBPs are positioned near the N- and C-terminus respectively (Ghosh et al. 2008; Romeis and Höltje, 1998; Machowski et al., 2014).

The Class B HMW PBP lack catalytic activity at the N-terminal domain, possessing only the transpeptidase domain at the C-terminal end (Höltje, 1998; Ghosh et al., 2008; Romeis and Höltje, 1998; Machowski et al., 2014). The N-terminal domain of Class B HMW PBPs is predicted to interact with various proteins that regulate bacterial cell morphogenesis (Höltje, 1998). In mycobacteria, the class A HMW PBPs includes PonA1, PonA2 and a second homologue of PonA2 annotated as PonA3 in *M. smegmatis* (Machowski et al., 2014; Patru and Pavelka, 2010; Billman-Jacobe et al., 1999). The mycobacterial Class B HMW PBPs include PBPA and PBPB and BPB-lipo (Machowski et al., 2014; Sauvage et al., 2008). The transpeptidase activity of PBPs is involved in the formation of 4→3 cross-links, figure 1.1.4. This involves binding of the donor pentapeptide side chain by the transpeptidase domain, followed by the formation of an acyl-enzyme intermediate complex facilitated by the active site serine that attacks the D-Ala-D-Ala bond. The intermediate complex is then hydrolysed, followed by the transfer of the peptide bond to the adjacent side chain *meso*-DAP of the tripeptide acceptor stem to form 4→3 cross-links (McDonough et al., 2002; lovering et al., 2012)



The second group of PBPs is the LMW PBPs, also referred to as Class C PBPs, which can be further categorized into 3-subgroups using *E. coli* as the representative species. These include the monofunctional DD-Carboxypeptidase (DD-CPases), the  $\beta$ -lactamases (Ghuysen, 1996; Massova and Mobashery, 1998; Navratna et al., 2010) and the PBP4, sub-family of bifunctional LMW PBPs with both DD-CPase and transpeptidase domains (Nelson and Young, 2001). The LMW PBPs share a common structural organisation consisting of a penicillin binding domain and a transmembrane segment for membrane anchoring at the C-terminus (Jacoby, 2009). This MSc is focused on class C PBPs, particularly the characterization of mycobacterial DD-CPases.

### **1.5.2.3. DD-Carboxypeptidases**

DD-CPases are acyl serine transferases that retain signature motifs such as the Ser-Xaa-Xaa-Lys, Ser-Xaa-Asn and Lys-Thr-Gly triad (Nicholas et al., 2003; Goffin and Ghuysen, 1998). This group of proteins is involved in the final periplasmic stage of PG biosynthesis. They regulate the level of PG cross-linking by hydrolyzing the terminal D-Alanine from the pentapeptide side chain of nascent PG subunits, producing a tetrapeptide stem that cannot act as a donor for PG crosslinking (Strominger, 1969; Lawrence and Strominger, 1970; Leyh-Bouille et al., 1972), figure 1.1.4. The LMW PBPs, as demonstrated in *E. coli* possess DD-CPases activity, but their biological significance has not been demonstrated in various species (Ghosh et al., 2008; Nelson and Young, 2000). Many organisms harbour a multiplicity of DD-CPases, which are predicted to be functionally redundant in *E. coli*, which codes for at least 12 PBPs, of which 4 possess DD-CPases activity (Massova and Mobashery, 1998; Holtje, 1998; Denome et al., 1999; Sauvage et al., 2008). Consistent with this notion, deletion of individual DD-CPases in *E. coli* did not result in growth defects. However, combinatorial deletion of the different LMW PBPs implicated PBP5 (encoded by *dacA*) to

be important in maintaining normal bacterial cell shape (Nelson and Young, 2001; Holtje, 1998). PBP5 in *E. coli* is further implicated in regulating bacterial cell elongation, due to the observation that deletion of PBP2 inhibits cylindrical PG synthesis during growth thus producing spherical cells, a phenotype reversed by ectopic expression of PBP5. PBP5 is also implicated in mediating cell division as demonstrated by the inability to separate daughter cells in a PBP5-AmiC double mutant (Priyadarshini et al., 2006)

*Bacillus subtilis*, a gram positive rod-shaped model organism encodes four DD-CPase homologues (PBP5 encoded by *dacA* and *dacB*, PBP4a and DacF, Popham et al., 1999; Atrih et al., 1999; Pedersen et al., 1998). In this organism, PG maturation is mediated by DacB (Popham et al., 1999; Atrih et al., 1999; Pedersen et al., 1998) and synthesis of the spore cortex PG in matured *B. subtilis* spores is mediated by DacA and DacF respectively (Pedersen et al., 1998; Popham et al., 1999).

The observed genetic multiplicity with DD-CPases in both *E. coli* and *B. subtilis*, and the lack of these proteins in the genome of other organisms such as *Caulobacter crescentus* and *Helicobacter pylori* (Koyasu et al., 1980; Krishnamurthy et al., 1999; Ghosh et al., 2008), suggests they are most likely individually non-essential with overlapping functions. This would explain their accessory roles in bacterial elongation and division, in *E. coli* and *B. subtilis*. In mycobacterial species, DD-CPases are relatively uncharacterized and this study will focus on shedding light on physiological function of mycobacterial DD-CPase homologues.

### **1.6.1. Mycobacterial DD-CPases**

As with other organisms, mycobacteria have multiple DD-CPases homologues. *M. smegmatis* has four DD-CPase homologues (designated MSMEG\_1661, MSMEG\_2432/3 and

MSMEG\_6113, Machowski et al., 2014). Currently, a single study has been conducted on *M. smegmatis* DD-CPase by Bansal et al., (2015), which focused on MSMEG\_2433 and demonstrated that MSMEG\_2433 actively binds fluorescent penicillin, a characteristic of PBPs, and that heterologous expression of MSMEG\_2433 rescues the cell morphology defects of the septuple *E. coli* mutant generated by Ghosh & Young, (2003), lacking a combination of various PBPs. Furthermore, heterologous expression of MSMEG\_2433 in the septuple mutant restored  $\beta$ -lactam antibiotic resistance. Purified MSMEG\_2433 displayed ability to hydrolyse artificial PG substrates and also deacylate  $\beta$ -lactam antibiotics. *M. tuberculosis* encodes three DD-CPase homologues (designated Rv2911, Rv3330 and Rv3627c). Bourai et al., (2012) revealed a role for Rv2911 in maintaining various cellular processes when ectopically expressed in *M. smegmatis* including colony morphology (see results and discussion). Furthermore, they demonstrated that deletion of Rv2911 from wild type *M. tuberculosis* affects bacterial growth in acidic media at low oxygen tensions, accompanied by increased survival in ThP-1 cells (Boura et al., 2012). These two studies implicate mycobacterial DD-CPases in regulating various cellular processes but do not provide insight on functional redundancy or possible roles in regulating cell wall synthesis.

Cell division and elongation are tightly regulated, and the effectors of both processes exert their effect through interaction with various partners (Singh et al., 2006; Kieser, and Rubin, 2014). As such, it is unclear whether the mycobacterial DD-CPase homologues act as single enzymes or exert their function through interaction with various partners, as observed for other PBPs. Additionally; the mycobacterial DD-CPase homologues remain uncharacterized. Considering this, the specific aims and objectives of this MSc are listed below.

### **1.7.1. Hypothesis**

It is hypothesized that Mycobacterial DD-CPases play important roles in cell elongation and division, possibly through interaction with various proteins. It is further speculated that there is some degree of overlap of function between the multiple DD-CPase homologues present in *M. tuberculosis*.

## **1.8. Aims and objectives of this study**

### **1.8.1. Study aims**

- I. To identify putative interacting partners for MSMEG\_2433 and MSMEG\_6113. These two proteins were chosen based on the observation in our laboratory that the former was expressed in high transcript abundance and the latter was essential for growth (C.S Ealand and B. Kana, unpublished)
- II. To interrogate the functionality (redundancy vs. specialist function) of the *M. tuberculosis* DD-CPases through ectopic expression in wild type *M. smegmatis* and *M. tuberculosis* H<sub>37</sub>RvS.

### **1.8.2. Study objectives**

- I. To construct two bait vectors carrying MSMEG\_2433 and MSMEG\_6113 fused to mycobacterial dihydrofolate reductase fragment 3 in pUAB400. These will serve as the bait vector.
- II. To design a genomic DNA library with overlapping fragments with a size range of 0.5-5.0 kbps, which will be fused to the mycobacterial dihydrofolate reductase fragment 1 and 2 in pUAB300. This will serve as the prey for assaying protein interaction.

- III. To assay protein interaction of the baits (MSMEG\_2433 and MSMEG\_6113) against the prey (genomic DNA library) using the mycobacterial Protein Fragment Complementation assay (mPFC).
- IV. To sequence and identify putative interacting partners of MSMEG\_2433 and MSMEG\_6113.
- V. To clone Rv2911, Rv3330 and Rv3627c into pSE100 for ectopic expression in wild type *M. smegmatis* and *M. tuberculosis*.
- VI. To assess the following in the heterologous *M. smegmatis* and *M. tuberculosis* strains:
  - Bacterial colony morphology
  - Bacterial sliding
  - Biofilm formation
  - Growth kinetics
  - Cell surface morphology by scanning and transmission electron microscopy
- VII. To create C-terminally tagged rseGFP derivatives of *M. tuberculosis* DD-CPases.
- VIII. To ectopically express the fusion proteins in wild type *M. smegmatis* and monitor cellular localization of these proteins in the heterologous strain.

## **2. Materials and methods**

### **2.1.1. Plasmids used and constructs generated in this study**

The plasmids and strains used in this are listed in table 2.1.1 and 2.2.2 respectively.

**Table 2.1.1.** Plasmid generated and/or used in this study.

| Plasmid         | Genotype  | Source/Reference     |
|-----------------|---|----------------------|
| pUAB300         | <i>E. coli</i> -Mycobacterium shuttle plasmid carrying the mDHFR fragment 1 and 2, together with the glycine linker; Hyg <sup>r</sup> | Singh et al., (2006) |
| pUAB400         | <i>E. coli</i> -Mycobacterium shuttle plasmid carrying mDHFR fragment 3; Kan <sup>r</sup>   | Singh et al., (2006) |
| pSE100          | <i>E. coli</i> -Mycobacterium shuttle plasmid carrying P <sub>sync</sub> tetO tetracycline regulated operator; Hyg <sup>r</sup>       | Erhrt et al., (2005) |
| pUAB3145        | Derivative of pUAB300 carrying the complete MSMEG_3145 open reading frame; Hyg <sup>r</sup>   | This study           |
| pUAB5439        | Derivative of pUAB400 carrying the complete MSMEG_5439 open reading frame; Kan <sup>r</sup>   | This study           |
| pUAB2433        | Derivative of pUAB400 carrying the complete MSMEG_2433 open reading frame; Kan <sup>r</sup>   | This study           |
| pUAB6113        | Derivative of pUAB400 carrying the complete MSMEG_6113 open reading frame; Kan <sup>r</sup>   | This study           |
| pSE2911         | Derivative of pSE100 carrying the Rv2911 gene; Hyg <sup>r</sup>   | This study           |
| pSE3330         | Derivative of pSE100 carrying the Rv3330 gene; Hyg <sup>r</sup>   | This study           |
| pSE3627c        | Derivative of pSE100 carrying the Rv3330 gene; Hyg <sup>r</sup>   | This study           |
| pSE2911-rseGFP  | Derivative of pSE100 carrying Rv2911 gene with a C-terminal rseGFP; Hyg <sup>r</sup>  | This study           |
| pSE3330-rseGFP  | Derivative of pSE100 carrying Rv3330 gene with a C-terminal rseGFP; Hyg <sup>r</sup>  | This study           |
| pSE3627c-rseGFP | Derivative of pSE100 carrying Rv3627c gene with a C-terminal rseGFP; Hyg <sup>r</sup>   | This study           |

Kan<sup>r</sup>, kanamycin resistance; Hyg<sup>r</sup>, hygromycin resistance.

**Table 2.1.2.** Strains used and/or generated in this study.

| Strain                               | Description  | Source/Reference     |
|--------------------------------------|--|----------------------|
| <i>Escherichia coli</i> DH5 $\alpha$ | <i>SupE44 <math>\Delta</math>lacU169 hsdR17 recA1 endA1 gyrA96 thi-1 relA1</i>   | Promega, Madison, WI |
| mc <sup>2</sup> 155                  | High frequency transformation mutant of <i>M. smegmatis</i> ATCC 607   | Snapper et al., 1990 |
| H <sub>37</sub> RvS                  | Laboratory H <sub>37</sub> Rv strain   | Ioerger et al., 2010 |
| mc <sup>2</sup> (pSE100)             | Derivative of mc <sup>2</sup> 155 expressing the pSE100 vector, Hyg <sup>r</sup>   | This study           |
| mc <sup>2</sup> (pSE2911)            | Derivative of mc <sup>2</sup> 155 ectopically expressing Rv2911 from pSE2911 vector, Hyg <sup>r</sup>  | This study           |
| mc <sup>2</sup> (pSE3330)            | Derivative of mc <sup>2</sup> 155 ectopically expressing Rv3330 from pSE3330 vector, Hyg <sup>r</sup>  | This study           |
| mc <sup>2</sup> (pSE3627c)           | Derivative of mc <sup>2</sup> 155 ectopically expressing Rv3627c from pSE3627c vector, Hyg <sup>r</sup>  | This study           |
| mc <sup>2</sup> (pSE2911-rseGFP),    | Derivative of mc <sup>2</sup> 155 ectopically expressing a C-terminal rseGFP-tagged derivative of Rv2911, expressed from the pSE2911-rseGFP vector; Hyg <sup>r</sup>   | This study           |
| mc <sup>2</sup> (pSE3330-rseGFP)     | Derivative of mc <sup>2</sup> 155 ectopically expressing a C-terminal rseGFP-tagged derivative of Rv3330, expressed from the pSE3330-rseGFP vector; Hyg <sup>r</sup>   | This study           |
| mc <sup>2</sup> (pSE3627c-rseGFP)    | Derivative of mc <sup>2</sup> 155 ectopically expressing a C-terminal rseGFP-tagged derivative of Rv3627c, expressed from the pSE3627c-rseGFP vector; Hyg <sup>r</sup> | This study           |
| H <sub>37</sub> RvS(pSE2911),        | Derivative of H <sub>37</sub> RvS ectopically expressing Rv2911 from the pSE2911 vector; Hyg <sup>r</sup>  | This study           |
| H <sub>37</sub> RvS(pSE3330),        | Derivative of H <sub>37</sub> RvS ectopically expressing Rv3330 from the pSE3330 vector; Hyg <sup>r</sup>  | This study           |
| H <sub>37</sub> RvS(pSE3627c)        | Derivative of H <sub>37</sub> RvS ectopically expressing Rv3627c from the pSE3627c vector; Hyg <sup>r</sup>  | This study           |

|  |  |            |
|--|--|------------|
| H <sub>37</sub> RvS(pSE100)              | Derivative of H <sub>37</sub> RvS expressing the pSE100 vector, Hyg <sup>r</sup>   | This study |
| mc <sup>2</sup> 155::pUAB400 (pUAB300)   | Derivative of mc <sup>2</sup> 155 carrying pUAB400 integrated at the <i>attP</i> site and pUAB300 an episomal plasmid, Hyg <sup>r</sup> Kan <sup>r</sup> | This study |
| mc <sup>2</sup> 155::pUAB2433 (pUAB300)  | Derivative of mc <sup>2</sup> 155 expressing pUAB2433 integrated at the <i>attP</i> site and episomal pUAB300, Hyg <sup>r</sup> Kan <sup>r</sup>         | This study |
| mc <sup>2</sup> 155::pUAB5439 (pUAB3145) | Derivative of mc <sup>2</sup> 155 expressing pUAB5439 integrated at the <i>attP</i> site and episomal pUAB3145; Hyg <sup>r</sup> Kan <sup>r</sup>        | This study |

Hyg<sup>r</sup>, hygromycin resistance; Kan<sup>r</sup>, kanamycin resistance.

## 2.2. Bacterial growth conditions

### 2.1 Growth conditions for *E. coli* DH5 $\alpha$ and derivatives.

*E. coli* DH5 $\alpha$  strains were streaked on Luria-Agar (LA) to obtain single colonies. A single colony was picked and inoculated into Luria Bertani (LB) or 2xTY at 37<sup>0</sup>C with shaking at 250 rpm. Derivatives of *E. coli* DH5 $\alpha$ , transformed with plasmids were cultured on LA, LB, or 2xTY supplemented with appropriate antibiotics. Recipes for all media used are in the Appendix (Appendix F). The antibiotic concentrations used in this study are as follows: Hygromycin (Hyg) 200  $\mu$ g/ml and Kanamycin (Kan) 50  $\mu$ g/ml. The volume of liquid media was adjusted depending on the type of experiment conducted with each strain (e.g. bulk vs. small scale DNA extraction).

#### 2.2.2. Growth conditions for *M. smegmatis* and *M. tuberculosis*.

The wild type mc<sup>2</sup>155 and derivative strains were cultured on Middlebrook 7H10 agar and in Middlebrook 7H9 broth, herein referred to as 7H10 and 7H9 respectively. 7H10 was supplemented with 0.2% glucose, 0.5% glycerol, 0.085% NaCl. 7H9 was supplemented with 0.2% glucose, 0.2% glycerol, 0.085% NaCl, 0.05% tween80. In the case of H<sub>37</sub>RvS and



derivative strains, 7H9 was supplemented with OADC (oleic acid albumin dextrose catalase) enrichment, 0.2% glycerol and 0.05% tween80 and Middlebrook 7H11 was supplemented with OADC enrichment and 0.2% glycerol. A single colony for each strain was picked from solid agar and propagated in 7H9 supplemented with the appropriate antibiotics. The mc<sup>2</sup>155 strain and derivatives were cultured at 37<sup>0</sup>C with shaking at 100 rpm. The H<sub>37</sub>RvS strain and derivatives were cultured at 37<sup>0</sup>C in disposable tissue culture flasks without agitation. Antibiotics were used at the following concentrations: Kan 25 µg/ml and Hyg 50 µg/ml.

### **2.3. Mycobacterial DNA extractions**

#### **2.3.1. Large scale DNA extraction for PCR.**

The Cetyltrimethylammonium bromide (CTAB) DNA extraction protocol was used for large scale DNA extraction from both *M. smegmatis* and *M. tuberculosis* strains. The mc<sup>2</sup>155 and derivative strains were cultured on solid media to obtain a lawn of cells and the H<sub>37</sub>RvS and derivative strains were cultured in liquid media. Cells were harvested by scraping the lawn of cells off the agar plates or by centrifugation (12 470 X g, 10 min) for mc<sup>2</sup>155 and H<sub>37</sub>RvS respectively. The cells were resuspended in 500 µl TE buffer (10 mM tris-HCl pH 8.0, 10 mM EDTA dissolved in dH<sub>2</sub>O). Following resuspension, 50 µl lysozyme (10 mg/ml) was added to the cells, followed by incubation for 1 hour at 37<sup>0</sup>C. Thereafter, 70 µl SDS (10%) and 6 µl proteinase K (10 mg/ml) was added to the mixture, with further incubation at 65<sup>0</sup>C for 1-2 hours. Following this, 100 µl NaCl (5M) and 80 µl CTAB/NaCl buffer (4.1 % NaCl, 10% N-cetyl-N,N, N-trimethyl ammonium bromide dissolved in dH<sub>2</sub>O) were added, followed by mixing and incubation at 65<sup>0</sup>C for 10 min. An equal volume of chloroform:isoamyl alcohol (24:1 ratio) was added and mixed by inverting tubes, followed by centrifugation (12 470 X g, 5 min). The top aqueous layer was aspirated and transferred to a fresh tube, followed by the addition of 0.6 volume isopropanol. The tubes were placed

on ice or at  $-20^{\circ}\text{C}$  for 20 min, followed by centrifugation (12 470 X g, 30 min) to pellet the DNA. The DNA pellet was washed with 70% EtOH and dried using an Eppendorf Concentrator 530. The lyophilized DNA was resuspended in an appropriate amount of nuclease free water and quantified using the NanoDrop ND-1000 Spectrophotometer (NanoDrop technologies). To assess the quality of the DNA, an aliquot was electrophoresed on 1% agarose gel with molecular weight markers, Appendix (A.1.1.1). Extracted DNA was stored at  $-20^{\circ}\text{C}$  for subsequent use.

### **2.3.2. Small scale DNA extraction for genotypic confirmation**

A colony boil protocol was used for small scale DNA extraction. A single colony (either *M. smegmatis* or *M. tuberculosis*) was resuspended in 10  $\mu\text{l}$   $\text{sdH}_2\text{O}$ , followed by addition of 100  $\mu\text{l}$  chloroform, mixing and incubation at  $65^{\circ}\text{C}$  for 15 min. Thereafter, the mixture was centrifuged (12 470 X g, 15 min) and the top aqueous layer extracted without breaking the interface. The top aqueous layer was transferred to a fresh tube and 5  $\mu\text{l}$  was used for PCR.

## **2.4. *E. coli* plasmid DNA extraction**

### **2.4.1. Bulk DNA extraction**

The Nucleobond DNA extraction kit (Macherey Nagel) was used for bulk plasmid DNA extraction from *E. coli* DH5 $\alpha$  derivatives. Briefly, the strains were cultured overnight in 50 ml LB or 2xTY supplemented with the appropriate antibiotics and DNA was extracted following instructions specified by the manufacturer.

### **2.4.2. Small scale plasmid DNA extraction**

The alkaline lysis miniprep protocol was used for small scale DNA extractions. Strains were cultured overnight in 2 ml LB or 2xTY supplemented with the appropriate antibiotics as

described in section 2.2.1. Cells were harvested by centrifugation (12 470 X g, 5 min) followed by resuspension in 100 µl ice-cold solution I (50mM glucose, 25mM Tris-HCl (pH 8), 10 mM EDTA dissolved in dH<sub>2</sub>O). Following this, 200 µl freshly prepared solution II (1% SDS, 0.2 M NaOH dissolved in sdH<sub>2</sub>O) was added. The suspension was mixed gently by inverting the tubes and incubated on ice for 5 min. Thereafter, 150 µl ice-cold solution III (3 M potassium acetate, 11.5% acetic acid dissolved in sdH<sub>2</sub>O) was added to the sample, followed by mixing and incubation on ice for 10 min. The sample was centrifuged (12 470 X g, 30 min) and the supernatant transferred to a fresh tube. DNA was precipitated as described in section 2.3.1 by adding 0.6 volume isopropanol followed by centrifugation (12 470 X g, 30 min). The pellet was washed with 70% EtOH and dried as described in section 2.3.1. The dried pellet was resuspended in an appropriate volume of nuclease free water and stored at -20<sup>0</sup>C for subsequent use.

## **2.5. DNA clean-up and removal of contaminating proteins**

### **2.5.1. Sodium acetate precipitation**

Extracted chromosomal or plasmid DNA was sodium-acetate precipitated to remove contaminating proteins, salts and other impurities. Briefly, 1/10 volume sodium acetate (3M, pH 5.2) was added to the DNA followed by the addition of 3X volume of ice-cold 100% EtOH. The sample was mixed and centrifuged (12 470 X g, 30 min). For genomic DNA precipitation, 1/10 volume sodium acetate (3 M, pH 5.2) and 3X volume of ice-cold 100% EtOH was added to DNA, followed by incubation at -20<sup>0</sup>C for 20 min. After centrifugation (12 470 X g, 30 min), the supernatant was discarded and the DNA pellet dried as described in section 2.3.1. The dried pellet was resuspended in an appropriate amount of nuclease free water and stored at -20<sup>0</sup>C for subsequent use.

## **2.6. Restriction profiling**

Restriction profiling of vector backbones, PCR products and recombinant plasmids generated in this study was carried out using restriction enzymes from Fermentas (Fermentas), NEB (New England Biolabs) and Roche (Roche Applied Sciences) following instructions specified by the manufacturer unless stated otherwise. Briefly, restriction digests were carried out in a 10 µl reaction volume with approximately 1 µg DNA, 1 µl buffer, 1 U enzyme and made up to 10 µl with nuclease free water. The digests were incubated at 37<sup>0</sup>C for 1 hour unless stated otherwise by the manufacturer, before running on a 1% agarose and imaging using the Bio-Rad Gel Doc (Bio-Rad). BSA (Bovine serum albumin) was added to the restriction digests if necessary, to a final concentration of 10 µg/ml.

## **2.7. Agarose gel electrophoresis**

Extracted DNA, PCR reactions and restriction digests were run on a 1 % agarose gel made with 1X TAE buffer (1 mM EDTA and 40 mM Tris-acetate). Electrophoresis was conducted in 1X TAE buffer at 90 V for 45-50 min using a Bio-Rad electrophoresis tank (Bio-Rad). Following every run, the gels were imaged with the Bio-Rad Gel Doc (Bio-Rad). The DNA molecular weight markers used in this study are shown in the Appendix (A1.1.1).

## **2.8. DNA cloning**

### **2.8.1. Vector backbone confirmation.**

All the vector backbones were confirmed by restriction profiling with at least 4 enzymes before cloning. Briefly, *E. coli* DH5 $\alpha$  derivatives carrying the vector backbone were cultured overnight as described in section 2.2.1 for large/small scale DNA extraction. The extracted plasmid DNA was verified by restriction profiling as described in section 2.6.

### **2.8.2. PCR reactions.**

Gradient PCR (with annealing temperature range of 70<sup>0</sup>C-80<sup>0</sup>C) was carried out to determine the optimal annealing temperature for each primer set. The primer sets used in this study are listed in the Appendix (Appendix B). Following the determination of the optimal annealing temperature for each primer pair, PCR was carried out with the appropriate controls. The controls included the positive control (*narB*), no template control, no forward primer control, no reverse primer control and the test PCR with the template, forward and reverse primers. For cloning, PCR was carried out with the high fidelity Phusion DNA Polymerase (NEB). PCR reactions were set up to a final volume of 25 µl containing 5X HF buffer, DMSO, 50 ng template DNA, 0.2 mM dNTPs, 1 µM forward and reverse primer, 2 U high fidelity Phusion DNA polymerase enzyme. The cycling conditions were as follows; one cycle of initial denaturation (95 or 98<sup>0</sup>C, 4 min), 30-35 cycles of denaturation (95 or 98<sup>0</sup>C, 30 sec), annealing (70 to 80<sup>0</sup>C, 45 sec), elongation (72<sup>0</sup>C, 30 sec), one cycle of final elongation (72<sup>0</sup>C, 7 min). Following PCR amplification, the amplicon was run on a 1% gel and visualized as described in section 2.7. PCR reactions which yielded the expected DNA size were used for cloning.

### **2.8.3. PCR and plasmid DNA digestion**

Cloning strategies that employed either a single or two inserts were used in this study. The PCR product(s) and vector backbone were digested with selected restriction enzymes listed in the Appendix (Appendix B). The restriction digests were set up as described in section 2.6. Restriction enzymes that shared the same restriction buffer were used concurrently in one reaction. For restriction digests with two restriction enzymes that do not share the same reaction conditions, sequential digests were set up, which involved digestion with one enzyme, DNA clean up as per section 2.5.1, followed by digestion with the second enzyme.

Following digestion, DNA was run on a 1% low melting agarose gel for DNA purification with agarase as described below.

#### **2.8.4. Agarase DNA recovery and clean-up for cloning.**

The agarase protocol was used for recovery of DNA from agarose gels for cloning purposes. Following restriction digests, the vector backbone and PCR product(s) were run on a low melting agarose gel. After electrophoresis, the bands were visualized under UV (ultraviolet) light and excised from the gel. Following this, the excised gel slice with the desired band was weighed and incubated at 70<sup>0</sup>C until the agarose was completely melted. The melted gel was equilibrated at 42<sup>0</sup>C for 5 min and 1 U of Agarase was added per 100 mg of liquefied gel, followed by incubation at 42<sup>0</sup>C for 30 min. Thereafter, sodium acetate was added to the reaction mixture to a final concentration of 2.5 M. The mixture was placed on ice, followed by centrifugation (12 470 X g, 10 min). The supernatant was then transferred to a fresh tube and 2.5 volumes of isopropanol was added, mixed and incubated for 1 hour at room temperature. After incubation, the DNA was harvested by centrifugation (12 470 X g, 15 min) and dried as described in section 2.3.1. The pellet was resuspended in an appropriate volume of nuclease free water and stored at -20<sup>0</sup>C for subsequent use.

#### **2.8.5. Dephosphorylation of plasmid DNA**

Plasmid DNA was dephosphorylated to remove phosphate groups at the 5' end of linearized plasmid DNA with Antarctic Phosphatase (NEB) as per manufacturer's instructions. This was done to prevent self-ligation of the vector backbone during cloning.

### **2.8.6. DNA ligations**

Ligations of PCR product(s) into plasmid DNA was carried out using the Fast-link DNA ligation Kit (Epicentre) following instructions specified by the manufacturer. For increased ligation efficiency, different ligation ratios (molar ratio of vector: insert) were used. The standard ligation ratios used were 1:1, 1:3, 1:5 (vector: insert) for 2-way cloning and 1:1, 1:3:3 and 1:5:5:5 (vector: insert) for 3-way cloning. These ratios were adjusted depending on the concentration of insert recovered from gel purification. The concentration of the vector DNA was kept at 50 ng for all ligations. The following formula was used to calculate the amount of insert required for a 1:1 ratio with 50 ng of vector backbone.

$$\text{ng of insert} = \frac{\text{ng of plasmid DNA (50 ng)} \times \text{size of insert (bps)}}{\text{Size of plasmid (bps)}}$$

The final volume for each ligation was kept between 15-20  $\mu\text{l}$ . The ligations were incubated at room temperature for 1-2 hours. Following incubation, the ligase was heat inactivated (70<sup>0</sup>C, 15 min).

## **2.9. Preparation and transformation of chemically competent *E. coli* DH5 $\alpha$**

### **2.9.1. Preparation of chemically competent *E. coli* DH5 $\alpha$**

Chemically competent *E. coli* DH5 $\alpha$  was prepared as follows: A single colony was inoculated into 5 ml LB or 2xTY and cultured overnight at 37<sup>0</sup>C with shaking at 250 rpm. Fresh 100 ml LB or 2xTY was inoculated with 1 ml of pre-culture and incubated under the same conditions. The optical density (OD<sub>600</sub>) was monitored until log phase (OD<sub>600</sub>= 0.5-0.9) and cells were harvested by centrifugation (3 901 X g, 3 min, 4<sup>0</sup>C). The cells were gently resuspended in 20 ml ice-cold CaCl<sub>2</sub> (0.1 M) and placed on ice for 20 min. This procedure was repeated and following two washes, the cells were resuspended in 4 ml ice-cold CaCl<sub>2</sub>

(0.1 M). For increased transformation efficiency, competent cells were placed on ice for 2 hours before transformation.

### **2.9.2. Transformation of chemically competent *E. coli* DH5 $\alpha$**

DNA ligations prepared as described in section 2.8.6 were mixed with 100  $\mu$ l of freshly prepared competent cells and placed on ice for 15 minutes. Cells were transformed by heat shock (42<sup>0</sup>C, 90 sec) and immediately placed on ice for 5 min, followed by the addition of 750  $\mu$ l LB or 2xTY. The transformation reactions were transferred to a 37<sup>0</sup>C incubator with shaking at 250 rpm for 1 hour, to allow for expression of the antibiotic selectable marker. Thereafter, cells were harvested by centrifugation (12 470 X g, 1 min), resuspended in 100  $\mu$ l LB or 2xTY and plated on LA supplemented with the appropriate antibiotic. The plates were incubated overnight at 37<sup>0</sup>C and single colonies picked for screening of putative positive clones as described below, section 2.10.1.

## **2.10. Screening and confirmation of positive clones**

### **2.10.1. Screening for putative clones**

Putative positive clones were screened as follows: Plasmid DNA from selected transformed colonies was extracted using the small scale alkaline lysis miniprep as described in section 2.4.2. Clones were screened with a single enzyme first and a single positive clone, which yielded the expected band size following screening with a single enzyme, was further verified by restriction profiling as described in section 2.6 with at least four restriction enzymes. Following restriction profiling, the insert was sequenced to ensure that no mutations were introduced during the PCR and cloning steps.



### **2.10.2. Sequencing**

The constructs were sent to the Stellenbosch University DNA sequencing facility for sequencing. Following DNA extractions with the Nucleobond Plasmid extraction kit, the constructs were sequenced using the BigDye Terminator V3.1 sequencing kit (Applied Biosystems) following instructions supplied by the manufacturer.

### **2.11. Transformation of *M. smegmatis***

#### **2.11.1. Preparation of electro-competent mc<sup>2</sup>155**

Cells were grown to log phase ( $OD_{600} = 0.5-0.9$ ) and harvested by centrifugation (2 360 X g, 10 min, 4<sup>0</sup>C). The cells were then washed three times by gentle resuspension in 10 ml ice-cold 10% glycerol with harvesting by centrifugation (2 360 X g, 10 min, 4<sup>0</sup>C) between washes. Following these washes, the cells were resuspended in 4 ml ice-cold 10% glycerol and used immediately.

#### **2.11.2. Transformation of electro-competent mc<sup>2</sup>155**

For transformation, 400 µl of electro-competent cells were transferred to a 0.2 cm electroporation cuvette (Bio-Rad) together with plasmid DNA obtained following confirmation of the construct by restriction digest and sequencing. The Gene PulserX cell (Bio-Rad) was used for electroporation and the conditions were as follows: 2.5 KV, 25 µF and 1000 Ω with a path length of 0.2 cm. Following pulsing, cells were immediately rescued with 800 µl LB or 2xTY for 3 hours or overnight at 37<sup>0</sup>C with shaking at 100 rpm. The rescued cells were plated on 7H10 agar supplemented with the appropriate antibiotic. The plates were incubated for at least 3-4 days to allow colonies to emerge.

## **2.12. Transformation of H<sub>37</sub>RvS**

### **12.2.1. Preparation of electro-competent H<sub>37</sub>RvS**

Electro-competent *M. tuberculosis* H<sub>37</sub>RvS cells were prepared as follows. Cultures were grown to log phase as described in section 2.2.2 and the cells harvested by centrifugation (2360 X g, 10 min). The pelleted cells were washed three times with room temperature 10% glycerol. Following the last wash, cells were resuspended in 4 ml of room temperature 10% glycerol and immediately used for electroporation with The Gene PulserX cell (Bio-Rad).

### **2.12.2. Transformation of electro-competent H<sub>37</sub>RvS**

Plasmid DNA was damaged by UV irradiation (100 mJ cm<sup>-2</sup>) using the Uvitech CL503G, which allows for increased transformation efficiencies. Following UV irradiation, 400 µl of electro-competent H<sub>37</sub>RvS, together with damaged DNA, was transferred to 0.2 cm electroporation cuvettes (Bio-Rad) and pulsed as described in section 2.11.2. Thereafter, cells were immediately rescued with 800 µl 7H9, followed by incubation overnight at 37<sup>0</sup>C without shaking. The transformations were plated on 7H11 supplemented with the appropriate antibiotic and incubated at 37<sup>0</sup>C for at least 5 weeks for colonies to emerge.

## **2.13. Genotypic confirmation of recombinant strains**

The mc<sup>2</sup>155 and H<sub>37</sub>RvS and their derivatives were confirmed as follows. After transformation, a single strain was picked and DNA extracted by colony boil described in section 2.3.2. PCR with Fast-start Taq DNA polymerase (Roche) was used for genotypic confirmation with gene specific primers listed in the Appendix (Appendix B). PCR reactions were set up in a final volume of 25 µl, with the following contents: 1X recommended PCR buffer supplied by the manufacturer, 1X GC rich solution, dNTPs to a

final concentration of 0.2 mM, reverse and forward primers each at a final concentration of 1  $\mu$ M, DNA template (5  $\mu$ l) and 0.2 U Fast-start Taq polymerase. The PCR cycling conditions were the same as described in section 2.8.2.

## **2.14. Genomic DNA library construction**

### **2.14.1. Genomic DNA extraction and restriction digest**

The mc<sup>2</sup>155 genomic DNA was extracted using the CTAB method as described in section 2.3.1 and run on a 1% gel along with molecular weight marker to determine quality. DNA was quantified with the NanoDrop ND-1000 Spectrophotometer (NanoDrop Technologies). The library was designed by setting up a 2-fold dilution series of a *TaqI* restriction enzyme digest as follows: A series of reaction mixtures with equal amounts of DNA (8  $\mu$ g), buffer and nuclease free water were set up to final volume of 40  $\mu$ l. *TaqI* 10 U from NEB was added to the first tube, mixed and a 2-fold serial dilution of the enzyme was carried out. Dilution, was carried out to ensure partial digestion of genomic DNA with overlapping fragments. The reaction digests were incubated at 37<sup>0</sup>C for 1.5 hours. Thereafter, the enzyme was heat inactivated by incubation at 80<sup>0</sup>C for 20 min. Following this, 5  $\mu$ l of the partial digests was run on a 1% gel as described in section 2.7 to identify a digest with a 0.5-5.0 kbps fragment size range. The selected digest was sodium-acetate precipitated as described in section 2.5.1 and run on a 1% gel to ensure that the fragment size range was still between 0.5-5.0 kbps and no shearing had occurred during the clean-up. The prey vector (pUAB300) was linearized with *ClaI* and ligations were carried out using the following vector: insert ratio; 1:1, 1:3 and 1:5 and 2:1. A cut and ligate control was also carried out.

### **2.14.2. Preparation of electro-competent *E. coli* DH5 $\alpha$**

A pre-culture of *E. coli* DH5 $\alpha$  was set up by inoculating a single colony into 5 ml 2xTY and incubated overnight at 37<sup>0</sup>C with shaking at 250 rpm. The pre-culture was used to inoculate 100 ml fresh 2xTY, which was allowed to grow to log-phase. Cells were placed on ice for 10 min followed by centrifugation (3 901 X g, 3 min, 4<sup>0</sup>C). The cells were gently washed three times in ice-cold 10% glycerol, with harvesting by centrifugation (308.1 X g, 10 min, 4<sup>0</sup>C) between washes. After the final wash step, cells were resuspended in 4 ml ice-cold 10% glycerol and immediately used for transformation.

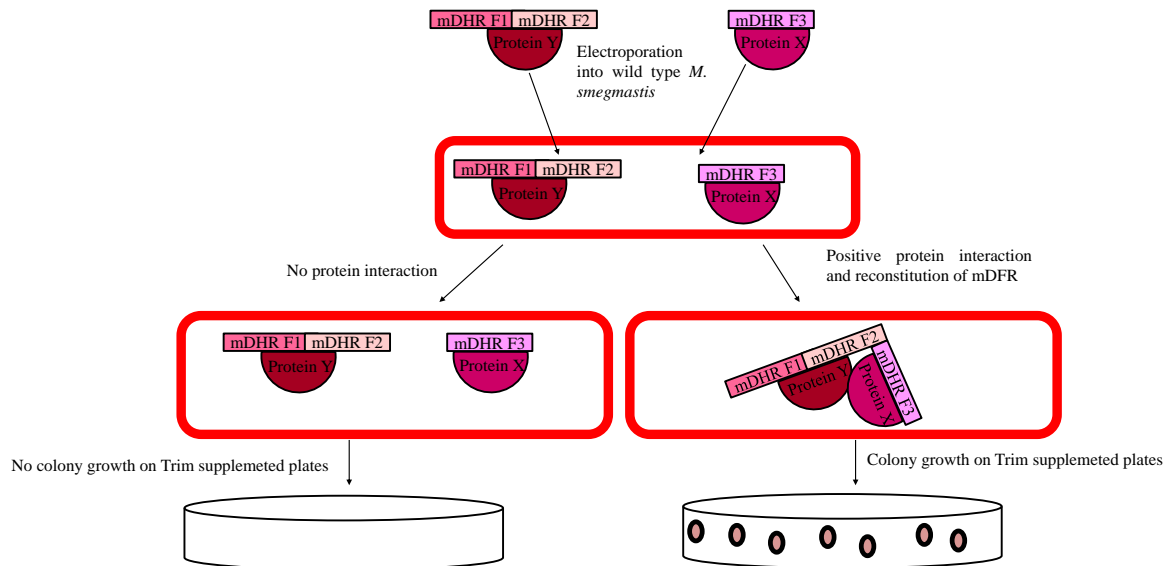
### **2.14.3. Transformation of electro-competent *E. coli* DH5 $\alpha$**

The ligation reactions and 40  $\mu$ l of electro-competent cells were transferred to a 0.1 cm electroporation cuvette (Bio-Rad) and pulsed with the Gene PulserX cell (Bio-Rad) with the following conditions: 1.8 KV, 600  $\Omega$ , 10  $\mu$ F and a path length of 0.1 cm. Following electroporation, cells were immediately recovered in 800  $\mu$ l 2xTY for 1 hour at 37<sup>0</sup>C and plated on LA supplemented with the appropriate antibiotic. The plates were incubated at 37<sup>0</sup>C overnight. The next day, 10 colonies were randomly picked and digested for confirmation for the presence of insert (data not shown). Following this, cells were scraped off and plasmid DNA extracted using the nucleobond Plasmid Purification kit, as described in section 2.4.1. This constituted the plasmid DNA for genomic library.

## **2.15. Identification of the respective MSMEG\_2433 and MSMEG\_6113 putative interacting partners**

### **2.15.1 Assaying for putative interacting partners for MSMEG\_2433 and MSMEG\_6113.**

The interaction between the proteins encoded on pUAB(3145) (RipA) and pUAB::5439 (RpfB) served as the positive control for this study. To confirm this, mc<sup>2</sup>155 was transformed with these two vectors and plated on TRIM (Figure 3.1.9). For negative controls the empty pUAB300 vector was used in conjunction with the pUAB6113 and pUAB2433 to create two strains, mc<sup>2</sup>::2433 (pUAB300) and mc<sup>2</sup>::6113 (pUAB300) – that displayed no growth on plates as expected (Table 3.1.9). The positive control were chosen based on experimental data that demonstrated an interaction between MSMEG\_5439 (RpfB) and MSMEG\_3154 (RipA), which results in synergistic degradation of septal peptidoglycan (Hett et al., 2007, Hett et al., 2008) (II) The mc<sup>2</sup>::pUAB5439 was generated by co-electroporation of pUAB5439 and pUAB3145 recombinant plasmids into mc<sup>2</sup>155. The mc<sup>2</sup>::pUAB2433 and mc<sup>2</sup>pUAB6113 strains were generated by transformation of mc<sup>2</sup>155 with pUAB2433 and pUAB6113 respectively. To assay for putative interacting partners, the library DNA was introduced into mc<sup>2</sup>::pUAB2433 and mc<sup>2</sup>::pUAB6113 strains by electroporation as described in section 2.11.2. After electroporation, cells were rescued as with 800 µl 2xTY and plated on 7H10 with Hyg/Kan. Following 3-4 days of incubation, cells were scraped off, resuspended in 1 ml 7H9 and plated on 7H10 Hyg/Kan supplemented with 7.5 µg/ml Trim (trimethoprim). Plates were incubated for 7 days and growth was scored as positive interaction. A graphical representation of the principles of the mPFC assay is shown below, figure 2.1.1



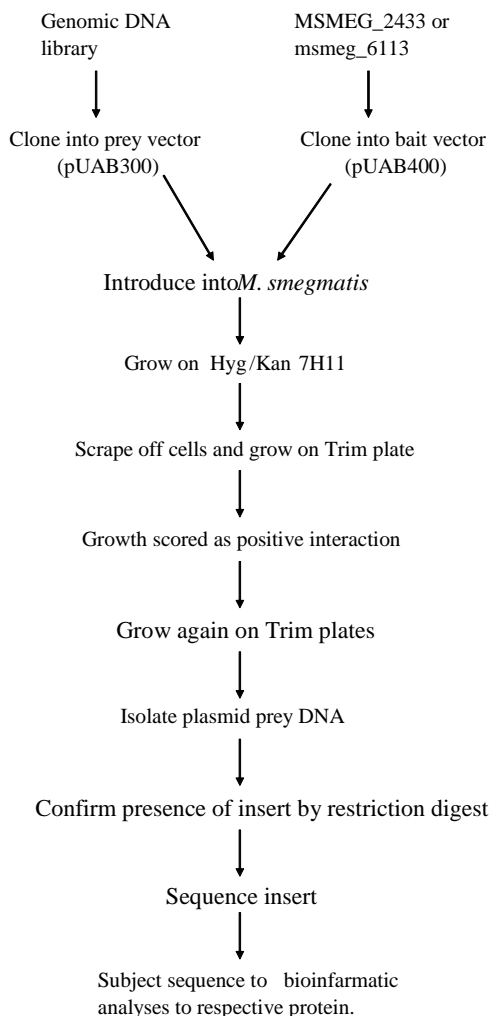
**Figure 2.1.1.** The concept of the mPFC assay. The system requires the introduction of two proteins (X and Y) tagged with the mycobacterial dihydrofolate reductase fragments (1 and 2) and fragment 3 respectively. In the case of no protein interaction between the two proteins there will be failure to reconstitute the mycobacterial dihydrofolate reductase (mDFR) and no growth will be observed on trimethoprim (Trim) supplemented plates. Positive interaction between protein X and Y results in the reconstitution of the mDHFR, which hydrolyses Trim allowing for colonies to emerge on Trim supplemented plates (Singh et al., 2006)

### 2.15.2. Sequencing and identification of the respective interacting partners

A colony boil was carried out as described in section 2.3.2 to extract the prey vector carrying the respective putative interacting partners. The extracted plasmid DNA was introduced into chemically competent *E. coli* DH5 $\alpha$  prepared as described in section 2.9.1. The transformants were cultured in 2xTY supplemented with the appropriate antibiotic followed by plasmid DNA extraction using the small scale alkaline lysis miniprep protocol as described in section 2.2.2 for sequencing. The sequences were analysed using Blastx (), Blastn (<http://blast.ncbi.nlm.nih.gov/Blast.cgi>)

and Smart blast (<http://blast.st-va.ncbi.nlm.nih.gov/blast/smartblast/>) from NCBI. The BioCyc (<http://biocyc.org/MSME246196/blast.html>) data base was also used to analyse protein domains (see discussion).

### Strategy of the mPFC assay used in this study



**Figure 2.1.2.** The strategy employed using the mPFC assay to identify putative interacting partners for MSMEG\_2433 and MSMEG\_6113. The genomic DNA library cloned in the prey vector was introduced into wild type *M. smegmatis* together with MSMEG\_2433 or MSMEG\_6113 cloned into the bait vector. Colonies on Hyg/Kan plates were scraped and sub-cultured on Trim supplemented solid agar and growth was scored as positive interaction, followed by isolation of prey vector plasmid DNA and confirmation of insert by sequencing.

The resulting sequence was subjected to various bioinformatics analysis to identify the putative interacting partners.

## **2.16. Phenotypic characterization of recombinant strains**

### **2.16.1. Assessment of mycobacterial colony morphology**

The heterologous *M. smegmatis* strains ectopically expressing *M. tuberculosis* DD-CPase homologues and the control strains were grown to log phase ( $OD_{600} = 0.5-0.9$ ) and 100  $\mu$ l spotted on 7H10 agar supplemented with the appropriate antibiotic. The recombinant *M. tuberculosis* H<sub>37</sub>RvS derivatives ectopically expressing the *M. tuberculosis* DD-CPase homologues were grown similarly to log phase and plated on 7H11 supplemented with the appropriate antibiotics. The colonies were imaged using a standard digital camera and bacterial cording was assessed using the Zeiss STEMI-2000c dissecting microscope.

### **2.16.2. Assessment of mycobacterial biofilm formation**

The air-media interface protocol as published by Ojha et al., (2008) was used for assessment of biofilm formation for the *M. smegmatis* and *M. tuberculosis* derivatives that ectopically express the *M. tuberculosis* DD-CPase homologues. Cells were grown to stationary phase ( $OD_{600} = 2.0$ ) and cultures that exceeded an  $OD_{600} = 2.0$  were adjusted by dilution. The cells were washed two times in Sauton's minimal media (refer to Appendix G), pH 7.3. Following the washes, serial dilutions for each strain ( $10^0-10^5$ ) were carried out and 100  $\mu$ l of each dilution, inoculated into 10 ml Sauton's media in a 6-well microtitre plate. The CFU/ml was scored for each dilution to ensure that the amount of inoculum for each strain at each dilution is uniform as variations in inoculum could result in aberrant biofilm formation. The plates were sealed with biohazard tape to prevent evaporation and incubated at 37<sup>0</sup>C before viewing with the Zeiss STEMI-2000c dissecting microscope.



### **2.16.3. Assessment of bacterial sliding motility**

Sliding motility of *M. smegmatis* derivatives was assayed on semi-solid media as previously described by Martinez et al., (2001). Single colonies of each strain were placed on the surface of 7H9 solidified with 0.3% agar or agarose (refer to Appendix G). The plates were sealed with parafilm and incubated for two weeks at 37<sup>0</sup>C for assessment of bacterial sliding. As an alternative, the strains were grown to log-phase (OD<sub>600</sub> = 0.5-0.9) and 10 µl of the log-phase cultures were stab-inoculated into 7H9 solidified with 0.3% agar. The stab-inoculated plates were sealed as described above and incubated at 37<sup>0</sup>C for 3 days. Following the incubation period, the plates were imaged with the Bio-Rad Gel Doc.

### **2.16.4. Assessment of mycobacterial growth**

Growth was determined by monitoring the OD<sub>600</sub> and plating for CFU/ml. Growth of the *M. smegmatis* strains was monitored in 7H9 and plating for CFU/ml on 7H10 supplemented with the appropriate antibiotic. Growth of the *M. tuberculosis* strains was assayed in 7H9 and 7H11 supplemented with the appropriate antibiotic. For *M. smegmatis*, a pre-culture was set up by inoculating 1 ml of freezer stock in 10 ml 7H9. The pre-culture was grown overnight at 37<sup>0</sup>C with shaking at 100 rpm to start a growth curve with a starting OD<sub>600</sub> = 0.01. Growth rates were assayed by monitoring the OD<sub>600</sub> and plating for CFU/ml at 3-hour intervals. For *M. tuberculosis* H<sub>37</sub>RvS derivatives, a pre-culture was set up by inoculating 1 ml freezer stock in 10 ml 7H9 supplemented with the appropriate antibiotics. The pre-culture for each strain was grown for 3 days before inoculation into 50 ml fresh media to a starting OD<sub>600</sub> = 0.05. Growth of the *M. tuberculosis* H<sub>37</sub>RvS strains was assayed daily by monitoring the OD<sub>600</sub> and plating for CFU/ml.

### **2.16.5. Scanning electron microscopy preparation and imaging**

To assess cell surface morphology by scanning electron microscopy (SEM), a growth curve for *M. smegmatis* and *M. tuberculosis* was started as described above. Cells were harvested by centrifugation (3 901 X g, 10 min) at lag, log and stationary phases of growth for SEM. The *M. tuberculosis* cultures were killed by resuspension in 100 µl formaldehyde (4%), followed by incubation at 37<sup>0</sup>C for 1 hour. The cells were washed twice in 0.1 M PBS (Phosphate buffered saline) with centrifugation steps in between washes (3 901 X g, 10 min) and the supernatant discarded after the final wash step. Cells were then fixed overnight at 4<sup>0</sup>C in a fixative solution of 2.5% glutaraldehyde in 0.1 M PBS, pH7.4. Following this, cells were washed three times in PBS with centrifugation steps in between (12 470 X g, 10 min) and stained with 100 µl osmium (2%) for 1 hour. After staining, cells were washed three times in PBS as previously described and samples dehydrated by washing with increasing EtOH concentrations (30%, 50%, 70% and 100%) for 2 min. The dehydration step was repeated once more with 100% EtOH and the samples were stored in 100% EtOH at room temperature for imaging. Samples were then spotted on a filter and coated twice with carbon for imaging with the FEI Nova NanoSEM 230 scanning electron microscope

### **2.16.6. Transmission electron microscopy preparation and imaging**

Growth curves were started as described in section 2.16.4 and cells were harvested at lag, log, and stationary phases of growth for transmission electron microscopy (TEM). The *M. tuberculosis* strains were killed and washed in PBS as described above. Cells were then fixed in 500 µl TEM fixative solution (0.1M HEPES, 2.5% glutaraldehyde, 2% formaldehyde and 0.05% ruthenium red) at room temperature for 1 hour. After chemical fixation, the samples were washed three times with PBS as described above and stained with 100 µl osmium (2%) for 1 hour. The samples were dehydrated with

increasing concentrations of EtOH (30%, 50% and 100%). The samples were then washed twice in propylene oxide and then transferred to a propylene oxide:resin (1:1 ratio) solution for 1 hour. Cells were harvested by centrifugation (12 470 X g, 10 min) and stored overnight at room temperature in 100% resin (5.62 g araldite, 7.75 epon 812 and 15 g DDSA). Following overnight incubation, cells were pelleted and transferred to fresh resin containing DMP30 accelerator (1:40). The samples were incubated at room temperature for one hour followed by incubation at 60<sup>0</sup>C for 48 hours. The solidified samples were sectioned with the Relchert Ultracut Ultramicrotome (Leica-Reichert) and imaged with Tecnai F20 Transmission Electron Microscope.

### **2.17. Fluorescence microscopy**

The *M. smegmatis* derivatives carrying the rseGFP fusion proteins were cultured to log phase (OD<sub>600</sub> = 0.5-0.9) in 7H9 supplemented with the appropriate antibiotic. Following this, cells were harvested by centrifugation (12 470 X g, 1 min) and washed twice in PBS. Thereafter, 3 µl was spotted and spread evenly on cover slips before heat fixation at 60<sup>0</sup>C on a heating block for 30 sec. Cells were mounted on slides with fluoromount and allowed to dry before viewing with the Zeiss 100x, 1.46 numerical aperture objective mounted to an Axio Observer Z1 base. The images were processed using the Zen lite blue edition (2012) version 1.1.2.0. Any brightness/contrast manipulations were applied to the entire image and not specific sections.

### **2.18. Statistical analyses**

The GraphPad Prism 6 was used for statistical analysis of the standard error and P-values (Student's t-test at 95% confidence level) for all assays that required statistical analysis. The P-values illustrate the statistical difference and abbreviated as follows; P<0.01; data is not

statistically significant,  $P < 0.001$ ; data is moderately significant,  $P < 0.0001$ ; data is strongly significant)

### **3. Results**

#### **3.1. Protein interaction**

One of the aims of this MSc was to identify putative interacting partners for two *M. smegmatis* DD-CPases, MSMEG\_2433 and MSMEG\_6113, using the mPFC assay. The rationale for choosing these two particular DD-CPases was based on the observation from unpublished work (C.S Ealand and B. Kana) in our laboratory demonstrating that MSMEG\_6113 is essential for growth and that MSMEG\_2433 is expressed at comparatively higher transcript abundance when compared to other DD-CPase-encoding genes in *M. smegmatis*. The approach in this regard first involved the construction of vectors that would serve as positive controls to confirm the accuracy of the read-out. Following this, MSMEG\_6113 and MSMEG\_2433 were cloned into bait vectors, followed by construction of a representative genomic DNA library of *M. smegmatis* to screen for putative interacting partners.

##### **3.1.1. Confirming the efficacy of the mPFC assay by assessing protein-interaction of the two peptidoglycan hydrolases, RipA and RpfB**

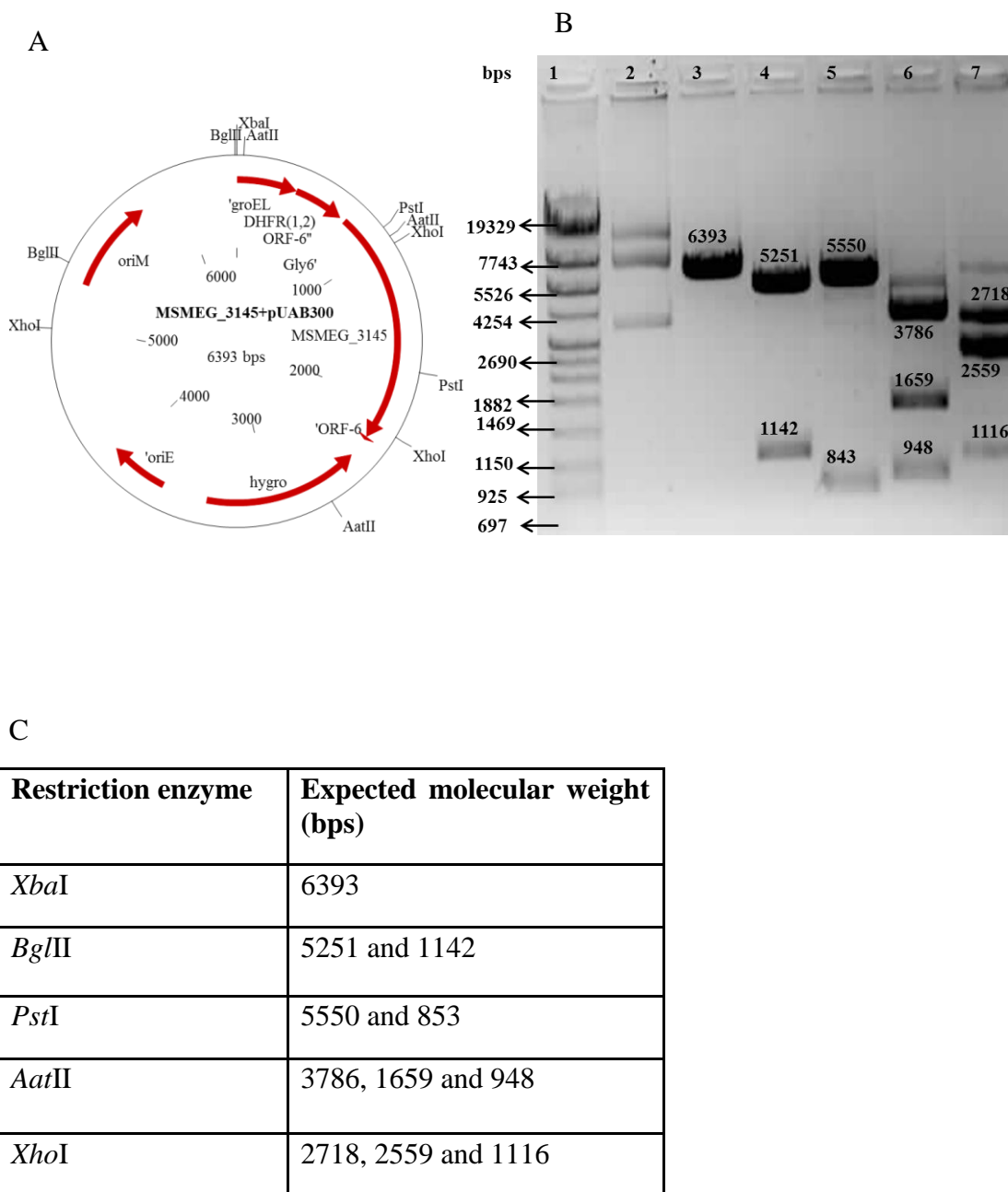
The mPFC assay uses two vectors; these include an integrating (pUAB400) and episomal (pUAB300) plasmid. *E. coli* DH5 $\alpha$  cells carrying the respective vectors were streaked on LA supplemented with the appropriate antibiotic and a single colony was picked, cultured overnight as detailed in section 2.2.1 for large scale plasmid extraction using the Macherey-Nagel Nucleobond Plasmid Extraction Kit, following instructions specified by the manufacturer. The vectors were verified by restriction profiling with at least four different

restriction enzymes. The restriction maps that were obtained are given in the Appendix (A.1.1.5 and A.1.1.6)

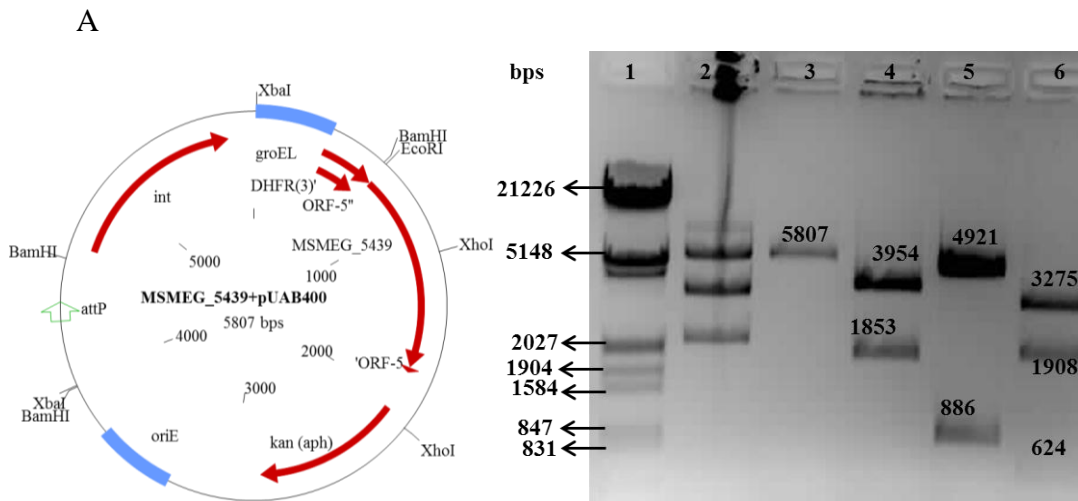
The screening procedure required positive controls to confirm functionality of the system. For this, we selected the resuscitation promoting factor B (RpfB- a lytic transglycosylase) and the Rpf interacting protein A (RipA- an endopeptidase) for the following reasons: (I) A series of studies have demonstrated an interaction RpfB and RipA, which results in synergistic degradation of septal peptidoglycan (Hett et al., 2007, Hett et al., 2008) (II) Both these proteins co-localize to the septum during growth (Hett et al., 2007) (III) These are periplasmic proteins and better reflect the cellular location expected for DD-CPases than cytoplasmic enzymes (Hett et al., 2008) (IV) Synergistic degradation of cell wall material by these two enzymes is expected to release products that allow for reactivation of dormant bacteria (Kana et al., 2008; Nikitushkin et al., 2015), further substantiating the physiological relevance of their interaction in *M. smegmatis*.

RipA and RpfB are encoded by MSMEG\_3154 and MSMEG\_5439 respectively. These genes were PCR amplified with the primer set listed in the Appendix (Appendix B). Directional cloning with *Bam*HI+*Hind*III for RipA and *Eco*RI+*Hind*III for RpfB into pUAB300 and pUAB400 respectively was carried out as detailed in section 2.8.6. Chemically competent CaCl<sub>2</sub> *E. coli* DH5α were transformed with the ligations and propagated in LB as detailed in section 2.2.1. The recombinant plasmid DNA from transformed colonies was isolated using the small scale alkaline lysis miniprep DNA extraction protocol as detailed in section 2.4.2 and putative positive clones were identified by screening with a single enzyme. A single putative clone was taken forward and further verified by restriction profiling with at least four enzymes and sequencing. The restriction

profiles for *ripA* (MSMEG\_3145) and *rpfB* (MSMEG\_5439) cloned into pUAB300 and pUAB400 respectively are given figure 3.1.2 and figure 3.1.3 respectively.



**Figure 3.1.2.** Restriction profiling of MSMEG\_3145 cloned into pUAB300. (A) Vector map of MSMEG\_3145 cloned in pUAB300. (B) Restriction profile of MSMEG\_3145 cloned into pUAB300. Lane 1= Marker IV, Lane 2= Uncut pUAB300, Lane 3= *Xba*I, Lane 4= *Bg*II, Lane 5= *Pst*I, Lane 6= *Aat*II, Lane 7= *Xho*I. (C) Table showing the expected banding patterns for MSMEG\_3145 cloned into pUAB300 with the restriction enzymes listed.

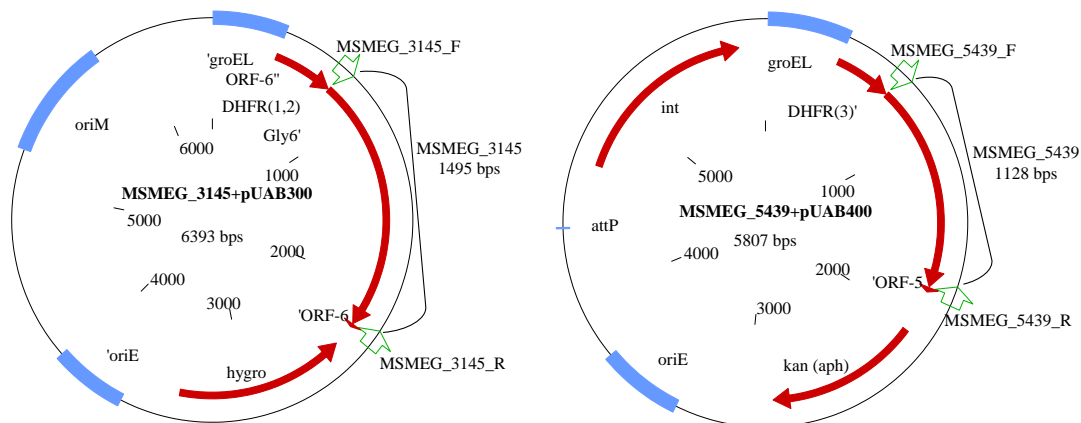


**Figure 3.1.3.** Restriction profiling MSMEG\_5439 cloned into pUAB400. (A) Vector map of RpfB cloned into pUAB400. (B) Restriction profile of MSMEG\_5439 cloned into pUAB400. Lane 1= Marker IV, Lane 2= Uncut pUAB400, Lane 3= *EcoRI*, Lane 4= *XbaI*, Lane 5= *XhoI*, Lane 6= *BamHI*. (C) Table showing the expected banding patterns for MSMEG\_5439 cloned into pUAB400 with the restriction enzymes listed.

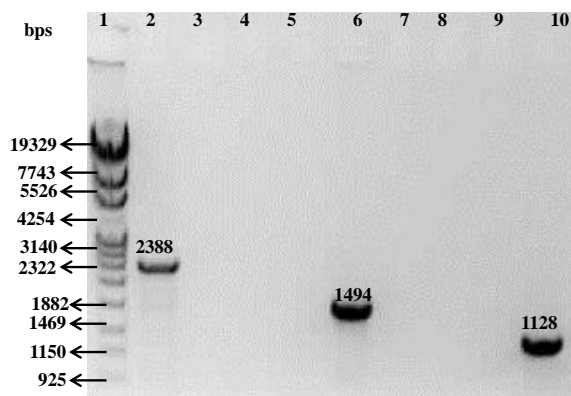
Co-electroporation of  $mc^2155$  with the above constructs was carried out as detailed in section 2.11.2 to generate the  $mc^2::pUAB5439$  (pUAB3145) strain carrying both tagged derivatives of RpfB and RipA. This strain was propagated on solid 7H10 media supplemented with Hyg and Kan. To confirm that the selected clone carried the desired gene, a colony boil was carried out as detailed in section 2.3.2 for PCR confirmation of the inserts using gene specific primers listed in the Appendix (Appendix B). Figure 3.1.4 shows the

primer binding sites of the PCR confirmation primers for MSMEG\_3145 and MSMEG\_5439 cloned into pUAB300 and pUAB400 respectively, and PCR confirmation of MSMEG\_3145 and MSMEG\_5439 respectively.

A.



B.



**Figure 3.1.4.** PCR confirmation of strains carrying control vectors. (A) The primer binding sites for PCR confirmation are indicated by the green marker arrows. Primer pairs (MSMEG\_3145\_F+MSMEG\_3145\_R) and (MSMEG\_5439\_F+MSMEG\_5439\_R) were used for PCR confirmation of MSMEG\_3145 and MSMEG\_543 respectively. (B) PCR confirmation of MSMEG\_3145 and MSMEG\_5439 cloned into pUAB300 and pUAB400. MSMEG\_3145 and MSMEG\_5439 were PCR amplified with an annealing temperature of 70<sup>0</sup>C and 72<sup>0</sup>C respectively. Lane 1= Marker IV, Lane 2= *narB* (positive control), Lane 3= No template control, Lane 4= No forward primer control, Lane 5= No reverse primer control, Lane 6= MSMEG\_3145, Lane 7= No template control, Lane 8= No forward primer control, Lane 9= No reverse primer control, Lane 10= MSMEG\_5439.



To assay for protein interaction, the mc<sup>2</sup>::pUAB5439 (pUAB3145) strain was cultured on 7H10 Hyg/Kan media supplemented with Trim to a final concentration of 30 µg/ml. It was decided to monitor colony growth on a daily basis since the time at which colonies emerge is determined by multiple factors including the strength of interaction between two proteins, with colonies representing weaker interactions emerging later compared to colonies from stronger interactions (Singh et al., 2006). The culture plates were incubated for 3 days at 37<sup>0</sup>C, which is generally the time it takes for *M. smegmatis* colonies to emerge. No growth was observed for the mc<sup>2</sup>::pUAB5439 (pUAB3145) strain after the 3 day incubation period (data not shown).

To address this, growth of the mc<sup>2</sup>::pUAB5439 (pUAB3145) strain was monitored for 7 days. No colony growth was observed following the 7-day incubation period (data not shown). Following these unsuccessful attempts, it was hypothesized that the mc<sup>2</sup>::pUAB5439 (pUAB3145) strain required additional growth enhancers not contained in Middlebrook 7H10 agar. The strain was cultured on Middlebrook 7H11 agar, a modified form of 7H10 Middlebrook agar, enriched with casein hydrolysate that supports the growth of *M. tuberculosis* (Cohn et al., 1968). No growth was observed for the mc<sup>2</sup>::pUAB5439 (pUAB3145) strain on 7H11 Middlebrook agar with the same Trim concentration used previously (data not shown). This suggested that a different factor, other than growth supplements contained in the media was inhibiting growth of the mc<sup>2</sup>::pUAB5439 (pUAB3145) strain.

Given that changing the growth media had no effect, we next hypothesized that the concentration of Trim was toxic, preventing growth of the mc<sup>2</sup>::pUAB5439 (pUAB3145) strain. To test this, the concentration of Trim was gradually decreased by 5 µg/ml intervals from 30 to 10 µg/ml, and when no growth was observed (data not shown), it was further

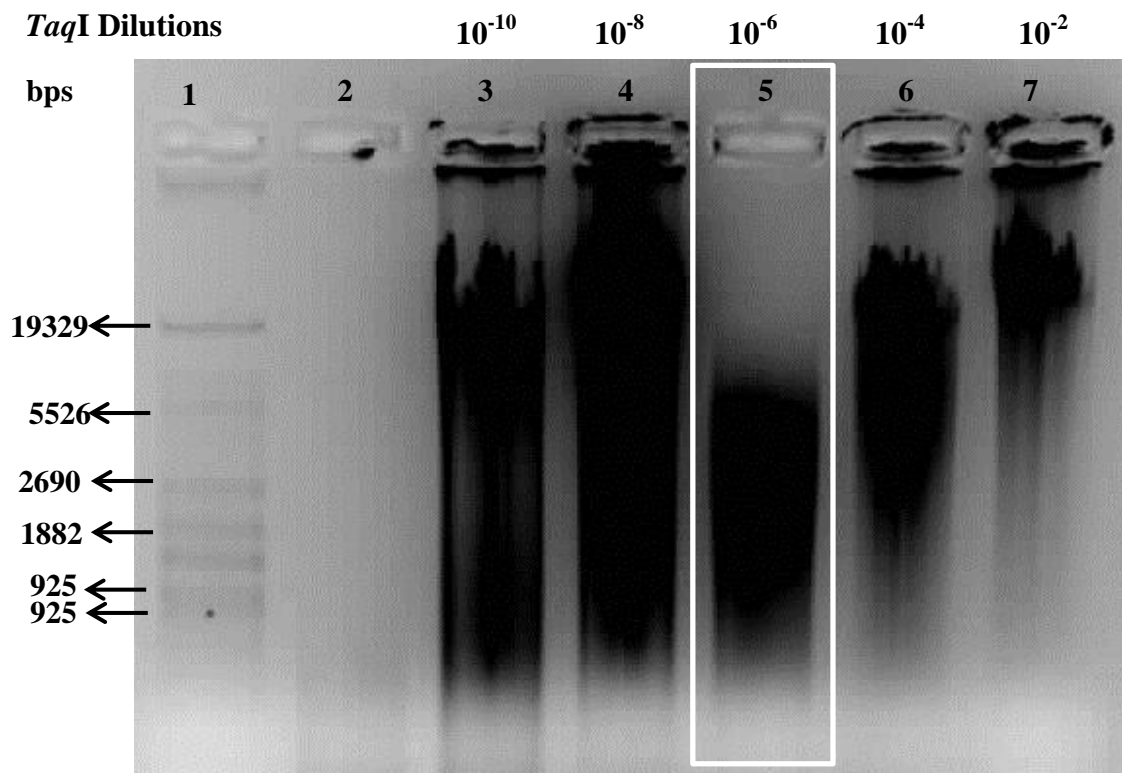
decreased to 7.5 µg/ml, which allowed for growth of the  $mc^2::pUAB5439$  (pUAB3145) strain after 7 days of incubation. The results for the  $mc^2::pUAB5439$  (pUAB3145) cultured on 7.5 µg/ml are reported in figure 3.1.9 and table and table 3.1.1.

### **3.1.2. Construction and generation of wild type $mc^2155$ genomic DNA library.**

Genomic DNA library construction for studying protein interaction requires highly concentrated DNA of good quality. To obtain this,  $mc^2155$  was cultured on 7H10 solid media and incubated as previously described to obtain a lawn of cells. The lawn was scraped off and genomic DNA extracted following the large scale genomic DNA extraction protocol as detailed in section 2.3.1. The genome of mycobacterial species, including  $mc^2155$ , has a high G+C content. Based on this, it was decided to use a restriction enzyme with an A+T recognition site, which will cut within the genome less frequently. Higher concentrations of restriction endonuclease digest genomic DNA to completion. Hence, setting up a dilution series with reducing amount of enzyme results in partial digestion of genomic DNA with overlapping fragments of a specific range (in this study, a range of 0.5-5 kbps was considered enough for full coverage). The enzyme of choice was *TaqI* (recognition site: T<sup>^</sup>CGA). A restriction digest of the genomic DNA was carried out by serial dilutions of the restriction enzyme as described in section 2.14.1 and the dilution series was incubated at 37<sup>0</sup>C for 1.5 hours. The digests were visualized on a 1% agarose gel to observe which dilution of the restriction enzyme resulted in partial fragments, with high a concentration of fragments in the range between 0.5 and 5.0 kbps, figure 3.1.5.

A 6-fold dilution of *TaqI* (lane 5 in figure 3.1.5) yielded fragments in the range of 0.5-7.0 kbps. It was decided not carry out a gel extraction procedure since low yields of DNA are obtained after gel extraction. Therefore, the digest was sodium-acetate precipitated as

described in section 2.5.1. The genomic DNA was resuspended in nuclease free water and this constituted the genomic DNA library.



**Figure 3.1.5.** Genomic DNA library of *mc*<sup>2155</sup> designed with *TaqI*. Lane 1: Marker IV, Lane 7-3: Partial digests of *mc*<sup>2155</sup> genomic DNA. Lane 5 shows a partial digest of genomic DNA after a 6-fold dilution of the original restriction digest, with a range of between 7.0 and approximately 0.5 Kbps, which was within the expected range.

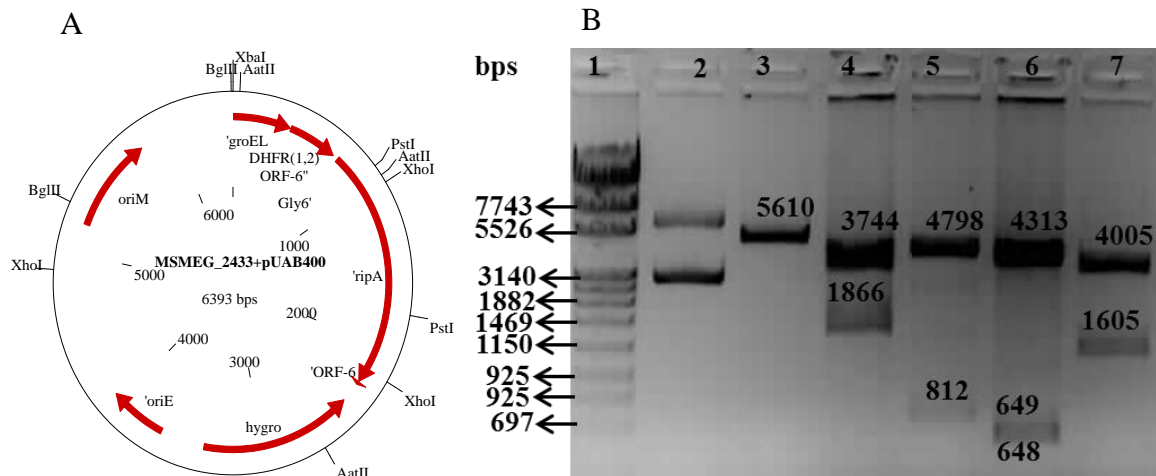
The prey vector, pUAB300, was linearized with *ClaI* for ligation with digested genomic DNA as described in section 2.14.1. Electro-competent *E. coli* DH5 $\alpha$  cells were prepared with ice-cold 10% glycerol as described in section 2.14.2 and transformed with the library ligations using conditions described in section 2.14.3. The transformations were grown on LA Hyg plates. A transformation efficiency > 10<sup>5</sup> is generally considered sufficient for coverage (Miller, 1972; Hannah, 1985) and the efficiency from these reactions was estimated to be ca. 10<sup>5</sup> CFU/ml, representing sufficient coverage of the library. All colonies were

scraped off, followed by a large-scale plasmid DNA extraction, carried out as described in 2.4.1.

### **3.1.3. Cloning and PCR confirmation of MSMEG\_2433 and MSMEG\_6113 into the bait vector, pUAB400**

MSMEG\_2433 and MSMEG\_6113 were PCR amplified and cloned as detailed in section 2.8.6. *E. coli* DH5 $\alpha$  was transformed with the ligations and a single putative clone of each was verified by restriction profiling and sequencing. The restriction profiles for MSMEG\_2433 and MSMEG\_6113 cloned into pUAB400 are shown in figure 3.1.6 and 3.1.7 respectively.

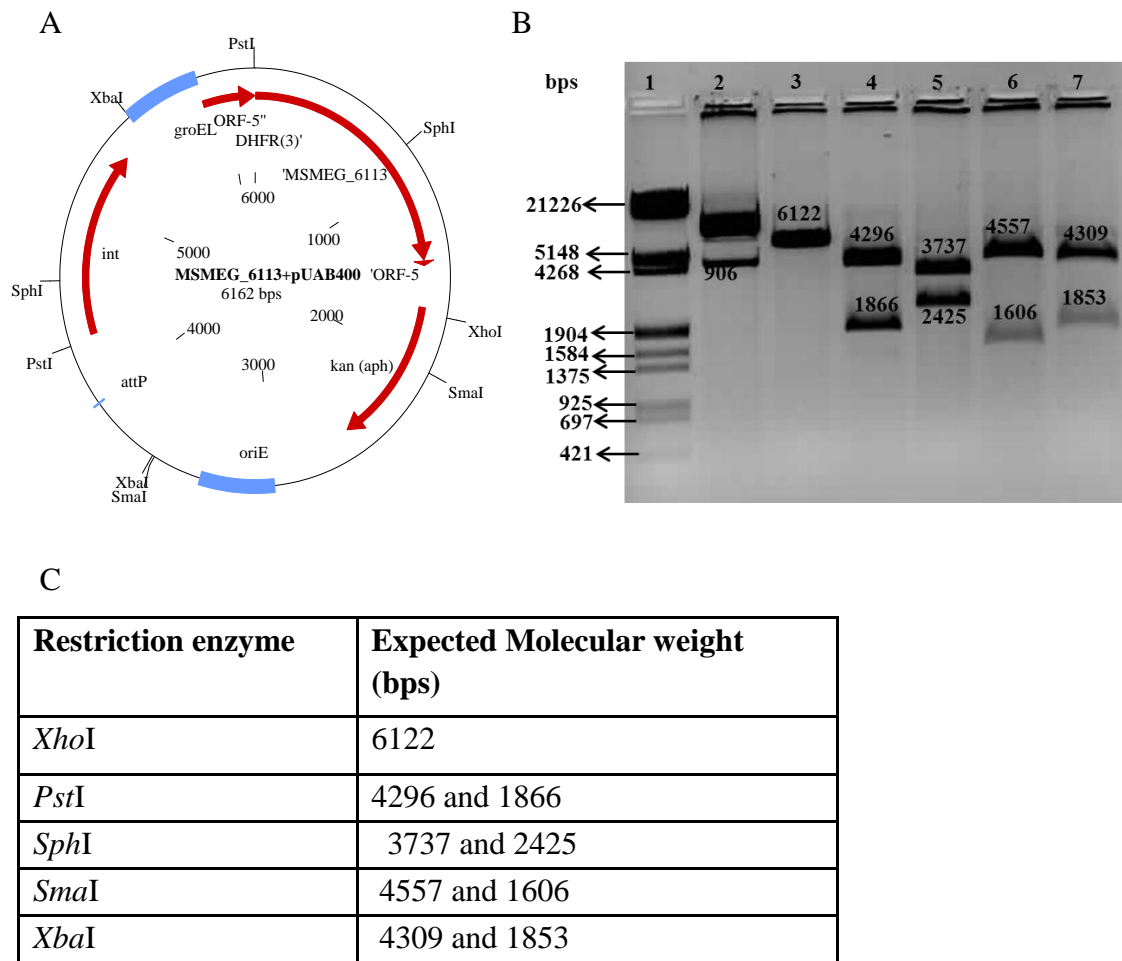
The mc<sup>2</sup>::pUAB2433 and mc<sup>2</sup>::pUAB6113 strains were generated by electroporation of these constructs into mc<sup>2</sup>155 section, 2.11.2. A colony boil and PCR confirmation was carried out using gene specific primers listed in the Appendix (Appendix B). Figure 3.1.8 show the primer binding sites of the PCR confirmation primers for MSMEG\_2433 and MSMEG\_6113 cloned into pUAB400 respectively, and PCR confirmation of the mc<sup>2</sup>::pUAB2433 and mc<sup>2</sup>::pUAB6113, following transformation of mc<sup>2</sup>155 with the above constructs.



**C**

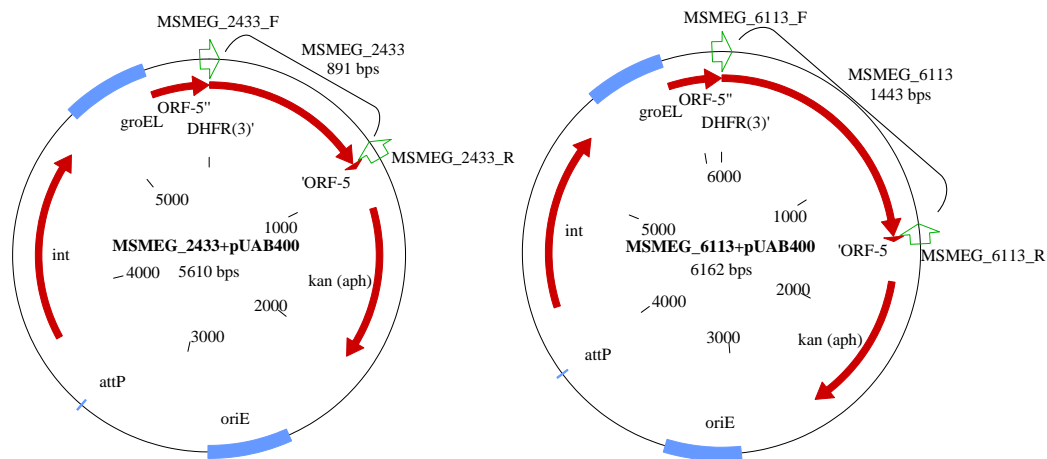
| Restriction enzyme | Expected Molecular weight (bps) |
|--------------------|---------------------------------|
| <i>HindIII</i>     | 5610                            |
| <i>PstI</i>        | 3744 and 1866                   |
| <i>XhoI</i>        | 4798 and 812                    |
| <i>PvuI</i>        | 4313, 649 and 648               |
| <i>SmaI</i>        | 4005 and 1605                   |

**Figure 3.1.6.** Restriction profiling MSMEG\_2433 cloned into pUAB400. (A) Vector map of MSMEG\_2433 cloned into pUAB400. (B) Restriction profile of MSMEG\_2433 cloned into pUAB400. Lane 1= Marker IV, Lane 2= Uncut pUAB400, Lane 3= *HindIII*, Lane 4= *PstI*, Lane 5= *XhoI*, Lane 6= *PvuI*, Lane 7= *SmaI*. (C) Table showing the expected banding patterns for MSMEG\_2433 cloned into pUAB400 with the listed restriction enzymes.

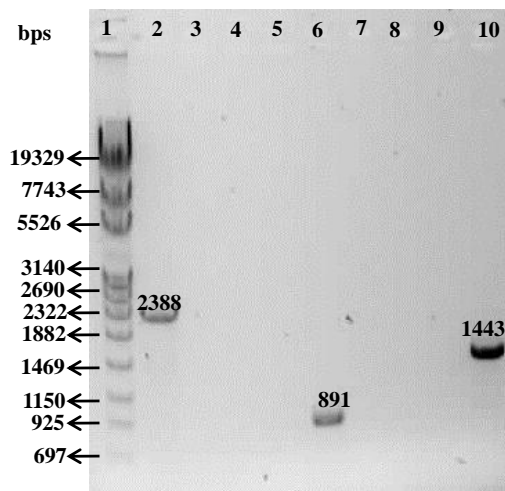


**Figure 3.1.7.** Restriction profiling of MSMEG\_6113 cloned into pUAB400. (A) Vector map of MSMEG\_6113 in pUAB400. (B) Restriction profile of MSMEG\_6113 cloned into pUAB400. Lane 1= Marker IV, Lane 2= Uncut pUAB400, Lane 3= *XhoI*, Lane 4= *PstI*, Lane 5= *SphI*, Lane 6= *SmaI*, Lane 7= *XbaI*. (C) Table showing the expected banding patterns for MSMEG\_6113 cloned into pUAB400 with the restriction enzymes listed.

A



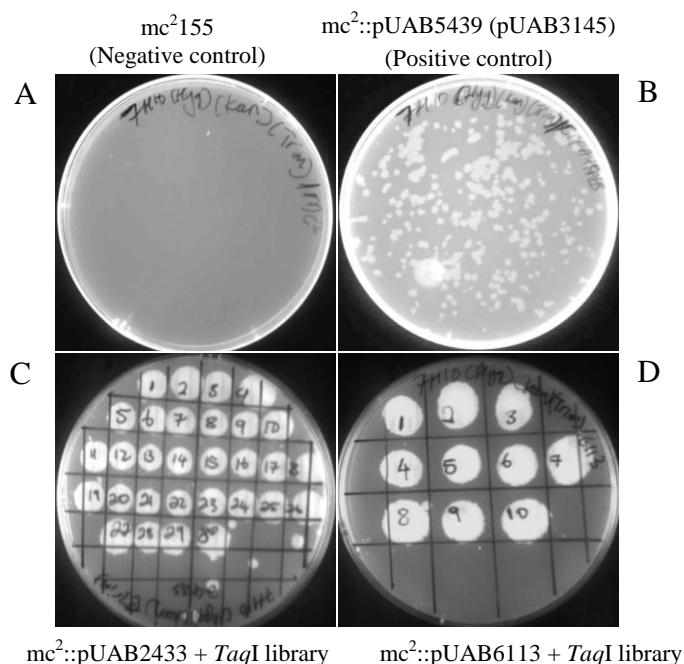
B



**Figure 3.1.8.** Genotypic confirmation of the bait strains. (A) The primer binding sites for PCR confirmation of MSMEG\_2433 and MSMEG\_6113 cloned into pUAB400. The primer binding sites are indicated by the green marker arrows. Primer pairs (MSMEG\_2433\_F+MSMEG\_2433\_R) and (MSMEG\_6113\_F+MSMEG\_6113\_R) were used for PCR confirmation of the respective genes. (B) MSMEG\_2433 and MSMEG\_6113 PCR confirmation with annealing temperature at 76<sup>o</sup>C and 70<sup>o</sup>C respectively. Lane 1= Marker IV, Lane 2= *narB* (Positive control), Lane 3= No template control, Lane 4= No forward primer control, Lane 5= No reverse primer control, Lane 6= MSMEG\_2433, Lane 7= No template control, Lane 8= No forward primer control, Lane 9= No reverse primer control, Lane 10= MSMEG\_6113.

### 3.1.4. Screening for interaction partners using the mPFC assay and Trim resistance.

To screen for putative DD-CPase interacting partners, the bait vector (carrying either MSMEG\_2433 or MSMEG\_6113) were transformed into *M. smegmatis* as detailed in section 2.15.1. Following this, the genomic DNA library carried in the prey vector (pUAB300) was introduced into the  $mc^2::pUAB2433$  and  $mc^2::pUAB6113$  strains by electroporation and the transformations were plated on 7H11 Hyg/Kan solid agar. Colonies from 7H11 Hyg/Kan were sub-cultured on 7H11 Hyg/Kan supplemented with 7.5  $\mu\text{g/ml}$  Trim and any putative interactions would score as growth on agar plates. A total of 30 and 10 putative positive clones were obtained for MSMEG\_2433 and MSMEG\_6113 respectively. Table 3.1.1 and figure 3.1.9 summarizes the results obtained for MSMEG\_2433 and MSMEG\_6113 interaction using mPFC assay, including all the controls.



**Figure 3.1.9.** The results obtained using the mPFC assay for screening of putative MSMEG\_2433 and MSMEG\_6113 interacting partners. (A) Wild type  $mc^2155$  cells only negative control. (B) RpfB+RipA positive control. (C) Putative positive interacting partners for MSMEG\_2433. (D) Putative positive interacting partners for MSMEG\_6113. A total of 30 and 10 putative interacting partners were identified for MSMEG\_2433 and MSMEG\_6113 using the mPFC assay.



**Table 3.1.1.** The total number of colonies for each test conducted for screening of putative MSMEG\_2433 and MSMEG\_6113 interacting partners including the appropriate controls using the mPFC assay.

| Test  | Positive(-) or Negative(+) | Total number of colonies |
|---|----------------------------|--------------------------|
| mc <sup>2</sup> 155   | -                          | 0                        |
| mc <sup>2</sup> 155::pUAB6113 (pUAB300)                         | -                          | 0                        |
| mc <sup>2</sup> 155::pUAB2433 (pUAB300)                         | -                          | 0                        |
| mc <sup>2</sup> 155::pUAB5439(pUAB3145)                         | +                          | 224                      |
| mc <sup>2</sup> 155::pUAB2433 + <i>TaqI</i> genomic DNA library | +                          | 30                       |
| mc <sup>2</sup> 155::pUAB6113 + <i>TaqI</i> genomic DNA library | +                          | 10                       |

### 3.1.5. Identification of the respective MSMEG\_2433 and MSMEG\_6113 putative interacting partners

The plasmids carried in the above-mentioned positive clones were isolated from *M. smegmatis*, transformed into *E. coli* DH5 $\alpha$ , isolated again and sequenced to determine the identity of the inserts. The plasmid inserts were sequenced using the recommended sequencing primers for the mPFC system for identification of the putative interacting partners (Singh et al., 2006). Due to cost constraints, it was decided to sequence only 15 putative interacting clones for MSMEG\_2433 and 9 sequences were obtained for MSMEG\_6113.

To confirm the identity of the respective inserts, the nucleotide sequences obtained were analyzed using the Blastx (<http://blast.ncbi.nlm.nih.gov/Blast.cgi>) search tool from NCBI, to


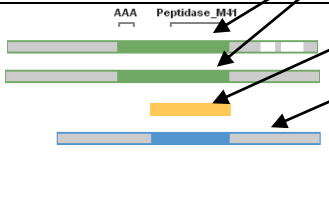

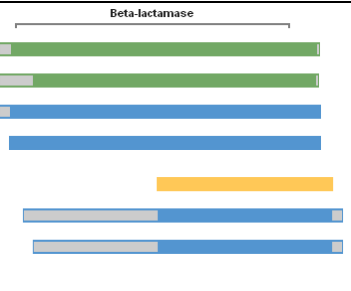
obtain the full length gene of the putative interacting partner. A list of genes was generated by Blastx, and only those with a high percentage identity to the query sequence (viz. nucleotide sequences that we obtained and used to search the database) were considered for further analysis. To identify the corresponding protein for each respective putative interacting partner, the sequences generated through Blastx were further analysed by Blastn (<http://blast.ncbi.nlm.nih.gov/Blast.cgi>) also from NCBI. Table 3.1.2 and table 3.1.3 report on the respective putative interacting partners identified for MSMEG\_2433 and MSMEG\_6113 respectively using the above mentioned bioinformatics tools. The assay revealed that MSMEG\_2433 and MSMEG\_6113 possibly interact with various proteins, including PBPs, identified to be present at the poles of actively growing cells or the divisome of dividing cells. These included PonA1, PbpA and PbpB. The assay also revealed that the two *M. smegmatis* DD-CPases possibly interact with transcription (DNA polymerase subunit III subunit delta) and translation (RNA polymerase sigma factor E) machinery. Hypothetical proteins including several uncharacterized proteins in mycobacteria were also identified to possibly interact with MSMEG\_2433 and MSMEG\_6113.

To study the domain composition of the putative interacting partners, the sequences from Blastn were further analyzed using the BioCyc protein-protein Blast search tool (<http://biocyc.org/MSME246196/blast.html>). Table 3.1.2 and 3.1.3 report on the domain composition for the respective proteins identified to possibly interact with MSMEG\_2433 and MSMEG\_6113 respectively. The domains for the interacting partners include the transpeptidase, glycosyltransferase and penicillin binding domains. These domains are contained within the well characterized PG remodelling enzymes, suggestive of a role of the two *M. smegmatis* DD-CPases in effecting PG remodelling at the poles of actively growing

cells or the divisome of dividing cells, through associating with the PG remodelling enzymes.

The location of the inserts obtained within the full-length gene was determined. Considering the nature of the mPFC assay, it was hypothesized that the insert sequences within the putative positive clones probably contain residues that are essential for protein interaction or are within a domain involved in protein interaction. To assess this, the Smart Blast search tool from NCBI was used. The complete protein sequence of each putative interacting partner was analysed through Smart Blast to obtain the domain organization of the entire protein. The nucleotide sequence for each positive insert from the library screen was then translated using the ExPASy translate tool (<http://web.expasy.org/translate/>), and the output sequence was further analysed through Smart Blast (<http://blast.st-va.ncbi.nlm.nih.gov/blast/smartblast/>) which gives a summary of the best matches for the query sequence, including the conserved domains. The results obtained for each putative interacting partner using Smart Blast are reported in table 3.1.2 and table 3.1.3 for MSMEG\_2433 and SMEG\_6113 respectively. The green regions represent the best matches for the full length protein sequence. The query sequence is shown in yellow and the sequence which best matches the query sequence is indicated in blue.

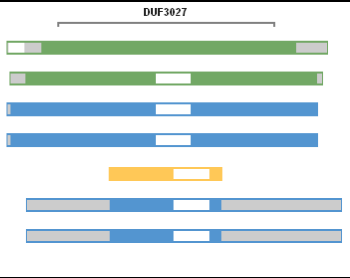

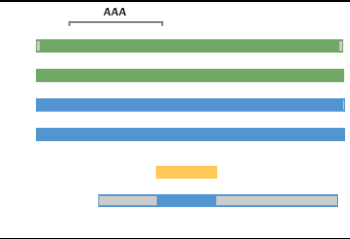

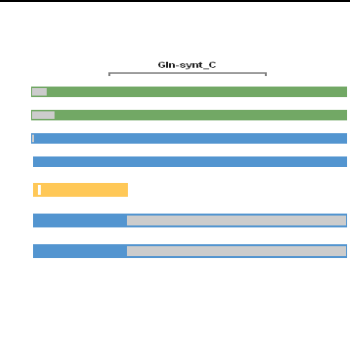

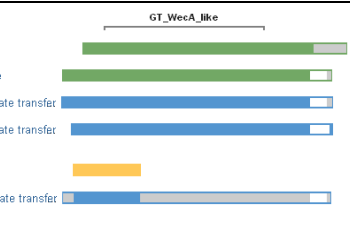
**Table 3.1.2.** Putative MSMEG\_2433 interacting partners obtained using the mPFC assay. The MSMEG-, NCBIWP- and SMEI- number for each putative MSMEG\_2433 are listed including the domain organization and the region that the sequenced putative interacting partner occupies within the full length protein.

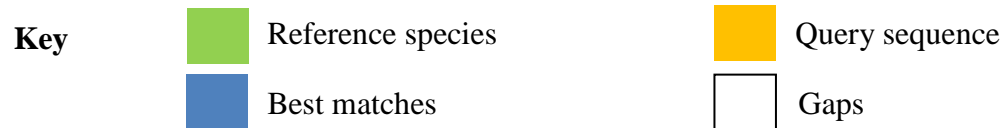
| Protein                                 | MSMEG number<br>NCBI WP number<br>SMEI number | Conserved domain   | Position of putative interacting partner within the full length protein sequence  |
|---|---|--|---|
| ATP-dependent zinc metalloprotease FtsH | MSMEG_6105<br>WP_003897506.1<br>MSMEI_5946    |    | <p>Conserved domains for the query:<br/>cell division protein FtsH-like protein<br/>zinc metalloprotease FtsH</p> <p>Your query: unnamed protein product<br/>cell division protein FtsH</p>  <p>Reference species<br/>Query sequence<br/>Best match</p>      |
| Hypothetical protein                    | MSMEG_4337<br>WP_014878005.1<br>MSMEI_4237    |  | <p>Conserved domains for the query:<br/>hypothetical protein SC02380<br/>hypothetical protein Rv2257c<br/>serine hydrolase<br/>beta-lactamase</p> <p>Your query: unnamed protein product<br/>serine hydrolase<br/>beta-lactamase</p>  <p>Beta-lactamase</p> |

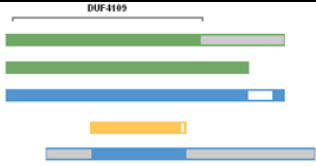


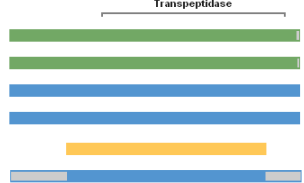

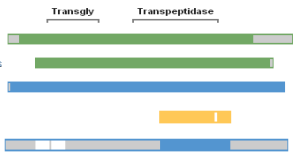
  

**Key**

- Reference species
- Query sequence
- Best matches
- Gaps

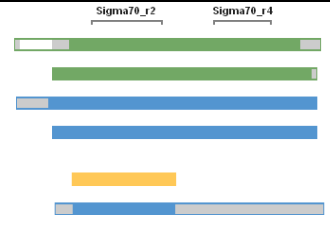
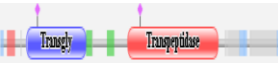
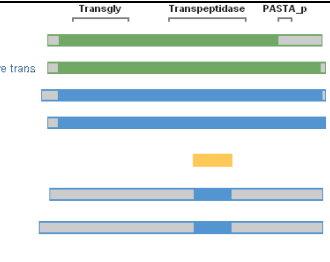

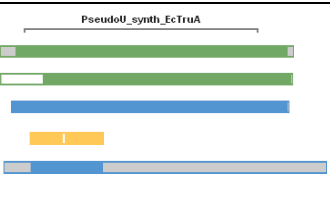

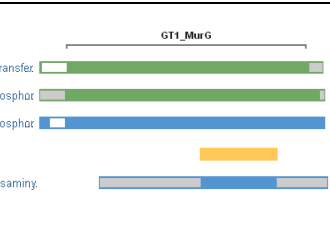
|  |   |  |   |
|--|---|--|---|
| <p>Conserved hypothetical protein</p>  | <p>MSMEG_5691<br/>WP_011730713.1<br/>MSMEI_5541</p> | <p>No data obtained</p>  | <p>Conserved domains for the query:</p> <p>hypothetical protein SCO4330<br/>hypothetical protein R0877<br/>hypothetical protein<br/>hypothetical protein</p> <p><b>Your query: unnamed protein product</b><br/>hypothetical protein<br/>hypothetical protein D806_5766</p>   |
| <p>DNA polymerase III subunit delta</p>  | <p>MSMEG_6153<br/>WP_011731078.1<br/>MSMEI_5996</p> |    | <p>Conserved domains for the query:</p> <p>DNA polymerase III subunit delta'<br/>DNA polymerase<br/>DNA polymerase III subunit delta'<br/>DNA polymerase III subunit delta'</p> <p><b>Your query: unnamed protein product</b><br/>DNA-directed DNA polymerase III subunit delta'</p>   |
| <p>Glutamine synthetase</p>  | <p>MSMEG_3561<br/>WP_014877747.1<br/>MSMEI_3480</p> |    | <p>Conserved domains for the query:</p> <p>glutamine synthetase<br/>glutamine synthetase GlnA<br/>glutamine synthetase<br/>glutamine synthetase, catalytic domain protein</p> <p><b>Your query: unnamed protein product</b><br/>glutamine synthetase, catalytic domain protein<br/>glutamine synthetase</p>   |
| <p>Glycosyl transferase/undecaprenyl-phosphate alpha-N-acetylglucosaminyltransferase</p> | <p>MSMEG_4947<br/>WP_011730204.1<br/>MSMEI_4819</p> |  | <p>Conserved domains for the query:</p> <p>transferase<br/>decaprenyl-phosphate N-acetylglucosaminylphosphotransferase<br/>undecaprenyl-phosphate alpha-N-acetylglucosaminyl 1-phosphate transfer<br/>undecaprenyl-phosphate alpha-N-acetylglucosaminyl 1-phosphate transfer</p> <p><b>Your query: unnamed protein product</b><br/>undecaprenyl-phosphate alpha-N-acetylglucosaminyl 1-phosphate transfer</p>  |



|  |   |   |   |
|--|---|---|---|
| <p>Hypothetical protein</p>  | <p>MSMEG_3858<br/>WP_003895305.1<br/>MSMEI_3768</p> | <p>No data obtained</p>   | <p>Conserved domains for the query:<br/>hypothetical protein SCO1421<br/>RNA polymerase-binding protein RbpA<br/>membrane protein<br/><b>Your query: unnamed protein product</b><br/>hypothetical protein</p>    |
| <p>Hypothetical protein</p>  | <p>MSMEG_5299<br/>WP_014878290.1<br/>MSMEI_5155</p> | <p>No data obtained</p>   | <p>Uncharacterised protein<br/><b>Your query: unnamed protein product</b><br/>hypothetical protein MSMEI_5155<br/>hypothetical protein</p>   |
| <p>Penicillin binding protein transpeptidase domain protein (PbpA)</p> | <p>MSMEG_0031<br/>WP_003891359.1<br/>MSMEI_0033</p> |   | <p>Conserved domains for the query:<br/>penicillin-binding protein<br/>penicillin-binding protein PbpA<br/>penicillin binding protein transpeptidase domain-containing protein<br/>penicillin-binding protein<br/><b>Your query: unnamed protein product</b><br/>penicillin-binding protein A</p>  |
| <p>bifunctional penicillin-binding protein 1A/1B ponA1</p>             | <p>MSMEG_6900<br/>WP_014878797.1<br/>MSMEI_6716</p> |  | <p>Conserved domains for the query:<br/>penicillin-binding protein<br/>bifunctional penicillin-insensitive transglycosylase/penicillin-sensitive trans<br/>penicillin-binding protein<br/><b>Your query: unnamed protein product</b><br/>penicillin-binding protein 1A</p>                        |

**Key**

- Reference species
- Best matches
- Query sequence
- Gaps

|  |   |   |   |
|--|---|---|---|
| <p>RNA polymerase sigma factor E</p>   | <p>MSMEG_1914<br/>WP_003893296.1<br/>MSMEI_1874</p> | <p>No data obtained</p>   | <p>Conserved domains for the query:</p> <ul style="list-style-type: none"> <li>RNA polymerase sigma factor RpoE</li> <li>ECF RNA polymerase sigma factor SigH</li> <li>RNA polymerase sigma-70 factor</li> <li>RNA polymerase subunit sigma</li> </ul> <p><b>Your query: unnamed protein product</b></p> <ul style="list-style-type: none"> <li>RNA polymerase subunit sigma</li> </ul>    |
| <p>Transglycosylase/<br/>penicillin-insensitive<br/>transglycosylase +<br/>penicillin-sensitive<br/>transpeptidase</p> | <p>MSMEG_6201<br/>WP_014878017.1<br/>MSMEI_4281</p> |   | <p>Conserved domains for the query:</p> <ul style="list-style-type: none"> <li>transpeptidase</li> <li>bifunctional penicillin-insensitive transglycosylase/penicillin-sensitive transglycosylase</li> <li>transglycosylase</li> <li>penicillin-binding protein</li> </ul> <p><b>Your query: unnamed protein product</b></p> <ul style="list-style-type: none"> <li>transglycosylase</li> <li>penicillin-binding protein</li> </ul>    |
| <p>tRNA pseudouridine synthase A</p>   | <p>MSMEG_1527<br/>WP_014877097.1<br/>MSMEI_1490</p> |   | <p>Conserved domains for the query:</p> <ul style="list-style-type: none"> <li>tRNA pseudouridine synthase A</li> <li>tRNA pseudouridine synthase A</li> <li>tRNA pseudouridine synthase A</li> </ul> <p><b>Your query: unnamed protein product</b></p> <ul style="list-style-type: none"> <li>tRNA pseudouridine(36-40) synthase</li> </ul>   |
| <p>UDP-diphospho-<br/>muramoylpentapeptide<br/>beta-N-<br/>acetylglucosaminyltrans<br/>ferase (MurG)</p>               | <p>MSMEG_4227<br/>WP_011729656.1<br/>MSMEI_4127</p> |  | <p>Conserved domains for the query:</p> <ul style="list-style-type: none"> <li>UDP-diphospho-muramoylpentapeptide beta-N- acetylglucosaminyltransferase</li> <li>UDP-N-acetylglucosamine-N-acetylmuramyl-(pentapeptide) pyrophosphatase</li> <li>UDP-N-acetylglucosamine-N-acetylmuramyl-(pentapeptide) pyrophosphatase</li> </ul> <p><b>Your query: unnamed protein product</b></p> <ul style="list-style-type: none"> <li>undecaprenyldiphospho-muramoylpentapeptide beta-N-acetylglucosaminyltransferase</li> </ul>  |

Key



Reference species




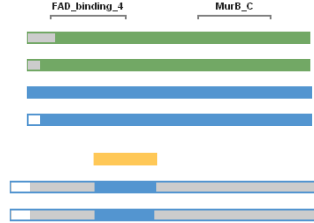
Query sequence







Best matches



Gaps


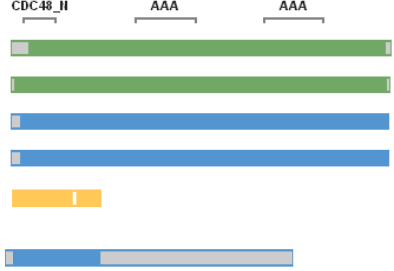

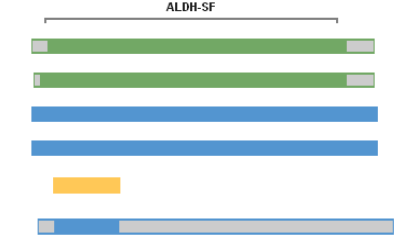
|   |   |  |  |
|---|---|--|--|
| <p>UDP-N-acetylenolpyruvoylglucosamine reductase (MurB)</p> | <p>MSMEG_0928<br/>WP_003892354.1<br/>MSMEI_0906</p> |  | <p><b>Conserved domains for the query:</b></p> <p>UDP-N-acetylenolpyruvoylglucosamine reductase</p> <p>UDP-N-acetylenolpyruvoylglucosamine reductase</p> <p>MULTISPECIES: UDP-N-acetylenolpyruvoylglucosamine reductase</p> <p>UDP-N-acetylenolpyruvoylglucosamine reductase</p> <p><b>Your query: unnamed protein product</b></p> <p>UDP-N-acetylenolpyruvoylglucosamine reductase</p> <p>UDP-N-acetylenolpyruvoylglucosamine reductase</p>  |
|---|---|--|--|

**Key**


|   |                   |   |                |
|---|-------------------|---|----------------|
|  | Reference species |  | Query sequence |
|  | Best matches      |  | Gaps           |





**Table 3.1.3.** Putative MSMEG\_6113 interacting partners obtained using the mPFC assay. The MSMEG-, NCBIWP- and SMEI- number for each putative MSMEG\_6113 are listed, including the domain organization and the region that the sequenced putative interacting partner occupies within the full length protein.


| Protein                             | SMEG number<br>NCBI number<br>SMEI number  | Conserved domain   | Position of putative interacting partner within the full length protein sequence   |
|-------------------------------------|--|--|--|
| Cell division control protein Cdc48 | MSMEG_0858<br>WP_014877228.1<br>MSMEI_1814 |    | <p>Conserved domains for the query:</p> <p>MULTISPECIES: ATPase</p> <p>ATPase</p> <p>ATPase</p> <p>ATPase</p> <p>Your query: unnamed protein product</p> <p>Cell division control protein Cdc48, AAA+ ATPase family</p>   |
| Coniferyl aldehyde dehydrogenase    | MSMEG_2242<br>WP_011728247.1<br>MSMEI_2187 |  | <p>Conserved domains for the query:</p> <p>coniferyl aldehyde dehydrogenase CalB</p> <p>coniferyl aldehyde dehydrogenase</p> <p>MULTISPECIES: aldehyde dehydrogenase</p> <p>aldehyde dehydrogenase</p> <p>Your query: unnamed protein product</p> <p>aldehyde dehydrogenase</p>  |


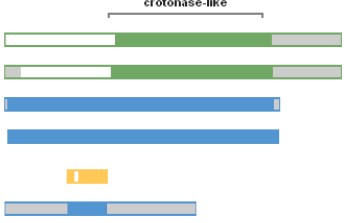
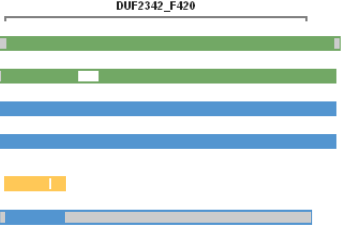
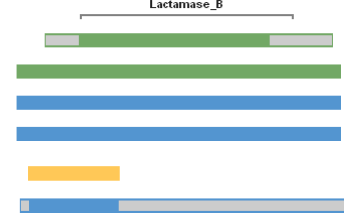

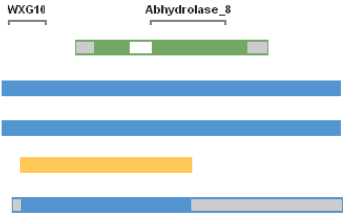
**Key**

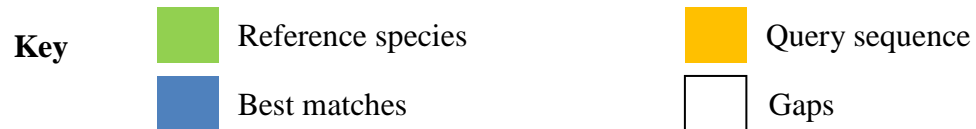
 Reference species

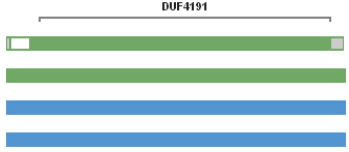

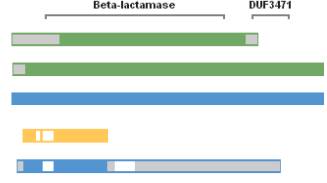
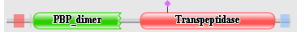
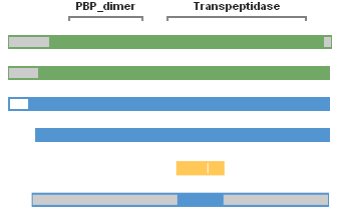
 Query sequence

 Best matches

 Gaps

|                                       |   |  |   |
|---------------------------------------|---|--|---|
| <p>Enoyl-CoA hydratase/isomerase</p>  | <p>MSMEG_0259<br/>WP_014876714.1<br/>MSMEI_0251</p> |    | <p>Conserved domains for the query:</p> <ul style="list-style-type: none"> <li>2,3-dehydroadipyl-CoA hydratase</li> <li>enoyl-CoA hydratase</li> <li>enoyl-CoA hydratase/isomerase</li> <li>enoyl-CoA hydratase</li> </ul> <p>Your query: unnamed protein product</p> <p>enoyl-CoA hydratase</p>           |
| <p>Conserved hypothetical protein</p> | <p>MSMEG_6112<br/>WP_011731046.1<br/>MSMEI_5953</p> | <p>No data obtained</p>  | <p>Conserved domains for the query:</p> <ul style="list-style-type: none"> <li>hypothetical protein SCO3407</li> <li>hypothetical protein Rv3626c</li> <li>hydrolase</li> <li>putative hydrolase</li> </ul> <p>Your query: unnamed protein product</p> <p>hydrolase</p>                                    |
| <p>Hypothetical protein</p>           | <p>MSMEG_0610<br/>WP_014878763.1<br/>MSMEI_6623</p> | <p>No data obtained</p>  | <p>Conserved domains for the query:</p> <ul style="list-style-type: none"> <li>hypothetical protein DR_1823</li> <li>beta-lactamase</li> <li>MULTISPECIES: MBL fold metallo-hydrolase</li> <li>MBL fold hydrolase</li> </ul> <p>Your query: unnamed protein product</p> <p>MBL fold metallo-hydrolase</p>  |
| <p>Hypothetical protein</p>           | <p>MSMEG_0365<br/>WP_011726883.1<br/>MSMEI_0358</p> |  | <p>Conserved domains for the query:</p> <ul style="list-style-type: none"> <li>hypothetical protein SCO3760</li> <li>hypothetical protein</li> <li>hypothetical protein</li> </ul> <p>Your query: unnamed protein product</p> <p>hypothetical protein</p>   |



|  |   |  |  |
|--|---|--|--|
| <p>Hypothetical protein</p>                      | <p>MSMEG_4287<br/>WP_003895683.1</p>                | <p>No data obtained</p>  | <p>Conserved domains for the query:</p> <ul style="list-style-type: none"> <li>hypothetical protein SCO2196</li> <li>transmembrane protein</li> <li>hypothetical protein</li> <li>membrane protein</li> </ul>   |
| <p>Beta lactamase penicillin-binding protein</p> | <p>MSMEG_5637<br/>WP_014876714.1<br/>MSMEI_0251</p> |  | <p>Conserved domains for the query:</p> <ul style="list-style-type: none"> <li>beta-lactamase family protein</li> <li>hypothetical protein Rv0907</li> <li>Putative beta-lactamase, penicillin-binding protein</li> </ul> <p>Your query: unnamed protein product</p> <ul style="list-style-type: none"> <li>Putative beta-lactamase, penicillin-binding protein</li> </ul>        |
| <p>Penicillin-binding protein B</p>              | <p>MSMEG_4233<br/>WP_011729661.1<br/>MSMEI_4133</p> |  | <p>Conserved domains for the query:</p> <ul style="list-style-type: none"> <li>cell division protein</li> <li>penicillin-binding membrane protein PbpB</li> <li>cell division protein FtsI</li> <li>peptidoglycan synthase FtsI</li> </ul> <p>Your query: unnamed protein product</p> <ul style="list-style-type: none"> <li>penicillin-binding membrane protein PbpB</li> </ul>  |

Key

|  |                   |  |                |
|--|-------------------|--|----------------|
|  | Reference species |  | Query sequence |
|  | Best matches      |  | Query sequence |

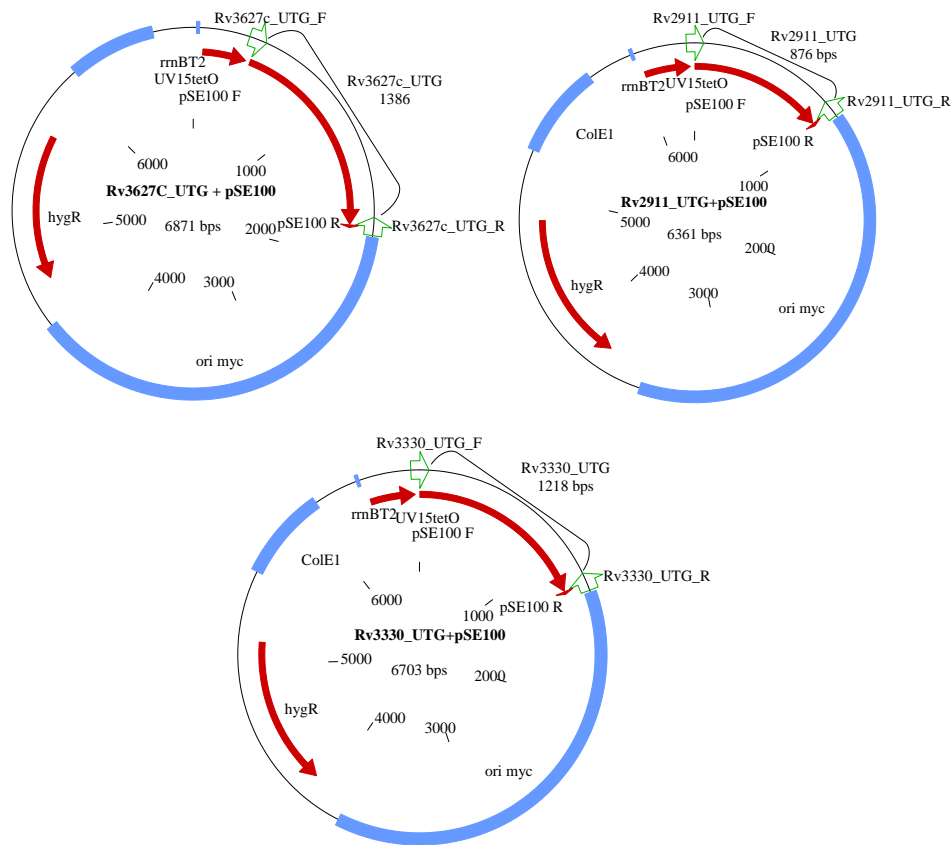
### **3.2. Ectopic expression of *M. tuberculosis* DD-CPases in *M. smegmatis*.**

As mentioned earlier, there is a multiplicity of DD-CPases in mycobacterial genomes and it is unclear if this is reflective of a redundancy in function or alternatively, the different homologues may retain specialist biological roles. The study by Bourai et al., (2012) demonstrated that heterologous expression of Rv2911 from *M. tuberculosis* in *M. smegmatis* leads to multiple defects including retarded growth, altered colony morphology, and aberrant sliding motility (Bourai et al., 2012). Considering this, in this study we aimed to characterize the physiological function of the different *M. tuberculosis* LMW PBPs, through ectopic expression in *M. smegmatis*. We recognize that heterologous expression has various limitations but hypothesized that a side-by-side assessment of the three homologues in the same heterologous host would provide some insight into specialist versus redundant function. For this, we constructed a set of recombinant *M. smegmatis* strains expressing Rv2911, Rv3330 and Rv3627c from the P<sub>sync</sub>tet promoter which is classified as the strongest promoter in mycobacteria for gene regulation studies (Ehrt et al., 2005). Based on this, we expect that expression from the P<sub>sync</sub>tet promoter results in high abundance of *M. tuberculosis* DD-CPases in *M. smegmatis*.

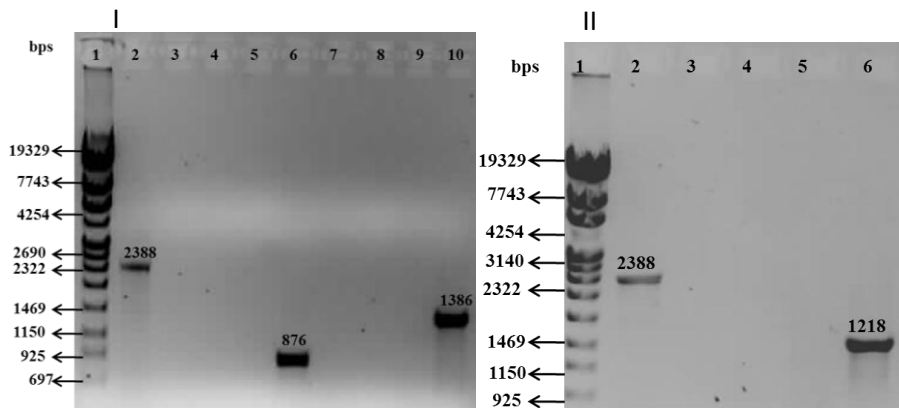
#### **3.2.1. Generation and genotyping of heterologous *M. smegmatis* strains ectopically expressing *M. tuberculosis* DD-CPases**

The episomal pSE100 vector, carrying Rv2911, Rv3330 and Rv3627c was constructed as detailed in section 2.8.6. The resulting constructs (pSE2911, pSE3330 and pSE3627c) were propagated in *E. coli* DH5 $\alpha$  and plasmid DNA was extracted as described in 2.4.2. The constructs were verified by restriction profiling and sequencing. The restriction maps are shown in Appendix (Appendix D). The mc<sup>2</sup>155 strain was transformed by electroporation as described in section 2.11.2 with these constructs to generate the mc<sup>2</sup>(pSE2911), mc<sup>2</sup>(pSE3330) and mc<sup>2</sup>(pSE3627c) strains. A negative control strain, mc<sup>2</sup>(pSE100), carrying the empty vector was also generated. A single colony of each strain was picked and DNA extracted as detailed in section 2.3.2 for PCR confirmation using gene specific primers listed in the Appendix (Appendix B), Figure 3.2.1.

A



B

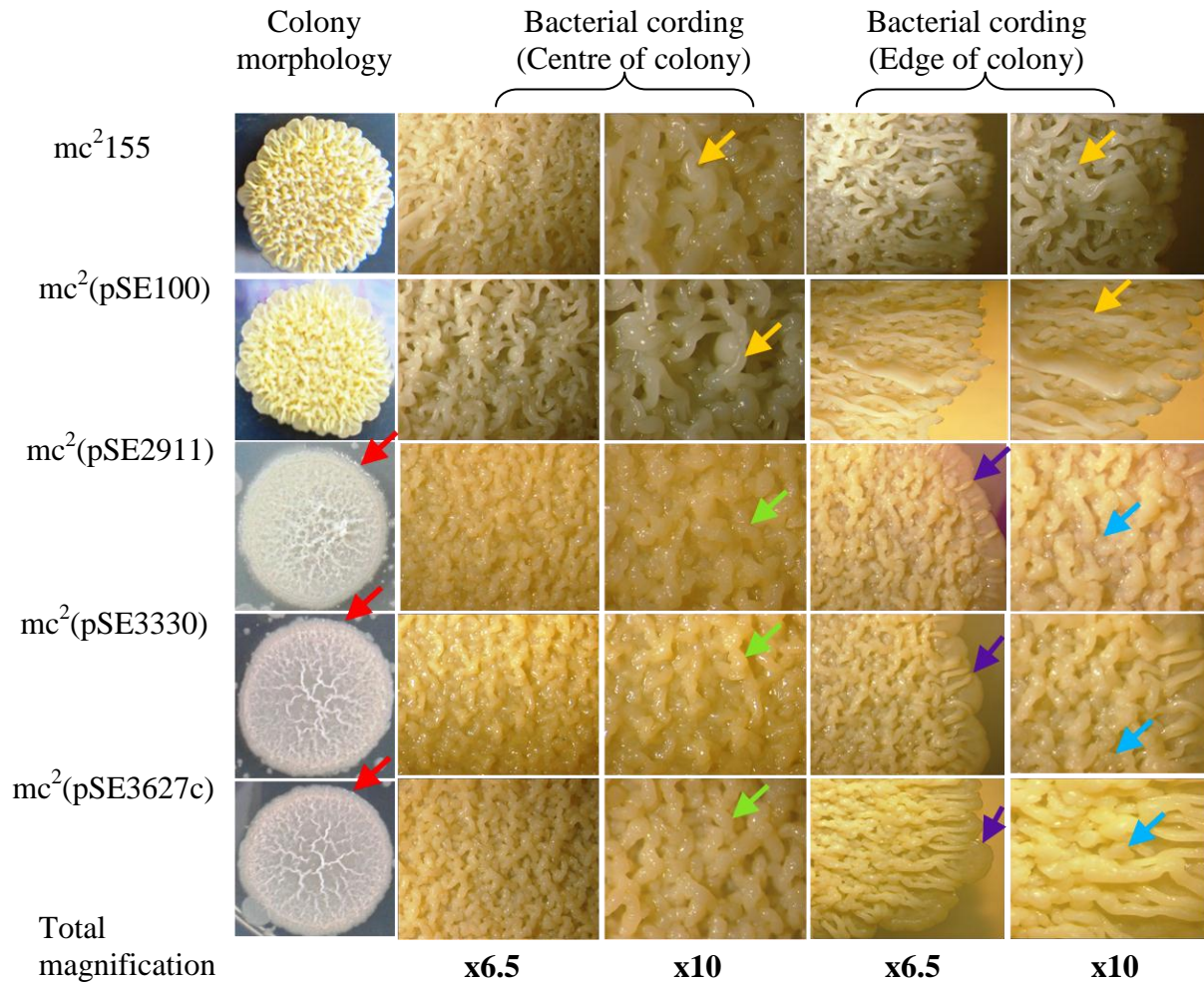


**Figure 3.2.1.** PCR confirmation of presence of *M. tuberculosis* DD-CPases in *M. smegmatis*. (A) Primer binding sites for PCR confirmation of *M. tuberculosis* DD-CPases cloned into pSE100. The primer binding sites are indicated by the green marker/arrows. Primer pairs (Rv2911\_UTG\_F+Rv2911\_UTG\_R), (Rv3330\_UTG\_F+Rv3330\_UTG\_R) and (Rv3627c\_UTG\_F+Rv3627c\_UTG\_F) were used for PCR confirmation of Rv2911, Rv3330 and Rv3627c respectively. (B) PCR confirmation of Rv2911 (I) and Rv3627c (II) with annealing temperature at 70°C and 72°C respectively. Lane 1= Marker IV, Lane 2= *narB* (Positive control), Lane 3= No template control, Lane 4= No forward primer control, Lane 5= No reverse primer control, Lane 6= Rv2911, Lane 7= No template control, Lane 8= No forward primer control, Lane 9= No reverse primer control, Lane 10= Rv3627c. (II) PCR confirmation of Rv3330 with annealing temperature of 70°C with primer pairs listed above. Lane 1= Marker IV, Lane 2= *narB* (Positive control), Lane 3= No template control, Lane 4= No forward primer control, Lane 5= No reverse primer control, Lane 6= Rv3330.

### **3.2.2. Ectopic expression of *M. tuberculosis* DD-CPases in *M. smegmatis* significantly affects bacterial colony morphology**

Following the generation of the heterologous *M. smegmatis* strains as described in section 2.11.2, we observed some defects in colony morphology where the resulting colonies were smooth with a distinct mucoïd surface surrounding the colony edge, figure 3.3.2. A similar defect was reported by Buorai et al., (2012) for the ectopic expression of Rv2911 and now we demonstrate that increased expression of any of the *M. tuberculosis* DD-CPases in *M. smegmatis* leads to similar defects.

The smooth colonies which also lacked defined surface cording, a characteristic unique to mycobacterial species, were further analysed using the Zeiss STEMI-2000c dissecting microscope. At high microscopic resolution, we determined that the strains were able to initiate cording, as demonstrated by the presence of short surface indentations that did not mature into the full serpentine cords displayed by the wild type mc<sup>2</sup>155 strain, figure 3.2.2. The short cords and surface indentations were exacerbated for the mc<sup>2</sup>(pSE2911) and mc<sup>2</sup>(pSE3330) strain, figure 3.2.2. In addition, the heterologous strains displayed an abnormal colony edge, distinct from that observed for the mc<sup>2</sup>155 and mc<sup>2</sup>(pSE100) control strains,



**Figure 3.2.2.** Colony morphology of the recombinant *M. smegmatis* strains ectopically expressing *M. tuberculosis* DD-CPases. The strains were grown in liquid culture to log phase (OD<sub>600</sub> 0.5-0.9) and 100 µl was spotted on 7H10 agar plates. Images were obtained using the Zeiss STEMI-2000c dissecting microscope after a 3-day incubation period at 37<sup>0</sup>C. The red arrows indicate smooth colonies with a mucoid surface edge. The yellow arrows illustrate wild type colony cording distinguished by clearly defined serpentine cords. The green arrows show short cords uncharacteristic of normal mycobacterial colony cording. The purple arrows point to the aberrant colony edge and the blues arrows indicate surface indentations.

### 3.2.3. Ectopic expression of *M. tuberculosis* DD-CPases affects bacterial sliding on semi-solid agar

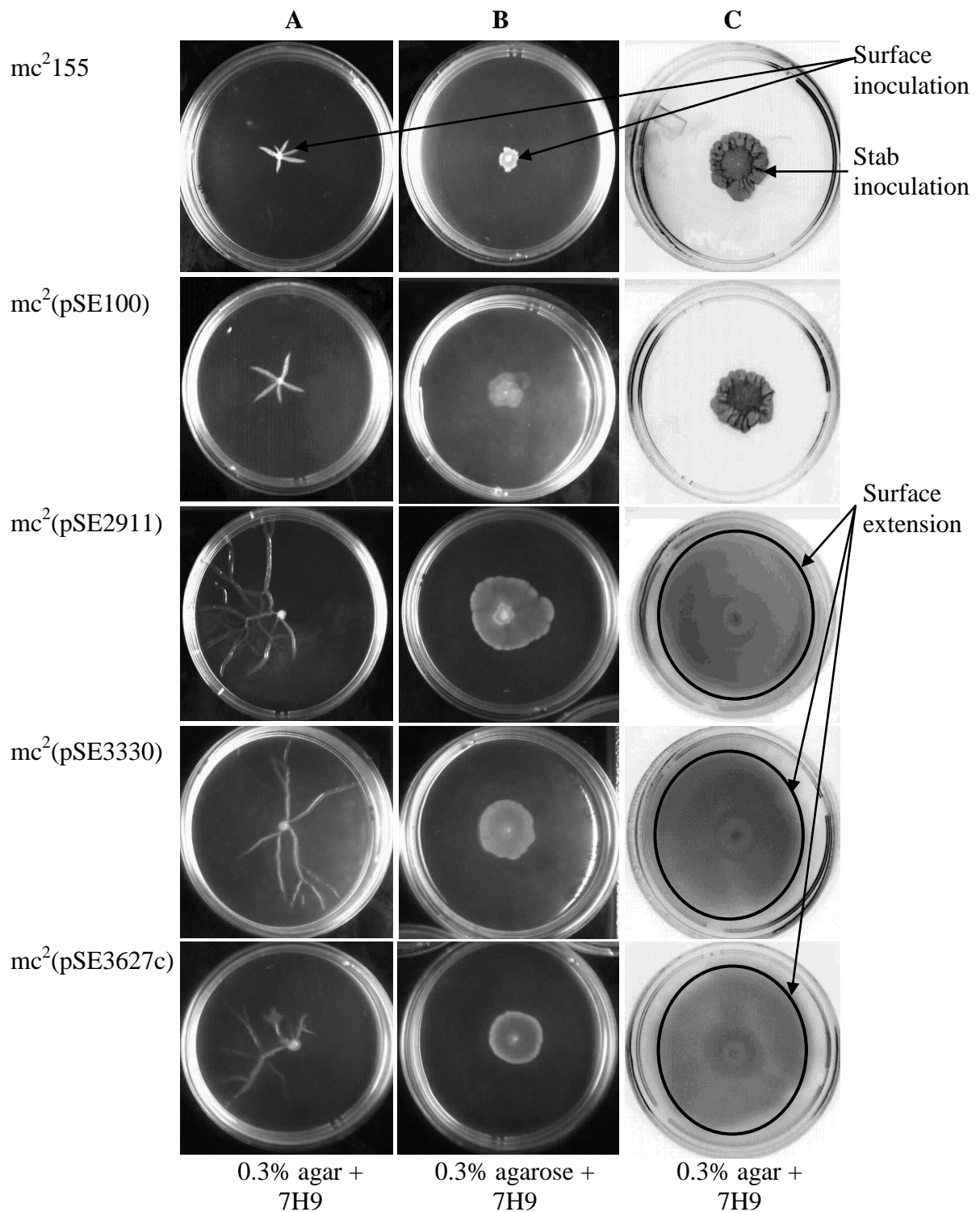
Previous studies have demonstrated that the formation of smooth colonies in mycobacterial species, as observed for our heterologous *M. smegmatis* strains, is related to modifications in cell wall components such as glycopeptidolipids (GPLs). In particular, an increase in the abundance of cell wall GPLs (Moya-Hoyos et al., 2015) or acetylation (Recht and kolter. 2001) directly

influence bacterial sliding on semi-solid media by considerably altering the surface hydrophobicity of cells. As a result, the surface of cells becomes less hydrophobic allowing for migration from the point of inoculation on semi-solid media. This type of motility is hypothesized to play a pivotal role in surface colonization, potentially leading to disease establishment and dissemination during mycobacterial infection (Recht et al., 200; Martínez et al., 2001)

Considering the colony forming defects noted above, we decided to assess sliding motility of the heterologous *M. smegmatis* strains on 7H9 media, with 0.3% agar or agarose as described in section 2.16.3. A freshly streaked colony of each respective heterologous strain was placed at the center of an agar or agarose solidified 7H9 plate and sliding was monitored as shown in figure 3.2.3 A and B. As an alternative, the strains were also stab-inoculated, figure 3.2.3 C.

In all cases, data revealed that ectopic expression of *M. tuberculosis* DD-CPases in *M. smegmatis* significantly influences bacterial sliding on semi-solid agar, where motility was greatly enhanced on 7H9 media solidified with agar as shown in both figure 3.2.3 A and C. In addition, stab inoculation resulted in increased sliding, with strains reaching the edge of plates after 3 days of incubation, when compared to the wild type and empty vector control strain. The sliding of the heterologous strains on agarose solidified media did not extend over to large surface areas as observed on agar solidified media. This is most likely due to high concentrations of agarose (0.2% or above), which results in media that is rigid, thus preventing bacterial translocation over a large surface (Martínez et al., 2001).





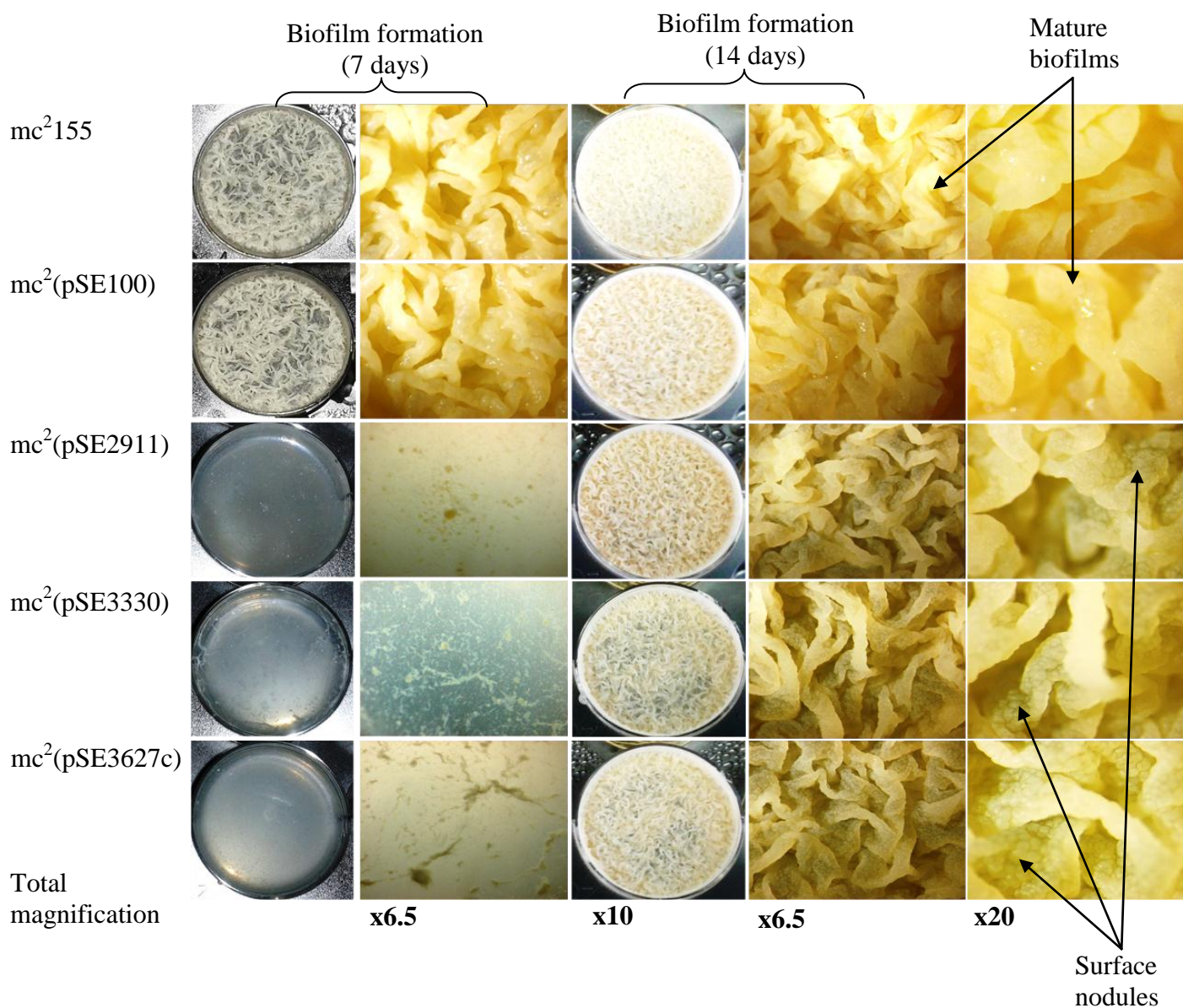
**Figure 3.2.3.** Sliding motility of the heterologous *M. smegmatis* strains on semi-solid media. Liquid 7H9 media was solidified with agar or agarose to a final concentration of 0.3%. A 3-day old freshly streaked colony of the heterologous strain was surface inoculated on (A) agar or (B) agarose solidified 7H9. Additionally, agar solidified 7H9 was stab inoculated with 10  $\mu$ l liquid culture grown to log-phase (C).

### **3.2.4. Ectopic expression of *M. tuberculosis* DD-CPases in *M. smegmatis* results in delayed and aberrant biofilm formation**

The observed defects in colony morphology and sliding on semi-solid agar were suggestive of alterations in cell surface properties for the heterologous strains. This prompted us to further assess whether cell-cell interaction/communication including arrangement in an organized bacterial community, is retained upon ectopic expression of *M. tuberculosis* DD-CPases in *M. smegmatis*. Biofilms represent one of the best-studied models of cellular communities and we turned our attention to using this system to assess the behavior of our heterologous strains. A series of studies have demonstrated that both *M. tuberculosis* and *M. smegmatis* are capable of forming biofilms on both polyvinyl chloride and the air-media interface (Ojha et al., 2005; Ojha and Hatfull, 2007; Ojha et al., 2012). The air-media interface protocol to assess biofilm formation of the heterologous *M. smegmatis* strains. Biofilms were prepared in 6-well microtitre plates using Sauton's minimal media as described in section 2.16.2. The plates were sealed with biohazard tape and incubated at 37<sup>0</sup>C in a standing incubator. The plates were viewed at 7 and 14 days respectively using the Zeiss STEMI-2000c dissecting microscope.

At day 7, the mc<sup>2</sup>155 and mc<sup>2</sup>(pSE100) control strains formed mature biofilms, figure 3.2.4. The recombinant strains showed no indication of biofilm formation at this point and to further confirm whether these strains were competent for biofilm formation, the cultures were incubated under the same conditions for a further 7 days. After 14 days of incubation, mature biofilms were observed for the heterologous *M. smegmatis* strains. However, when viewed at high resolution with the Zeiss STEMI-2000c dissecting microscope, the biofilms were unevenly textured with severe surface nodules when compared to the mc<sup>2</sup>155 and mc<sup>2</sup>(pSE100) control strains. The data demonstrated that ectopic expression of *M. tuberculosis* DD-CPases in *M. smegmatis* significantly delays the efficiency at which cells switch from planktonic growth to a spontaneously self-assembled community in the form of biofilms. In addition, the data demonstrated that ectopic expression of *M. tuberculosis* DD-CPases in *M. smegmatis* significantly affects biofilm

maturation, with the heterologous strains unable to form robust and mature biofilms when compared to the  $mc^2$ 155 and  $mc^2$ (pSE100) control strains.



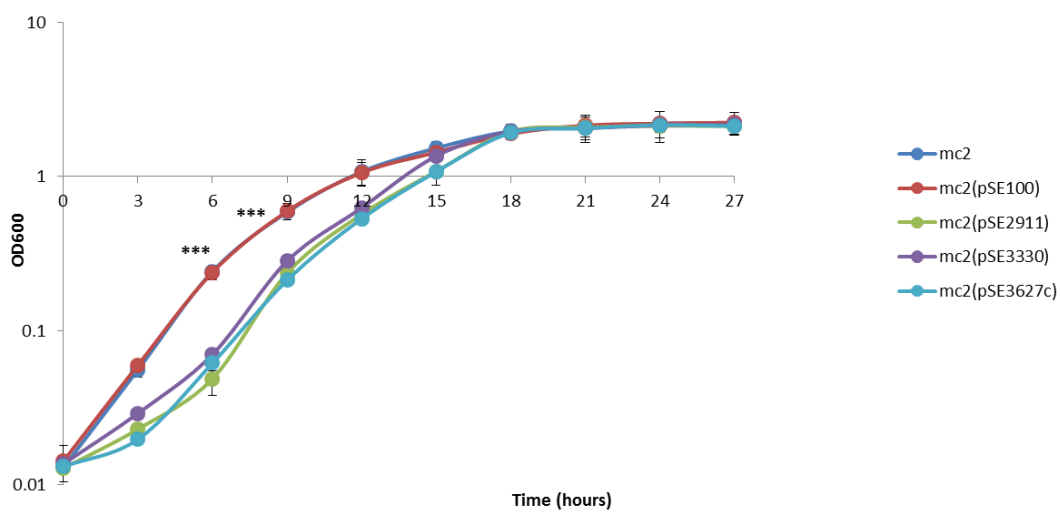
**Figure 3.2.4.** Biofilm formation of the heterologous *M. smegmatis* strains ectopically expressing *M. tuberculosis* DD-CPases. The heterologous strains displayed delayed biofilm formation, with mature biofilms forming after a 14 day incubation period at 37<sup>0</sup>C. The resulting biofilms were unevenly textured with severe nodules.

### 3.2.5. Ectopic expression of *M. tuberculosis* DD-CPases in *M. smegmatis* results in retarded growth in axenic culture

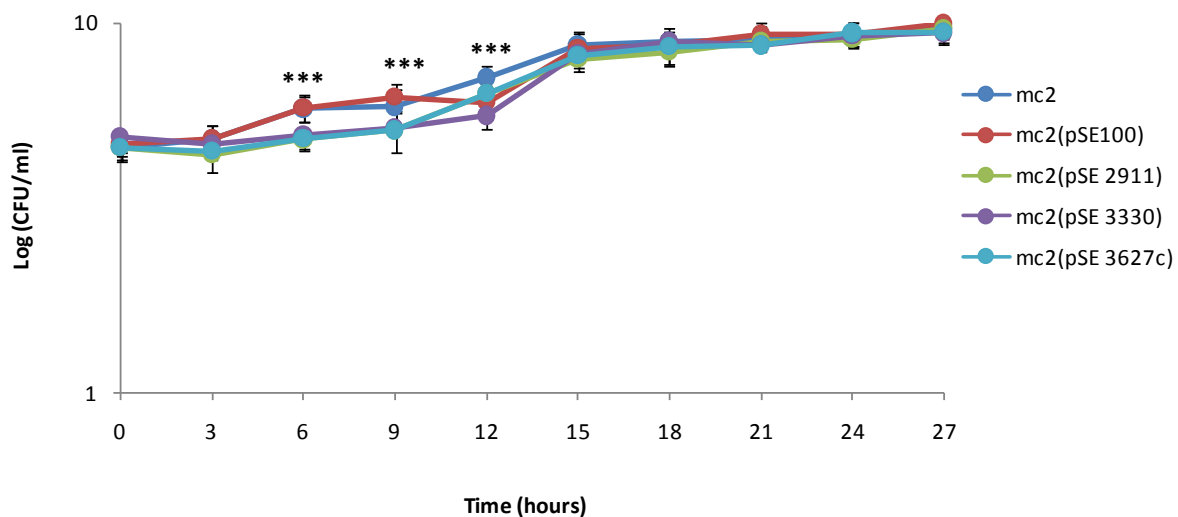
To further understand the physiological role of the *M. tuberculosis* DD-CPases, a growth curve was conducted to evaluate the effect of ectopic expression of these proteins on growth rates of

heterologous *M. smegmatis*. Growth curve cultures were started as detailed in section 2.16.6. The heterologous strains displayed retarded growth at the onset of the log-phase, an effect that was lost during later stages of growth where these strains displayed similar levels of growth and biomass as those obtained for mc<sup>2</sup>155 and mc<sup>2</sup>(pSE100) strains, figure 3.2.5. Clumping of cultures was observed after 18 hours of growth and to circumvent this, cultures were gently swirled to disengage clumps before measuring the OD<sub>600</sub> and plating for CFU/ml.

A



B



**Figure 3.2.5.** Growth curve analysis of the heterologous *M. smegmatis* strains. Growth was monitored by measuring the OD<sub>600</sub> (A) and plating for CFU/ml (B) at 3-hour intervals. The growth curve was started at OD<sub>600</sub> = 0.1 in liquid 7H9 media. (\*\*\*, P<0.0001).

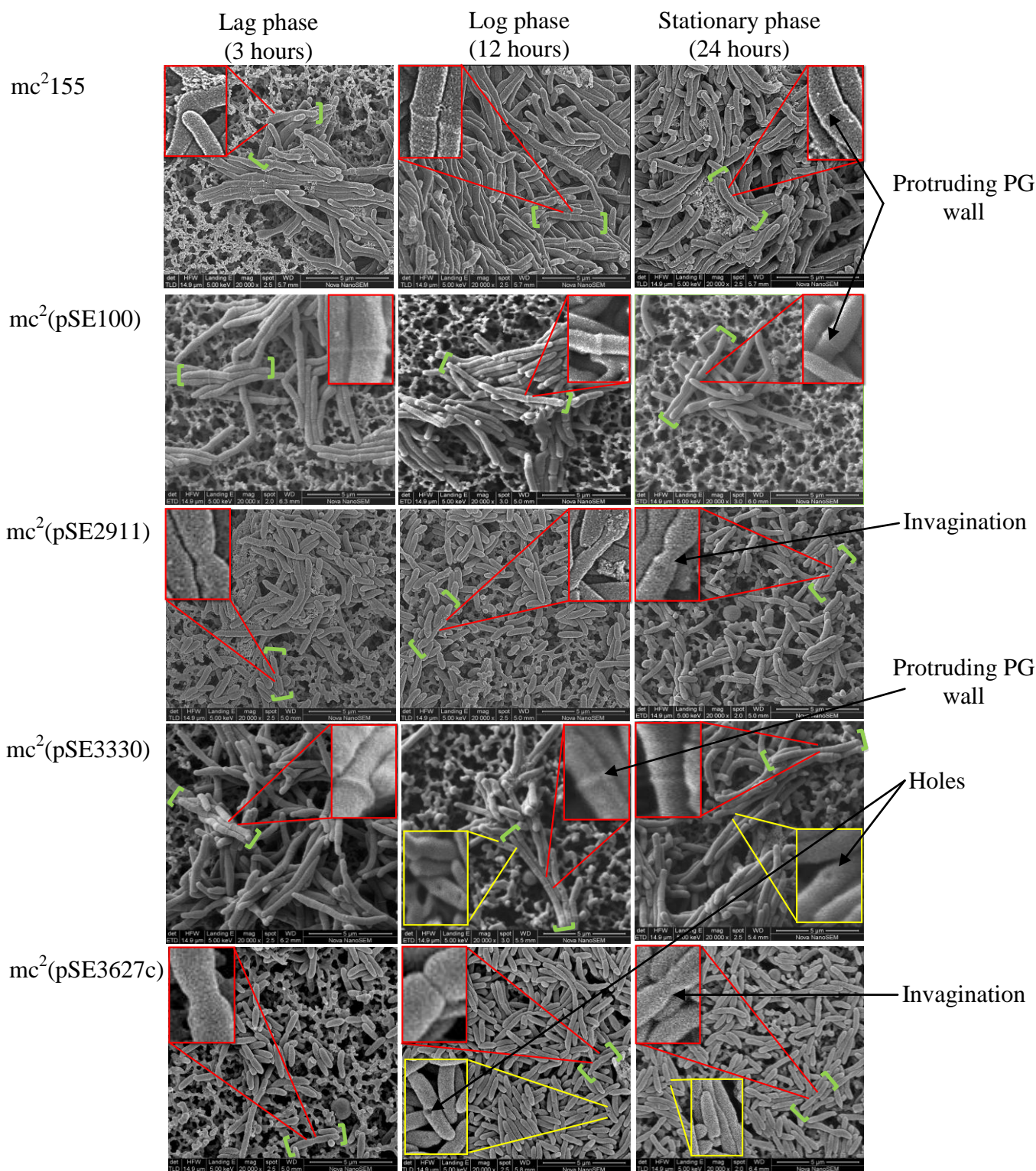
### **3.2.6. Ectopic expression of Rv2911 and Rv3627c significantly alters mycobacterial cell length and mechanisms of division.**

We next decided to study cell wall morphology using SEM to assess the impact of ectopic expression of *M. tuberculosis* DD-CPases in *M. smegmatis*. Cells were harvested at 3, 12 and 24 hours representing the lag, log and stationary phases of growth. The OD<sub>600</sub> of each strain was measured before harvesting cells to confirm that the cultures had reached the growth phase in question. Cells were prepared for SEM as detailed in section 2.16.5 and imaged using the high resolution FEI Nova NanoSEM 230 scanning electron microscope.

Ectopic expression of Rv2911 and Rv3627c resulted in reduced bacterial cell size, figure 3.2.6. To further confirm that cell size was greatly reduced in the mc<sup>2</sup>(pSE2911) and mc<sup>2</sup>(pS3627c) strains, the distribution of cell lengths for the heterologous strains was measured and expressed as percentage of the total population. The control strains and the mc<sup>2</sup>(pSE3330) strain have a majority of cells with a size range of between 4-6 μm. We noted a shift in the distribution of cell lengths in the majority of cells towards a cell size ranging <2 μm for the mc<sup>2</sup>(pSE2911) and mc<sup>2</sup>(pSE3627c) strains, during all stages of growth, Figure 3.2.7. This suggested that ectopic expression of these two DD-CPases caused dysregulation of cell elongation or division process.

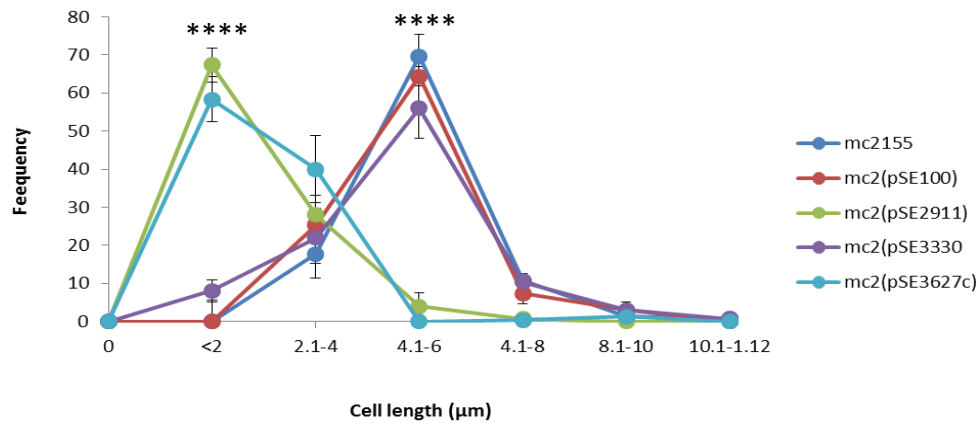
In addition to reduced cell length, the mc<sup>2</sup>(pSE2911) and mc<sup>2</sup>(pSE3627c) strains lacked the protruding peptidoglycan noted with proper septum formation for all cells undergoing division, seen in the enlarged inserts, figure 3.2.6. Furthermore, the septum of all cells undergoing division for these strains appears to invaginate as cells divide. This feature contrasts with that observed for the control and mc<sup>2</sup>(pSE3330) strains. The mc<sup>2</sup>(pSE3330) and mc<sup>2</sup>(pSE3627c) strains had cells with holes following ectopic expression of Rv3330 and Rv3627c respectively, figure 3.2.6.



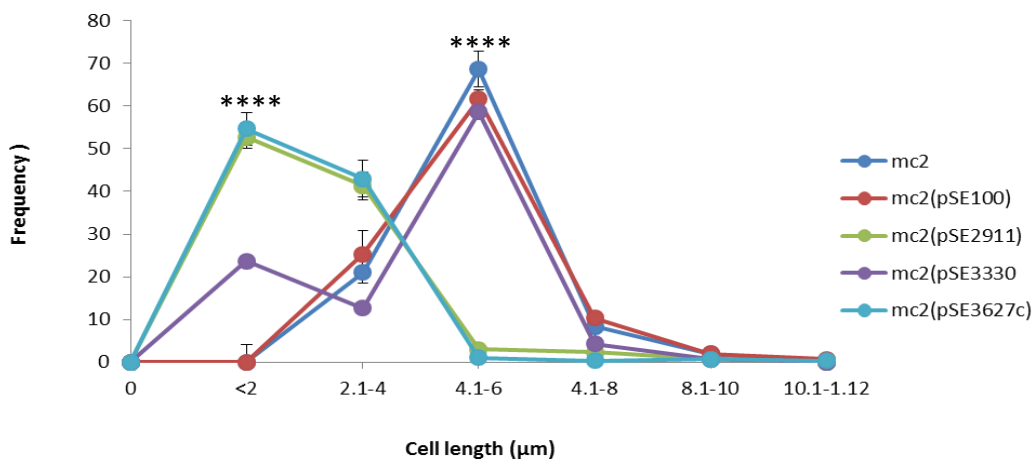


**Figure 3.2.6.** Cell length alteration and division defects displayed by the heterologous *M. smegmatis* strains as a result of ectopic expression of *M. tuberculosis* DD-CPases. The strains were cultured in liquid 7H9 (starting  $OD_{600} = 0.05$ ) and sampled at 3, 12 and 24 hours representing the lag, log and stationary phases of growth for SEM. The green parenthesis delineates the size of a single cell. The enlarged insert in red demonstrates the division site. The enlarged inserts in yellow indicate holes observed for the  $mc^2(pSE3330)$  and  $mc^2(pSE3627c)$ . Scale bar= 5  $\mu$ m

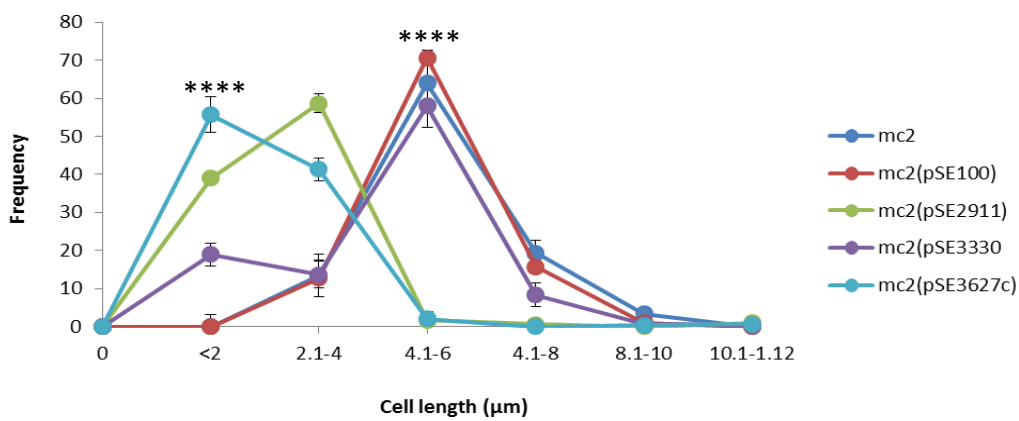
A



B



C

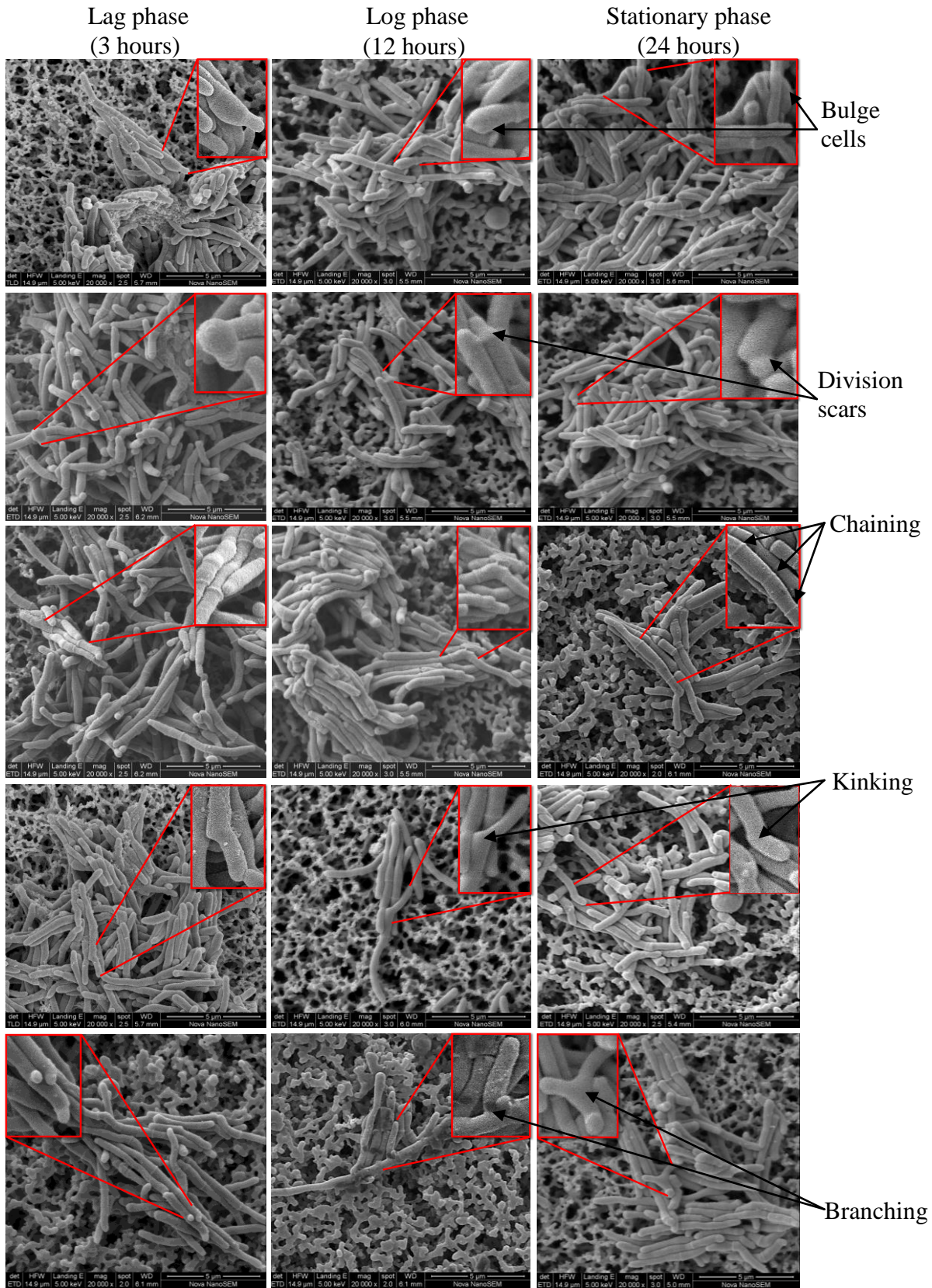


**Figure 3.2.7.** Cell length distribution of the heterologous *M. smegmatis* strains. Graph A, B and C represent cell length distribution of the heterologous strains at lag, log and stationary phases of growth respectively. The mc<sup>2</sup>155, mc<sup>2</sup>(pSE100) and mc<sup>2</sup>(pSE3330) strains displayed cell length distribution of between 4-6 µM. A shift to the left in cell length, with cell size <2 µM was observed for the mc<sup>2</sup>(pSE2911) and mc<sup>2</sup>(pSE3627c) strains. (n=100 ; \*\*\*\*, P<0.00001).

### **3.2.7. Ectopic expression of Rv3330 in *M. smegmatis* significantly affects cellular morphology**

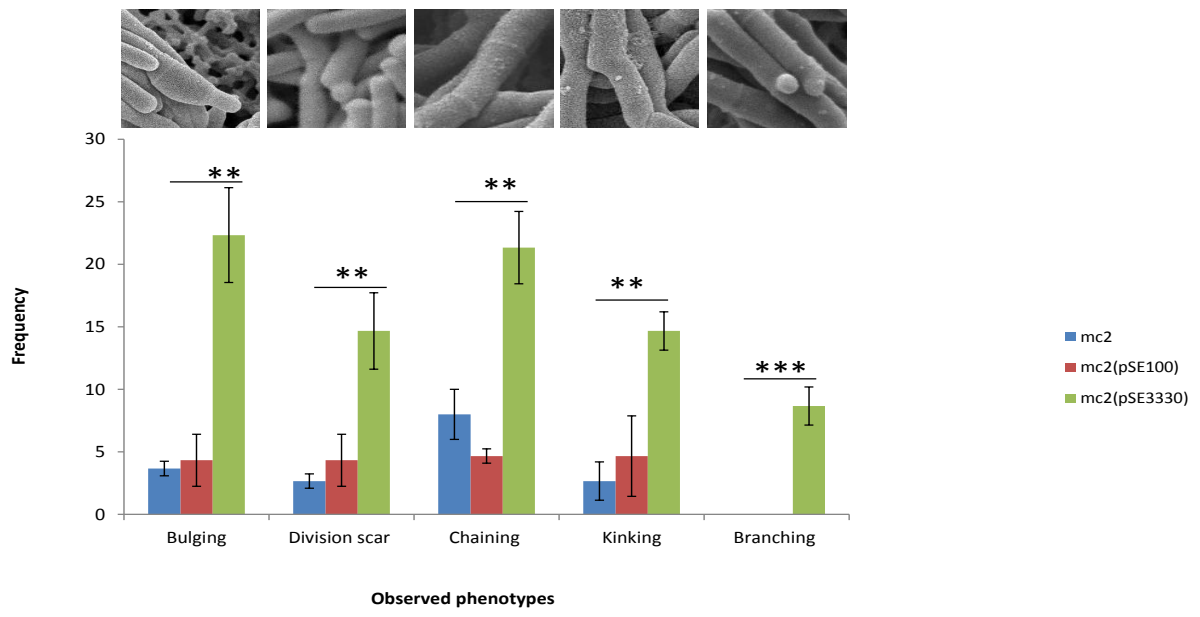
The mc<sup>2</sup>(pSE3330) strain displayed robust morphological defects as revealed by SEM, that were not noted in the other strains. The defects include the formation of cells with bulges, division scars, chaining of cells, kinking and branching/lateral growth, figure 3.2.8. The phenotypes were quantified and expressed as a percentage of the total population for cells in lag, log and stationary phases of growth. An increase in the number of cells showing abnormal cellular morphology was observed for the mc<sup>2</sup>(pSE3330) strain, figure 3.2.9. Another important observation is the lateral branching/growth of cells, exclusively observed for the mc<sup>2</sup>(pSE3330) strain, further substantiating that ectopic expression of Rv3330 in *M. smegmatis* affects normal cellular morphology.



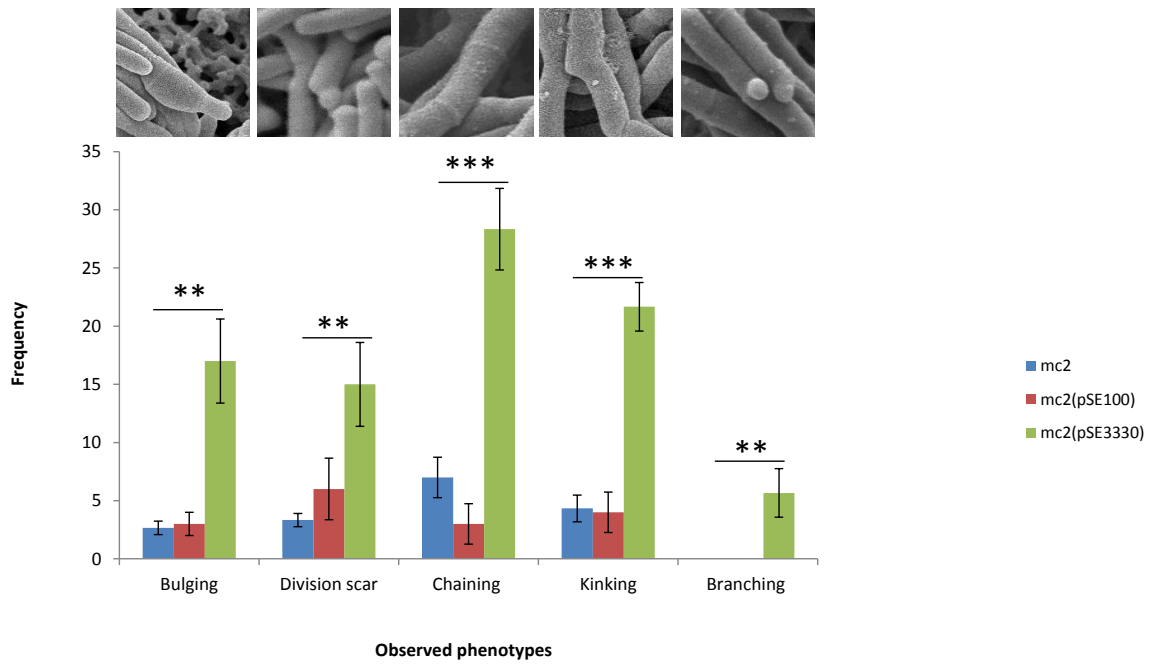


**Figure 3.2.8.** Abnormal cell wall morphology displayed by the *mc*<sup>2</sup>(pSE3330) strain. The insert in each image represent the enlarged cell morphology defect. The morphological defects include bulging of cells, division scars, chaining, kinking and lateral branching/growth of cells. Scale bar= 5 µm

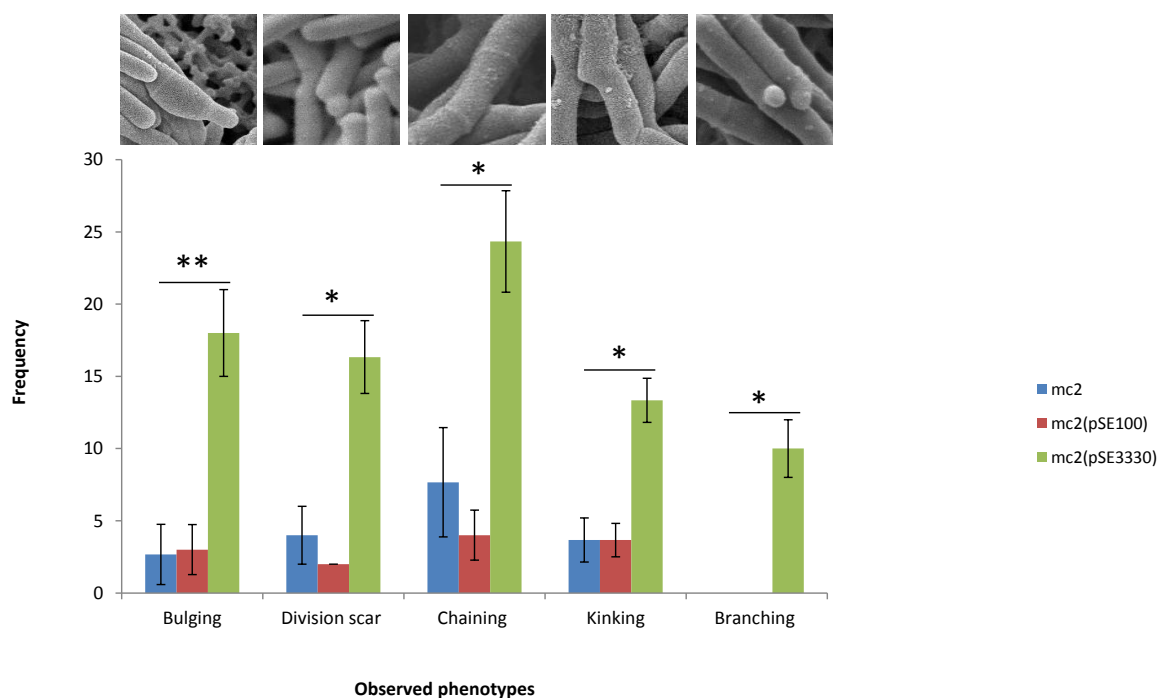
A



B



C



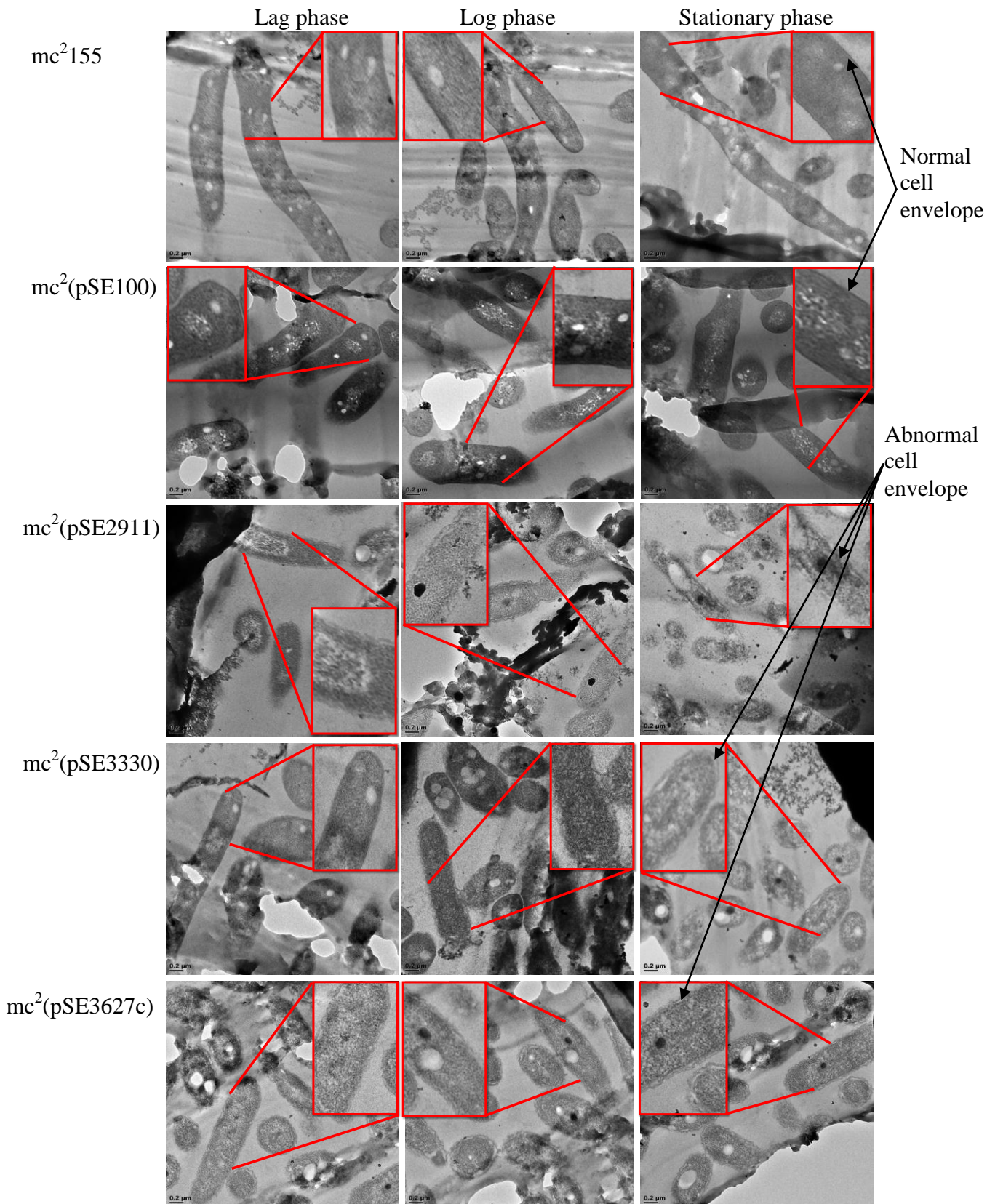
**Figure 3.2.9.** Quantification of abnormal cellular morphology resulting from ectopic of Rv3330 in *M. smegmatis*. Graph A, B and C represents the quantified phenotypes for each population of cells harvested at lag, log and stationary phases of growth respectively. The data shows a significant increase in cells that form chains, bulges and division scars for the mc<sup>2</sup>(pSE3330) strain relative to the mc<sup>2</sup>155 and mc<sup>2</sup>(pSE100) control strains. ( $n= 100$ ; \*,  $P<0.01$ ; \*\*,  $P<0.001$ ; \*\*\*,  $P<0.0001$ , \*\*\*\*;  $P<0.0001$ )

### 3.2.8. Ectopic expression of *M. tuberculosis* DD-CPases disrupts normal cell wall architecture in *M. smegmatis*

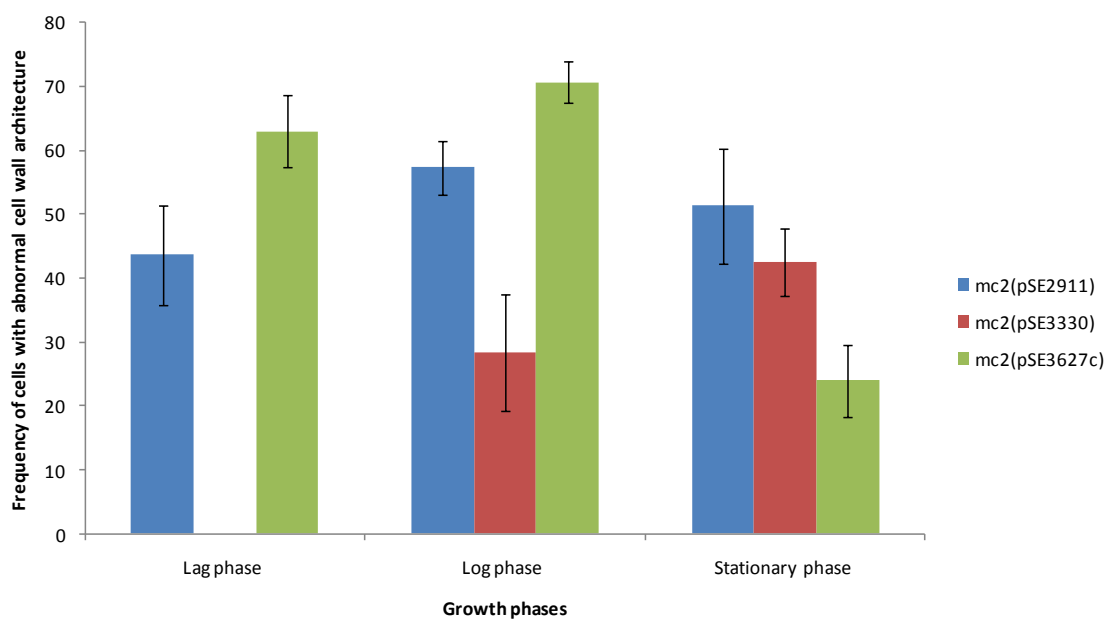
Examination of the cell surface by SEM revealed distinct cell morphology defects for the heterologous strains. To follow up on the effect of ectopic expression of *M. tuberculosis* DD-CPases on cell morphology, TEM was conducted on the recombinant strains. The strains were cultured as previously described and sampled at lag, log and stationary phases of growth. The samples were prepared for TEM as detailed in sections 2.16.6 and imaged with the Tecnai F20 Transmission Electron Microscope. TEM revealed two distinct cell wall defects for the heterologous strains: (I) the thickness of the wall was greatly increased and (II) the cell envelope displayed partial detachment from the cytoplasm, figure 3.2.10. To further demonstrate that the observed cell wall defects were significant, we quantified the total number of cells with abnormal

cell wall architecture and expressed as a percentage of the entire population, figure 3.2.11. The data revealed a significant increase of the abnormal cell wall phenotype for the  $mc^2(pSE2911)$  strain at 3 and 9 hours. The abnormal cell wall architecture for the  $mc^2(pSE3330)$  strain was only observed at log phase with abnormal cell wall defects observed at all growth phases for the  $mc^2(pSE2911)$  and  $mc^2(pSE3627c)$  strains.





**Figure 3.2.10.** Transmission electron micrographs of the heterologous *M. smegmatis* strains ectopically expressing *M. tuberculosis* DD-CPases at lag, log and exponential phases of growth. The inserts show an enlarged section of cells displaying abnormal cell wall architecture. The data demonstrated that ectopic expression of *M. tuberculosis* DD-CPases interferes with normal cell wall formation, resulting in cells with uneven cell wall architecture that appears to partially detach from the cytoplasm. Scale bar= 0.2 μm.



**Figure 3.2.11.** Quantification of cells displaying aberrant cell wall architecture resulting from increased expression of *M. tuberculosis* DD-CPases in *M. smegmatis* as revealed by TEM. The heterologous strain displayed abnormal cell wall characterized by increased thickness and partial detachment of the cell envelope from the cytoplasm. The frequency of cells displaying the cell wall defects increased for the mc<sup>2</sup>(pSE2911) and mc<sup>2</sup>(pSE3627c) at log phase with the mc<sup>2</sup>(pSE3330) strain displaying cell wall defects at log and stationary phases of growth. (*n*= 100)

### 3.3. Ectopic expression of *M. tuberculosis* DD-CPase homologues in wild type H<sub>37</sub>RvS strain

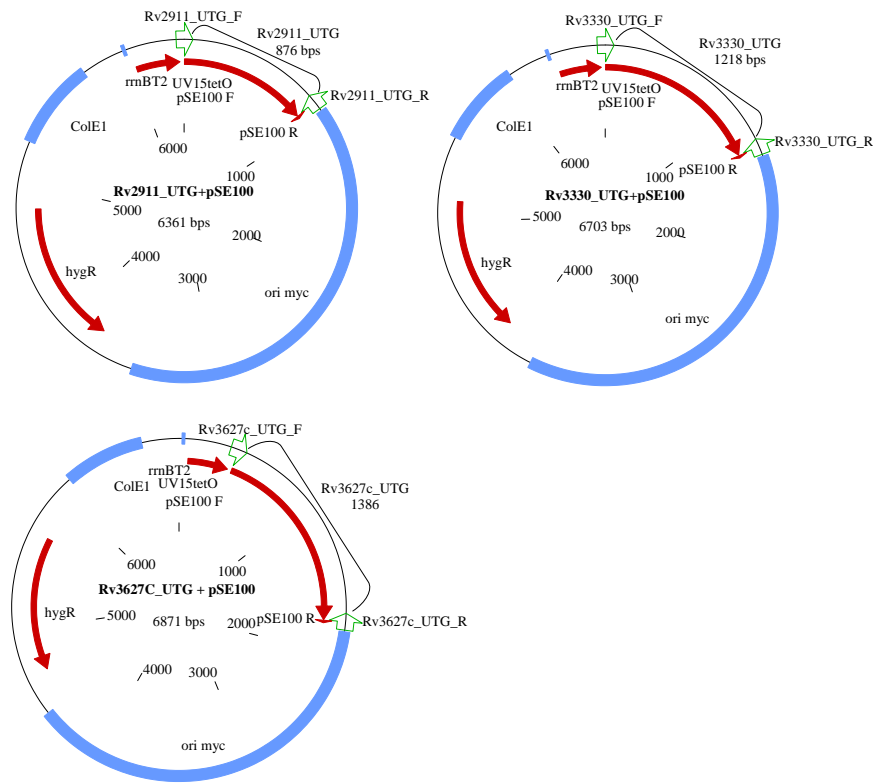
Data obtained for the heterologous *M. smegmatis* strains thus far strongly implicated *M. tuberculosis* DD-CPases in maintaining bacterial colony morphology, surface structure and sliding propensity, biofilm formation/maturation, growth in broth culture and normal cell length/division. We recognize that heterologous expression in *M. smegmatis* is a suitable system for characterization of the respective *M. tuberculosis* DD-CPase homologues, but there are various limitations of this system. The most important being that the biology of cell division may be different between *M. smegmatis* and *M. tuberculosis*. Considering this, we hypothesized that a side-by-side assessment of the three homologues in the native host would provide additional insight into the biological role of these proteins. In this component of the study, we aimed to

characterize the physiological function of *M. tuberculosis* DD-CPase homologues (previously expressed in *M. smegmatis*) through ectopic expression in wild type *M. tuberculosis* H<sub>37</sub>RvS.

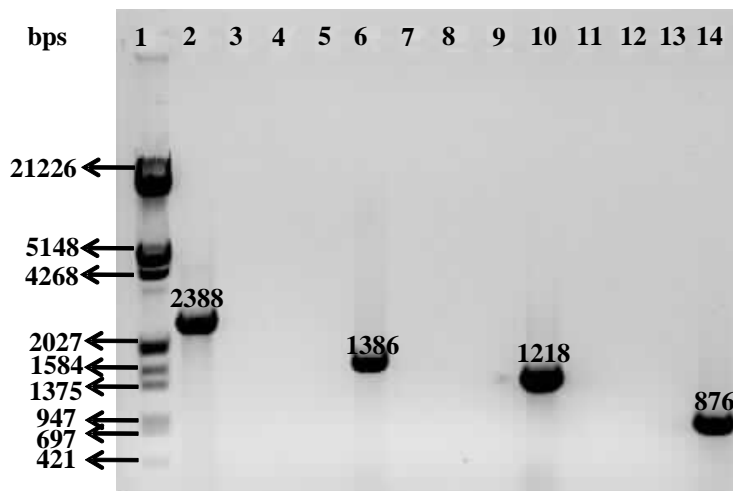
### **3.3.1. Construction and genotypic analysis of H<sub>37</sub>RvS strains that ectopically express individual DD-CPase-encoding genes**

The constructs carrying the untagged *M. tuberculosis* DD-CPases previously used for generation of the heterologous *M. smegmatis* strains as reported in section 3.2 were introduced into the wild type *M. tuberculosis* H<sub>37</sub>RvS strain by electroporation as described in section 2.12.2 to generate the H<sub>37</sub>RvS(pSE2911), H<sub>37</sub>RvS(pSE3330), H<sub>37</sub>RvS(pSE3627c) recombinant strains. The H<sub>37</sub>RvS(pSE100) control strain, that carried the empty vector, was also generated. In each case, a single transformant was selected and DNA extracted for PCR confirmation of whether the selected strain carried the correct gene as described in section 2.3.2. The PCR confirmation primers used for confirmation of the heterologous *M. smegmatis* strains were employed for confirmation of the recombinant H<sub>37</sub>RvS strains. PCR analysis of each strain confirmed that they carried the expected *M. tuberculosis* DD-CPase, figure 3.1.3.

A



B



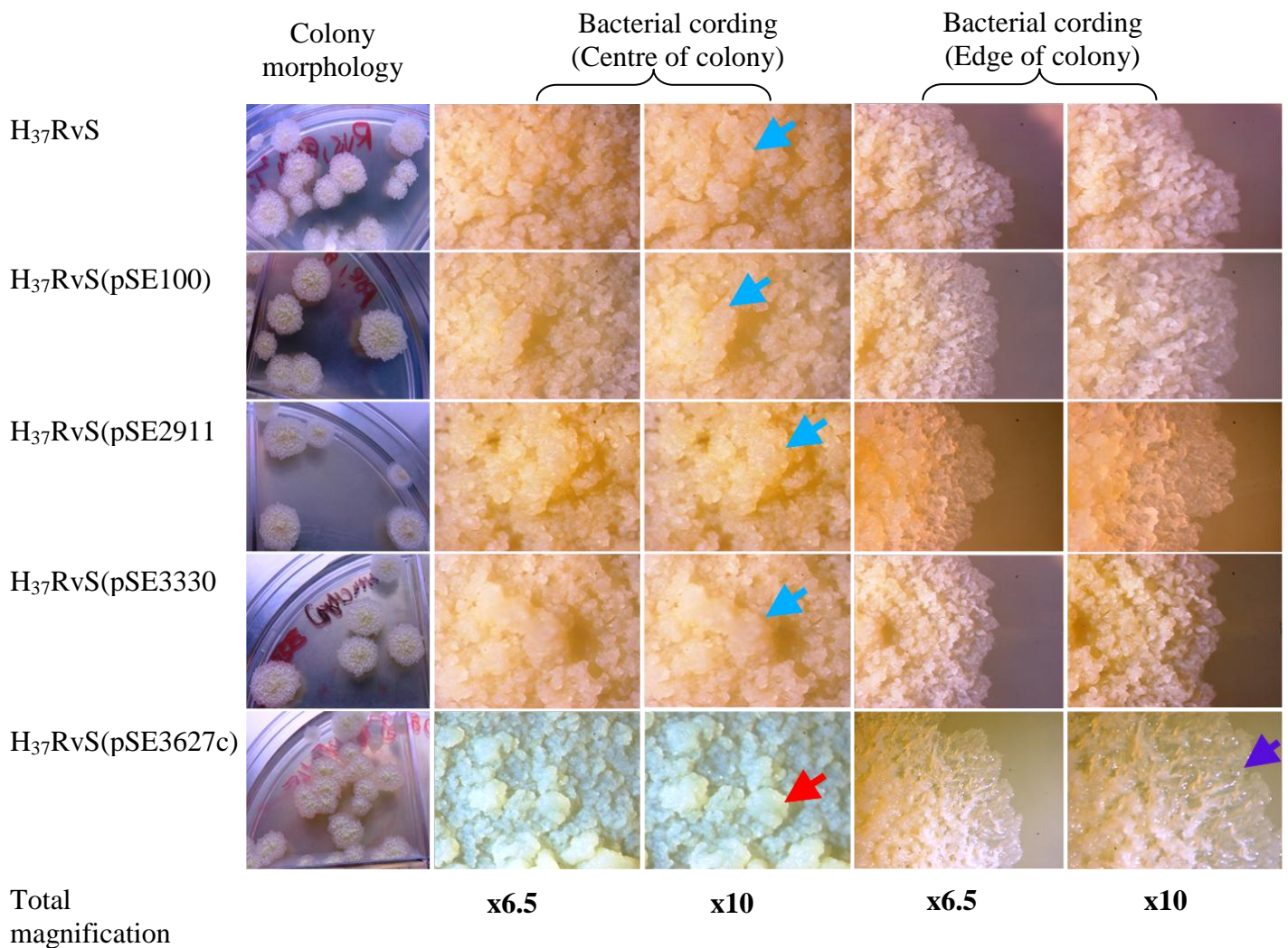
**Figure 3.3.1.** PCR confirmation of recombinant H<sub>37</sub>RvS strains carrying the *M. tuberculosis* DD-CPases ectopically expressed in H<sub>37</sub>RvS. (A) Primer binding sites for PCR confirmation. The primer binding sites are indicated by the green marker/arrows. Primer pairs (Rv2911\_UTG\_F+Rv2911\_UTG\_R), (Rv3330\_UTG\_F+Rv3330\_UTG\_R) and (Rv3627c\_UTG\_F+Rv3627c\_UTG\_R) were used for PCR confirmation of Rv2911, Rv3330 and Rv3627c, respectively. (B) PCR confirmation of Rv3627c, Rv3330 and Rv2911, respectively. Lane 1= Marker III, Lane 2= *narB* (Positive control), Lane 3= No template control, Lane 4= No forward primer control, Lane 5= No reverse primer control, Lane 6= Rv3627c, Lane 7= No template control, Lane 8= No forward primer control, Lane 9= No reverse primer control, Lane 10=



Rv3330, Lane 11= No template control, Lane 12= No forward primer control, Lane 13= No reverse primer control, Lane 14= Rv2911.

### **3.3.2 Ectopic expression of Rv3627c in H<sub>37</sub>RvS significantly affects bacterial cording**

The heterologous *M. smegmatis* strains displayed robust colony morphology and cording defects on solid 7H10 media when viewed at high microscopic resolution. To determine whether these are involved in maintaining normal colony morphology in H<sub>37</sub>RvS, single isolated colonies from the respective H<sub>37</sub>RvS recombinant strains were analysed using the Zeiss STEMI-2000c dissecting microscope as described in section 2.16.1. The recombinant H<sub>37</sub>RvS strains displayed no gross colony defects on plates as previously observed for the heterologous *M. smegmatis* strains and were characterized by surface cording comparable to wild type H<sub>37</sub>RvS colonies, figure 3.3.2. This suggested that the *M. tuberculosis* DD-CPase homologues are not involved in maintaining normal bacterial colony morphology in the H<sub>37</sub>RvS strain. To further confirm this, the resulting colonies of the recombinant strains were analysed for cording defects with the Zeiss STEMI-2000c dissecting microscope as described in section 2.16.1. At high microscopic resolution, we observed that the H<sub>37</sub>RvS(pSE2911) and H<sub>37</sub>RvS(pSE3330) recombinant strains were able to initiate cord formation which developed into the full serpentine cords comparable to those observed for the wild type H<sub>37</sub>RvS, figure 3.3.2. The H<sub>37</sub>RvS(pSE3627c) strain was also able to initiate cord formation but was unable to complete this process as demonstrated by the presence of short cords, which were not able to mature into the full serpentine cords as observed for the other strains, figure 3.3.2. This strain also displayed an abnormal colony edge, predominantly characterized by severe surface extensions with no observable serpentine cording. The data strongly demonstrated that Rv3627c is solely involved in maintaining normal bacterial cording in the H<sub>37</sub>RvS strain, with the remaining homologues displaying no observable role in this regard.



**Figure 3.3.2.** Colony morphology of the recombinant H<sub>37</sub>RvS strains ectopically expressing *M. tuberculosis* DD-CPases. The strains were cultured to log phase (OD<sub>600</sub>= 0.5-0.9) and plated on Middlebrook 7H11 agar to obtain single isolated colonies which were viewed at high microscopic resolution for cording defects. The blue arrows illustrate wild type colony cording distinguished by clearly defined serpentine cords. The H<sub>37</sub>RvS(pSE3627c) strain displayed short cords with surface extension that displayed no observable cording as shown by the red and purple arrows.

### 3.3.3. Ectopic expression of Rv3627c in H<sub>37</sub>RvS significantly delays biofilm formation and maturation

As mentioned earlier, colony defects are suggestive of alterations in cell surface properties that abolish cell-cell interaction/communication. We next sought to further study this by assessing the capacity of the H<sub>37</sub>RvS(pSE3627c) strain, which displayed colony morphology defects, to initiate and form mature biofilms. For comparison, we tested all the other strains, using the adopted air-media interface protocol as described in section 2.6.2. *M. tuberculosis* is a slow growing organism

and the formation of mature biofilms is different from *M. smegmatis*, requiring at least 5-weeks incubation at 37<sup>0</sup>C (Ojha et al., 2005., Ojha et al., 2008, Ojha et al., 2010 and Kulka et al., 2012). Based on this, biofilms were prepared in 6-well microtitre plates in minimal Sauton's media and sealed with biohazard tape for 6 weeks.

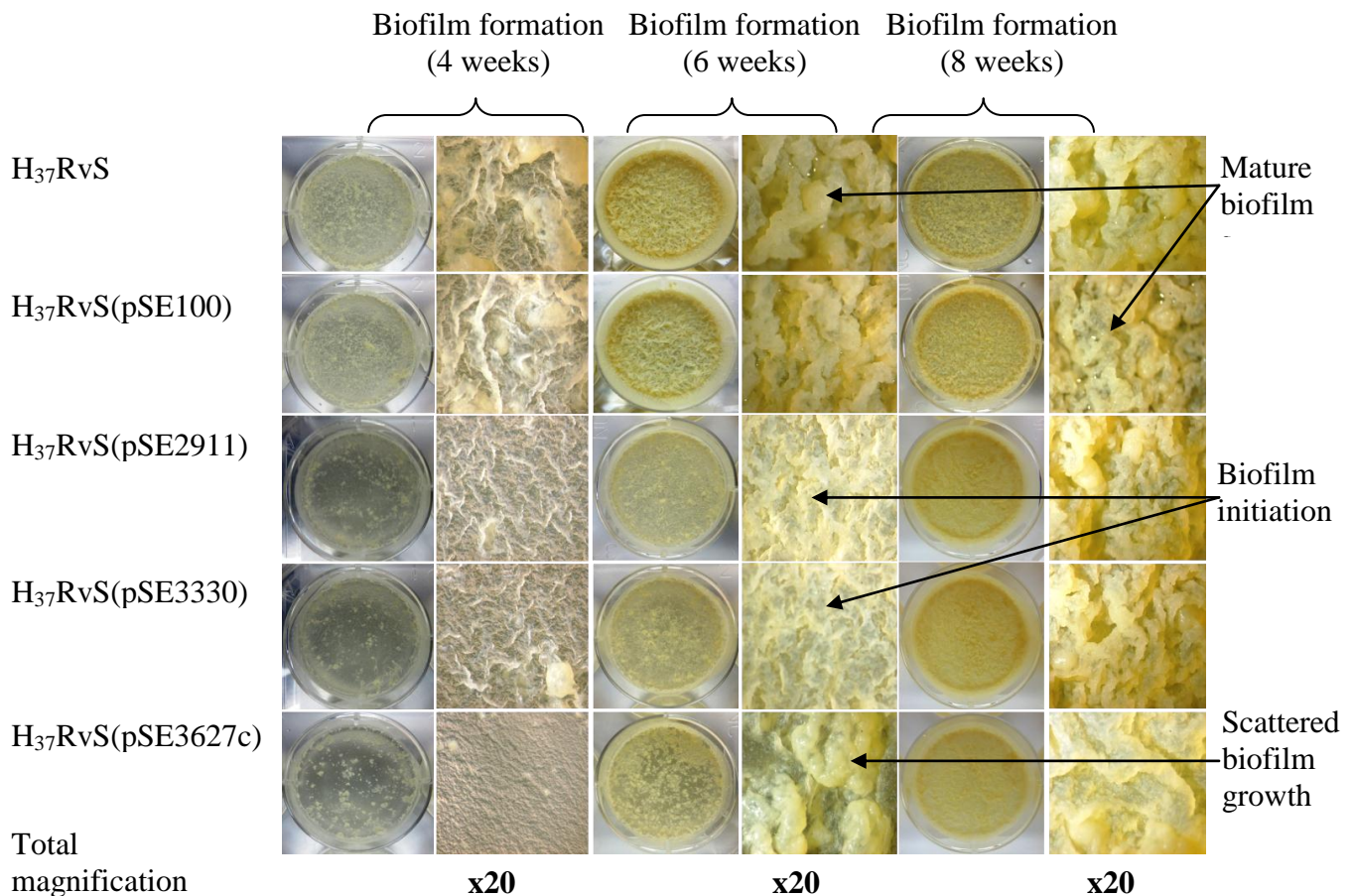
Following the 6 week incubation period, biofilm formation was assessed using the Zeiss STEMI-2000c dissecting microscope as described in section 2.16.2. Mature biofilms were observed for the H<sub>37</sub>RvS and H<sub>37</sub>RvS(pSE100) control strains after the 6-weeks of incubation. The recombinant H<sub>37</sub>RvS strains that ectopically expressed DD-CPases displayed indications of initiating biofilm formation but at this point, it was not conclusive whether these strains were competent to form mature biofilms, as previously reported for the heterologous *M. smegmatis* strains. To address this, it was decided to assess biofilm formation of the recombinant H<sub>37</sub>RvS strains at 4, 6 and 8 weeks after incubation, as this might provide more insight into the biofilm forming capacity of these strains.

Following the 4-week incubation period, the recombinant H<sub>37</sub>RvS strains displayed little initiation of biofilm formation when compared to the wild type H<sub>37</sub>RvS and H<sub>37</sub>RvS(pSE100) control strains, figure 3.3.3. Following the 6-week incubation period, the control strains formed fully mature biofilms as previously observed. The H<sub>37</sub>RvS(pSE2911) and H<sub>37</sub>RvS(pSE3330) strains displayed robust biofilm initiation after six weeks compared to that observed after 4-weeks. The H<sub>37</sub>Rv(pSE3627c) strain displayed poor biofilm initiation, accompanied by scattered biofilm growth after 6-weeks of incubation, figure 3.3.3.

Based on the observed biofilm initiation phenotype displayed by the recombinant H<sub>37</sub>RvS strains, it was hypothesized that these strains are competent for biofilm formation but require extended incubation. To address this, the strains were incubated for an additional 2 weeks. Following the 8 week incubation period, mature biofilms, comparable to wild type H<sub>37</sub>RvS and H<sub>37</sub>RvS(pSE100) control strains, were observed for the H<sub>37</sub>RvS(pSE2911) and H<sub>37</sub>RvS(pSE3330) strains. The

H<sub>37</sub>RvS(pSE3627c) at this point displayed robust biofilm initiation accompanied by slight biofilm maturation, figure 3.3.3.

The series of data obtained, from initiation of biofilm formation to maturation demonstrated that adherence is a prerequisite for biofilm growth and maturation as observed for the recombinant strains, which firstly displayed a gradual increase in the robustness of biofilm initiation then followed by biofilm maturation. The data demonstrated that in *M. tuberculosis*, colony morphology (or lack thereof) is not predicative of biofilm forming capacity. This is based on the observation for the recombinant H<sub>37</sub>RvS strains, with the H<sub>37</sub>RvS(pSE2911) and H<sub>37</sub>RvS(pSE3330) strains, which displayed no colony morphology defects but yielding delayed biofilm formation and maturation. Furthermore, the data point to a differential role for the respective DD-CPases in maintaining normal biofilm formation and maturation, with Rv3627c playing an important role in governing the rate at which biofilms form and mature.



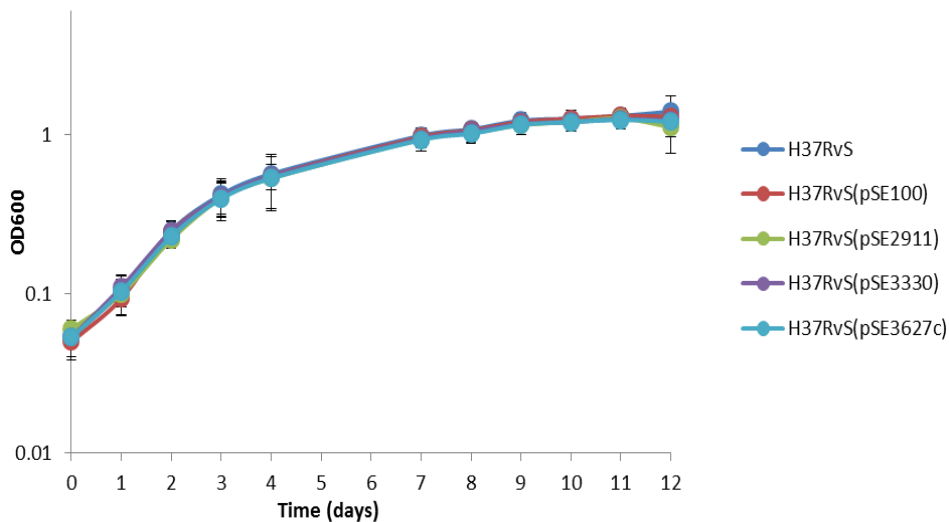
**Figure 3.3.3.** Biofilm formation of the recombinant H<sub>37</sub>RvS strains ectopically expressing *M. tuberculosis* DD-CPase homologues. The H<sub>37</sub>RvS(pSE2911) and H<sub>37</sub>RvS(pSE3330) strains displayed delayed biofilm formation at week 4 and 6, followed by the formation of fully mature biofilms after 8 weeks of incubation at 37<sup>0</sup>C. The H<sub>37</sub>RvS(pSE3627c) strain also displayed a similar delay in the biofilm formation but failed to form mature biofilms following the 8 week incubation period.

### 3.3.4. The H<sub>37</sub>RvS recombinant strains ectopically expressing the *M. tuberculosis* DD-CPases displayed no growth retardation in liquid 7H9 media

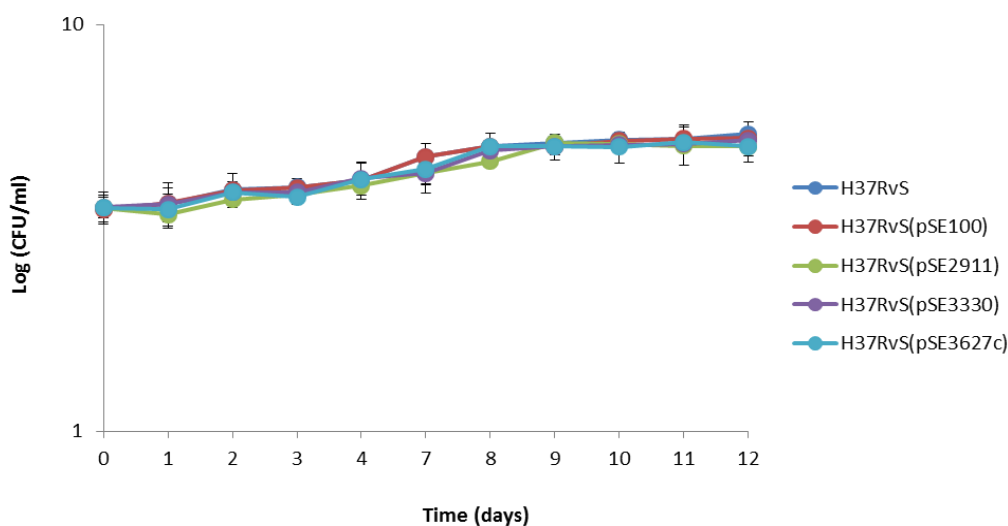
To further understand the physiological role of DD-CPases in bacterial proliferation, growth of the recombinant H<sub>37</sub>RvS strains was assayed in Middlebrook 7H9 media by monitoring the optical density of cultures at 600 nm (OD<sub>600</sub>) and plating for CFU/ml as described in section 2.16.4. The growth assay for the recombinant strains was started at OD<sub>600</sub> = 0.05 and monitored on a daily basis. The recombinant H<sub>37</sub>RvS strains displayed growth rates comparable to the H<sub>37</sub>RvS and H<sub>37</sub>RvS(pSE100) control strains, figure 3.3.4 A. The data suggested that ectopic expression of the respective *M. tuberculosis* DD-CPase homologues does not alter growth rates in H<sub>37</sub>RvS, in contrast to what was observed for the heterologous *M. smegmatis* strains. To validate this, the

CFU/ml for each strain was also plotted and compared to that of the H<sub>37</sub>RvS and H<sub>37</sub>RvS(pSE100) control strains, figure 3.3.4 B. The data confirmed that growth of the recombinant H<sub>37</sub>RvS strains was comparable to that of the H<sub>37</sub>RvS and H<sub>37</sub>RvS(pSE100) controls, with the recombinant strains displaying similar biomass at each time point.

A



B



**Figure 3.3.4.** Growth of the recombinant H<sub>37</sub>RvS strains in Middlebrook 7H9 media. (A) OD<sub>600</sub> and (B) CFU/ml of the recombinant H<sub>37</sub>RvS strains compared to the H<sub>37</sub>RvS and H<sub>37</sub>RvS(pSE100) control strains. The recombinant strains displayed growth rates comparable to the H<sub>37</sub>RvS and H<sub>37</sub>RvS(pSE100) control strains, suggesting that the respective *M. tuberculosis* DD-CPase homologues are not involved in regulating growth in *M. tuberculosis*.



### **3.3.5. Recombinant H<sub>37</sub>RvS strains ectopically expressing *M. tuberculosis* DD-CPases displayed an increase in bacterial cell length as revealed by scanning electron microscopy (SEM)**

To assess the impact of ectopic expression of *M. tuberculosis* DD-CPase homologues on cell surface structure of the recombinant H<sub>37</sub>RvS strains, SEM images were obtained for these strains as described in section 2.16.5. Briefly, cells were harvested at day 3, 7 and 10 representing the lag, log and stationary phases of growth. The OD<sub>600</sub> of each strain was measured before harvesting cells to confirm that the cultures had reached the growth phase in question. Cells were prepared for SEM and imaged using the high resolution FEI Nova NanoSEM 230 scanning electron microscope as described in section 2.16.5.

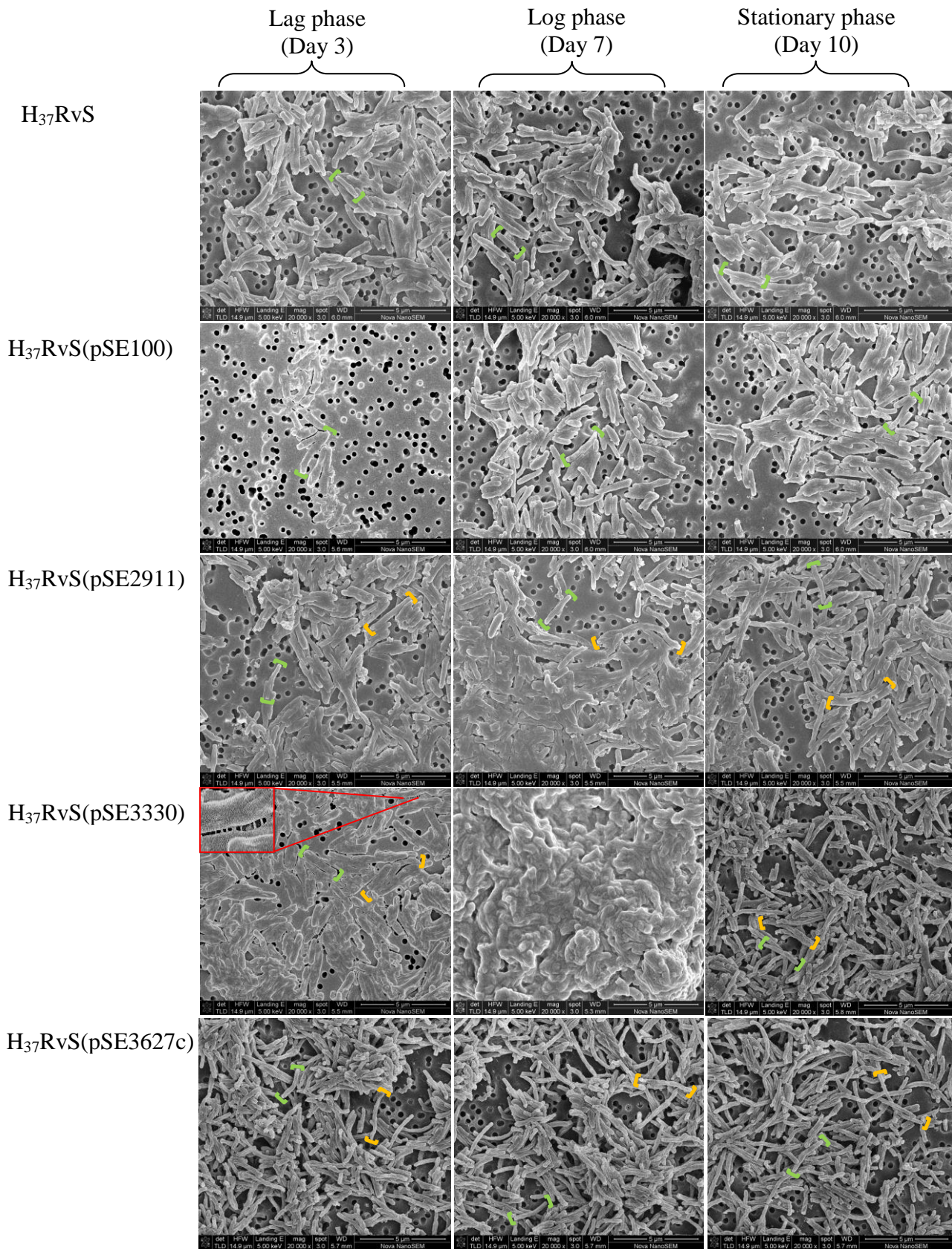
Ectopic expression of Rv2911 and Rv3627c in mc<sup>2</sup>155 reduced bacterial cell size as previously observed, pointing to a possible role for these proteins in maintaining cell length and/or rates of cellular elongation. Ectopic expression of these DD-CPases in H<sub>37</sub>RvS resulted in a mixed population of cells with varying cell length, displaying both normal and increased cell size, figure 3.3.5. To further substantiate that ectopic expression of DD-CPases results in an increase in the proportion of cells with increased cell length, cell size distribution of the recombinant strains was measured and compared to that of the control strains, figure 3.3.6. The data demonstrated an increase in the population of cells with a 3.5-5.0 µm cell size range. The increase in the proportion of cells with longer cell length point to a redundant role for the *M. tuberculosis* DD-CPases in maintaining normal bacterial cell length.

The recombinant H<sub>37</sub>RvS strains displayed none of the cell surface morphology defects previously observed for the heterologous *M. smegmatis* strains. Surface extensions were observed on cells harvested at lag phase for the H<sub>37</sub>RvS(pSE3330) strain as shown by the large insert in figure 3.3.5. These surface extensions, which are present on and around the majority of cells, appeared to be involved in cell-cell adhesion, with adjacent cells linked together by these surface

structures. In some cases, we observed breakage of the extensions linking the two separate cells, figure 3.3.5. To address the concern that the surface extensions could have arisen from the preparation procedure, we assessed SEM micrographs of the wild type and H<sub>37</sub>RvS(pSE100) control strains and found that they were absent from these strains. This suggested that the surface extensions arose directly from ectopic expression of Rv3330.

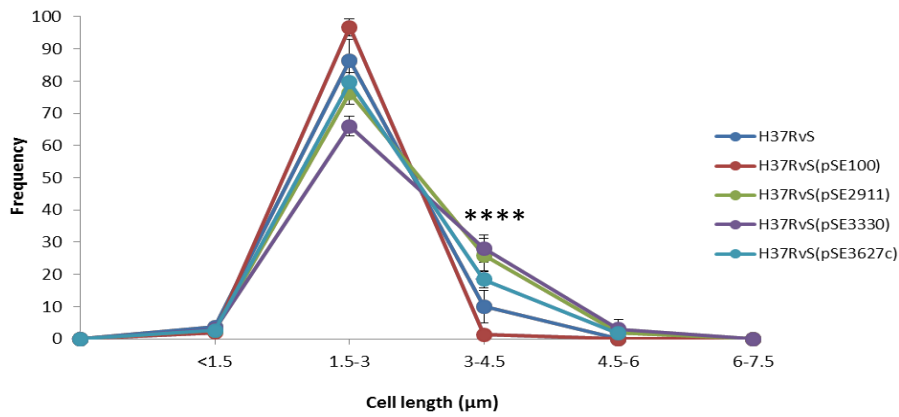
This is further substantiated by the observation that on SEM micrographs, this strain appeared as bacterial clusters for log phase cultures, further confirming that the observed surface extensions are not a result of the preparation procedure but are undoubtedly as a result of ectopic expression of Rv3330 in H<sub>37</sub>RvS. The physiological significance of the observed surface extensions as a result of ectopic expression of Rv3330, however, remains unclear and is beyond the scope of the current study.



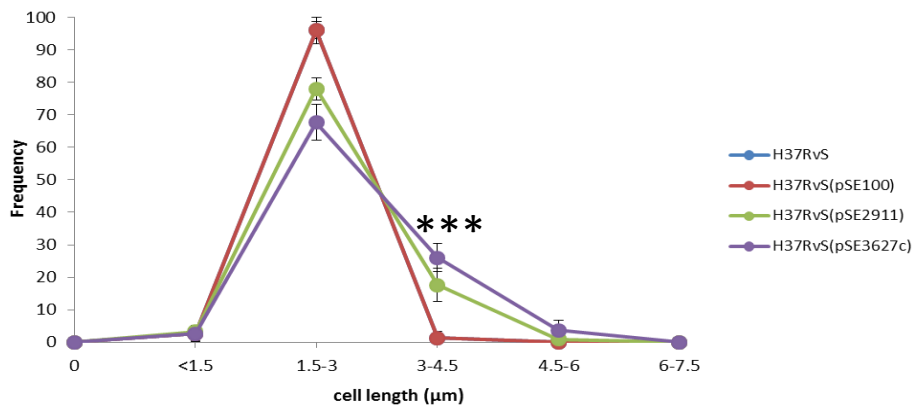


**Figure 3.3.5.** Cell surface of the recombinant H<sub>37</sub>RvS strains at lag, log and stationary phases of growth as revealed by SEM. The green parenthesis delineate a single cell of normal size with a 1.5-3 μm cell size range. The yellow parenthesis delineates cells with increased cell length with a cell size range of 3-4.5 μm observed for the recombinant strains. The enlarged insert demonstrates surface extensions/structures observed for H<sub>37</sub>RvS(pSE3330) strain at lag phase. Scale = 5 μm

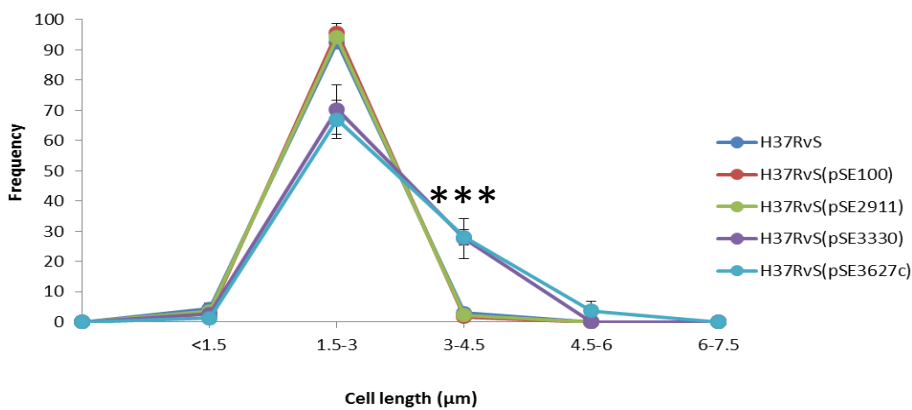
A



B



C



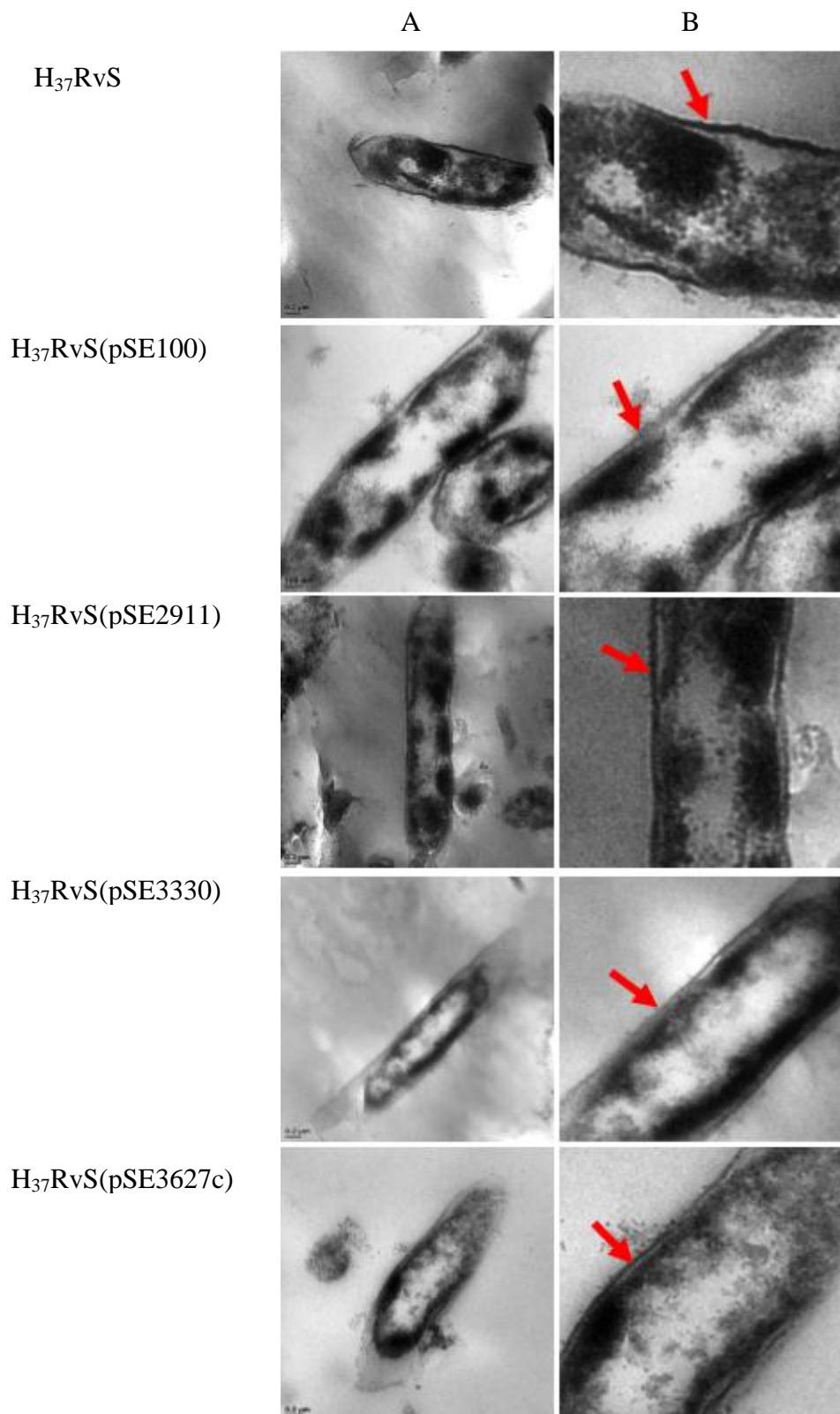
**Figure 3.3.6.** Cell length distribution of the recombinant H<sub>37</sub>RvS strains. The graphs represent cell length distribution at lag (A), log (B) and stationary (C) phases of growth. *M. tuberculosis* strains ectopically expressing DD-CPases displayed an increase in the proportion of cells with a 3-4.5 µm size range. In graph B, the cell length of the H<sub>37</sub>RvS(pSE3330) is excluded because of clumping of cells which precluded measurement of cell length for single. (n=100; \*\*\*, P<0.001; \*\*\*\*, P<0.00001)

### **3.3.6. Ectopic expression of *M. tuberculosis* DD-CPases in H<sub>37</sub>RvS does not affect normal bacterial cell wall architecture as revealed by transmission electron microscopy (TEM)**

Ectopic expression of *M. tuberculosis* DD-CPases in the heterologous *M. smegmatis* strains revealed a possible role for maintaining normal bacterial cell wall architecture. To examine these enzymes in the recombinant H<sub>37</sub>RvS strains, TEM was performed as detailed in section 2.16.6. Cells were harvested at lag, log and stationary phase for imaging with the Tecnai F20 Transmission Electron Microscope.

TEM requires large cultures volumes at each time point to obtain grids with sufficient cells for viewing. This is dependent on the growth phase, with lag phase cultures requiring at least 30 ml culture volume compared to stationary phase cultures. Due to strict operating conditions in the BSLIII laboratory, the culture volume was greatly reduced to 5 ml at each time point. This was a major disadvantage as empty grids for all strains were obtained for cultures harvested at lag and log phases of growth. A few images for each strain were obtained with stationary phase cultures and the micrographs demonstrated that ectopic expression of *M. tuberculosis* DD-CPase homologues does not affect cell wall morphology, figure 3.3.7. At this point, this conclusion is based on the micrographs obtained for the recombinant strains at stationary phase only, which may not appropriately represent the entire population.



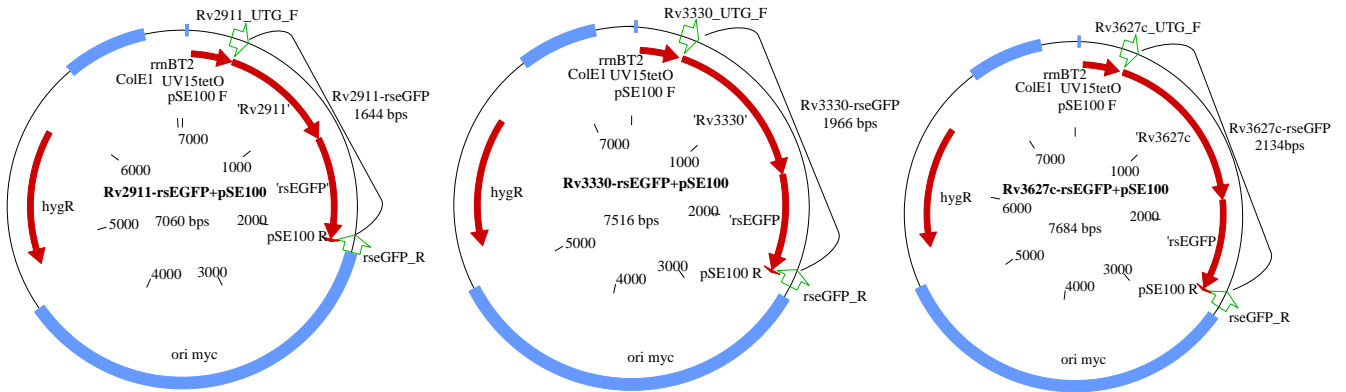


**Figure 3.3.7.** Transmission electron micrographs of the recombinant H<sub>37</sub>RvS strains obtained for stationary phase cultures. (A) scanning electron micrographs at x5700 magnification (B) depicts the zoomed images shown in A for each strain. The red arrows point to the enlarge cell wall/envelope of the respective strains. The data demonstrated that ectopic expression of the respective *M. tuberculosis* DD-CPase homologues in H<sub>37</sub>RvS does not affect bacteria cell wall architecture. Scale bar=0.2

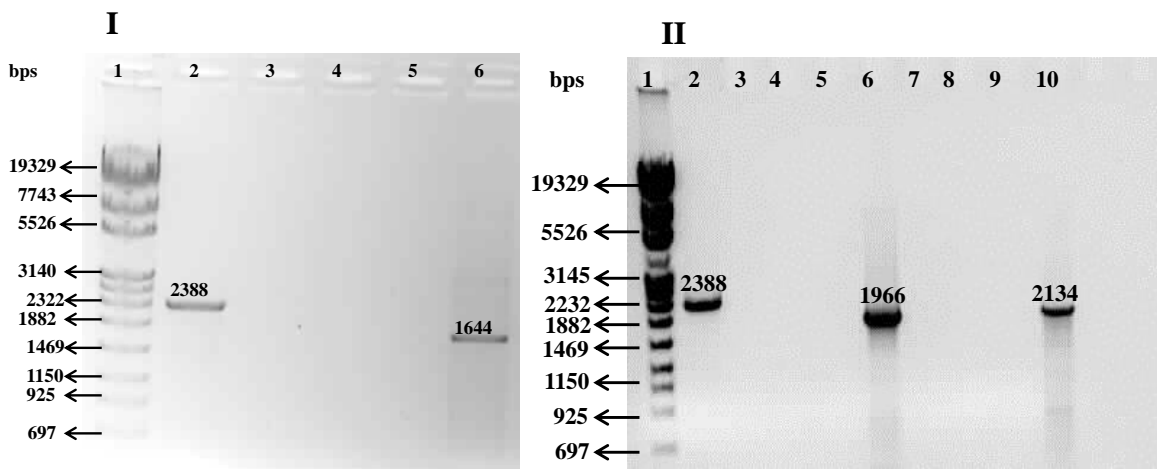
### **3.4. *M. tuberculosis* rseGFP tagged DD-CPase derivatives displayed polar, mid-cell and quarter cell position localization when ectopically expressed in *M. smegmatis***

Our data thus far strongly suggest that *M. tuberculosis* DD-CPases are involved in maintaining a variety of cellular processes. To understand where in the cell these proteins exert their effects, cellular localization of rseGFP C-terminally tagged DD-CPase derivatives were constructed by 3-way cloning into pSE100 as described in section 2.8.6. The constructs were confirmed by restriction profiling and sequencing and introduced into mc<sup>2</sup>155 by electroporation to generate the mc<sup>2</sup>(pSE2911-rseGFP), mc<sup>2</sup>(pSE3330-rseGFP) and mc<sup>2</sup>(pSE3627c-rseGFP) strains. A single colony was picked and DNA extracted to confirm by PCR whether the selected strain express the correct protein fusion. The PCR confirmation primers are listed in the Appendix (Appendix B). Figure 3.4.1 shows the primer binding sites for PCR confirmation of the respective DD-CPase fusion proteins cloned into pSE100 for the selected strains and PCR confirmation of the respective DD-CPase fusion proteins.

A



B



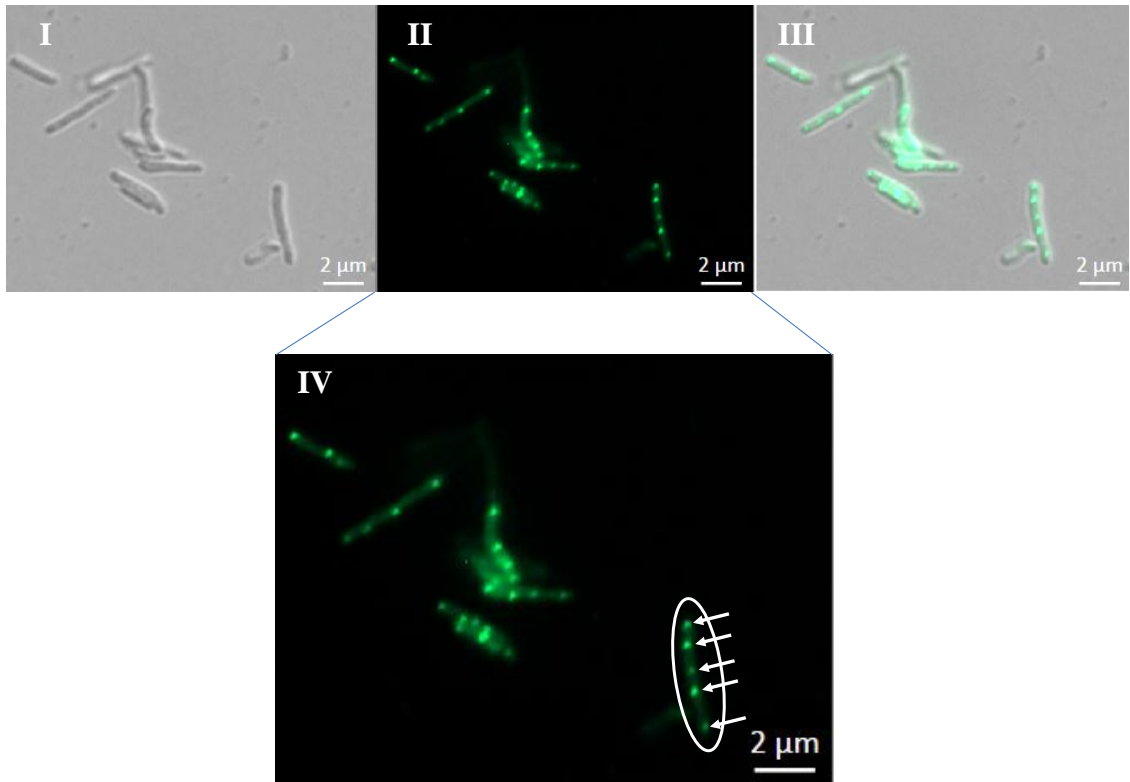
**Figure 3.4.1.** PCR confirmation of rseGFP C-terminally tagged *M. tuberculosis* DD-CPase derivatives. (A) Primer binding sites for PCR confirmation of rseGFP C-terminally tagged *M. tuberculosis* DD-CPase derivatives cloned into pSE100. The primer binding sites are indicated by the green marker arrows. Primer pair (Rv2911\_UTG\_F+rseGFP\_R), (Rv3627c\_UTG\_F+rseGFP\_R) and (Rv3330\_UTG\_F+rseGFP\_R) were used for PCR confirmation of Rv2911-*rseGFP*, Rv3330-*rseGFP* and Rv3627c-*rseGFP*. (B) PCR confirmation of rseGFP C-terminally tagged *M. tuberculosis* DD-CPase derivatives. (I) PCR confirmation of Rv2911-*rseGFP* fusion protein with annealing temperature at 72°C. Lane 1= Marker IV, Lane 2= *narB* (Positive control), Lane 3= No template control, Lane 4= No forward primer control, Lane 5= No reverse primer control, Lane 6= Rv2911-*rseGFP* protein fusion. (II) PCR confirmation of Rv3330-*rseGFP* and Rv3627c-*rseGFP* protein fusions with annealing temperature at 70°C and 72°C respectively. Lane 1= Marker IV, Lane 2= *narB* (Positive control), Lane 3= No template control, Lane 4= No forward primer control, Lane 5= No reverse primer control, Lane 6= Rv3330-*rseGFP* fusion, Lane 7= No template control, Lane 8= No forward primer control, Lane 9= No reverse primer control, Lane 10= Rv3627c-*rseGFP*.

The heterologous *M. smegmatis* strains ectopically expressing the fusion proteins were subjected to the same assays conducted for the heterologous *M. smegmatis* strains ectopically expressing the untagged DD-CPases as reported in section 3.2 to confirm that the rseGFP fluorescence tag is functional and does not interfere with the activity of the respective DD-CPases. The strains ectopically expressing the untagged and rseGFP tagged protein derivatives yielded similar results for the assays conducted (data not shown), confirming that the rseGFP fluorescent tag is functional and that its activity does not interfere with that of the respective DD-CPases.

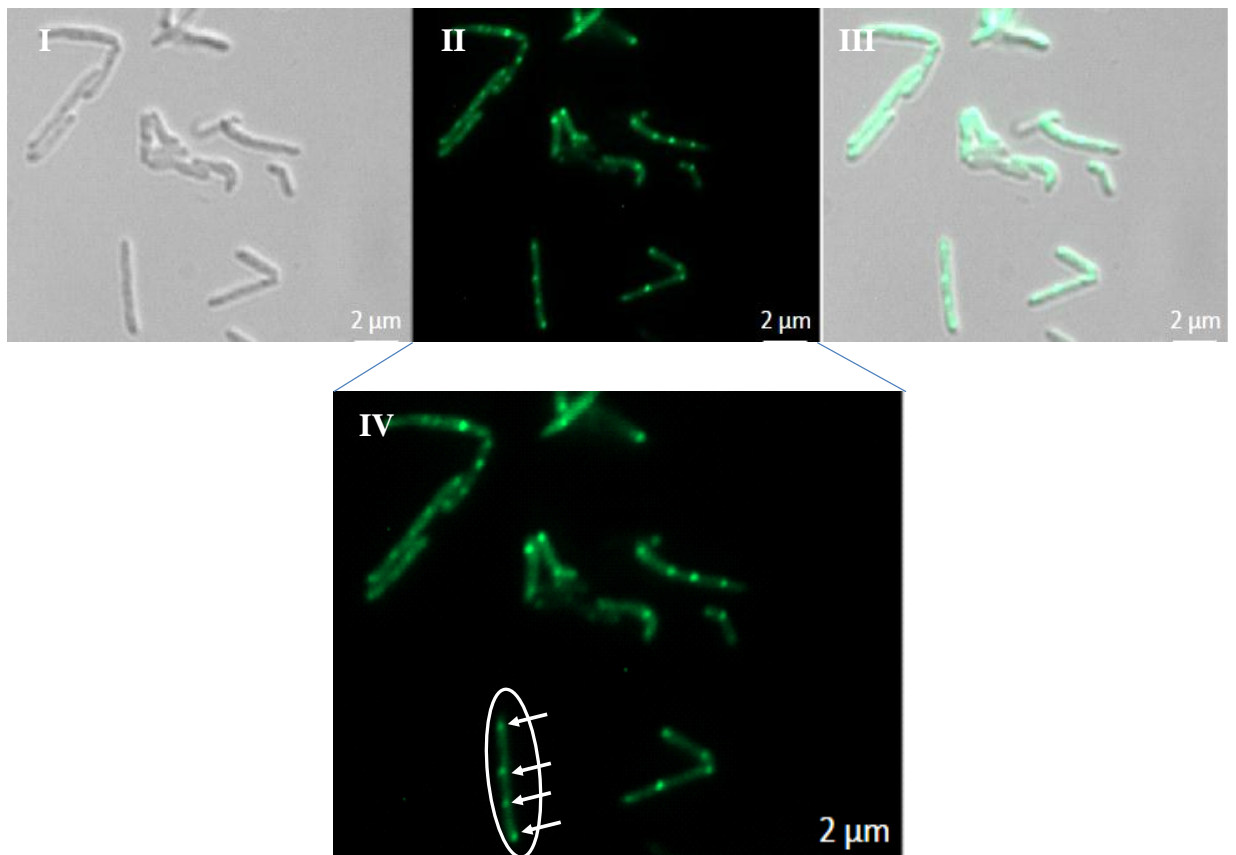
The heterologous *M. smegmatis* strains carrying the fusion proteins were cultured in 7H9 to log phase ( $OD_{600} = 0.5-0.9$ ). Cells were heat fixed on cover slips after three times washes with PBS as detailed in section 2.17, heat fixed and mounted on slides with fluoromount for imaging with the Zeiss 100x, 1.46 numerical aperture objective mounted to an Axio Observer Z1 base. The images obtained for cellular localization of the DD-CPase in the heterologous strains are shown in figure 3.4.2.

The *M. tuberculosis* DD-CPases displayed various patterns of localization, figure 3.4.2. To determine the most consistent pattern of localization for each fusion protein in each strain, we quantified distribution of the different localization patterns displayed by respective DD-CPase fusion proteins, Figure 3.4.3. A unique pattern of cellular localization for the *M. tuberculosis* DD-CPases in the heterologous strains with foci observed at both poles, mid-cell and quarter cell position was determined to be the most consistent pattern of localization, figure 3.4.3. To our knowledge, the observed cellular localization for the *M. tuberculosis* DD-CPase fusion proteins in *M. smegmatis*, has not been reported for any of the known proteins involved in PG remodelling.

Rv2911 localization

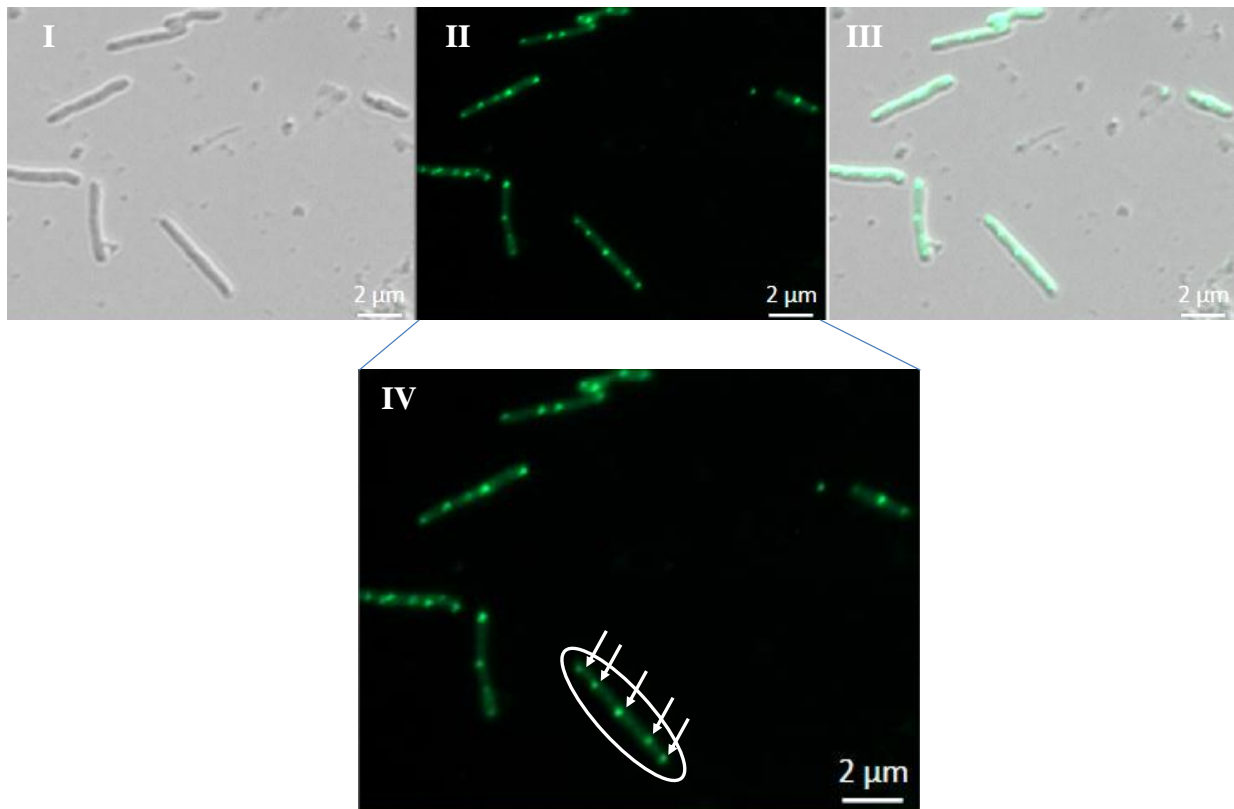


Rv3330 localization

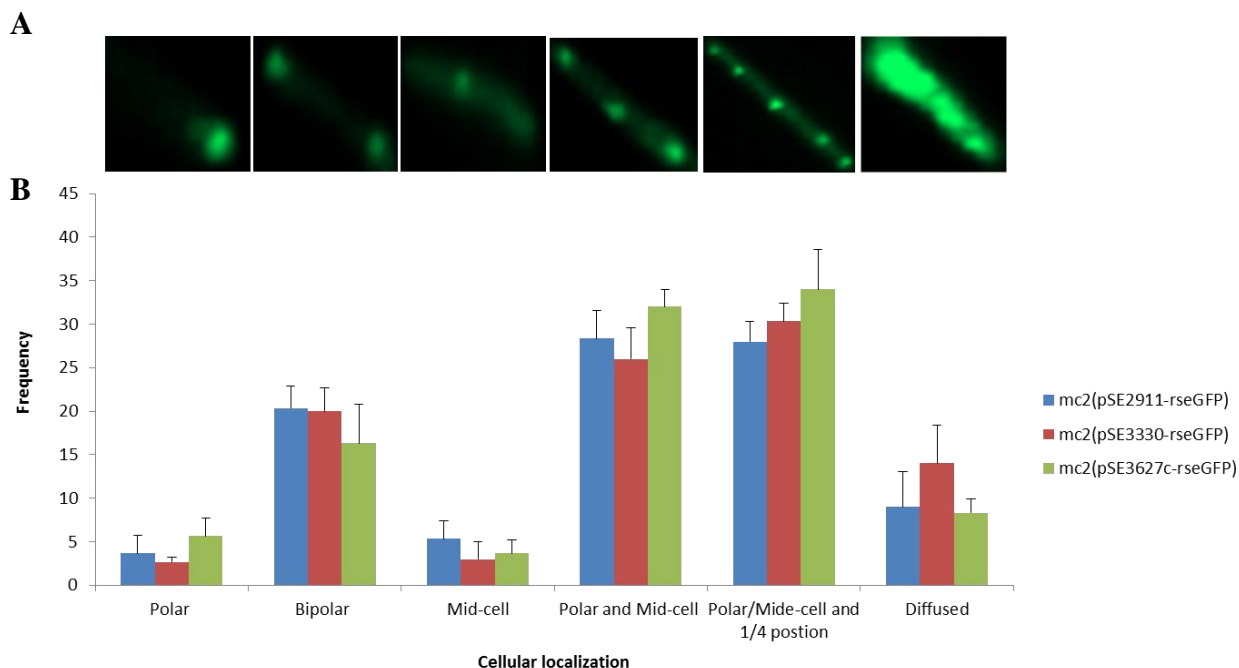




### Rv3627c localization



**Figure 3.4.2.** Cellular localization of C-terminally tagged rseGFP *M. tuberculosis* DD-CPase derivatives in *M. smegmatis*. The heterologous strains were cultured to log phase and heat fixed before mounting on slides with fluoromount for imaging. The panels marked (I), (II) and (III) show the images obtained through the DIC channel, fluorescence channel and a merge of both the DIC and fluorescence channel respectively. The panel marker (IV) shows an enlarged image obtained through the fluorescence channel



**Figure 3.4.3.** Quantification of cellular localization of rseGFP tagged *M. tuberculosis* DD-CPase fusion proteins ectopically expressed in mc<sup>2</sup>155. The image labeled (A) shows the different patterns of localization observed for the *M. tuberculosis* DD-CPase derivatives and (B) is a graphic representation of the distribution of cellular localization for the fusion proteins. The data revealed that the three proteins localize at both poles, mid-cell and quarter cell position. ( $n=100$ )

#### 4. Discussion

As with any infectious agent, the successful nature of *M. tuberculosis* as a pathogen is primarily related to its inherent ability to grow and proliferate in the presence of both immune and drug assault. Consequently, a substantial understanding of the different processes that underpin growth and cell division in this organism is of utmost importance for the design of effective, target based novel anti-TB drugs. Bacterial growth and division is a sophisticated process, involving the coordinated expansion and cleavage of the different layers in the cell envelope, a process mediated by multiple enzymes. In this study, we focused our attention on the mycobacterial PG degrading DD-CPases, a group of enzymes implicated in maintaining normal growth and survival in other organisms (Nelson and Young, 2001). Disease progression and viability of *M. tuberculosis*, involves the maintenance of a structurally functional cell wall and the PG layer in this case is of particular importance as it anchors the MAs and AG to create the PG-AG-MAs

complex. As mentioned earlier, PG remodelling involves the activity of multiple enzymes, some of which interact with various proteins to fulfil their function. One of the aims of this study was to determine whether mycobacterial DD-CPases exert their effect as singular enzymes or through interaction with various proteins as observed for other PG remodelling enzymes. This research question was based on two important observations, which include: (I) In other organisms, experimental and crystallographic data point to an interaction between PBPs, to allow for PG remodelling during cellular growth or division (Kuzin et al., 1995; Sauvage et al., 2008; van der Ploeg et al., 2013, Hett et al., 2007, Hett et al., 2008) (II) available data on mycobacterial elongation and division, demonstrated that these two processes are dynamic, directed by protein complexes requiring the participation of PBPs (Mukherjee et al., 2009; Hett et al., 2010; Kieser and Rubin, 2014). Considering this, we sought to determine if mycobacterial DD-CPases, which are predicted to be important in maintaining normal mycobacterial growth and survival by regulation of the amount of PG cross-linking, are part of any of the identified cell wall remodelling complexes, the divisome and/or elongasome.

To further expand on the current knowledge and physiological function of mycobacterial DD-CPases, we identified putative interacting partners for two *M. smegmatis* DD-CPases, MSMEG\_2433 and MSMEG\_6113, using the mPFC assay. These two proteins were chosen based on unpublished data from the CBTBR which suggested that the former was expressed in high transcript abundance and the latter was essential for growth (C. Ealand and B. Kana, unpublished). The assay revealed multiple putative interacting partners for these proteins demonstrating that they possibly exert their effect through multi-protein complexes, table 3.1.2 and table 3.1.3. Whilst we identified numerous partners, in the discussion that follows, we focus on those that are either periplasmic/membrane bound and have been reported to be involved in PG remodelling, with predicted effects on cell elongation or division.

## **4.1. Interaction between MSMEG\_2433 and MSMEG\_6113 with PBPs**

### **4.1.1. MSMEG\_6113 and Beta lactamase penicillin-binding protein**

$\beta$ -lactamases are a group of proteins with the ability to bind and hydrolyse  $\beta$ -lactam antibiotics such as penicillin and are the major contributing factor to  $\beta$ -lactam resistance (Bush et al., 1995). Deletion of BlaC and BlaS, the major  $\beta$ -lactamases in *M. smegmatis* and *M. tuberculosis*, abolished the intrinsic resistance of these strains to  $\beta$ -lactam antibiotics (Flores et al., 2005). This observation demonstrated an essential role of  $\beta$ -lactamases for cell survival and viability in mycobacteria. Putative interaction of MSMEG\_6113 with a  $\beta$ -lactamase, points to an additional role for this DD-CPase in maintaining cell survival either through the modulation of  $\beta$ -lactamase activity or by modifying PG during  $\beta$ -lactam treatment.

### **4.1.2. MSMEG\_2433 and Penicillin binding protein transpeptidase domain protein (PbpA)**

PbpA is a class B PBP that plays a role in bacterial growth (Wei et al., 2003). In *M. smegmatis*, PbpA localizes at the septum with a significant role in cell division as demonstrated by cell division defects in the PbpA mutant (Dasgupta et al., 2006). Genetic complementation of a PbpA *M. smegmatis* mutant with the *M. tuberculosis* counterpart reverses the cell growth and division defects (Dasgupta et al., 2006), suggesting a conserved physiological role for this protein in mediating cell division. Amino acid sequence comparison of PbpA from five mycobacterial species revealed that this protein is indeed highly conserved (Dasgupta et al., 2006). It has been demonstrated that the phosphorylation status of PbpA, by either protein kinase PknA or PknB regulates the activity of PbpA (Kang et al., 2005; Dasgupta et al., 2006; Kieser et al., 2015; Chaba et al., 2002).

These protein kinases are in turn regulated by autophosphorylation or through phosphatase activity. In *M. tuberculosis*, PknB is regulated by a phosphatase, PstP (Boitel et al., 2003). It is unclear whether the same system prevails in *M. smegmatis*. Cellular localization data places PbpA at the septum and poles of dividing cells (Kieser et al., 2015). Considering that PbpA is involved

in synthesis of the PG polymer, the interaction between this protein and MSMEG\_2433, suggests that the latter may be involved in regulating PG synthesis at the cell poles and septum.

#### **4.1.3. MSMEG\_2433 and the bifunctional penicillin-binding protein A1/1B (PonA1)**

PonA1, encoded by MSMEG\_6900 in *M. smegmatis* is a bi-functional class A PBP, with separate domains that harbour transglycosylation and transpeptidation activities, which are required for cross-linking of new PG units to the existing polymer in the periplasm (Machowski et al., 2014). PonA1 localizes at the poles and at the septum of actively growing cells (Hett et al., 2010). In mycobacteria, PonA1 is involved in the regulation of multiple cellular processes, with the transpeptidase domain being dispensable for growth and viability (Kieser et al., 2015). The PonA1-regulated processes include the maintenance of normal bacterial cell length and morphology and the establishment of new poles, both of which are required for virulence during the murine model of TB infection (Kieser et al., 2015). As previously mentioned for PbpA, the activity of PonA1 is also subject to regulation by phosphorylation (Prisic et al., 2010; Kieser et al., 2015), further signifying the role of protein kinases in regulating key cell division processes. The interaction of MSMEG\_2433 with PonA1 suggests that PonA1 recruits MSMEG\_2433 at the poles following establishment of the new pole. This also suggests that in addition to FtsH (predicted in this study to inhibit FtsZ (see section 4.2.1), PBPs may also be involved in the septal recruitment of MSMEG\_2433 at the division site.

#### **4.1.4. MSMEG\_2433 and the penicillin-insensitive transglycosylase/penicillin-sensitive transpeptidase (PonA2)**

PonA2 is also a bifunctional class A PBP (Machowski et al., 2014). *M. smegmatis* and other soil mycobacteria encode an additional homologue of PonA2, annotated as PonA3 (Patru and Pavels, 2010; Machowski et al., 2014). PonA2 in *M. smegmatis* is implicated in maintaining viability under nutrient starvation or during stationary phase growth (Keer et al., 2000; Patru and Pavels, 2010). The mechanism leading to PonA2 adaptation to these conditions is unclear, with opposing

ideas proposed with respect to how PonA2 contributes to cell viability under stressful conditions (Goffin and Ghuysen, 2002; Mainard et al., 2000; Mainard et al., 2005). The study by Patru and Pavels, 2010 suggested that adaptation to stressful environment requires the maintenance of cell wall integrity facilitated by PonA2 (Patru and Pavels, 2010).

Currently, it is unknown whether PonA2 is part of the divisome or elongasome complex in mycobacteria. The protein harbours a PASTA domain, previously identified in other PG associated proteins such as PbpA, which is proposed to direct proteins to the division site (Dasgupta et al., 2016). In addition to the PASTA domain, PonA2 also consists of a proline-rich region predicted to mediate protein interaction. Based on these two features we propose that PonA2 is first recruited to the division site of actively growing cells and following the correct placement at the septum by the PASTA domain, the proline-rich region recruits MSMEG\_2433 through protein interaction, facilitating proper septum cleavage. The septal localization of PonA2 has been confirmed in a study demonstrating that PonA2 acts to modulate the synergistic association of RpfB and RipA (Hett and Rubin, 2010), both of which co-localize at the septum (Hett et al., 2007; Hett et al., 2008).

#### **4.1.5. MSMEG\_6113 and Penicillin binding proteins B (PbpB)**

PbpB is a class B PBP and shares similar characteristics with PbpA. This protein is recruited to the septum of dividing *M. smegmatis* cells, mediating cell division as deletion of PbpB results in altered cell length (Dasgupta et al., 2006). The interaction of MSMEG\_6113 with PbpB suggests a possible role in cell division.

### **4.2. Interaction between MSMEG\_2433 and MSMEG\_6113 with other periplasmic/membrane bound proteins**

#### **4.2.1. MSMEG\_2433 and the ATP-dependent zinc metalloprotease FtsH**

FtsH is a membrane anchored ATP-dependent, zinc metalloprotease belonging to the AAA family of ATPases (Herman et al., 1995). It is conserved in prokaryotes but also found in chloroplasts

and mitochondria of eukaryotic species (Ito and Akiyama. 2015; Lindahl et al., 1996). In prokaryotes, it acts as a quality control protein (Fischer et al., 2002), assisting in protein folding and degradation, directly maintaining cell viability during bacterial development (Gottesman, 1996). In *B. subtilis*, a GFP tagged FtsH fusion displayed mid-cell localization, a preferential site for FtsZ polymerization in actively growing cells (Wehrl et al., 2000). In addition, deletion of this gene in *B. subtilis* results in the formation of cellular filaments (Wehrl et al., 2000). This observation points to two possible roles for FtsH, either as a component of the divisome complex where it facilitates cleavage of the septum or as a direct inhibitor of FtsZ polymerization at inappropriate sites during cell growth. The latter is substantiated by demonstration that in *E. coli*, *in vitro* assays confirmed that FtsZ is subjected to degradation by FtsH (Anilkumar et al., 2001; Srinivasan et al., 2006; Srinivasan et al., 2008), suggesting that FtsH is a negative regulator of FtsZ. Genetic complementation of a *E. coli* FtsH mutant with *M. tuberculosis* FtsH, further revealed that the latter is proteolytically active against the heat shock transcription factor  $\sigma^{32}$ , phage  $\lambda$ CII and the SecY proteins, which are the other substrates of FtsH (Srinivasan et al., 2006). Based on this observation, we predict that the mycobacterial FtsH might also be active against FtsZ, inhibiting its polymerization over replicating chromosomal DNA during cell growth and division. In *C. crescentus*, overproduction of FtsH resulted in increased tolerance to stress, with mutant strains showing reduced efficiency in differentiation of swarmer cells into stalk cells, accompanied by cell division defects (Fischer et al., 2002), further signifying the role of FtsH in maintaining normal cellular development, probably through regulation of FtsZ activity. The possible interaction of MSMEG\_2433 with FtsH, most likely at the septum, suggests that MSMEG\_2433 may be involved in the pathway(s) that mediate correct spatial and temporal placement of the septum.

#### **4.2.3. MSMEG\_2433 and UDP-diphospho-muramoylpentapeptide beta-N-acetylglucosaminyltransferase (MurG)**

The MurG glycosyltransferase catalyzes the final cytoplasmic step of PG biogenesis, mediating the transfer of GlcNAc from UDP-GlcNAc to lipid I (Mengin-Lecreux et al., 1991, Tayler et al., 2010). The product of this reaction, Lipid II, is translocated across the membrane for processing and incorporation into the existing PG polymer by PBPs. In *E. coli*, MurG displayed scattered localization over the entire length of the cell with a distinct preference for the mid-cell (Mohammadi et al., 2007). Further analysis of MurG localization revealed that this mid-cell localization of MurG was dependent on the formation of a mature divisome, and that lateral localization was dependent on the presence of MreCD (Mohammadi et al., 2007), required for shape maintenance in rod-shaped bacteria. The observed lateral and mature divisome dependent localization suggest a possible role for MurG in regulating lateral growth and PG synthesis at the septum. In mycobacteria, a recently identified FtsZ-interacting protein, SepF, also interacts with MurG (Gupta et al., 2015), implicating MurG in linking the two distinct processes, PG biogenesis and cell division. Our identification of possible interaction between MSMEG\_2433 and MurG is indicative of further complexity in these and related processes.

#### **4.2.4. MSMEG\_2433 and UDP-N-acetylenolpyruvoylglucosamine reductase (MurB)**

UDP-N-acetylenolpyruvoylglucosamine reductase is encoded by MurB. This protein is involved in the second cytoplasmic step of PG biogenesis. Following MurA mediated production of UDPGlcNAcEP, MurB reduces the phosphoenolpyruvate to produce UDPMurNAc (Matsaou et al., 2003). Currently, there is no literature linking the activity of the MurB reductase to either cell division or elongation and its interaction with MSMEG\_2433 requires further confirmation.

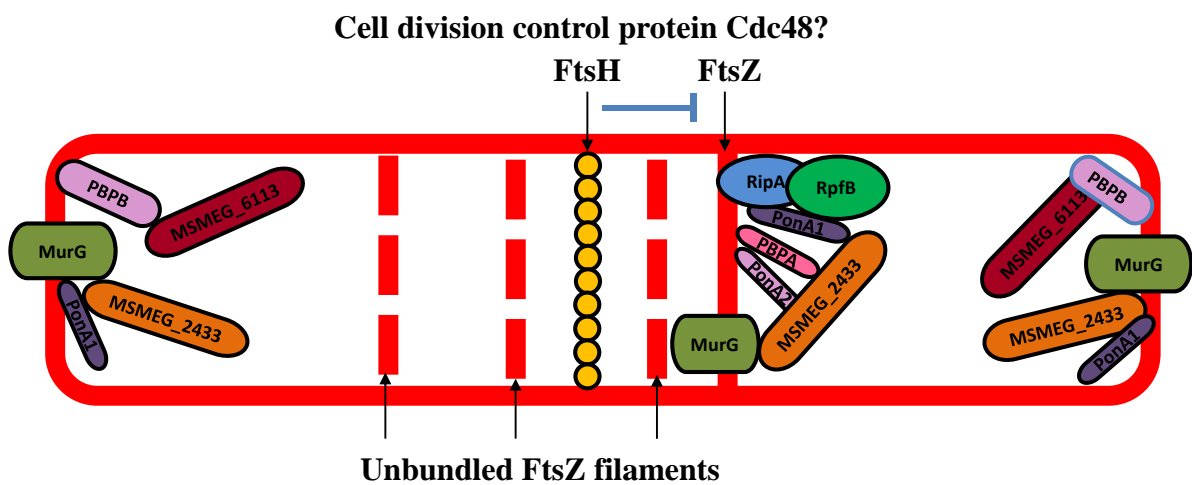


#### 4.2.5. MSMEG\_6113 and the cell division control protein Cdc48

The Cdc48 cell division protein is relatively uncharacterized in prokaryotes, belonging to the ATPase family of proteins along with FtsH that acts as molecular chaperone and negative regulator of FtsZ. Thus, it is unclear whether this protein also affects cell division in a mechanism mediated by FtsH, or whether it is involved in regulating other cellular processes unrelated to FtsH. In *Saccharomyces cerevisiae*, this protein is required for spindle disassembly at the end of mitosis (Cao et al., 2003), suggestive of a cell-cycle regulatory role for Cdc48 in mycobacteria.

#### 4.3. Proposed model for biological role of MSMEG\_2433 and MSMEG\_6113

Considering the above-mentioned protein interactions, and the cellular localization of the interacting partners we propose a model for the cellular localization and physiological role of MSMEG\_2433 and MSMEG, figure 4.1.1.



**Figure 4.1.1.** A proposed model for the function of MSMEG\_2433 and MSMEG\_6113. Shown are MSMEG\_2433 and MSMEG\_6113 and their putative interacting partners, with proposed roles, either in cell elongation or division. Based on protein interaction data, we predict that both MSMEG\_2433 and MSMEG\_6113 are present at the pole and at mid-cell, interacting with well-known proteins involved in either cell elongation or division. Additionally, the model proposes that MSMEG\_2433 is involved in the correct placement of FtsZ, through interaction with FtsH.

#### 4.4. Ectopic expression of *M. tuberculosis* DD-CPase homologues

##### 4.4.1. *M. tuberculosis* DD-CPases and maintenance of normal colony morphology

Colony morphology of infectious pathogenic bacteria influences virulence and disease progression (Simpson et al., 1987; Darzins and Fahr, 1956; Bernut et al., 2014). Therefore, an enhanced understanding of the different factors that contribute to changes in colony morphology is crucial for drug development (Kansal et al., 1998). In mycobacteria, the maintenance of normal colony morphology is dependent on multiple factors, including *pcaA* and *lsr2* gene products (Glickman et al., 2000; Chen et al., 2006). Bourai et al., (2012) demonstrated a role for *M. tuberculosis* Rv2911-encoded DD-CPase in maintaining normal colony morphology when ectopically expressed in *M. smegmatis*. In our study, we sought to build on these observations by carrying out a side-by-side assessment of functionality of all three DD-CPase encoding genes in *M. tuberculosis*. We appreciate that ectopic expression in a heterologous host has limitations which include: (I) differences in cell division between hosts (II) variation between hosts in the complement of interacting partners and (III) increased expression can lead to non-specific effects on cell division/morphology. However, we had chosen to ectopically express the three *M. tuberculosis* DD-CPases in the same vector backbone, using the same promoter (*pmyctet*) and consequently, we predicted that any differential effects that result from over-expression of these genes could provide an insight into biological roles and functional redundancy. We demonstrated that ectopic expression of the *M. tuberculosis* DD-CPase homologues affects colony morphology in both *M. smegmatis* and *M. tuberculosis*. The resulting colonies were smooth, surrounded by a mucous surface and lacked the fully matured bacterial cords observed for the mc<sup>2</sup>155 strain. These data suggested a redundant role of these proteins in maintaining normal colony morphology in *M. smegmatis*. However, further analysis through ectopic expression in H<sub>37</sub>RvS revealed that increased expression of Rv3627c significantly alters bacterial colony morphology, thus highlighting a role for Rv3627c in mediating the organization of individual cells into colonies on agar plates in *M. tuberculosis*.

#### **4.4.2. *M. tuberculosis* DD-CPases and their role in bacterial motility**

Bacterial sliding on semi-solid media is a characteristic that is directly linked to alterations in cell surface properties in mycobacteria. The increase in cell wall GPLs or acetylation significantly affects bacterial sliding (Moya-Hoyos et al., 2015; Recht and kolter, 2001). Additionally, the phosphorylation activity of protein kinase (PknF) also alters sliding motility in *M. tuberculosis* (Gopaldaswamy et al., 2008)

Ectopic expression of *M. tuberculosis* DD-CPase homologues in *M. smegmatis* resulted in defects in surface sliding. Bourai et al., (2012) demonstrated a similar role for Rv2911 in regulating bacterial sliding using the heterologous approach that we employed for characterization of the *M. tuberculosis* DD-CPase homologues. Our data also implicates Rv3330 and Rv3627c in regulating bacterial sliding, suggestive of a role for DD-CPases in modulating either the GPL content in the mycobacterial cell wall or other aspects of PG biology that affect the bio-physical characteristics of the cell.

#### **4.4.3. *M. tuberculosis* Rv3627c and biofilm formation**

Biofilm formation in pathogenic bacteria is illustrative of a survival strategy to survive during periods of stress and antibiotic treatment. Multiple factors are implicated in maintaining normal biofilm formation in mycobacteria. This includes alterations in surface GPLs (Milena Moya-Hoyos et al., 2015; Recht and kolter, 2001), the GroEL1 chaperone (Ojha et al., 2005), the phosphorylation activity of PknF (Gopaldaswamy et al., 2007), the dependence on various metal ions ( $\text{Ca}^{2+}$ ,  $\text{Mg}^{2+}$  and  $\text{Zn}^{2+}$ ) (Carter et al., 2003; Ojha and Hatfull, 2007), free MAs (Ojha et al., 2008), the biological activity of the Polyketide PksI protein (Pang et al., 2012) and the Lsr2 protein (Chen et al., 2006). Our study further implicates mycobacterial DD-CPases in maintaining normal biofilm formation based on the following observations: (I) ectopic expression of *M. tuberculosis* DD-CPase homologues in *M. smegmatis* significantly delayed biofilm formation and (II) further assessment of the role of these proteins in maintenance of biofilm formation in the recombinant *M. tuberculosis* H<sub>37</sub>RvS strain substantiated that they regulate the rate at which

biofilms form and mature. In our analysis, the H<sub>37</sub>RvS(pSE3627c) strain displayed notably delayed kinetics in biofilm formation, suggesting a hierarchy in the role of DD-CPases in biofilm formation, with Rv3627c ranking the highest.

#### **4.4.4. *M. tuberculosis* DD-CPases and their role in bacterial growth**

The capacity of a pathogen to grow is critical for survival and disease progression. In this study, we assayed growth of heterologous *M. smegmatis* strains ectopically expressing *M. tuberculosis* DD-CPases in nutrient rich Middlebrook 7H9 media and observed notable defects. The heterologous strains displayed growth retardation, which was exacerbated at log phase, suggesting that *M. tuberculosis* DD-CPase homologues play a prominent role when bacteria are replicating rapidly. However, similar assessment of the impact of over-expression of DD-CPases in *M. tuberculosis* yielded contrary results where ectopic expression resulted in no changes in growth rates. Consequently, the role of the *M. tuberculosis* DD-CPases in growth requires further study and in this regard, it is noteworthy that Rv3627c has been annotated as essential for growth *in vitro* (Griffin et al., 2011).

#### **4.4.5. *M. tuberculosis* Rv2911 and Rv3627c and their role in maintaining normal bacterial cell length and mechanisms of cells division**

Using SEM, we identified a role for Rv2911 and Rv3627c in regulating bacterial cell length in *M. smegmatis*. Ectopic expression of these two DD-CPases in wild type *M. tuberculosis* H<sub>37</sub>RvS, also resulted in an increase in cell size. Combinatorial deletion of multiple *E. coli* PG hydrolases significantly affects bacterial cell size, with cells losing the natural rod-shape and adopting an almost spherical shape (Heidrich et al., 2002). This observation, together with our data implicates PG hydrolases such as DD-CPases in regulating bacterial cell length.

However, we noted differential effects on cell length in *M. smegmatis* and *M. tuberculosis* where in the former we observed an increase in the populations of cells with reduced cell size for mc<sup>2</sup>(pSE2911) and mc<sup>2</sup>(pSE3627c) strains [and with mc<sup>2</sup>(pSE3330) to a lesser extent]. However, in *M. tuberculosis*, we observed growth-stage specific changes in cell length, table 4.1.1. These

data suggests that the two mycobacterial strains used in this study compensate differentially in response to increased expression of DD-CPases and also point to important differences in the biological function of PG remodelling enzymes between these two strains.

**Table 4.1.1.** Cell length displayed by the heterologous *M. smegmatis* and recombinant *M. tuberculosis* H<sub>37</sub>RvS strains at different phases. The data illustrates that the two strains, mc<sup>2</sup>155 and H<sub>37</sub>RvS, compensate differentially following ectopic expression of the *M. tuberculosis* DD-CPases. (\*, not done).

| <b>Recombinant strain</b>     | <b>Lag Phase</b>         | <b>Log Phase</b>         | <b>Stationary Phase</b>  |
|-------------------------------|--------------------------|--------------------------|--------------------------|
| <i>M. smegmatis</i>           |                          |                          |                          |
| mc <sup>2</sup> (pSE2911)     | Reduction in cell length | Reduction in cell length | Reduction in cell length |
| mc <sup>2</sup> (pSE3330c)    | No change in cell length | Reduction in cell length | Reduction in cell length |
| mc <sup>2</sup> (pSE3627c)    | Reduction in cell length | Reduction in cell length | Reduction in cell length |
|                               |                          |                          |                          |
| <i>M. tuberculosis</i>        |                          |                          |                          |
| H <sub>37</sub> RvS(pSE2911)  | Increased cell length    | Increased cell length    | No change in cell length |
| H <sub>37</sub> RvS(pSE3330c) | Increased cell length    | Not done*                | Increased cell length    |
| H <sub>37</sub> RvS(pSE3627c) | Increased cell length    | Increased cell length    | Increased cell length    |

Electron micrographs for the H<sub>37</sub>RvS(pSE3330) strain were characterized by large numbers of clumped cells. These precluded the characterization of cell length in this strain.

The short cells observed for the heterologous *M. smegmatis* strains ectopically expressing Rv2911 and Rv3627c suggest that these strains likely commit to division too early during growth, thus resulting in the production cells with reduced length. At this point, it is unclear if the replicated chromosome partitions completely in these strains. In *M. tuberculosis*, the increase in the population of cells with longer cell sizes suggests division and daughter cell separation is delayed when DD-CPases are over-expressed. Our study represents the first report that implicates

mycobacterial DD-CPases in regulating bacterial cell length and mechanisms of cell division and now provides exciting avenues for further study.

#### **4.4.6. *M. tuberculosis* Rv3330 and bacterial cell morphology**

Ectopic expression of Rv3330 in *M. smegmatis* revealed a role for this protein in governing bacterial cell morphology. The mc<sup>2</sup>(pSE3330) strain displayed a majority of cells with abnormal cell morphology, including bulges, division scars at the poles, chaining and kinking along the lateral axis of the cell. However, morphological assessment of the recombinant H<sub>37</sub>RvS strains ectopically expressing Rv3330 revealed none of the defects displayed by the mc<sup>2</sup>(pSE3330) strain, once again highlighting key differences between *M. tuberculosis* and *M. smegmatis*. The cell surface defects displayed by the heterologous *M. smegmatis* strain ectopically expressing Rv3330 are similar to those observed in *E. coli*, where deletion of PBP5, a direct homologue of MSMEG\_6113, significantly affected bacterial cell shape (Nelson and Young, 2001; Ghosh et al., Young 2006). Genetic complementation of *E. coli* mutants with MSMEG\_2433 reversed morphological defects of the mutant strain (Bansal et al., 2015), indicative of a role of MSMEG\_2433, a direct homologue of Rv3330 in *M. tuberculosis*, in regulating mycobacterial cell morphology.

Cell morphology in mycobacteria is dependent on multiple factors. Schoonmaker et al., (2014) identified a role for *M. tuberculosis* Ldts in regulating cell size and morphology. Deletion of Ldt<sub>m1</sub> and Ldt<sub>m2</sub> from *M. tuberculosis* genome resulted in various effects, including reduction of bacterial cell size and alterations of cell morphology amongst others (Schoonmaker et al., 2014). DivIVA, the polar localizing protein that drives polar elongation in actinomycetes and other rod-shaped bacteria such as *B. subtilis* (Halbedel et al., 2009; Letel et al., 2009) is also implicated in regulating bacterial cell morphology (Kang et al., 2008). Reduced expression of DivIVA in *M. smegmatis* leads to robust morphological changes such as bulging at the pole of actively growing cells, a defect arising from abnormal PG synthesis at the poles (Kang et al., 2008). This suggests that the polar defects observed for the mc<sup>2</sup>(pSE3330) strain (viz. kinking, division scars and

bulging), following ectopic expression of Rv3330, might potentially result from direct or indirect dysregulation of DivIVA activity by Rv3330, since the latter also localizes at both poles, as demonstrated in this study.

#### **4.4.7. DD-CPases and the bacterial cell envelope**

Ectopic expression of *M. tuberculosis* DD-CPase homologues in wild type *M. smegmatis* caused significant disruptions of bacterial cell envelope architecture. The thickness of the envelope was increased and appeared to partially detach from the cytoplasm. However, these effects did not occur in *M. tuberculosis*. At this point, it is difficult to draw definite conclusions regarding this observation as the TEM data obtained for the recombinant H<sub>37</sub>RvS strains was not a representation of the entire population for all strains at different growth phases. These cell wall defects we noted in *M. smegmatis* were reported in *M. tuberculosis* following the loss of Ldt<sub>m1</sub> and Ldt<sub>m2</sub> (Schoonmaker et al., 2014), suggestive of a possible interplay between PG-hydrolase (viz. DD-CPases) and synthases (viz. LD-transpeptidases).

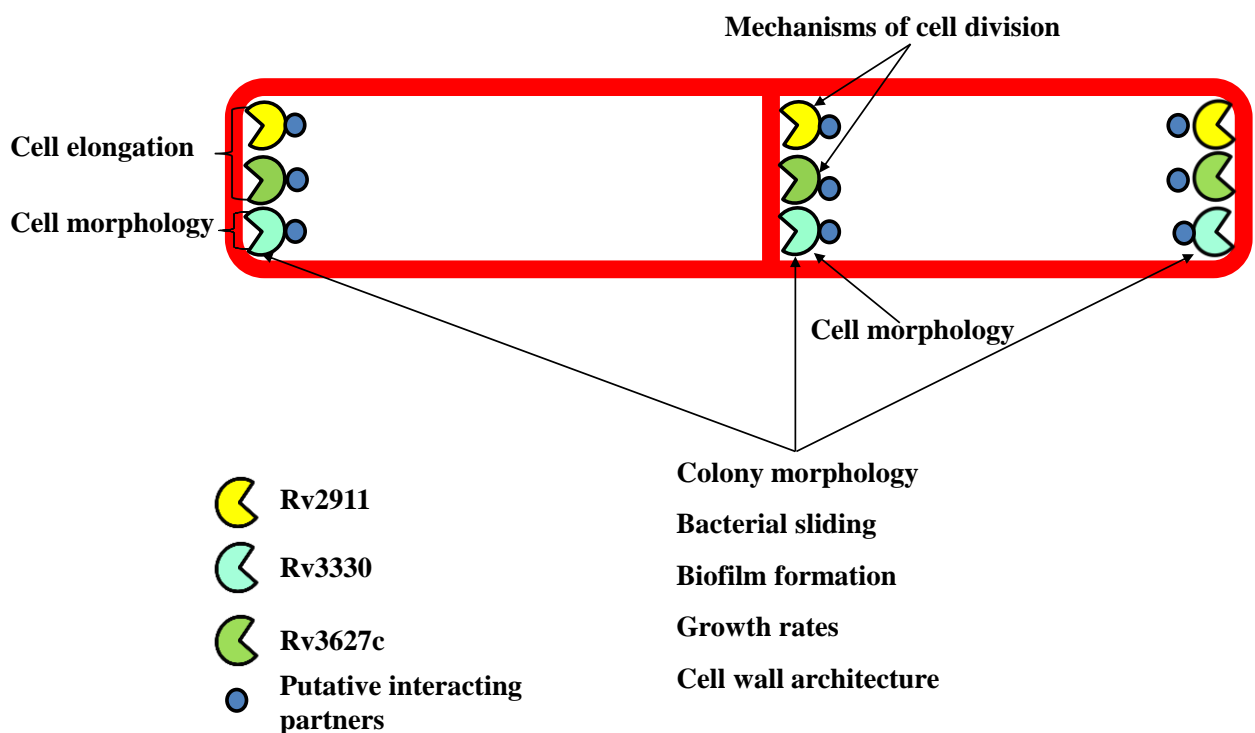
#### **4.5. Polar, mid-cell and quarter cell position localization of rseGFP tagged *M. tuberculosis* DD-CPase homologues**

Cellular localization studies of rseGFP tagged *M. tuberculosis* DD-CPase protein derivatives revealed a unique pattern of localization. The three proteins displayed a similar pattern of localization, at the poles, mid-cell and quarter cell positions. This pattern of localization suggests a role for *M. tuberculosis* DD-CPase homologues in elongation and division in mycobacteria. Numerous well characterized *M. tuberculosis* PG remodelling enzymes, are documented to be present at the poles of actively growing cells or the divisome of dividing cells (Kieser and Rubin, 2014; Machowski et al., 2014). The most intriguing site of localization for the three homologues is at the quarter cell position, which we hypothesize serves to identify or mark future division sites. Another possible reason for localization at this position is to facilitate nucleoid partitioning during cell growth. We were unable to address this by DAPI staining of chromosomal DNA, as the fluorescence from the rseGFP and DAPI run through the same channel in our microscope.

Future studies will involve tagging the *M. tuberculosis* DD-CPase homologues with another fluorescent tag, such as mRFP, to definitively assess whether these proteins are involved in nucleoid occlusion or not.

#### 4.6. A proposed model for the function of *M. tuberculosis* DD-CPases

A combination of the protein interaction data with the phenotypes displayed by the heterologous *M. smegmatis* strains, ectopically expressing the *M. tuberculosis* DD-CPases and localization analysis, allowed for the construction of a hypothetical model for the physiological role of DD-CPase, and the sites at which they exert their effect, figure 4.1.2.



**Figure 4.1.2.** A model depicting the role *M. tuberculosis* DD-CPase homologues. The three proteins localize at both poles and mid-cell, with Rv2911 and Rv3627c regulating rates of cell elongation at the poles and mechanisms of cell division at the septum. Rv3330 at the poles and septum is predominantly involved in regulating cell morphology. The quarter cell localization is not included mainly because it is unclear of what role these proteins play at those specific sites. The model predicts that these proteins exert their effect through interaction with various partners identified to be present at the poles or septum.

## 5.1. Conclusion and future prospects

### 5.1.1 Conclusion



Collectively, this study demonstrated the importance of mycobacterial DD-CPases in cellular elongation, division and maintenance of normal cell morphology. We also confirmed that mycobacterial DD-CPases do not function as single entities, but through interaction with various partners, present at the poles and septum of actively growing cells. Interrogation of the functionality of *M. tuberculosis* DD-CPase homologues by heterologous expression in *M. smegmatis* revealed that despite the observed genetic multiplicity, these proteins are not functionally redundant, with over-expression of Rv2911 and Rv3627c resulting in defective cell elongation and division while Rv3330 is involved in maintaining normal bacterial cell morphology. This is the first study that assigns a role for *M. tuberculosis* DD-CPases in maintaining normal bacterial colony morphology, sliding, biofilm formation and growth rates. Analysis of the functionality of the *M. tuberculosis* DD-CPase homologues in the native *M. tuberculosis* host did not yield conclusive results as observed for the heterologous *M. smegmatis* strains. Therefore, interrogation of the functionality of these proteins in *M. tuberculosis*, through gene knockout is of utmost importance since a side-by-side assessment of the physiological function of these homologues in a heterologous system points to important, non-redundant roles for DD-CPases in mycobacteria.

### **5.1 Future prospects**

The heterologous *M. smegmatis* system revealed an important role of the *M. tuberculosis* DD-CPases homologues in maintaining a variety of biological processes. Thus different approaches to further understand their role in *M. tuberculosis* will allow for detailed characterization of the physiological function in mycobacteria. Considering the limitations of this study, we therefore propose the following future studies:

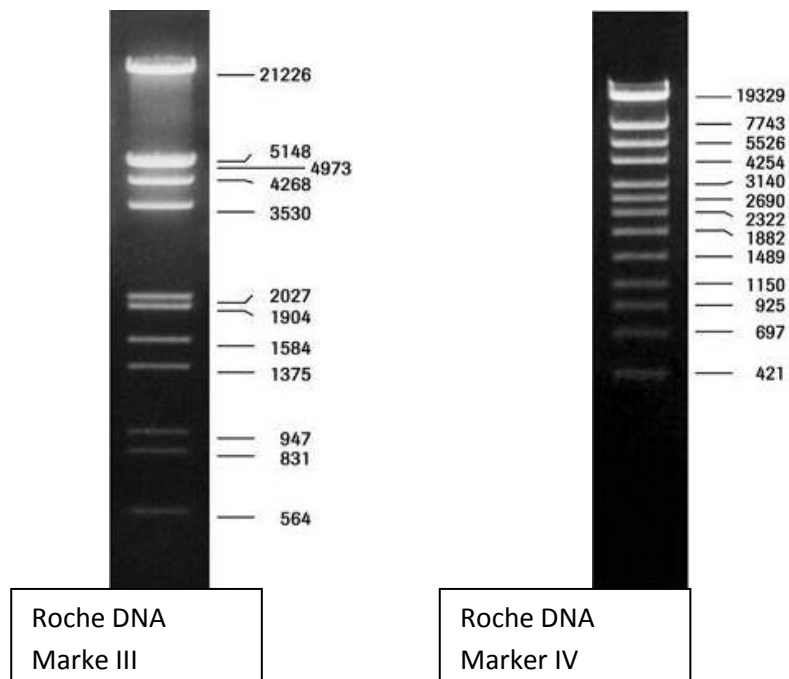
- I. At this point, the transcript levels of the ectopically expressed DD-CPase homologues were not determined in both the heterologous *M. smegmatis* and the recombinant *M. tuberculosis* strains. Therefore, determining and comparing transcript levels by qPCR will shed light on whether these proteins are expressed at similar levels in the two organisms.

- II. Single and combination knockout of the three DD-CPases in *M. tuberculosis*. It should be noted that Rv3627c is essential, a feature which will necessitate a knockdown approach. The resulting strains should be characterized for morphological and virulence defects.
- III. Further validation of putative interacting partners identified in this study using a co-immune precipitation (pull-down) approach. Biochemical characterization of the *M. tuberculosis* DD-CPases and their interacting partners.

## 6. Appendices

### 6.1 Appendix A: DNA molecular weight markers used in this study

#### (A.1.1.1) Roche marker III and IV



**Figure A.1.1.1.** Molecular weight DNA markers.

**6.2. Appendix B: Gene specific primers used for PCR amplification of genes and genotypic confirmation of strains generated in this study.**

**Table. A.1.1.1.** Bacterial two hybrid primers.

| Primer pair                      | Primer sequence  | Restriction site                 |
|----------------------------------|--|----------------------------------|
| <i>narB</i> _F<br><i>narB</i> -R | TCATGGCTCGCACAGACCGGATC<br>CTCTCAGAGGTGTTCTCGGCGA                      | None                             |
| MSMEG_3145_F<br>MSMEG_3145_R     | CGCGCGGGATCCATGAGACGTACCGTCCGCGCT<br>GCGCGCAAGCTTTCAGTATTCGATGAGCCGGGT | <i>Bam</i> HI<br><i>Hind</i> III |
| MSMEG_5439_F<br>MSMEG_5439_R     | CGCGCGGAATTCATGCTTCGAGGAGTTGTGGGT<br>GCGCGCAAGCTTTCAGCGCGCCCAATCCTCCC  | EcoRI<br><i>Hind</i> III         |
| MSMEG_2433_F<br>MSMEG_2433_R     | CGCGCGGAATTCATGTGGAGGTACGCCTTCGGG<br>GCGCGCAAGCTTTCAGAGCGCCCGATGCTCGC  | EcoRI<br><i>Hind</i> III         |
| MSMEG_6113_F<br>MSMEG_6113_R     | CGCGCGGAATTCATGAGCGATAGGCTGACGCGC<br>GCGCGCAAGCTTTCATGCGCCGCATCCGCAGCT | EcoRI<br><i>Hind</i> III         |

**Table A.1.1.2.** Untagged *M. tuberculosis* DD-CPase primer sets for cloning into pSE100 and genotypic confirmation of generated strains.

| Primer pair                    | Primer sequence  | Restriction site              |
|--------------------------------|--|-------------------------------|
| Rv2911_UTG_F<br>Rv2911_UTG_R   | GCGCAGATCTTTAAACTCTGCGCCCATGCGA<br>GCGCGCATCGATCTAGAGCGAGCCGACGCT    | <i>Bgl</i> II<br><i>Cla</i> I |
| Rv3330_UTG_F<br>Rv3330_UTG_R   | GGCCAGATCTTACTCTGCACAGACGATGGCC<br>GCGCGCATCGATCTAGTGCTGCGGCCGGCGG   | <i>Bgl</i> II<br><i>Cla</i> I |
| Rv3627c_UTG_F<br>Rv3627c_UTG_R | GCGCAGATCTAAGGCAGGAGAGCTCATGGGT<br>GCGCGCATCGATTCACGTCGTGCACCCGCAGAA | <i>Bgl</i> II<br><i>Cla</i> I |

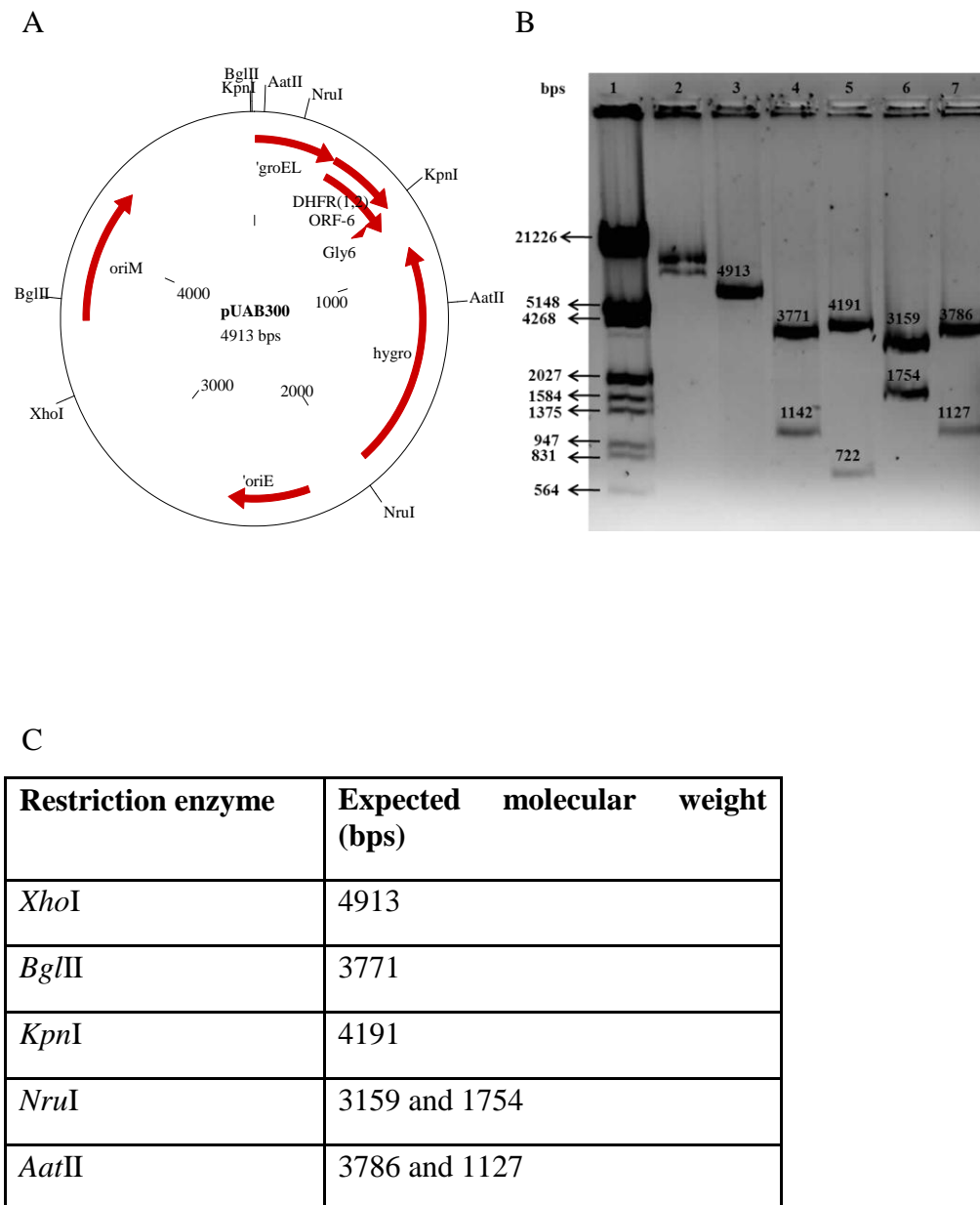
**Table A.1.1.3.** rseGFP and *M. tuberculosis* DD-CPase primer sets for 3-way cloning into pSE100 and genotypic confirmation of generated strains.

| Primer pair                | Primer sequence  | Restriction site             |
|----------------------------|--|------------------------------|
| rseGFP_F<br>rseGFP_R       | CGCGCG <u>GAATTC</u> ATGGTGAGCAAGGGCGAGGA<br>GCGCGC <u>CTGCAG</u> AGGAGTCCAAGCTCAGCTAA | <i>EcoRI</i><br><i>PstI</i>  |
| Rv2911_UTG_F<br>Rv2911_R   | GCGC <u>AGATCT</u> TTAAACTCTGCGCCCATGCGA<br>GGCC <u>GAATTC</u> GAGCGAGCCGACGCTGGCCTG   | <i>BglII</i><br><i>EcoRI</i> |
| Rv3330_UTG_F<br>Rv3330_R   | GGCC <u>AGATCT</u> TACTCTGCACAGACGATGGCC<br>GCGCGAATTCGTGCTGCGGCCGGCGGTTTCAT           | <i>BglII</i><br><i>EcoRI</i> |
| Rv3627c_UTG_F<br>Rv3627c_R | GCGC <u>AGATCT</u> AAGGCAGGAGAGCTCATGGGT<br>GGCC <u>GAATTC</u> CGTCGTGCACCCGCAGAACCA   | <i>BglII</i><br><i>EcoRI</i> |

### 6.3. Appendix C: Restriction digests

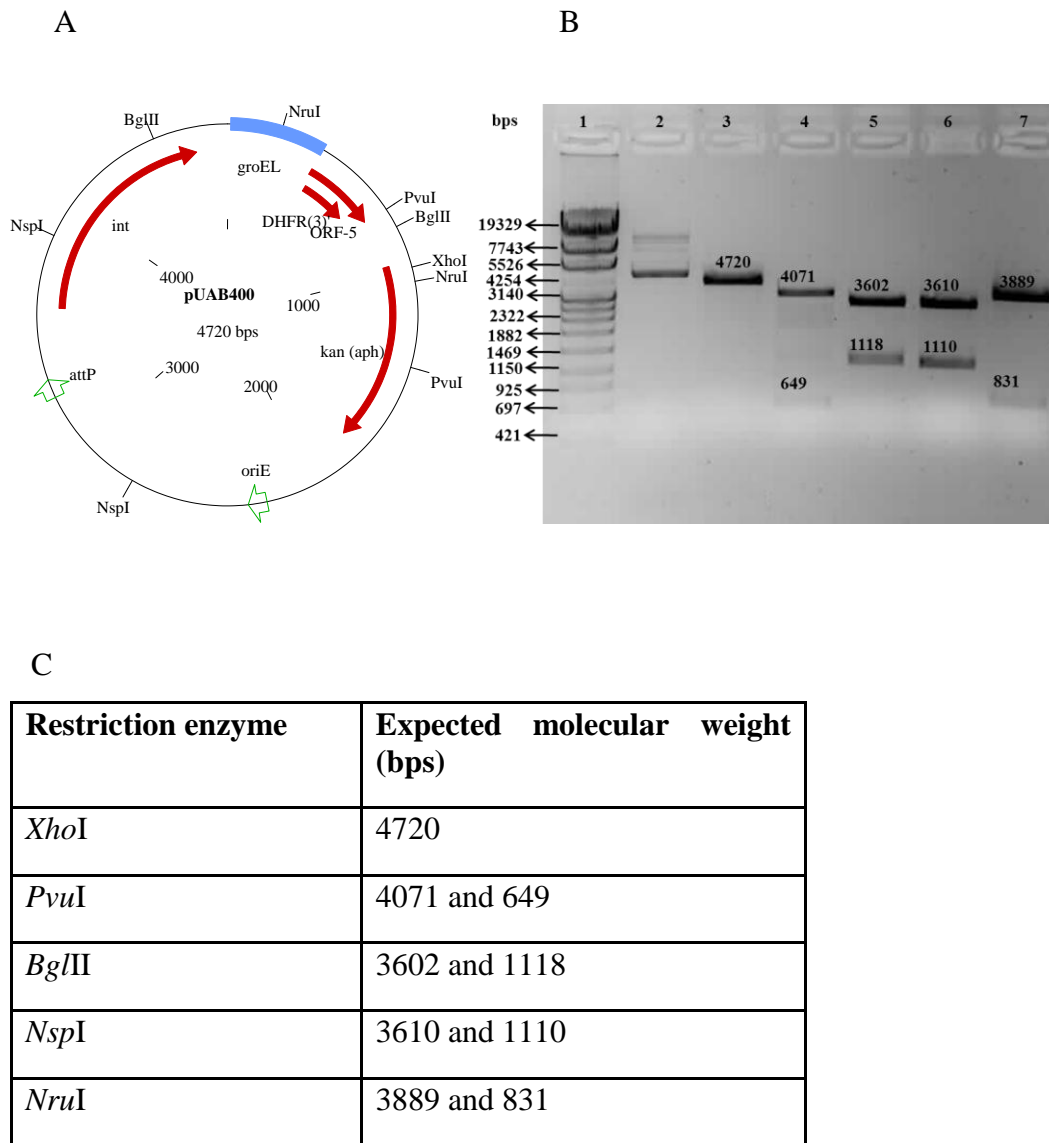
#### 6.3.1 Restriction profile of the mPFC backbone vectors

##### 6.3.1.1. Restriction profile of pUAB300



**Figure A.1.1.2.** Restriction profiling of the mPFC prey vector, pUAB300. (A) plasmid map of pUAB300. (B) Restriction profile of pUAB300. Lane 1= marker III, Lane 2= uncut pUAB300, Lane 3= *XhoI*, Lane 4= *BglII*, Lane 5= *KpnI*, Lane 6= *NruI*, Lane 7= *AatII*. (C) Table showing the expected banding profiles for pUAB300 restricted with the listed restriction enzymes.

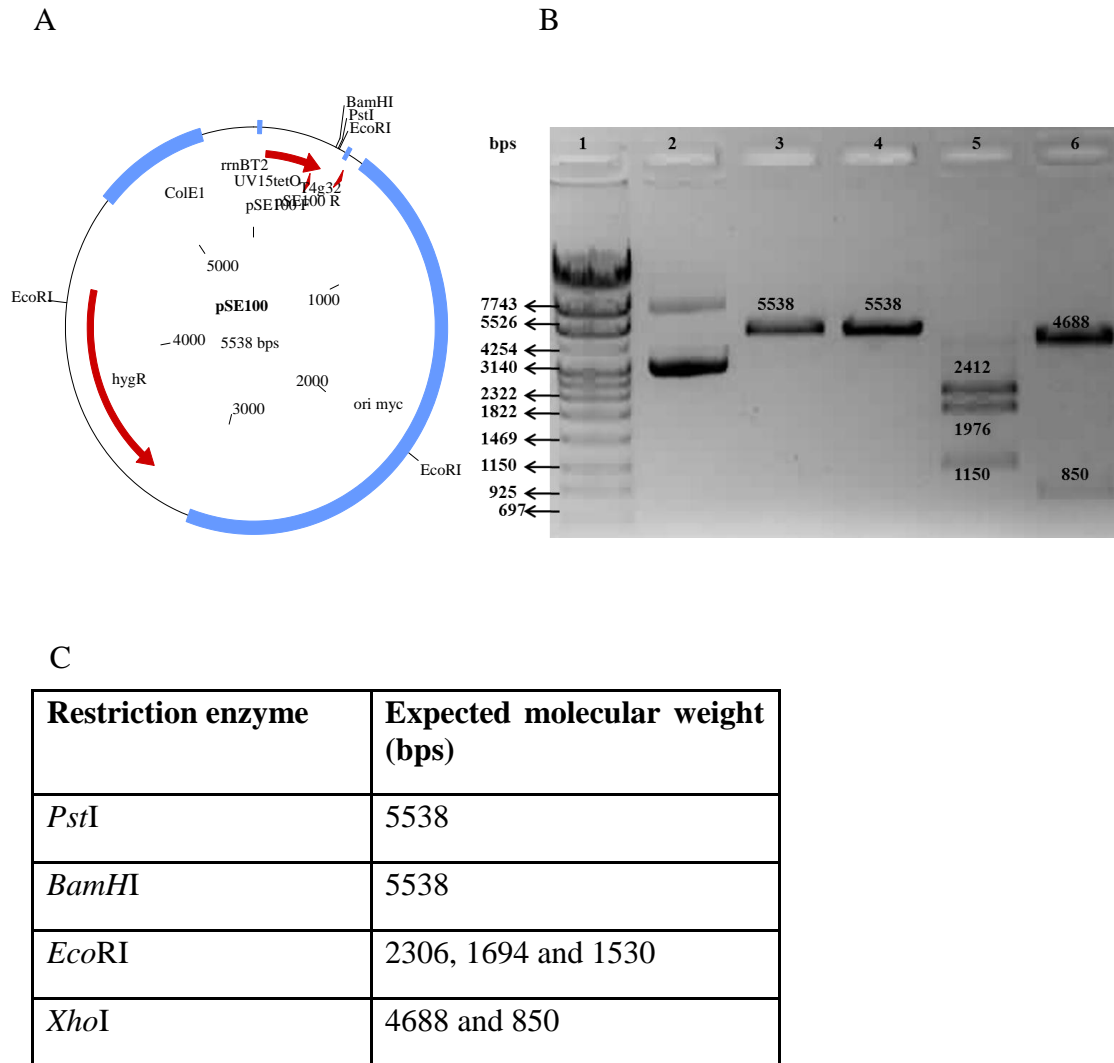
### 6.3.1.2. Restriction profile of pUAB400



**Figure A.1.1.3.** Restriction profiling of the mPFC bait vector, pUAB400. (A) Plasmid map of pUAB400. (B) Restriction profile of pUAB400. Lane 1= marker IV, Lane 2= uncut pUAB400, Lane 3= *XhoI*, Lane 4= *PvuI*, Lane 5= *BglII*, Lane 6= *NspI*, Lane 7= *NruI*. (C) Table showing the expected banding profiles for pUAB300 restricted with the listed restriction enzymes.

## 6.4. Appendix D: Restriction profile of pSE100 vector backbone and derivatives.

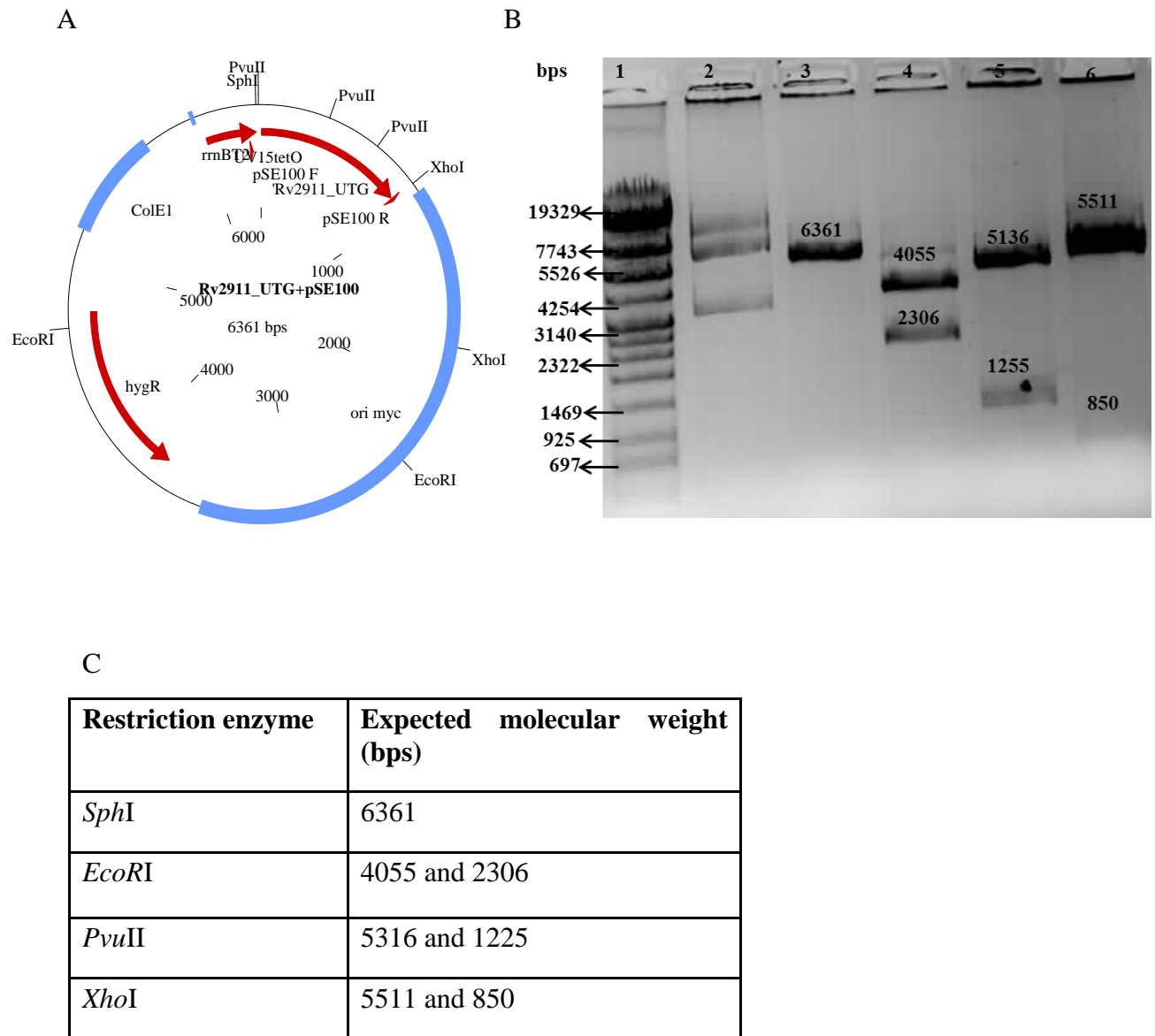
### 6.4.1. Restriction profile of pSE100 vector backbone



**Figure A.1.1.4.** Restriction profiling of pSE100. (A) Plasmid map of pSE100. (B) Restriction profile of pSE100. Lane 1= marker IV, Lane 2= uncut pSE100, Lane 3=, *Pst*I, Lane 4= *Bam*HI, Lane 5= *Eco*RI, Lane 6= *Xho*I . (C) Table showing the expected banding profiles of pSE100 restricted with the listed restriction enzymes.

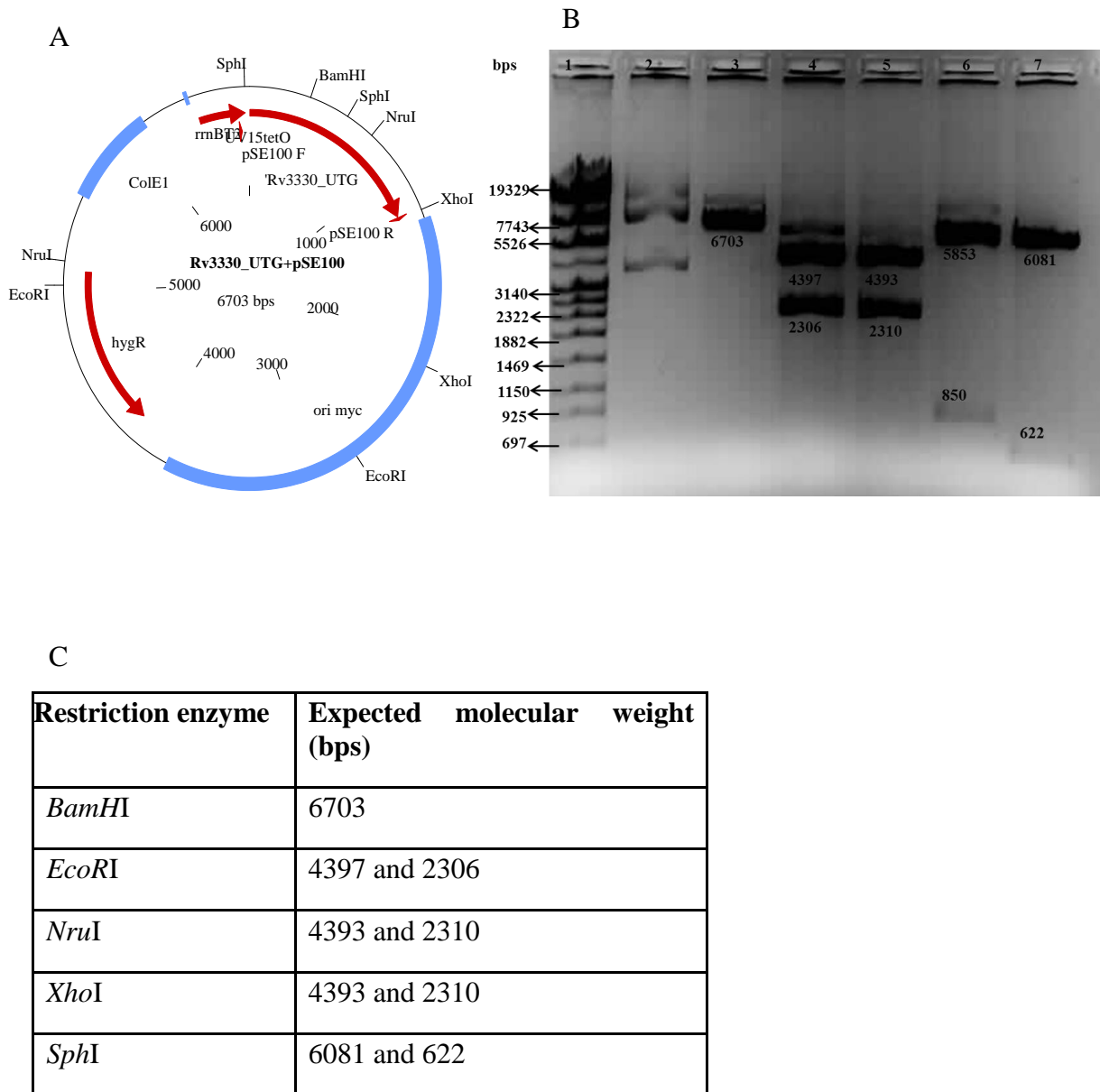


### 6.4.2. Restriction profile of untagged Rv2911 cloned into pSE100



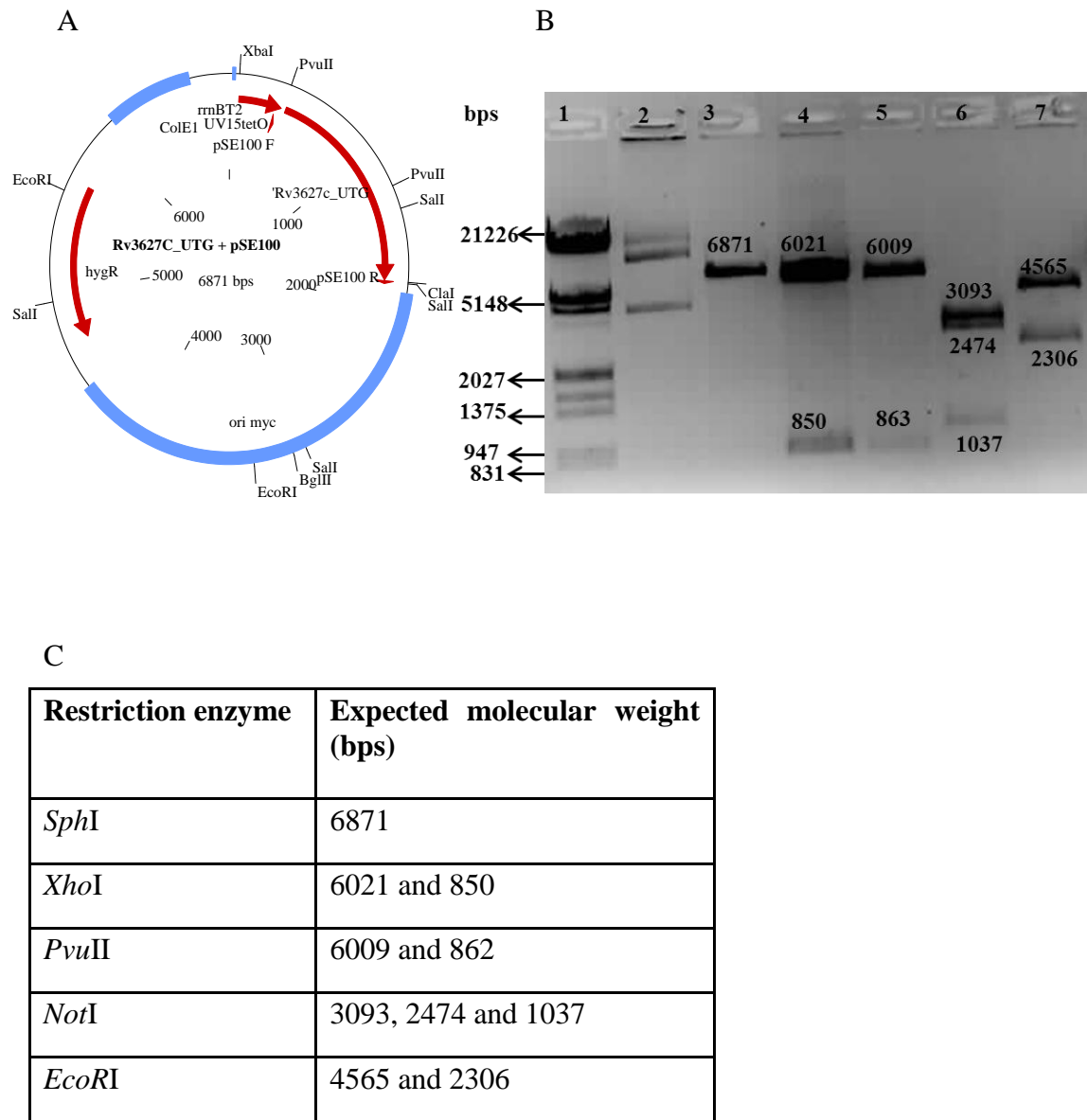
**Figure A.1.1.5.** Restriction profiling of untagged Rv2911 cloned into pSE100 producing the pSE2911 construct. (A) Vector map showing untagged Rv2911 cloned into pSE100. (B) Restriction profile pSE2911 construct. Lane 1= Marker IV, Lane 2= Uncut pSE100, Lane 3= *SphI*, Lane 4= *EcoRI*, Lane 5= *PvuI*, Lane 6= *XhoI*. (C) Table showing the expected banding profiles of pSE2911 construct restricted with the listed restriction enzymes.

### 6.4.3. Restriction profile of untagged Rv3330 cloned into pSE100



**Figure A.1.1.6.** Restriction profiling of untagged Rv3330 cloned into pSE100 to generate the pSE3330 construct. (A) Vector map showing untagged Rv3330 cloned into pSE100. (B) Restriction profiling of pSE3330 construct. Lane 1= Marker IV, Lane 2= uncut pSE100, Lane 3= *BamHI*, Lane 4= *EcoRI*, Lane 5= *NruI*, Lane 6= *XhoI*, Lane 7= *SphI*. (C) Table showing the expected banding profiles of pSE3330 construct restricted with the listed restriction enzymes

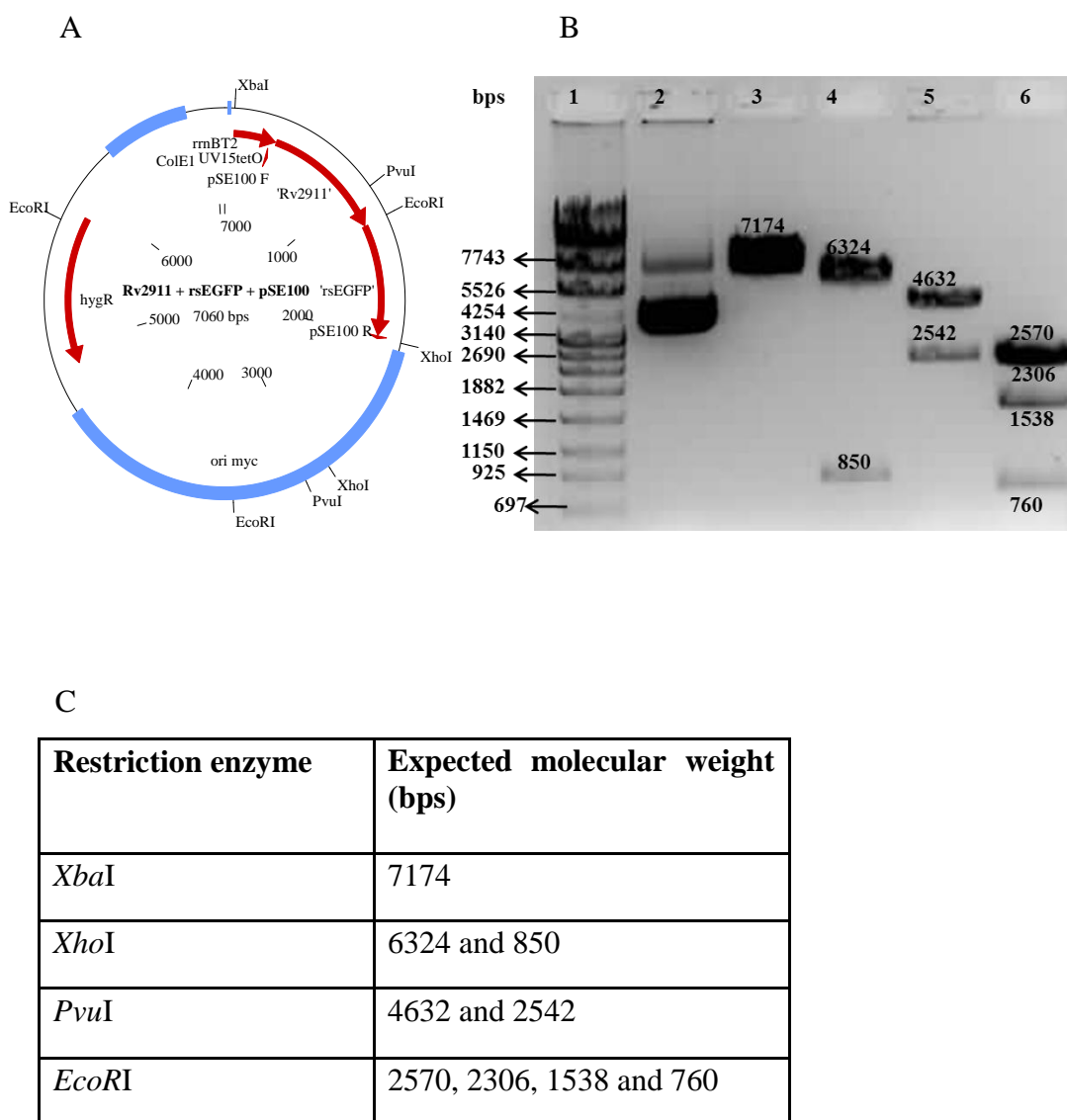
#### 6.4.4. Restriction profile of untagged Rv3627c cloned into pSE100



**Figure A.1.1.7.** Restriction profiling of untagged Rv3627c cloned into pSE100 to generate the pSE3627c construct. (A) Vector map showing untagged Rv3627c cloned into pSE100. (B) Restriction profiling of pSE3627c construct. Lane I= Marker III, Lane 2= uncut pSE100, Lane 3= *SphI*, Lane 4= *XhoI*, Lane 5=*PvuII*, Lane 6= *NotI*, Lane 7= *EcoRI*. (C) Table showing the expected banding profiles of pSE3627c construct restricted with the listed restriction enzymes.

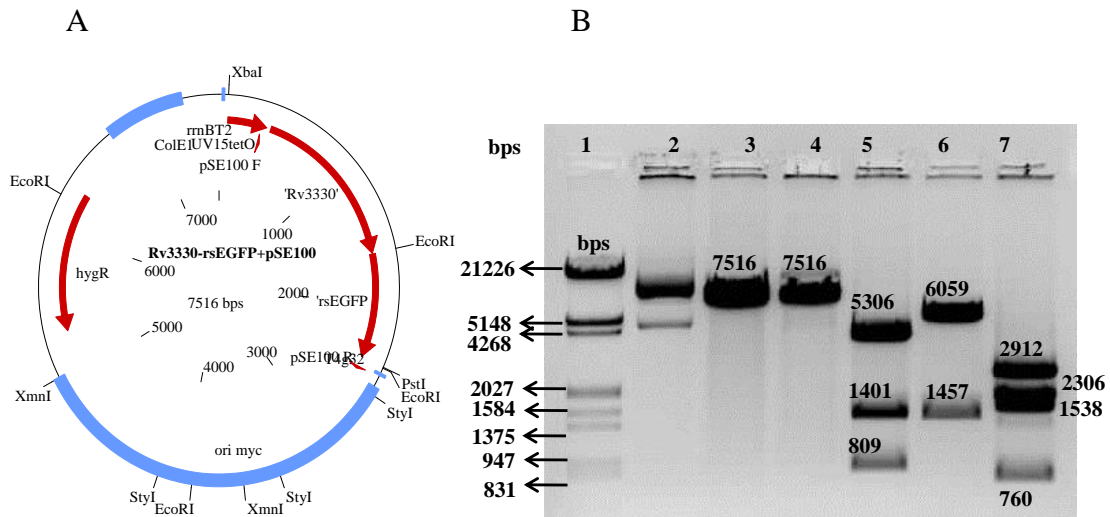
## 6.5. Appendix E: Restriction profiling of rseGFP tagged *M. tuberculosis* DD-CPase derivatives into pSE100

### 6.5.1. Restriction profiling of C-terminally rseGFP tagged Rv2911 cloned into pSE100



**Figure A.1.1.8.** Restriction profiling of rseGFP C-terminally tagged Rv2911 cloned into pSE100 to generate the pSE2911-rseGFP construct. (A) Vector map showing rseGFP C-terminally tagged Rv2911. (B) Restriction profiling of pSE2911-rseGFP construct. Lane 1= Marker IV, Lane 2=uncut pSE100, Lane 3= *Xba*I, Lane 4= *Xho*I, Lane 5=*Pvu*I, Lane 6= *Eco*RI. (C) Table showing the expected banding profiles of pSE2911-rseGFP construct with the listed restriction enzymes.

### 6.5.2. Restriction profiling of C-terminally rseGFP tagged Rv3330 cloned into pSE100.

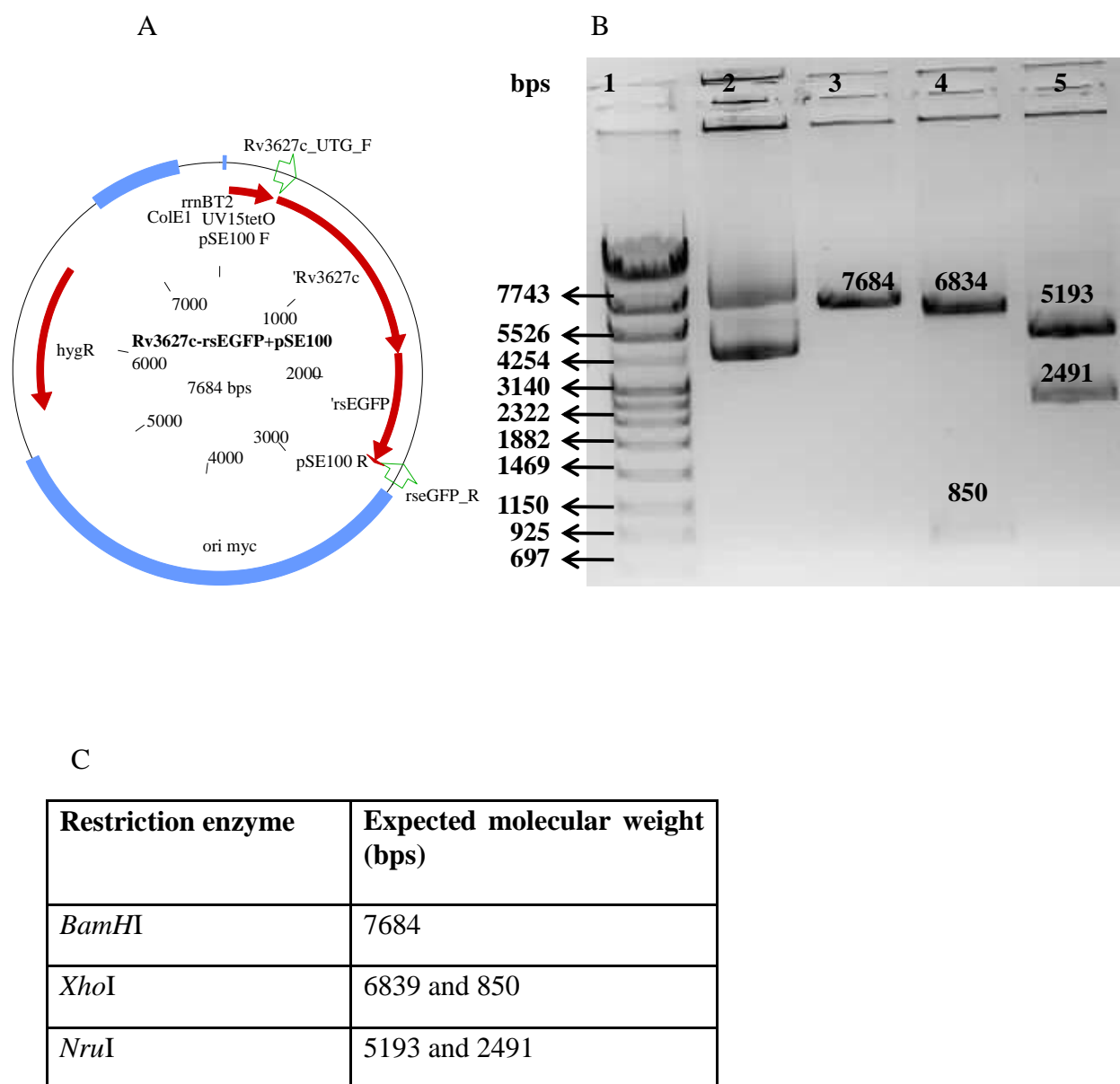


**C**

| Restriction enzyme | Expected molecular weight (bps) |
|--------------------|---------------------------------|
| <i>XbaI</i>        | 7516                            |
| <i>PstI</i>        | 7516                            |
| <i>styI</i>        | 5306, 1401 and 809              |
| <i>XmnI</i>        | 6059 and 1457                   |
| <i>EcoRI</i>       | 2921, 2306, 1538 and 760        |

**Figure A.1.1.9.** Restriction profiling of rseGFP C-terminally tagged Rv3330 cloned into pSE100 to generate the pSE3330-rseGFP construct. (A) Vector map showing rseGFP C-terminally tagged Rv3330. (B) Restriction profiling of pSE3330-rseGFP construct. Lane I= Marker III, Lane 2= uncut pSE100, Lane 3= *XbaI*, Lane 4= *PstI*, Lane 5= *StyI*, Lane 6= *XmnI*, Lane 7= *EcoRI*. (C) Table showing the expected banding profiles of pSE3330-rseGFP construct with the listed restriction enzymes.

### 6.5.3. Restriction profiling of C-terminally rseGFP tagged Rv3627c cloned into pSE100.



**Figure A.1.1.10.** Restriction profiling of rseGFP C-terminally tagged Rv3627c cloned into pSE100 to generate the pSE3627c-rsEGFP construct. (A) Vector map showing rseGFP C-terminally tagged Rv3627c. (B) Restriction profiling of pSE3627c-rsEGFP construct. Lane 1= Marker IV, Lane 2= uncut pSE100, Lane 3= *Bam*HI, Lane 4= *Xho*I, Lane 5=*Nru*I. (C) Table showing the expected banding profiles for pSE3627c-rsEGFP construct with the listed restriction enzymes

## 6.6. Appendix F: Culture media:

### 6.6.1. *E. coli* culture media

|      |  |
|------|--|
| LB   | 10 g tryptone, 10 NaCl, 5 g yeast extract in 1 L dH <sub>2</sub> O           |
| 2xTY | 20 g tryptone, 10 g NaCl, 10 g yeast extract in 1 L dH <sub>2</sub> O        |
| LA   | 10 g tryptone, 5 NaCl, 5 g yeast extract, 15 g agar in 1 L dH <sub>2</sub> O |

### 6.6.2. *M. smegmatis* culture media

|                    |  |
|--------------------|--|
| Middlebrook 7H9    | 4.7 g Middlebrook 7H9, 10 ml of 100x glucose salts, 2 ml glycerol, , 2 ml 25% Tween80 in 1 L dH <sub>2</sub> O |
| Middlebrook 7H10   | 19 g Middlebrook 7H10, 10 ml of 100x glucose salts, 5 ml glycerol in 1 l dH <sub>2</sub> O                     |
| 100x glucose salts | 20 g glucose, 8.5 g NaCl dissolved in 100 ml dH <sub>2</sub> O   |

### 6.6.2. *M. tuberculosis* culture media

|                  |  |
|------------------|--|
| Middlebrook 7H9  | 4.7 g Middlebrook 7H9, 100 ml OADC, 2 ml glycerol, , 2 ml 25% Tween80 in 1 L dH <sub>2</sub> O |
| Middlebrook 7H11 | 19 g Middlebrook 7H10, 100 ml OADC, 5 ml glycerol in 1 l dH <sub>2</sub> O                     |

## 6.7. Appendix G: Specialised media

|                                  |  |
|----------------------------------|--|
| 6.7.2. Minimal Souton's media    | 4 g asparagine, 0.5 MgSO <sub>4</sub> , 2 g citric acid, 0.5 g KH <sub>2</sub> PO <sub>4</sub> , 0.005 g ammonium ferric acids, 60 ml glycerol in 1 L dH <sub>2</sub> O. Adjust pH to 7.3. |
| 6.7.3. Molality semi-solid media | 4.7 g Middlebrook 7H9, 2 ml glycerol, agar or agrose to a final concentration of 0.3% and allow to dry overnight at room temperature   |

## 6.8. Appendix H: DNA extraction solutions

### 6.8.1. Plasmid DNA extraction for *E. coli* solutions

|              |   |
|--------------|---|
| Solution I   | 50 mM glucose, 25 mM Tris-HCl (pH 8), 10 mM EDTA in dH <sub>2</sub> O   |
| Solution II  | 1% SDS, 0.2 M NaOH dissolved in dH <sub>2</sub> O                       |
| Solution III | 3 M potassium acetate, 11.5% acetic acid dissolved in dH <sub>2</sub> O |

### 6.8.2. Genomic DNA extraction solutions for mycobacteria

|                             |  |
|-----------------------------|--|
| CTAB                        | 4.1 % NaCl, 10% N-cetyl-N,N, N-trimethyl ammonium bromide dissolved in dH <sub>2</sub> O |
| TE Buffer                   | 10 mM Tris-HCl (pH 8), 10 mM EDTA dissolved in dH <sub>2</sub> O                         |
| Chloroform: Isoamyl alcohol | 24 ml chloroform, 1 ml isoamyl alcohol   |
| Phenol:chloroform           | 1 ml phenol, 1 ml chloroform   |
| Sodium acetate              | 3M sodium acetate dissolved in dH <sub>2</sub> O, pH 5.2                                 |



## Bibliography

- Ahmad, S. (2010). Pathogenesis, immunology, and diagnosis of latent *Mycobacterium tuberculosis* infection. Clinical and Developmental Immunology **2011**.
- Alcaide, F., G. E. Pfyffer and A. Telenti (1997). Role of *embB* in natural and acquired resistance to ethambutol in mycobacteria. Antimicrobial agents and chemotherapy **41**(10): 2270-2273.
- Alsteens, D., C. Verbelen, E. Dague, D. Raze, A. R. Baulard and Y. F. Dufrêne (2008). Organization of the mycobacterial cell wall: a nanoscale view. European Journal of Physiology **456**(1): 117-125.
- Andersen, P. and T. M. Doherty (2005). The success and failure of BCG—implications for a novel tuberculosis vaccine. Nature Reviews Microbiology **3**(8): 656-662.
- Anilkumar, G., R. Srinivasan, S. P. Anand and P. Ajitkumar (2001). Bacterial cell division protein FtsZ is a specific substrate for the AAA family protease FtsH. Microbiology **147**(3): 516-517.
- Asselineau, J. and E. Lederer (1950). Structure of the mycolic acids of mycobacteria. Nature **166**: 782 - 783
- Astarie-Dequeker, C., L. Le Guyader, W. Malaga, F.-K. Seaphanh, C. Chalut, A. Lopez and C. Guilhot (2009). Phthiocerol dimycocerosates of *M. tuberculosis* participate in macrophage invasion by inducing changes in the organization of plasma membrane lipids. PLoS Pathog **5**(2): e1000289.
- Atrih, A., G. Bacher, G. Allmaier, M. P. Williamson and S. J. Foster (1999). Analysis of peptidoglycan structure from vegetative cells of *Bacillus subtilis* 168 and role of PBP 5 in peptidoglycan maturation. Journal of bacteriology **181**(13): 3956-3966.
- Bansal, A., D. Kar, R. A. Murugan, S. Mallick, M. Dutta, S. D. Pandey, C. Chowdhury and A. S. Ghosh (Year). A putative low-molecular mass (LMM) penicillin-binding protein (PBP) of *Mycobacterium smegmatis* exhibits prominent physiological characters of DD-Carboxypeptidase and beta-lactamase. Microbiology, **161**(5), 1081-1091
- Begg, K. J. and W. D. Donachie (1985). Cell shape and division in *Escherichia coli*: experiments with shape and division mutants. Journal of bacteriology **163**(2): 615-622.
- Belanger, A. E., G. S. Besra, M. E. Ford, K. Mikusová, J. T. Belisle, P. J. Brennan and J. M. Inamine (1996). The *embAB* genes of *Mycobacterium avium* encode an arabinosyl transferase involved in cell wall arabinan biosynthesis that is the target for the antimycobacterial drug ethambutol. Proceedings of the National Academy of Sciences **93**(21): 11919-11924.
- Bernhardt, T. G. and P. A. De Boer (2003). The *Escherichia coli* amidase AmiC is a periplasmic septal ring component exported via the twin-arginine transport pathway. Molecular microbiology **48**(5): 1171-1182.
- Bernut, A., J.-L. Herrmann, K. Kissa, J.-F. Dubremetz, J.-L. Gaillard, G. Lutfalla and L. Kremer (2014). *Mycobacterium abscessus* cording prevents phagocytosis and promotes abscess formation. Proceedings of the National Academy of Sciences **111**(10): E943-E952.
- Bhamidi, S., M. S. Scherman, V. Jones, D. C. Crick, J. T. Belisle, P. J. Brennan and M. R. McNeil (2011). Detailed structural and quantitative analysis reveals the spatial organization of

the cell walls of in vivo grown *Mycobacterium leprae* and in vitro grown *Mycobacterium tuberculosis*. Journal of Biological Chemistry **286**(26): 23168-23177.

Bhutani, H., S. Singh and K. Jindal (2005). Drug-drug interaction studies on first-line anti-tuberculosis drugs. Pharmaceutical development and technology **10**(4): 517-524.

Billman-Jacobe, H., R. E. Haites and R. L. Coppel (1999). Characterization of a *Mycobacterium smegmatis* mutant lacking penicillin binding protein 1. Antimicrobial agents and chemotherapy **43**(12): 3011-3013.

Boddingius, J. and H. P. Dijkman (1989). Immunogold labeling method for *Mycobacterium leprae*-specific phenolic glycolipid in glutaraldehyde-osmium-fixed and Araldite-embedded leprosy lesions. Journal of Histochemistry & Cytochemistry **37**(4): 455-462.

Boitel, B., M. Ortiz-Lombardía, R. Durán, F. Pompeo, S. T. Cole, C. Cerveñansky and P. M. Alzari (2003). PknB kinase activity is regulated by phosphorylation in two Thr residues and dephosphorylation by PstP, the cognate phospho-Ser/Thr phosphatase, in *Mycobacterium tuberculosis*. Molecular microbiology **49**(6): 1493-1508.

Boneca, I. G., O. Dussurget, D. Cabanes, M.-A. Nahori, S. Sousa, M. Lecuit, E. Psylinakis, V. Bouriotis, J.-P. Hugot and M. Giovannini (2007). A critical role for peptidoglycan N-deacetylation in *Listeria* evasion from the host innate immune system. Proceedings of the National Academy of Sciences **104**(3): 997-1002.

Bonfiglio, G., G. Russo and G. Nicoletti (2002). Recent developments in carbapenems." Expert opinion on investigational drugs **11**(4): 529-544.

Boots, J.-W. P., R. E. Spelbrink, G. M. Kool, E. Breukink, J. A. Killian and B. de Kruijff (2003). Membrane interaction of the glycosyltransferase MurG: a special role for cardiolipin. Journal of bacteriology **185**(13): 3773-3779.

Bouhss, A., A. E. Trunkfield, T. D. Bugg and D. Mengin-Lecreulx (2008). The biosynthesis of peptidoglycan lipid-linked intermediates. FEMS microbiology reviews **32**(2): 208-233.

Bourai, N., W. R. Jacobs and S. Narayanan (2012). Deletion and overexpression studies on DacB2, a putative low molecular mass penicillin binding protein from *Mycobacterium tuberculosis* H 37 Rv. Microbial pathogenesis **52**(2): 109-116.

Bush, K., G. A. Jacoby and A. A. Medeiros (1995). A functional classification scheme for beta-lactamases and its correlation with molecular structure. Antimicrobial agents and chemotherapy **39**(6): 1211.

Cao, K., R. Nakajima, H. H. Meyer and Y. Zheng (2003). The AAA-ATPase Cdc48/p97 regulates spindle disassembly at the end of mitosis. Cell **115**(3): 355-367.

Cato 3rd, A., J. Cavanaugh, H. Shi, A. Hsu, J. Leonard and R. Granneman (1998). The effect of multiple doses of ritonavir on the pharmacokinetics of rifabutin. Clinical pharmacology and therapeutics **63**(4): 414-421.

Chaba, R., M. Raje and P. K. Chakraborti (2002). Evidence that a eukaryotic-type serine/threonine protein kinase from *Mycobacterium tuberculosis* regulates morphological changes associated with cell division. European Journal of Biochemistry **269**(4): 1078-1085.

- Chen, J. M., G. J. German, D. C. Alexander, H. Ren, T. Tan and J. Liu (2006). Roles of Lsr2 in colony morphology and biofilm formation of *Mycobacterium smegmatis*. Journal of bacteriology **188**(2): 633-641.
- Cloud, K. A. and J. P. Dillard (2002). A lytic transglycosylase of *Neisseria gonorrhoeae* is involved in peptidoglycan-derived cytotoxin production. Infection and Immunity **70**(6): 2752-2757.
- Cohen-Gonsaud, M., N. H. Keep, A. P. Davies, J. Ward, B. Henderson and G. Labesse (2004). Resuscitation-promoting factors possess a lysozyme-like domain. Trends in biochemical sciences **29**(1): 7-10.
- Cohn, M. L., R. F. Waggoner and J. K. McClatchy (1968). The 7H11 Medium for the Cultivation of Mycobacteria 1. American Review of Respiratory Disease **98**(2): 295-296.
- Colditz, G. A., T. F. Brewer, C. S. Berkey, M. E. Wilson, E. Burdick, H. V. Fineberg and F. Mosteller (1994). "Efficacy of BCG vaccine in the prevention of tuberculosis: meta-analysis of the published literature. Jama **271**(9): 698-702.
- Centers for Disease Control and Prevention (2006). Emergence of Mycobacterium tuberculosis with extensive resistance to second-line drugs--worldwide, 2000-2004. MMWR. Morbidity and mortality weekly report **55**(11): 301.
- Corbett, E. L., C. J. Watt, N. Walker, D. Maher, B. G. Williams, M. C. Raviglione and C. Dye (2003). The growing burden of tuberculosis: global trends and interactions with the HIV epidemic. Archives of internal medicine **163**(9): 1009-1021.
- Daffe, M. and G. Etienne (1999). The capsule of *Mycobacterium tuberculosis* and its implications for pathogenicity. Tubercle and Lung Disease **79**(3): 153-169.
- Daffé, M. and P. Draper (1997). The envelope layers of mycobacteria with reference to their pathogenicity. Advances in microbial physiology **39**: 131-203.
- Darzins, E. and G. Fahr (1956). Cord-forming property, lethality and pathogenicity of Mycobacteria. CHEST Journal **30**(6): 642-648.
- Dasgupta, A., P. Datta, M. Kundu and J. Basu (2006). The serine/threonine kinase PknB of *Mycobacterium tuberculosis* phosphorylates PBPA, a penicillin-binding protein required for cell division. Microbiology **152**(2): 493-504.
- Davis, K. M. and J. N. Weiser (2011). Modifications to the peptidoglycan backbone help bacteria to establish infection. Infection and Immunity **79**(2): 562-570.
- de Requena, D. G., S. Bonora, S. Garazzino, M. Sciandra, A. d'Avolio, R. Raiteri, R. Marrone, M. Boffito, F. De Rosa and A. Sinicco (2005). Nevirapine plasma exposure affects both durability of viral suppression and selection of nevirapine primary resistance mutations in a clinical setting. Antimicrobial agents and chemotherapy **49**(9): 3966-3969.
- Dean, G. L., S. G. Edwards, N. J. Ives, G. Matthews, E. F. Fox, L. Navaratne, M. Fisher, G. P. Taylor, R. Miller and C. B. Taylor (2002). Treatment of tuberculosis in HIV-infected persons in the era of highly active antiretroviral therapy. Aids **16**(1): 75-83.

- Denome, S. A., P. K. Elf, T. A. Henderson, D. E. Nelson and K. D. Young (1999). *Escherichia coli* mutants lacking all possible combinations of eight penicillin binding proteins: viability, characteristics, and implications for peptidoglycan synthesis. Journal of bacteriology **181**(13): 3981-3993.
- Domenech, P., M. B. Reed and C. E. Barry (2005). Contribution of the *Mycobacterium tuberculosis* MmpL protein family to virulence and drug resistance. Infection and Immunity **73**(6): 3492-3501.
- Dougherty, T. J., K. Kennedy, R. E. Kessler and M. J. Pucci (1996). Direct quantitation of the number of individual penicillin-binding proteins per cell in *Escherichia coli*. Journal of bacteriology **178**(21): 6110-6115.
- Draper, P. and R. Rees (1973). The nature of the electron-transparent zone that surrounds *Mycobacterium lepraemurium* inside host cells. Microbiology **77**(1): 79-87.
- Du, W., J. R. Brown, D. R. Sylvester, J. Huang, A. F. Chalker, C. Y. So, D. J. Holmes, D. J. Payne and N. G. Wallis (2000). Two active forms of UDP-*N*-acetylglucosamine enolpyruvyl transferase in gram-positive bacteria. Journal of bacteriology **182**(15): 4146-4152.
- Dubnau, E., J. Chan, C. Raynaud, V. P. Mohan, M. A. Lan elle, K. Yu, A. Qu emard, I. Smith and M. Daff  (2000). Oxygenated mycolic acids are necessary for virulence of *Mycobacterium tuberculosis* in mice. Molecular microbiology **36**(3): 630-637.
- Duncan, K. (2003). Progress in TB drug development and what is still needed. Tuberculosis **83**(1): 201-207.
- Dworkin, J. (2014). The medium is the message: interspecies and inter-kingdom signaling by peptidoglycan and related bacterial glycans. Annual review of microbiology **68**: 137-154.
- Dye, C., G. P. Garnett, K. Sleeman and B. G. Williams (1998). Prospects for worldwide tuberculosis control under the WHO DOTS strategy. The Lancet **352**(9144): 1886-1891.
- Ehrt, S., X. V. Guo, C. M. Hickey, M. Ryou, M. Monteleone, L. W. Riley and D. Schnappinger (2005). Controlling gene expression in mycobacteria with anhydrotetracycline and Tet repressor. Nucleic acids research **33**(2): e21-e21.
- Elliott, A., S. Beming, M. Iseman and C. Peloquin (1995). Failure of drug penetration and acquisition of drug resistance in chronic tuberculous empyema. Tubercle and Lung Disease **76**(5): 463-467.
- Erdemli, S. B., R. Gupta, W. R. Bishai, G. Lamichhane, L. M. Amzel and M. A. Bianchet (2012). "Targeting the cell wall of *Mycobacterium tuberculosis*: structure and mechanism of L, D-transpeptidase 2." Structure **20**(12): 2103-2115.
- Fan, C., P. C. Moews and C. T. Walsh (1994). Vancomycin resistance: structure of D-alanine: D-alanine ligase at 2.3   resolution. Science **266**(5184): 439-443.
- Fischer, B., G. Rummel, P. Aldridge and U. Jenal (2002). The FtsH protease is involved in development, stress response and heat shock control in *Caulobacter crescentus*. Molecular microbiology **44**(2): 461-478.

- Flores, A. R., L. M. Parsons and M. S. Pavelka Jr (2005). Genetic analysis of the  $\beta$ -lactamases of *Mycobacterium tuberculosis* and *Mycobacterium smegmatis* and susceptibility to  $\beta$ -lactam antibiotics. Microbiology **151**(2): 521-532.
- Fox, W., G. A. Ellard and D. A. Mitchison (1999). Studies on the treatment of tuberculosis undertaken by the British Medical Research Council tuberculosis units, 1946–1986, with relevant subsequent publications. The International Journal of Tuberculosis and Lung Disease **3**(10s2): S231-S279.
- Gandhi, N. R., A. Moll, A. W. Sturm, R. Pawinski, T. Govender, U. Lalloo, K. Zeller, J. Andrews and G. Friedland (2006). Extensively drug-resistant tuberculosis as a cause of death in patients co-infected with tuberculosis and HIV in a rural area of South Africa. The Lancet **368**(9547): 1575-1580.
- Ghosh, A. S., C. Chowdhury and D. E. Nelson (2008). Physiological functions of D-alanine carboxypeptidases in *Escherichia coli*. Trends in microbiology **16**(7): 309-317.
- Ghuysen, J.M. (1991). Serine beta-lactamases and penicillin-binding proteins. Annual Reviews in Microbiology **45**(1): 37-67.
- Ghuysen, J.M. (1997). Penicillin-binding proteins. Wall peptidoglycan assembly and resistance to penicillin: facts, doubts and hopes. International journal of antimicrobial agents **8**(1): 45-60.
- Ghuysen, J.M., P. Charlier, J. Coyette, C. Duez, E. Fozze, C. Fraipont, C. Goffin, B. Joris and M. Nguyen-Disteche (1996). Penicillin and beyond: evolution, protein fold, multimodular polypeptides, and multiprotein complexes. Microbial Drug Resistance **2**(2): 163-175.
- Glickman, M. S., J. S. Cox and W. R. Jacobs (2000). A novel mycolic acid cyclopropane synthetase is required for cording, persistence, and virulence of *Mycobacterium tuberculosis*. Molecular cell **5**(4): 717-727.
- Goffin, C. and J.M. Ghuysen (1998). Multimodular penicillin-binding proteins: an enigmatic family of orthologs and paralogs. Microbiology and Molecular Biology Reviews **62**(4): 1079-1093.
- Goffin, C. and J.M. Ghuysen (2002). Biochemistry and comparative genomics of SxxK superfamily acyltransferases offer a clue to the mycobacterial paradox: presence of penicillin-susceptible target proteins versus lack of efficiency of penicillin as therapeutic agent. Microbiology and Molecular Biology Reviews **66**(4): 702-738.
- Gonzalez-Montaner, L., S. Natal, P. Yongchaiyud, P. Olliaro, E. Abbate, C. Mosca, G. Casado, M. Di Lonardo, G. Gerhart-Filho and I. Betjel (1994). Rifabutin for the treatment of newly-diagnosed pulmonary tuberculosis: a multinational, randomized, comparative study versus rifampicin. Tubercle and Lung Disease **75**(5): 341-347.
- Gopaldaswamy, R., S. Narayanan, W. R. Jacobs and Y. Av-Gay (2008). *Mycobacterium smegmatis* biofilm formation and sliding motility are affected by the serine/threonine protein kinase PknF. FEMS microbiology letters **278**(1): 121-127.
- Gottesman, S. (1999). Regulation by proteolysis: developmental switches. Current opinion in microbiology **2**(2): 142-147.

- Griffin, J. E., J. D. Gawronski, M. A. DeJesus, T. R. Ioerger, B. J. Akerley and C. M. Sassetti (2011). High-resolution phenotypic profiling defines genes essential for mycobacterial growth and cholesterol catabolism. PLoS Pathog **7**(9): e1002251.
- Gupta, R., M. Lavollay, J.L. Mainardi, M. Arthur, W. R. Bishai and G. Lamichhane (2010). "The *Mycobacterium tuberculosis* protein Ldt<sub>M2</sub> is a nonclassical transpeptidase required for virulence and resistance to amoxicillin. Nature medicine **16**(4): 466-469.
- Gupta, S., S. K. Banerjee, A. Chatterjee, A. K. Sharma, M. Kundu and J. Basu (2015). Essential protein SepF of mycobacteria interacts with FtsZ and MurG to regulate cell growth and division. Microbiology **161**(8): 1627-1638.
- Haas, D. W., S. L. Koletar, L. Laughlin, M. A. Kendall, C. Suckow, J. G. Gerber, A. R. Zolopa, R. Bertz, M. J. Child and L. Hoseney (2009). Hepatotoxicity and gastrointestinal intolerance when healthy volunteers taking rifampin add twice-daily atazanavir and ritonavir. Journal of acquired immune deficiency syndromes (1999) **50**(3): 290.
- Halbedel, S., L. Visser, M. Shaw, L. J. Wu, J. Errington, D. Marenduzzo and L. W. Hamoen (2009). Localisation of DivIVA by targeting to negatively curved membranes. The EMBO journal **28**(15): 2272-2282.
- Hammes, W. P. and H. Seidel (1978). The Activities in vitro of DD-Carboxypeptidase and LD-Carboxypeptidase of *Gaffkya homari* during Biosynthesis of Peptidoglycan. European Journal of Biochemistry **84**(1): 141-147.
- Hanahan, D. (1985). Techniques for transformation of *E. coli*. DNA cloning **1**: 109-135.
- Hanson, N. and C. Sanders (1999). Regulation of inducible AmpC beta-lactamase expression among Enterobacteriaceae. Current pharmaceutical design **5**(11): 881-894.
- Heidrich, C., A. Ursinus, J. Berger, H. Schwarz and J.-V. Hölftje (2002). "Effects of multiple deletions of murein hydrolases on viability, septum cleavage, and sensitivity to large toxic molecules in *Escherichia coli*. Journal of bacteriology **184**(22): 6093-6099.
- Heidrich, C., M. F. Templin, A. Ursinus, M. Merdanovic, J. Berger, H. Schwarz, M. A. De Pedro and J. V. Hölftje (2001). Involvement of *N*-acetylmuramyl-l-alanine amidases in cell separation and antibiotic-induced autolysis of *Escherichia coli*. Molecular microbiology **41**(1): 167-178.
- Herman, C., D. Thévenet, R. D'Ari and P. Boulloc (1995). Degradation of sigma 32, the heat shock regulator in *Escherichia coli*, is governed by HflB. Proceedings of the National Academy of Sciences **92**(8): 3516-3520.
- Hett, E. C. and E. J. Rubin (2008). Bacterial growth and cell division: a mycobacterial perspective. Microbiology and Molecular Biology Reviews **72**(1): 126-156.
- Hett, E. C., M. C. Chao and E. J. Rubin (2010). Interaction and modulation of two antagonistic cell wall enzymes of mycobacteria. PLoS Pathog **6**(7): e1001020.
- Hett, E. C., M. C. Chao, A. J. Steyn, S. M. Fortune, L. L. Deng and E. J. Rubin (2007). A partner for the resuscitation-promoting factors of *Mycobacterium tuberculosis*. Molecular microbiology **66**(3): 658-668.
- Hett, E. C., M. C. Chao, L. L. Deng and E. J. Rubin (2008). A mycobacterial enzyme essential for cell division synergizes with resuscitation-promoting factor. PLoS Pathog **4**(2): e1000001.

- Höltje, J., D. Mirelman, N. Sharon and U. Schwarz (1975). Novel type of murein transglycosylase in *Escherichia coli*. Journal of bacteriology **124**(3): 1067-1076.
- Höltje, J.V. (1998). Growth of the stress-bearing and shape-maintaining murein sacculus of *Escherichia coli*. Microbiology and Molecular Biology Reviews **62**(1): 181-203.
- Höltje, J.V. and C. Heidrich (2001). Enzymology of elongation and constriction of the murein sacculus of *Escherichia coli*. Biochimie **83**(1): 103-108.
- Hunter, S. and P. Brennan (1983). Further specific extracellular phenolic glycolipid antigens and a related diacylphthiocerol from *Mycobacterium leprae*. Journal of Biological Chemistry **258**(12): 7556-7562.
- Ioerger, T. R., Y. Feng, K. Ganesula, X. Chen, K. M. Dobos, S. Fortune, W. R. Jacobs, V. Mizrahi, T. Parish and E. Rubin (2010). Variation among genome sequences of H<sub>37</sub>Rv strains of *Mycobacterium tuberculosis* from multiple laboratories. Journal of bacteriology **192**(14): 3645-3653.
- Iseman, M. and L. Madsen (1991). Chronic tuberculous empyema with bronchopleural fistula resulting in treatment failure and progressive drug resistance. CHEST Journal **100**(1): 124-127.
- Ito, K. and Y. Akiyama (2005). Cellular functions, mechanism of action, and regulation of FtsH protease Annu. Rev. Microbiol. **59**: 211-231.
- Jacoby, G. A. (2009). AmpC  $\beta$ -lactamases. Clinical microbiology reviews **22**(1): 161-182.
- Jacoby, G. A. and D. L. Mayers (2009). Antimicrobial Drug Resistance: Mechanisms of Drug Resistance. Journal of Visualized Experiments **60**:pp.e3820-e3820
- Kana, B. D. and V. Mizrahi (2010). Resuscitation-promoting factors as lytic enzymes for bacterial growth and signaling. FEMS Immunology & Medical Microbiology **58**(1): 39-50.
- Kana, B. D., B. G. Gordhan, K. J. Downing, N. Sung, G. Vostroktunova, E. E. Machowski, L. Tsenova, M. Young, A. Kaprelyants and G. Kaplan (2008). The resuscitation-promoting factors of *Mycobacterium tuberculosis* are required for virulence and resuscitation from dormancy but are collectively dispensable for growth in vitro. Molecular microbiology **67**(3): 672-684.
- Kang, C.M., D. W. Abbott, S. T. Park, C. C. Dascher, L. C. Cantley and R. N. Husson (2005). The *Mycobacterium tuberculosis* serine/threonine kinases PknA and PknB: substrate identification and regulation of cell shape. Genes & development **19**(14): 1692-1704.
- Kang, C.M., S. Nyayapathy, J.-Y. Lee, J.-W. Suh and R. N. Husson (2008). Wag31, a homologue of the cell division protein DivIVA, regulates growth, morphology and polar cell wall synthesis in mycobacteria. Microbiology **154**(3): 725-735.
- Kansal, R. G., R. Gomez-Flores and R. T. Mehta (1998). Change in colony morphology influences the virulence as well as the biochemical properties of the *Mycobacterium avium* complex. Microbial pathogenesis **25**(4): 203-214.
- Kartmann, B., S. Stengler and M. Niederweis (1999). Porins in the Cell Wall of *Mycobacterium tuberculosis*. Journal of bacteriology **181**(20): 6543-6546.

- Keep, N., J. Ward, G. Robertson, M. Cohen-Gonsaud and B. Henderson (2006). Bacterial resuscitation factors: revival of viable but non-culturable bacteria. Cellular and molecular life sciences **63**(22): 2555-2559.
- Keer, J., M. J. Smeulders, K. M. Gray and H. D. Williams (2000). Mutants of *Mycobacterium smegmatis* impaired in stationary-phase survival. Microbiology **146**(9): 2209-2217.
- Khachi, H., R. O'Connell, D. Ladenheim and C. Orkin (2009). Pharmacokinetic interactions between rifabutin and lopinavir/ritonavir in HIV-infected patients with mycobacterial co-infection. Journal of antimicrobial chemotherapy **64**(4): 871-873.
- Kieser, K. J. and E. J. Rubin (2014). How sisters grow apart: mycobacterial growth and division. Nature Reviews Microbiology **12**(8): 550-562.
- Kieser, K. J., C. C. Boutte, J. C. Kester, C. E. Baer, A. K. Barczak, X. Meniche, M. C. Chao, E. H. Rego, C. M. Sasseti and S. M. Fortune (2015). Phosphorylation of the peptidoglycan synthase PonA1 governs the rate of polar elongation in mycobacteria. PLoS Pathog **11**(6): e1005010.
- Koraimann, G. (2003). Lytic transglycosylases in macromolecular transport systems of Gram-negative bacteria. Cellular and Molecular Life Sciences CMLS **60**(11): 2371-2388.
- Korsak, D., S. Liebscher and W. Vollmer (2005). Susceptibility to antibiotics and  $\beta$ -lactamase induction in murein hydrolase mutants of *Escherichia coli*. Antimicrobial agents and chemotherapy **49**(4): 1404-1409.
- Koul, A., E. Arnoult, N. Lounis, J. Guillemont and K. Andries (2011). The challenge of new drug discovery for tuberculosis. Nature **469**(7331): 483-490.
- Koyasu, S., A. Fukuda and Y. Okada (1980). The penicillin-binding proteins of *Caulobacter crescentus*. Journal of biochemistry **87**(1): 363-366.
- Kremer., W.R. Jacobs and G.F. Hatfull, G.F. (2008). Growth of *Mycobacterium tuberculosis*
- Krishnamurthy, P., M. H. Parlow, J. Schneider, S. Burroughs, C. Wickland, N. B. Vakil, B. E. Dunn and S. H. Phadnis (1999). Identification of a novel penicillin-binding protein from *Helicobacter pylori*. Journal of bacteriology **181**(16): 5107-5110.
- Kulka, K., G. Hatfull, and A.K. Ojha (2012). Growth of *Mycobacterium tuberculosis* biofilms. Journal of Visualized Experiments **60**: 3820-3820.
- Kumar, P., K. Arora, J. R. Lloyd, I. Y. Lee, V. Nair, E. Fischer, H. I. Boshoff and C. E. Barry (2012). "Meropenem inhibits DD-Carboxypeptidase activity in *Mycobacterium tuberculosis*. Molecular microbiology **86**(2): 367-381.
- Kuzin, A. P., H. Liu, J. A. Kelly and J. R. Knox (1995). Binding of cephalothin and cefotaxime to D-Ala-D-Ala-peptidase reveals a functional basis of a natural mutation in a low-affinity penicillin-binding protein and in extended-spectrum Beta.-lactamases. Biochemistry **34**(29): 9532-9540.
- Lan, N. T. N., N. T. N. Thu, A. Barrail-Tran, N. H. Duc, N. N. Lan, D. Laureillard, T. T. X. Lien, L. Borand, C. Quillet and C. Connolly (2014). Randomised pharmacokinetic trial of rifabutin with lopinavir/ritonavir-antiretroviral therapy in patients with HIV-associated tuberculosis in Vietnam. PloS one **9**(1): e84866.



- Lawrence, P. and J. Strominger (1970). The reversible fixation of radioactive penicillin G to the D-alanine Carboxypeptidase of *Bacillus subtilis*. J. Biol. Chem **245**: 3660-3666.
- Lee, M., W. Zhang, D. Heseck, B. C. Noll, B. Boggess and S. Mobashery (2009). Bacterial AmpD at the crossroads of peptidoglycan recycling and manifestation of antibiotic resistance. Journal of the American Chemical Society **131**(25): 8742-8743.
- Letek, M., M. Fiuza, E. Ordóñez, A. F. Villadangos, K. Flärdh, L. M. Mateos and J. A. Gil (2009). DivIVA uses an N-terminal conserved region and two coiled-coil domains to localize and sustain the polar growth in *Corynebacterium glutamicum*. FEMS microbiology letters **297**(1): 110-116.
- Leyh-Bouille, M., M. Nakel, J. M. Frere, K. Johnson, J. M. Ghuysen, M. Nieto and H. R. Perkins (1972). Penicillin-sensitive DD-carboxypeptidases from *Streptomyces* strains R39 and K11. Biochemistry **11**(7): 1290-1298.
- Liu, J., C. E. Barry, G. S. Besra and H. Nikaido (1996). Mycolic acid structure determines the fluidity of the mycobacterial cell wall. Journal of Biological Chemistry **271**(47): 29545-29551.
- Louw, G., R. Warren, N. G. Van Pittius, C. McEvoy, P. Van Helden and T. Victor (2009). A balancing act: efflux/influx in mycobacterial drug resistance. Antimicrobial agents and chemotherapy **53**(8): 3181-3189.
- Lovering, A. L., L. H. De Castro, D. Lim and N. C. Strynadka (2007). Structural insight into the transglycosylation step of bacterial cell-wall biosynthesis. Science **315**(5817): 1402-1405.
- Lovering, A. L., S. S. Safadi and N. C. Strynadka (2012). Structural perspective of peptidoglycan biosynthesis and assembly. Annual review of biochemistry **81**: 451-478.
- Macheboeuf, P., C. Contreras-Martel, V. Job, O. Dideberg and A. Dessen (2006). Penicillin binding proteins: key players in bacterial cell cycle and drug resistance processes. FEMS microbiology reviews **30**(5): 673-691.
- Machowski, E. E., S. Senzani, C. Ealand and B. D. Kana (2014). Comparative genomics for mycobacterial peptidoglycan remodeling enzymes reveals extensive genetic multiplicity. BMC microbiology **14**(1): 1.
- Mahapatra, S., T. Yagi, J. T. Belisle, B. J. Espinosa, P. J. Hill, M. R. McNeil, P. J. Brennan and D. C. Crick (2005). Mycobacterial lipid II is composed of a complex mixture of modified muramyl and peptide moieties linked to decaprenyl phosphate. Journal of bacteriology **187**(8): 2747-2757.
- Mainardi, J.L., M. Fourgeaud, J.E. Hugonnet, L. Dubost, J.-P. Brouard, J. Ouazzani, L. B. Rice, L. Gutmann and M. Arthur (2005). A novel peptidoglycan cross-linking enzyme for a  $\beta$ -lactam-resistant transpeptidation pathway. Journal of Biological Chemistry **280**(46): 38146-38152.
- Mainardi, J.L., R. Legrand, M. Arthur, B. Schoot, J. van Heijenoort and L. Gutmann (2000). Novel mechanism of  $\beta$ -lactam resistance due to bypass of DD-transpeptidation in *Enterococcus faecium*. Journal of Biological Chemistry **275**(22): 16490-16496.
- Markiewicz, Z., J. K. Broome-Smith, U. Schwarz and B. G. Spratt (1982). Spherical *E. coli* due to elevated levels of D-alanine Carboxypeptidase. Nature **297**, 702 - 704

- Marques, M. A. M., S. Chitale, P. J. Brennan and M. C. V. Pessolani (1998). Mapping and identification of the major cell wall-associated components of *Mycobacterium leprae*. Infection and Immunity **66**(6): 2625-2631.
- Martínez, A., S. Torello and R. Kolter (1999). Sliding motility in mycobacteria. Journal of bacteriology **181**(23): 7331-7338.
- Massova, I. and S. Mobashery (1998). Kinship and diversification of bacterial penicillin-binding proteins and  $\beta$ -lactamases. Antimicrobial agents and chemotherapy **42**(1): 1-17.
- Maya-Hoyos, M., J. Leguizamón, L. Mariño-Ramírez and C. Y. Soto (2015). Sliding Motility, Biofilm Formation, and Glycopeptidolipid Production in *Mycobacterium colombiense* Strains. BioMed research international. 2015, 11.
- McDonough, M. A., J. W. Anderson, N. R. Silvaggi, R. Pratt, J. R. Knox and J. A. Kelly (2002). Structures of two kinetic intermediates reveal species specificity of penicillin-binding proteins. Journal of molecular biology **322**(1): 111-122.
- McNeil, M., M. Daffe and P. J. Brennan (1990). Evidence for the nature of the link between the arabinogalactan and peptidoglycan of mycobacterial cell walls. Journal of Biological Chemistry **265**(30): 18200-18206.
- Mengin-Lecreulx, D., L. Texier, M. Rousseau and J. van Heijenoort (1991). The murG gene of *Escherichia coli* codes for the UDP-N-acetylglucosamine: N-acetylmuramyl-(pentapeptide) pyrophosphoryl-undecaprenol N-acetylglucosamine transferase involved in the membrane steps of peptidoglycan synthesis. Journal of bacteriology **173**(15): 4625-4636.
- Mikušová, K. N., T. Yagi, R. Stern, M. R. McNeil, G. S. Besra, D. C. Crick and P. J. Brennan (2000). Biosynthesis of the galactan component of the mycobacterial cell wall. Journal of Biological Chemistry **275**(43): 33890-33897.
- Miller, J. H. (1972). Experiments in molecular genetics. Cold Spring Harbor Laboratory, 35-105
- Mohammadi, T., A. Karczmarek, M. Crouvoisier, A. Bouhss, D. Mengin-Lecreulx and T. Den Blaauwen (2007). The essential peptidoglycan glycosyltransferase MurG forms a complex with proteins involved in lateral envelope growth as well as with proteins involved in cell division in *Escherichia coli*. Molecular microbiology **65**(4): 1106-1121.
- Moreno, C., A. Mehlert and J. Lamb (1988). The inhibitory effects of mycobacterial lipoarabinomannan and polysaccharides upon polyclonal and monoclonal human T cell proliferation. Clinical and experimental immunology **74**(2): 206.
- Mottl, H. and W. Keck (1991). Purification of penicillin-binding protein 4 of *Escherichia coli* as a soluble protein by dye-affinity chromatography. European Journal of Biochemistry **200**(3): 767-773.
- Mukamolova, G. V., A. S. Kaprelyants, D. I. Young, M. Young and D. B. Kell (1998). A bacterial cytokine. Proceedings of the National Academy of Sciences **95**(15): 8916-8921.
- Nachamkin, I., C. Kang and M. P. Weinstein (1997). Detection of resistance to isoniazid, rifampin, and streptomycin in clinical isolates of *Mycobacterium tuberculosis* by molecular methods. Clinical infectious diseases **24**(5): 894-900.

- Navratna, V., S. Nadig, V. Sood, K. Prasad, G. Arakere and B. Gopal (2010). Molecular basis for the role of *Staphylococcus aureus* penicillin binding protein 4 in antimicrobial resistance. Journal of bacteriology **192**(1): 134-144.
- Nelson, D. E. and K. D. Young (2000). Penicillin binding protein 5 affects cell diameter, contour, and morphology of *Escherichia coli*. Journal of bacteriology **182**(6): 1714-1721.
- Nelson, D. E. and K. D. Young (2001). Contributions of PBP 5 and DD-Carboxypeptidase Penicillin Binding Proteins to Maintenance of Cell Shape in *Escherichia coli*. Journal of bacteriology **183**(10): 3055-3064.
- Nicholas, R. A., S. Krings, J. Tomberg, G. Nicola and C. Davies (2003). Crystal structure of wild-type penicillin-binding protein 5 from *Escherichia coli* Implications for deacylation of the acyl-enzyme complex. Journal of Biological Chemistry **278**(52): 52826-52833.
- Nicoletti, G., G. Russo and G. Bonfiglio (2002). Recent developments in carbapenems. Expert opinion on investigational drugs **11**(4): 529-544.
- Nikitushkin, V. D., G. R. Demina, M. O. Shleeva, S. V. Guryanova, A. Ruggiero, R. Berisio and A. S. Kaprelyants (2015). A product of RpfB and RipA joint enzymatic action promotes the resuscitation of dormant mycobacteria. FEBS Journal **282**(13): 2500-2511.
- Ojha, A. and G. F. Hatfull (2007). The role of iron in *Mycobacterium smegmatis* biofilm formation: the exochelin siderophore is essential in limiting iron conditions for biofilm formation but not for planktonic growth. Molecular microbiology **66**(2): 468-483.
- Ojha, A.K., A.D. Baughn., D. Sambandan., T. Hsu., X. Trivelli., Y. Guerardel., A. Alahari., L. O'Toole, G., H. B. Kaplan and R. Kolter (2000). Biofilm formation as microbial development. Annual Reviews in Microbiology **54**(1): 49-79.
- Ojha, A.K., Baughn, A.D., Sambandan, D., Hsu, T., Trivelli, X., Guerardel, Y., Alahari, A., Kremer, L., Jacobs, W.R. and Hatfull, G.F., 2008. Growth of *Mycobacterium tuberculosis* biofilms containing free mycolic acids and harbouring drug-tolerant bacteria. Molecular microbiology, **69**(1):164-174.
- Ojha, A., Anand, M., Bhatt, A., Kremer, L., Jacobs, W.R. and Hatfull, G.F., 2005. GroEL1: a dedicated chaperone involved in mycolic acid biosynthesis during biofilm formation in mycobacteria. Cell **123**(5): 861-873.
- Pang, J. M., E. Layre, L. Sweet, A. Sherrid, D. B. Moody, A. Ojha and D. R. Sherman (2012). The polyketide Pks1 contributes to biofilm formation in *Mycobacterium tuberculosis*." Journal of bacteriology **194**(3): 715-721.
- Park, J. T. and T. Uehara (2008). How bacteria consume their own exoskeletons (turnover and recycling of cell wall peptidoglycan). Microbiology and Molecular Biology Reviews **72**(2): 211-227.
- Parrish, N. M., J. D. Dick and W. R. Bishai (1998). Mechanisms of latency in *Mycobacterium tuberculosis*. Trends in microbiology **6**(3): 107-112.
- Patru, M.-M. and M. S. Pavelka (2010). A role for the class A penicillin-binding protein PonA2 in the survival of *Mycobacterium smegmatis* under conditions of non-replication. Journal of bacteriology **192**(12): 3043-3054.

- Pedersen, L. B., T. Murray, D. L. Popham and P. Setlow (1998). Characterization of dacC, which encodes a new low-molecular-weight penicillin-binding protein in *Bacillus subtilis*. Journal of bacteriology **180**(18): 4967-4973.
- Pisabarro, A. G., M. A. de Pedro and D. Vázquez (1985). Structural modifications in the peptidoglycan of *Escherichia coli* associated with changes in the state of growth of the culture. Journal of bacteriology **161**(1): 238-242.
- Ploeg, R., J. Verheul, N. O. Vischer, S. Alexeeva, E. Hoogendoorn, M. Postma, M. Banzhaf, W. Vollmer and T. Blaauwen (2013). Co-localization and interaction between elongasome and divisome during a preparative cell division phase in *Escherichia coli*. Molecular microbiology **87**(5): 1074-1087.
- Popham, D. L., M. E. Gilmore and P. Setlow (1999). Roles of low-molecular-weight penicillin-binding proteins in *Bacillus subtilis* spore peptidoglycan synthesis and spore properties. Journal of bacteriology **181**(1): 126-132.
- Posey, J. E., T. M. Shinnick and F. D. Quinn (2006). Characterization of the twin-arginine translocase secretion system of *Mycobacterium smegmatis*. Journal of bacteriology **188**(4): 1332-1340.
- Prigozhin, D. M., D. Mavrici, J. P. Huizar, H. J. Vansell and T. Alber (2013). Structural and biochemical analyses of *Mycobacterium tuberculosis* N-acetylmuramyl-L-alanine amidase Rv3717 point to a role in peptidoglycan fragment recycling. Journal of Biological Chemistry **288**(44): 31549-31555.
- Prisic, S., S. Dankwa, D. Schwartz, M. F. Chou, J. W. Locasale, C.-M. Kang, G. Bemis, G. M. Church, H. Steen and R. N. Husson (2010). Extensive phosphorylation with overlapping specificity by *Mycobacterium tuberculosis* serine/threonine protein kinases. Proceedings of the National Academy of Sciences **107**(16): 7521-7526.
- Priyadarshini, R., D. L. Popham and K. D. Young (2006). Daughter cell separation by penicillin-binding proteins and peptidoglycan amidases in *Escherichia coli*. Journal of bacteriology **188**(15): 5345-5355.
- Prophet, E. B., B. Mills, J. B. Arrington and L. H. Sobin (1992). Laboratory methods in histotechnology, American Registry of Pathology Washington, DC.
- Qureshi, N., K. Takayama, H. C. Jordi and H. K. Schnoes (1978). Characterization of the purified components of a new homologous series of alpha-mycolic acids from *Mycobacterium tuberculosis* H<sub>37</sub>Ra. Journal of Biological Chemistry **253**(15): 5411-5417.
- Raviglione, M. C. and A. Pio (2002). Evolution of WHO policies for tuberculosis control, 1948–2001. The Lancet **359**(9308): 775-780.
- Recht, J. and R. Kolter (2001). Glycopeptidolipid acetylation affects sliding motility and biofilm formation in *Mycobacterium smegmatis*. Journal of bacteriology **183**(19): 5718-5724.
- Recht, J., A. Martínez, S. Torello and R. Kolter (2000). Genetic Analysis of Sliding Motility in *Mycobacterium smegmatis*. Journal of bacteriology **182**(15): 4348-4351.
- Ribera, E., L. Pou, R. M. Lopez, M. Crespo, V. Falco, I. Ocaña, I. Ruiz and A. Pahissa (2001). Pharmacokinetic interaction between nevirapine and rifampicin in HIV-infected patients with tuberculosis. JAIDS Journal of Acquired Immune Deficiency Syndromes **28**(5): 450-453.

- Rossi, E. D., J. A. Aínsa and G. Riccardi (2006). Role of mycobacterial efflux transporters in drug resistance: an unresolved question. FEMS microbiology reviews **30**(1): 36-52.
- Royet, J. and R. Dziarski (2007). Peptidoglycan recognition proteins: pleiotropic sensors and effectors of antimicrobial defences. Nature Reviews Microbiology **5**(4): 264-277.
- Sani, M., E. N. Houben, J. Geurtsen, J. Pierson, K. De Punder, M. van Zon, B. Wever, S. R. Piersma, C. R. Jiménez and M. Daffé (2010). Direct visualization by cryo-EM of the mycobacterial capsular layer: a labile structure containing ESX-1-secreted proteins. PLoS Pathog **6**(3): e1000794.
- Sauvage, E., F. Kerff, M. Terrak, J. A. Ayala and P. Charlier (2008). The penicillin-binding proteins: structure and role in peptidoglycan biosynthesis. FEMS microbiology reviews **32**(2): 234-258.
- Sauvage, E., F. Kerff, M. Terrak, J. A. Ayala and P. Charlier (2008). The penicillin-binding proteins: structure and role in peptidoglycan biosynthesis. FEMS microbiology reviews **32**(2): 234-258.
- Scheurwater, E. M. and L. L. Burrows (2011). Maintaining network security: how macromolecular structures cross the peptidoglycan layer. FEMS microbiology letters **318**(1): 1-9.
- Scheurwater, E., C. W. Reid and A. J. Clarke (2008). Lytic transglycosylases: bacterial space-making autolysins. The international journal of biochemistry & cell biology **40**(4): 586-591.
- Schoonmaker, M. K., W. R. Bishai and G. Lamichhane (2014). Nonclassical transpeptidases of *Mycobacterium tuberculosis* alter cell size, morphology, the cytosolic matrix, protein localization, virulence, and resistance to  $\beta$ -lactams. Journal of bacteriology **196**(7): 1394-1402.
- Severin, A. and A. Tomasz (1996). Naturally occurring peptidoglycan variants of *Streptococcus pneumoniae*. Journal of bacteriology **178**(1): 168-174.
- Shah, I. M., M.H. Laaberki, D. L. Popham and J. Dworkin (2008). A eukaryotic-like Ser/Thr kinase signals bacteria to exit dormancy in response to peptidoglycan fragments. Cell **135**(3): 486-496.
- Simpson, L., V. White, S. Zane and J. D. Oliver (1987). Correlation between virulence and colony morphology in *Vibrio vulnificus*. Infection and Immunity **55**(1): 269-272.
- Singh, A., D. Mai, A. Kumar and A. J. Steyn (2006). Dissecting virulence pathways of *Mycobacterium tuberculosis* through protein-protein association. Proceedings of the National Academy of Sciences **103**(30): 11346-11351.
- Smithwick, R.W., 1976. Laboratory manual for acid-fast microscopy Public Health Service, Center for Disease Control, Bureau of Laboratories. (p. 3)
- Spratt, B. G. (1977). Properties of the Penicillin-Binding Proteins of *Escherichia coli* K12. European Journal of Biochemistry **72**(2): 341-352.
- Spratt, B. G. (1983). Penicillin-binding Proteins and the Future of  $\beta$ -Lactam Antibiotics: The Seventh Fleming Lecture. Microbiology **129**(5): 1247-1260.

Srinivasan, R., G. Anilkumar, H. Rajeswari and P. Ajitkumar (2006). Functional characterization of AAA family FtsH protease of *Mycobacterium tuberculosis*. FEMS microbiology letters **259**(1): 97-105.

Srinivasan, R., H. Rajeswari and P. Ajitkumar (2008). Analysis of degradation of bacterial cell division protein FtsZ by the ATP-dependent zinc-metalloprotease FtsH *in vitro*. Microbiological research **163**(1): 21-30.

Strominger, J. L. (1969). Penicillin-sensitive enzymatic reactions in bacterial cell wall synthesis. Inhibitors Tools in Cell Research, Springer: 187-207.

Suárez, P. G., K. Floyd, J. Portocarrero, E. Alarcón, E. Rapiti, G. Ramos, C. Bonilla, I. Sabogal, I. Aranda and C. Dye (2002). Feasibility and cost-effectiveness of standardized second-line drug treatment for chronic tuberculosis patients: a national cohort study in Peru. The Lancet **359**(9322): 1980-1989.

Takayama, K., H. K. Schnoes, E. L. Armstrong and R. W. Boyle (1975). Site of inhibitory action of isoniazid in the synthesis of mycolic acids in *Mycobacterium tuberculosis*. Journal of lipid research **16**(4): 308-317.

Tayler, A. E., J. A. Ayala, P. Niumsup, K. Westphal, J. A. Baker, L. Zhang, T. R. Walsh, B. Wiedemann, P. M. Bennett and M. B. Avison (2010). Induction of  $\beta$ -lactamase production in *Aeromonas hydrophila* is responsive to  $\beta$ -lactam-mediated changes in peptidoglycan composition. Microbiology **156**(8): 2327-2335.

Telenti, A., P. Imboden, F. Marchesi, L. Matter, K. Schopfer, T. Bodmer, D. Lowrie, M. Colston and S. Cole (1993). Detection of rifampicin-resistance mutations in *Mycobacterium tuberculosis*. The Lancet **341**(8846): 647-651.

Telenti, A., W. J. Philipp, S. Sreevatsan, C. Bernasconi, K. E. Stockbauer, B. Wiele, J. M. Musser and W. R. Jacobs (1997). "The *emb* operon, a gene cluster of *Mycobacterium tuberculosis* involved in resistance to ethambutol. Nature medicine **3**(5): 567-570.

Tobian, A. A., N. S. Potter, L. Ramachandra, R. K. Pai, M. Convery, W. H. Boom and C. V. Harding (2003). Alternate class I MHC antigen processing is inhibited by Toll-like receptor signaling pathogen-associated molecular patterns: *Mycobacterium tuberculosis* 19-kDa lipoprotein, CpG DNA, and lipopolysaccharide. The Journal of Immunology **171**(3): 1413-1422.

Trunkfield, A. E., S. S. Gurcha, G. S. Besra and T. D. Bugg (2010). Inhibition of *Escherichia coli* glycosyltransferase MurG and *Mycobacterium tuberculosis* Gal transferase by uridine-linked transition state mimics. Bioorganic & medicinal chemistry **18**(7): 2651-2663.

Tufariello, J. M., J. Chan and J. L. Flynn (2003). Latent tuberculosis: mechanisms of host and bacillus that contribute to persistent infection. The Lancet infectious diseases **3**(9): 578-590.

Typas, A., M. Banzhaf, C. A. Gross and W. Vollmer (2012). From the regulation of peptidoglycan synthesis to bacterial growth and morphology. Nature Reviews Microbiology **10**(2): 123-136.

Tayler, A.E., Ayala, J.A., Niumsup, P., Westphal, K., Baker, J.A., Zhang, L., Walsh, T.R., Wiedemann, B., Bennett, P.M. and Avison, M.B., 2010. Induction of  $\beta$ -lactamase production in *Aeromonas hydrophila* is responsive to  $\beta$ -lactam-mediated changes in peptidoglycan composition. Microbiology**156**(8): 2327-2335.

- Vollmer, W., B. Joris, P. Charlier and S. Foster (2008). Bacterial peptidoglycan (murein) hydrolases. FEMS microbiology reviews **32**(2): 259-286.
- Wang, J. E., M. K. Dahle, M. McDonald, S. J. Foster, A. O. Aasen and C. Thiemermann (2003). Peptidoglycan and lipoteichoic acid in gram-positive bacterial species: receptors, signal transduction, biological effects, and synergism. Shock **20**(5): 402-414.
- Watanabe, M., Y. Aoyagi, M. Ridell and D. E. Minnikin (2001). Separation and characterization of individual mycolic acids in representative mycobacteria. Microbiology **147**(7): 1825-1837.
- Wei, Y., T. Havasy, D. C. McPherson and D. L. Popham (2003). Rod shape determination by the *Bacillus subtilis* class B penicillin-binding proteins encoded by pbpA and pbpH. Journal of bacteriology **185**(16): 4717-4726.
- Wietzerbin, J., B. C. Das, J. F. Petit, E. Lederer, M. Leyh-Bouille and J. M. Ghuysen (1974). Occurrence of D-alanyl-(D)-meso-diaminopimelic acid and meso-diaminopimelyl-meso-diaminopimelic acid interpeptide linkages in the peptidoglycan of Mycobacteria. Biochemistry **13**(17): 3471-3476.
- Winder, F. and P. Collins (1970). Inhibition by isoniazid of synthesis of mycolic acids in *Mycobacterium tuberculosis*. Microbiology **63**(1): 41-48.
- World Health Organization, W. H. (2015). Global tuberculosis report 2015.
- Young, K. D. (2006). The selective value of bacterial shape. Microbiology and Molecular Biology Reviews **70**(3): 660-703.
- Yuan, Y., R. E. Lee, G. S. Besra, J. T. Belisle and C. Barry (1995). Identification of a gene involved in the biosynthesis of cyclopropanated mycolic acids in *Mycobacterium tuberculosis*. Proceedings of the National Academy of Sciences **92**(14): 6630-6634.
- Zahrl, D., M. Wagner, K. Bischof, M. Bayer, B. Zavec, A. Beranek, C. Ruckstuhl, G. E. Zarfel and G. Koraimann (2005). Peptidoglycan degradation by specialized lytic transglycosylases associated with type III and type IV secretion systems. Microbiology **151**(11): 3455-3467.
- Zhang, Y. (2004). Persistent and dormant tubercle bacilli and latent tuberculosis. Frontiers in bioscience: a journal and virtual library **9**: 1136-1156.
- Zhang, Y. (2005). The magic bullets and tuberculosis drug targets. Annu. Rev. Pharmacol. Toxicol. **45**: 529-564.
- Zumla, A., P. Nahid and S. T. Cole (2013). Advances in the development of new tuberculosis drugs and treatment regimens. Nature reviews Drug discovery **12**(5): 388-404.

